National Library of Canada
Acquisitions and Bibliographic Services Branch
395 Wellington Street
Ottawa, Ontario
K1A 0N4

Bibliothèque nationale du Canada
Direction des acquisitions et des services bibliographiques
395, rue Wellington
Ottawa (Ontario)
K1A 0N4

Your file Votre référence

Our file Notre référence

NOTICE

The quality of this microform is heavily dependent upon the quality of the original thesis submitted for microfilming. Every effort has been made to ensure the highest quality of reproduction possible.

If pages are missing, contact the university which granted the degree.

Some pages may have indistinct print especially if the original pages were typed with a poor typewriter ribbon or if the university sent us an inferior photocopy.

Reproduction in full or in part of this microform is governed by the Canadian Copyright Act, R.S.C. 1970, c. C-30, and subsequent amendments.

AVIS

La qualité de cette microforme dépend grandement de la qualité de la thèse soumise au microfilmage. Nous avons tout fait pour assurer une qualité supérieure de reproduction.

S'il manque des pages, veuillez communiquer avec l'université qui a conféré le grade.

La qualité d'impression de certaines pages peut laisser à désirer, surtout si les pages originales ont été dactylographiées à l'aide d'un ruban usé ou si l'université nous a fait parvenir une photocopie de qualité inférieure.

La reproduction, même partielle, de cette microforme est soumise à la Loi canadienne sur le droit d'auteur, SRC 1970, c. C-30, et ses amendements subséquents.

Canada

SUBSTANCE P SENSORY FIBER INNERVATION OF CNS TARGET TISSUES IN TWO EXPERIMENTAL MODELS

by

WEIYA MA

A thesis submitted to the
Faculty of Graduate Studies and Research
in partial fulfilment of the requirement for the degree of
Doctor of Philosophy

Department of Pharmacology & Therapeutics
McGill University
Montreal, Quebec.

August, 1995

National Library
of Canada

Acquisitions and
Bibliographic Services Branch

395 Wellington Street
Ottawa, Ontario
K1A 0N4

Bibliothèque nationale
du Canada

Direction des acquisitions et
des services bibliographiques

395, rue Wellington
Ottawa (Ontario)
K1A 0N4

Your file Votre référence

Our file Notre référence

ISBN 0-612-12424-X

Canada

Dedicated to my husband, daughter and parents
for their everlasting selfless caring, loving and sacrifice

ABSTRACT

The aim of this thesis study was to investigate the substance P (SP)-immunoreactive (IR) sensory fiber innervation of CNS target tissues in two experimental models. In the first model, we examined the SP-IR boutons apposed to three functional types of dorsal horn neurons and their morphological interaction with calcitonin gene-related peptide (CGRP) and enkephalin (ENK) in the cat spinal cord, using a combination of intracellular electrophysiological recording and horseradish peroxidase injection with ultrastructural immunocytochemistry. In addition to SP-IR only boutons, we detected boutons co-localizing SP plus CGRP and SP plus ENK immunoreactivities presynaptic to nociceptive neurons. Quantitatively, significantly higher numbers of SP-IR, SP+CGRP-IR and SP+ENK-IR boutons were apposed to nociceptive neurons. Non-nociceptive neurons were rarely innervated by boutons which were SP-IR, SP+CGRP-IR and SP+ENK-IR. In contrast, ENK-IR only boutons innervated non-nociceptive neurons considerably. Boutons co-localizing SP and CGRP were considered as originating from primary sensory afferents. Most nociceptive neurons contained ENK immunoreactivity, but non-nociceptive neurons were never ENK-IR. The interaction of SP and γ-aminobutyric acid (GABA) in the superficial dorsal horn of the cat and rat spinal cord was also investigated. The co-localization of SP and GABA in axonal terminals was detected for the first time in the superficial layers of the dorsal horn of the cat, but not rat, spinal cord.

In the second model, we used immunocytochemistry to study the SP-IR fiber innervation of the white matter of transgenic mice expressing NGF in myelinating oligodendrocytes driven by a MBP promoter. SP-IR fibers were observed in the white matter

of the CNS of both transgenic and control mice from postnatal day 0 to day 2. From day 5 on, however, these SP-IR fibers increased markedly to become ectopic fibers in transgenic mice, but decreased dramatically, and finally disappeared, in control mice. The ectopic SP-IR fibers of transgenic mice persisted throughout adulthood. Capsaicin treatment abolished all ectopic SP-IR fibers, indicating their primary sensory origin.

In conclusion, SP-IR fibers specifically innervated nociceptive neurons and co-localized with CGRP, ENK and GABA in the cat dorsal horn. The finding provides anatomical substrates for roles of SP in nociception and for functional interactions of SP with ENK and GABA. Ectopic SP-IR fibers innervated the white matter of the CNS of transgenic mice where NGF was abnormally-produced.

RÉSUMÉ

Ces études avaient comme objectif l'investigation de l'innervation de tissus du système nerveux central par des fibres immunoréactives pour la substance P (SP), en utilisant deux modèles expérimentaux. Avec le premier modèle, nous avons examiné, sur le corne dorsal de la moelle épinière du chat, la distribution de terminaux axonaux immunoréactifs pour la SP qui étaient apposés à des neurones appartenant à trois types fonctionnels, et les interactions de ces terminaux-là avec le peptide alternatif du gène de la calcitonine (CGRP) et l'encéphaline (ENK). On a utilisé une combinaison d'enregistrement electrophysiologique intracellulaire, suivi d'injection de peroxydase de raifort, et d'immunohistochimie ultrastructurelle. On a observé, en plus de boutons axonaux réactifs uniquement pour la SP, d'autres qui étaient immunoreactifs pour la SP et la CGRP et aussi pour la SP et l'ENK, et qui établissaient des synapses avec des neurones nociceptifs. Du point de vue quantitatif, les cellules nociceptives recevaient significativement plus d'appositions de boutons immunoreactifs pour la SP, pour les SP+CGRP et pour les SP+ENK, que les neurones non-nociceptifs. Cependant, les cellules non-nociceptives étaient rarement innervées par des boutons immunoréactifs pour la SP, et pour les SP+CGRP ou SP+ENK. En contrepartie, ces cellules non-nociceptives recevaient un nombre considérable d'appositions de la part de boutons immunoréactifs uniquement pour l'ENK. Les boutons axonaux qui étaient immunoréactifs simultanément pour la SP et la CGRP ont été considérés comme appartenant à des afférents sensoriels primaires. La majorité des cellules nociceptives étudiées étaient immunoréactives pour l'ENK. Au contraire, les neurones non-nociceptifs n'étaient jamais immunoréactifs pour l'ENK. Nous avons aussi étudié les interactions entre la SP et l'acide

γ-aminobutyrique (GABA) dans la région superficielle du corne dorsal de la moelle épinière du chat et du rat. Nous avons détecté pour la première fois dans la littérature une co-localisation de SP et GABA dans des boutons axonaux de la moelle du chat, mais qui n'existait pas chez le rat.

En ce qui concerne les recherches avec le deuxième modèle expérimental, nous avons étudié avec immunohistochimie l'innervation, par des fibres immunoréactives pour la SP, de la substance blanche du système nerveux central de souris transgéniques. Ces souris synthétisaient du facteur de croissance nerveuse (NGF) dans des oligodendrocytes producteurs de myéline, sous le contrôle d'un promoteur de la protéine basique de la myéline (MBP). Nous avons observé des fibres immunoréactives pour la SP dans la substance blanche du système nerveux central de ces souris transgéniques et aussi des contrôles, du jour de naissance jusqu'à l'âge de 2 jours. Cependant, à partir de l'âge de 5 jours, ces fibres immunoréactives pour la SP augmentaient d'une façon remarquable en nombre et épaisseur chez les souris transgéniques, pour devenir de vraies fibres ectopiques. Chez les contrôles, ces fibres devenaient rares pour finalement disparaître. Ces fibres ectopiques des souris transgéniques persistaient pendant toute la vie adulte des souris. Ces fibres ectopiques immunoréactives pour la SP disparaissaient, cependant, après injection de capsaicine. Ce résultat indique que ces fibres ont une origine sensorielle primaire.

En conclusion, des fibres immunoréactives pour la SP innervaient d'une façon spécifique les neurones nociceptifs. En plus, dans quelques terminaux, cette immunoréactivité pour la SP était co-localisé avec celles pour la CGRP, l'ENK ou le GABA chez le chat. Ces résultats fournissent une base anatomique pour la participation de la SP dans les mécanismes nociceptifs et pour les interactions fonctionnelles entre la SP et l'ENK,

et la SP et le GABA. Des fibres ectopiques immunoréactives pour la SP innervaient la substance blanche du système nerveux central de souris transgéniques qui avaient une production ectopique de NGF par des oligodendrocytes.

TABLE OF CONTENTS

INDEX OF FIGURES

INDEX OF TABLES

ABBREVIATIONS

ABC Avidin-Biotin Complex
CGRP Calcitonin Gene-Related Peptide
DAB 3,3'-Diaminobenzidine Tetrahydrochloride
DRG dorsal root ganglion
EM electron microscopy
ENK Enkephalin
GABA γ-Aminobutyric Acid
HRP horseradish peroxidase
IR immunoreactive
LM light microscopy
MBP myelin basis protein
mg milligram
ml millilitre
NK-1 receptor neurokinin-1 receptor
NGF Nerve Growth Factor
PB Phosphate Buffer
PBS Phosphate Buffered Saline
PBS+T phosphate buffered saline containing 0.2% triton-100
POMC proopiomelanocortin
SP substance P

ACKNOWLEDGEMENT

First of all, I wish to express my sincere gratitude to the Faculty of Medicine, McGill University, for the award of the Special Chinese Studentship (2/1992-2/1994) and Internal Studentship (7/1994-7/1995) to support my graduate studies.

Throughout my three and half years of graduate studies in the Dept. of Pharmacology and Therapeutics, I was fortunate and privileged to interact with many professors, supporting staff members and fellow students. All of them helped me, directly or indirectly, to complete this thesis. I would like to take this opportunity to thank them:

I am grateful to my thesis supervisor, Dr. Alfredo Ribeiro-da-Silva for his encouragement and advice throughout the course of my research. I especially thank him for enriching my expertise in electron microscopic immunocytochemistry and leading me to the 'details' of the dorsal horn. I appreciate his helpful comments and suggestions in editing my manuscripts. I wish to express my great respect to him for his tolerance, generosity and understanding during these trying years. I derived great benefit from his skilled computer training, and I am particularly indebted to him for solving my many computer problems. I also thank him for translating the English abstract of this thesis into the French resume.

I express my thanks to Dr. A. Claudio Cuello for his encouragement and advice throughout the course of my study in his lab, and also for his financial support during my first two and half years. I especially thank him for providing an excellent academic environment in the department and his lab within which to work. I am grateful to him for allowing me to use the facilities in his lab. I appreciate his helpful comments in reading my several manuscripts.

I express my deep gratitude to my advisor Dr. Barbara Hales for always making time for me when I needed to talk, despite her extremely busy time schedule. I greatly appreciate her understanding, support and encouragement over these past trying years. Her attitude toward principle and people will be a model for me all my life. I am also indebted to her for helping me with my presentations, in which I was deeply impressed by her sound scientific judgment and insight, and extensive experience in training students. I also wish to thank her for helpful comments in reading one of my manuscripts, the general introduction and the final discussion of this thesis, and for her excellent skills in correcting my English. I was so fortunate to have her as my advisor.

I wish to thank Dr. Brian Collier for offering me a chance to discuss science with him. I was impressed by his kindness and humour. I am also grateful for his helpful comments and correction of my English when reading one of my manuscripts.

I wish to thank Dr. Rader Capek for his patience with me when I need help over the

years. His kindness and seriousness impressed me very much.

I wish to thank Dr. Paul B.S. Clarke for helpful discussions on the statistical analysis of my data, and for the loan of his handbook on the "SYSTAT" program.

I wish to thank Dr. Guillermina Almazan for helpful discussions on some of my data about oligodendrocytes.

I am most grateful to the excellent graduate courses offered to me by the professors in Dept. of Pharmacology and Therapeutics. Their lectures enlightened my thought and cultivated me to think independently and critically. Special appreciation go to: Dr. Clarke, Dr. Albert, Dr.Capek, Dr. Esplin, Dr. Hales, Dr.Quik, Dr.Collier, Dr. Robaire, Dr. Varma, Dr.Almazan, Dr. Trassler, Dr.Szyf, Dr.Saragovi and Dr.Maysinger.

I express my gratitude to Mrs. Marie Ballack for her excellent technical assistance in the EM preparation needed for this thesis, especially for her painstaking cutting of the ultrathin sections and post-embedding immunogold staining.

I would like to thank Mr.Alan Forster for his excellent photographic assistance during the course of my research, and for his patience with me when I asked for more demanding help.

I would like to thank Mr.Guillermo Besaccia and Mr.Mike Shen for their help in image analysis.

I wish to thank Marc Pinard for editing French Resume of this thesis.

My deepest thanks are extended to some special people in Dr. Cuello's lab, who make it a most pleasant environment to work in:

Mr. Sylvain Côté: for his help in preparing stock solutions and reagents in experiments, his kindness and expertise in solving problems with various facilities, and for his funny jokes, which usually made a stressful lab environment more relaxing.

Dr.Lorella Garofalo, Dr.Bonald Figueiredo de Cavalcante, Dr.Malgorzata Skup, Dr.Linsen Hu, Dr.Daochao Huang, Ms.Sue Grant: for their kindness and help with my presentations, for their encouraging words and thoughtful discussion in science.

Thanks are also due to the wonderful office staff for their support:

Mrs. Diane Plant: Over the years, Diane has helped me enormously with my various problems, ranging from the renewal of my student visa to providing me with a desk and a cabinet in the student editing room in my last days here. The depth of her help can be

measured by the size of my personal file in her office. I was greatly comforted by her kindness and benefited from her efficiency in dealing with various administrative problems.

Anne and Dawn: I thank them for correcting my English when I was preparing studentship applications and for their encouraging words during the course of my graduate studies.

Catherine and Pam: Thanks will go to Catherine and Pam for their patience in responding to my various questions about graduate studies and thesis preparation at McGill.

Mr.Sid Parkinson and Marsha: I wish to thank Mr.Sid Parkinson for his excellent editorial assistance in my several manuscripts and my thesis. I also thank Marsha for her editorial assistance in one of my manuscripts.

My deepest love and sincerest thanks go to my dear husband Aijia Chen and my lovely daughter Fan Chen, for their unbelievable support and understanding over those extremely hard years of separation. Without their selfless love, I could not have finished my Ph.D studies.

Finally, this thesis would not have been possible without my parents, whose selfless love and openness towards learning has been a constant source of strength to me over the years. That I have come this far is largely due to the example that they have set for me.

This thesis is humbly dedicated to my husband , daughter and parents.

STATEMENT OF AUTHORSHIP

The following is reproduced in full from the "Guidelines Concerning Thesis Preparation":

Manuscripts and authorship
Candidates have the option, **subject to the approval of their Department,** of including, as part of their thesis, copies of the text of a paper (s) submitted for publication, or the clearly-duplicated text of a published paper (s), provided that these copies are bound as an integral part of the thesis.
- If this option is chosen, **Connecting text, providing logical bridges between the different papers, are mandatory.**
- The thesis must still conform to all other requirements of the "Guidelines Concerning Thesis Preparation" and should be in a literary form that is more than a mere collection of manuscripts published or to be published. **The thesis must include, as separate chapters or sections:** (1) a Table of Contents, (2) a general abstract in English and French, (3) an introduction which clearly states the rationale and objectives of the study, (4) a comprehensive general review of the background literature to the subject of the thesis, when this review is appropriate, and (5) a final overall conclusion and/or summary.
- Additional material (procedural and design data, as well as descriptions of equipment used) must be provided where appropriate and in sufficient detail (eg. in appendices) to allow a clear and precise judgement to be made of the importance and originality of the research in the thesis.

- In the case of manuscripts co-authored by the candidate and others, **the candidate is required to make an explicit statement in the thesis of who contributed to such work and to what extent;** supervisors must attest to the accuracy of such claims at the Ph.D Oral Defence. Since the task of the examiners is made more difficult in these cases, it is in the candidate's interest to make perfectly clear the responsibilities of the different authors of co-authored papers.

Paper 1. Quantitative analysis of substance P immunoreactive boutons on physiologically characterized dorsal horn neurons in the cat lumbar spinal cord.
Weiya Ma, A.Ribeiro-da-Silva, Y.De Koninck, V.Radhakrishnan, J.L.Henry, A.C.Cuello
J. Comp. Neurol. in press.

Paper 2. Substance P and enkephalin immunoreactivities in axonal boutons presynaptic to physiological identified dorsal horn neurons.
An ultrastructural multiple-labelling study in the cat
Weiya Ma, A.Ribeiro-da-Silva, Y.De Koninck, V.Radhakrishnan, J.L.Henry and A.C.Cuello

submitted.

Paper 3. Substance P- and GABA-like immunoreactivities are co-localized in axonal varicosities in the superficial laminae of cat but not rat spinal cord.
Weiya Ma and A. Ribeiro-da-Silva
Brain Res. 692:99-110, 1995

Paper 4. Ectopic substance P and calcitonin gene-related peptide immunoreactive fibers in the spinal cord of transgenic mice over-expressing nerve growth factor.
Weiya Ma, A. Ribeiro-da-Silva, G. Noel, J.-P. Julien and A.C. Cuello
Eur. J. Neurosci. 7:2021-2035, 1995

Paper 5. Topographic and time course studies of ectopic substance P immunoreactive fibers in the CNS of transgenic mice which over-express nerve growth factor in myelinating oligodendrocytes.
Weiya Ma, A. Ribeiro-da-Silva, J.-P. Julien and A. C. Cuello
submitted

This thesis was generated based on the data described in the 5 papers listed above. The following statement describes the contributions of the each of the co-author.

Dr. A.Ribeiro-da-Silva: Principal investigator on all the projects and the main intellectual influence for the papers reported here. He also did quantification of Paper II.

Dr. A.C. Cuello: Full collaborator on all the projects and the person responsible for the conception of the transgenic mouse model.

Dr. J.L.Henry: Principal investigator on the projects involving electrophysiological studies. He and his assistants carried out the electrophysiological recordings and performed the intracellular injection of HRP into the dorsal horn neurons.

Dr.Y.De Koninck: At the time, a graduate student in Dr.Henry's lab. He conducted the electrophysiological recordings and intracellular injections of HRP into all dorsal horn neurons used in papers 1 and 2, except for neuron 339-1. He assisted in the editing of paper 1.

Dr.V.Radhakrishnan: A postdoctoral fellow in Dr. Henry's lab. He conducted the electrophysiological recording and intracellular injection of HRP into neuron 339-1, and assisted with editing of paper 1.

Drs. J.-P. Julien and G. Noel: Principal investigators of the transgenic mouse project. In collaboration with them, the MBP/NGF construct and the transgenic mice were produced, and the expression of the transgene in mice was studied.

Dr. Weiya Ma: I conducted all the immunocytochemical staining and the quantification of all papers (except quantification of Paper II) and performed all the surgical procedures except those in cats. I wrote the first version of all manuscripts included in this thesis which were finalized interacting with the other authors.

CHAPTER I

General introduction

Pain is an unpleasant sensation which occurs following the activation of special receptors, in the skin and deeper structures of the body. These "pain" receptors or nociceptors can be activated by noxious mechanical, thermal and chemical stimuli applied to the skin, muscles, joints and viscerae. There are two main types of nociceptors, myelinated nociceptors (Aδ nociceptors) and unmyelinated nociceptors (C-polymodal nociceptors), which occur respectively at the peripheral endings of thinly myelinated fibers (Aδ) and unmyelinated fibers (C). The nociceptive information originating from the peripheral tissues is conveyed by the two types of nociceptive fibers to the spinal and medullary dorsal horn, where it is modulated by both excitatory and inhibitory neurotransmitters or neuromodulators before being relayed to higher levels of the central nervous system (CNS) [for review, see (Willis et al., 1995)]. Substance P (SP), which occurs in Aδ and C fibers, has been considered a mediator of nociception in the spinal and medullary dorsal horns [for review, see (Henry, 1994)]. The detailed knowledge of the termination in the CNS of SP containing primary afferent fibers and of the synaptic interactions of these fibers with other systems under normal and abnormal experimental conditions is very important for the understanding of nociceptive mechanisms. This thesis project was designed to address the above issue in two experimental models. In the first experimental paradigm, the SP sensory fiber innervation of physiologically characterized dorsal horn neurons was investigated in the cat spinal cord. In the second experimental paradigm, the SP sensory fiber innervation of the white matter of the CNS of a transgenic mouse model which over-expresses nerve growth factor (NGF) was studied.

This general introduction therefore reviews aspects of the anatomy of the dorsal horn

related to nociception, the possible role of SP in nociception, the interaction of SP with calcitonin gene-related peptide (CGRP), enkephalin (ENK) and γ-aminobutynic acid (GABA), as well as the interaction of SP containing sensory neurons with NGF. Based on this background information, the objective and rationale of the current thesis project were formulated.

I. **Anatomical basis of nociceptive mechanisms in the dorsal horn**

The cat dorsal horn was divided by Rexed (1952; 1954) into six parallel laminae, on the basis of their cytoarchitecture. More recently, this classification has been extended to other mammalian species, including the rat (Molander et al., 1984). The transmission and modulation of nociception occur mostly in the superficial layers of the dorsal horn, particularly in lamina II of Rexed. Here, I will focus on the laminae of the dorsal horn which are thought to be involved in nociception. For a detailed description of the structure of the dorsal horn see Willis and Coggeshall (1991).

A. *Lamina I*

Lamina I (marginal zone) represents the dorsal-most part of the spinal grey matter. Morphologically, the neurons of lamina I were classically divided into large marginal cells and smaller neurons (Ramón y Cajal, 1909; Scheibel and Scheibel, 1968; Scheibel and Scheibel, 1969). More recently, several morphological types of cells were described in the cat (Gobel, 1978a), rat (Lima and Coimbra, 1986) and monkey (Beal et al., 1981), but these newer categories have yet to receive general agreement. Lamina I is composed primarily of

local interneurons (Golgi type II or intrinsic neurons) (Light et al., 1979; Cervero et al., 1979), but certain populations of neurons in lamina I are cells (Golgi type I or relay neurons) which project their axons to higher regions of the CNS (Lima and Coimbra, 1988; Lima and Coimbra, 1989; Lima and Coimbra, 1990; Lima et al., 1991). Thinly myelinated fibers (Aδ) are considered to provide most of the primary afferents to lamina I, although this lamina also receives a considerable number of unmyelinated fibers (C) (Willis and Coggeshall, 1991).

Functionally, lamina I cells were shown to respond to both noxious and non-noxious thermal and mechanical stimuli (Cervero et al., 1976; Light et al., 1979; Brown et al., 1981). These cells were characterized as nociceptive specific, wide dynamic range and non-nociceptive neurons based on their responses to noxious and non-noxious stimuli. Nociceptive specific neurons respond only to noxious stimuli; wide dynamic range neurons respond to both noxious and non-noxious stimuli; non-nociceptive neurons respond only to innocuous stimuli. Sixty-three percent of lamina I cells are nociceptive (Light, 1992).

B. *Lamina II*

Lamina II is also called the substantia gelatinosa of Rolando (Cervero and Iggo, 1980), for its gelatinous appearance due to the concentration of small neurons and the lack of myelinated fibers. Lamina II is further subdivided into outer lamina II (lamina IIo) and the inner lamina II (lamina IIi).

1. Cell types

Ramón y Cajal (1909) classified lamina II cells into central cells and limiting cells based on their morphological characteristics. In cat, the central cells and the limiting cells

were named as islet cells and stalked cells, respectively, by Gobel (1975; 1978b). The stalked, or limiting cells, occur along the lamina I-II border, while the islet, or central cells, are extensively distributed throughout the lamina. The dendritic trees of the stalked cells were characterized as cone shaped, radiating ventrally in laminae II from the cell bodies (Gobel, 1978b; Brown et al., 1981). Following electrophysiological characterization and intracellular horseradish peroxidase (HRP) injection, the stalked cells were thought to be either nociceptive specific or wide dynamic range neurons (Bennett et al., 1980). The dendritic trees of the islet cells was described as extending through the thickness of lamina II in a rostrocaudal orientation (Brown et al., 1981). The islet cells were reported either as nociceptive specific neurons or as mechanoreceptive neurons (Bennett et al., 1980).

According to Light (1992), 70% of cells in outer lamina II are nociceptive, receiving inputs from mechanical and polymodal nociceptors.

2. Glomeruli

The most striking feature of lamina II at the ultrastructural level is the existence of synaptic glomeruli. A glomerulus consists of a central terminal, which is in synaptic contact with several peripheral dendrites and axonal terminals. The central terminals, or central boutons (C), have been confirmed as representing terminals of primary sensory fibers (Duncan and Morales, 1978; Coimbra et al., 1984; Murray and Goldberger, 1986).

Two types of synaptic glomeruli were described in lamina II of the rat (Ribeiro-da-Silva and Coimbra, 1982; Ribeiro-da-Silva, 1995). Type I: represents the most commonly observed glomerular type. The central boutons (C_I) in this glomerular type are

relatively small and scalloped in shape, containing compact synaptic vesicles and very few mitochondria. The axoplasm is relatively electron dense. The central boutons likely represent the endings of unmyelinated nociceptive fibers, since they are capsaicin sensitive (Ribeiro-da-Silva and Coimbra, 1984). In rat, this type of glomerulus can be further divided into subtypes Ia and Ib (Ribeiro-da-Silva, 1995).

Type II: The central boutons (C_{II}) of this glomerular type are usually larger, of less scalloped contour, electron lucent and rich in mitochondria. Type II synaptic glomeruli can be further divided into subtype IIa, devoid of neurofilament bundles in the C bouton, and IIb, rich in neurofilament bundles in the C bouton. Based on the glomerular morphology of physiologically characterized fibers in the cat [for a review, see (Maxwell and Réthelyi, 1987)], the central boutons of type IIa glomeruli might be the termination of Aδ D-hair fibers, and those of type IIb, the termination of thicker fibers.

C. *Laminae III, IV and V*

Compared with lamina IV, lamina III is composed of relatively homogeneous and smaller cells. Lamina IV cells are heterogeneous in cell size, with the presence of some very large cells. The neurons in lamina III are mostly non-nociceptive neurons (Maxwell et al., 1983), but neurons which receive both innocuous and nociceptive inputs are also found (Light, 1992). The larger diameter (Aβ) sensory fibers, which do not convey nociceptive information, terminate mainly in laminae III-IV of the dorsal horn (Brown et al., 1981; Brown, 1982). The cells in lamina V are even more heterogeneous in size than those in lamina IV. Some neurons in lamina V have been shown to be nociceptive (De Koninck et

al., 1992). Lamina V also receives some high threshold mechanoreceptors (Light and Perl, 1979a).

II. Substance P and nociception

Substance P (SP) is a member of the neurokinin (tachykinin) family, which also includes neurokinin A (substance K) and neurokinin B. SP and neurokinin A share a single gene and are the products of alternative RNA splicing and/or post-translational processing. Therefore, they are closely related in structure and function. The functions of neurokinins in the mammalian CNS have been well described [for a review, see (Otsuka and Yoshioka, 1993)].

Unlike neurokinin A and neurokinin B which were found and characterized only recently (Nawa et al., 1983), SP was discovered in equine brain and intestine in 1931 by von Euler and Gaddum (1931), where it was shown to cause hypotension and smooth muscle contraction. In 1936, its peptide nature began to be known. However, it was not until 1971 that SP was purified and its undecapeptide sequence was revealed by Leeman and colleagues (Chang et al., 1971). Since then, the anatomical distribution and physiological roles of SP have been extensively studied. SP is widely distributed in the central and peripheral nervous systems and its physiological and pharmacological roles are diverse. Of these physiological roles, its role as a putative "pain" neurotransmitter in the dorsal horn has drawn great attention over the past two decades [for reviews, see (Otsuka and Yanagisawa, 1987; Otsuka and Yanagisawa, 1990)].

A. *Morphological evidence for a role of SP in nociception*

1. SP immunoreactivity in the dorsal horn

Immunocytochemically, SP was detected in high concentration in small diameter fibers in laminae I and II (Hökfelt et al., 1975a; Hökfelt et al., 1976; Cuello et al., 1978) and also in lamina V (Ruda et al., 1986). Unilateral multiple dorsal rhizotomies caused a marked reduction in SP immunoreactivity in these regions (Hökfelt et al., 1975a; Jessell et al., 1979), suggesting the presence of SP in primary afferent terminals. SP immunoreactivity was also found in neurons of laminae I and II (Hunt et al., 1981; Ljungdahl et al., 1978) and in descending pathways from the brainstem (Gilbert et al., 1982; Hökfelt et al., 1978). Ultrastructural studies have shown that SP immunoreactive (IR) terminals are presynaptic to dendrites in the superficial dorsal horn (Barber et al., 1979; Chan-Palay and Palay, 1977; Priestley et al., 1982b; DiFiglia et al., 1982; Ribeiro-da-Silva et al., 1989). In axonal terminals, SP immunoreactivity was mainly associated with large dense core vesicles (Barber et al., 1979; Priestley et al., 1982b; Ribeiro-da-Silva et al., 1989), particularly when using post-embedding immunogold protocols (Merighi et al., 1989).

2. SP immunoreactivity in primary sensory neurons

Using immunocytochemistry, SP immunoreactivity was first shown to be present in small size dorsal root ganglion (DRG) cells and in small diameter axons in the superficial dorsal horn by Hölkfelt and co-workers (Hökfelt et al., 1975a; Hökfelt et al., 1975b). A study (Tuchscherer and Seybold, 1985) showed that in the rat DRG, 6-20% cells were SP immunoreactive, most of which were of small size and only a few being of medium size. An

in situ hybridization study showed that approximately 20-30% of DRG cells in the rat and rabbit expressed preprotachykinin A mRNA (Boehmer et al., 1989). The mismatch of mRNA content and protein content suggests a fast SP turnover in small size DRG cells. Using a combination of electrophysiological recording and immunocytochemistry, SP immunoreactivity was observed in 50% of C-fiber neurons, in 20% of Aδ-fiber neurons, and in none of the Aα/β-neurons (McCarthy and Lawson, 1989). Subcutaneous administration of capsaicin to neonatal rats caused a selective degeneration of primary afferent C-fibers (Pignatelli et al., 1989), and concurrent depletion of SP from the DRG and dorsal horn (Nagy et al., 1981).

3. Distribution of SP receptors in the dorsal horn

SP, neurokinin A and neurokinin B are the preferred agonists for NK-1, NK-2 and NK-3 receptors, respectively, but these naturally occurring neurokinins are not completely selective for their respective receptor subtypes (Regoli et al., 1988). Using radioautography, high concentrations of SP receptor binding sites were shown in the superficial layers of the dorsal horn, particularly in laminae I and II (Quirion et al., 1983; Mantyh et al., 1989; Dam et al., 1990; Yashpal et al., 1990; Gouardères et al., 1993). More recent immunocytochemical studies provided results in apparent contradiction with the binding studies. A study showed that neurons with SP receptor immunoreactivity were located in lamina I and III of the trigeminal caudalis nucleus and in lamina I of the spinal cord (Nakaya et al., 1994). Similar results were obtained using a monoclonal antibody raised against the C-terminal of the NK-1 receptor, which revealed that most neurons possessing NK-1 receptor immunoreactivity were

located in lamina I and in lamina III-IV, and only very few were observed in lamina II (Bleazard et al., 1994). At the electron microscopy (EM) level, only 33% of SP-IR terminals were presynaptic to neurons expressing NK-1 receptors, indicating a mismatch between SP-IR terminals and SP receptors. In fact, the above studies favor the hypothesis that SP may be released at a distance from the postsynaptic targets expressing NK-1 receptors (Liu et al., 1994).

B. *SP and capsaicin*

Capsaicin is a pungent ingredient of certain hot peppers, which specifically interacts with small size primary sensory neurons. The detailed description of the effects of capsaicin on sensory neurons can be found in reviews of Holzer (1988; 1991) and Dray (1992). The effects of low doses of capsaicin are different quantitatively and qualitatively from those of high doses. At low doses (in the μg/kg body weight range), capsaicin exerts a powerful excitatory effect on peripheral sensory nerve terminals, and this effect is apparently confined to unmyelinated fibers (Szolcsanyi, 1977; Fitzgerald, 1983; Kenins, 1982). However, the inital excitation is soon followed by desensitization to chemical stimuli and by a blockade of nerve conduction (Fitzgerald, 1983). Systemic administration of capsaicin at high doses (in the mg/kg range) has a marked neurotoxic effect on a population of sensory neurons, mainly of small size. The extent of neuronal damage depends on the dosage, route of administration, animal species and age of the animals (Holzer, 1988). Administration of capsaicin to neonatal rats caused selective degeneration of up to 90% of the unmyelinated afferent fibers (Jancsó et al., 1977; Nagy et al., 1981; Nagy et al., 1983; Scadding, 1980).

Furthermore, SP and other neuropeptides were markedly depleted in the dorsal horn and the trigeminal nucleus (Cuello et al., 1981; Helke et al., 1981; Jancsó et al., 1981) and the pain threshold to noxious stimuli was increased (Holzer et al., 1979; Nagy et al., 1980; Nagy and Van der Kooy, 1983). Capsaicin treatment of adult rats results in less pronounced effects than in neonatal rats (Buck et al., 1982; Hayes et al., 1981; Jancsó et al., 1985; Jessell et al., 1978). Capsaicin induced analgesia is not only due to the depletion of SP from the unmyelinated fibers, but also due to its direct effects on the nociceptive neurons (Burks et al., 1985).

C. *Functional evidence for a role of SP in nociception*

1. Behavioral studies

Intrathecal SP injection in mice elicited tail-toward scratching and biting, behaviours suggesting pain perception (Hylden and Wilcox, 1981; Piercey et al., 1981). Neurokinin antagonists (Akerman et al., 1982) or anti-SP antibodies (Nance et al., 1987) administrated in the same route produced an analgesic effect. Intrathecal injection of SP in rats also facilitated a spinal nociceptive reflex (Yashpal and Henry, 1983; Yashpal and Henry, 1984; Cridland and Henry, 1988a) with a transient decrease in reaction time to tail withdrawal from a noxious radiant heat stimulus. Intrathecally injected SP increased the magnitude of the spinal flexion reflex elicited by noxious mechanical or thermal stimuli in the rat, suggesting that SP might be released from C-polymodal nociceptors (Wiesenfeld-Hallin, 1986a). More interestingly, familial dysautonomia patients, in which SP is depleted from the substantia gelatinosa of the spinal cord, exhibited severely diminished pain sensitivity (Pearson et al.,

1982).

2. Excitation of dorsal horn nociceptive neurons by SP

Electrophysiologically, SP was shown to excite specifically the dorsal horn neurons that respond to noxious cutaneous stimuli (Henry, 1976). A slow excitatory post-synaptic potential (EPSP) recorded from cat dorsal horn neurons following noxious cutaneous stimulation was blocked by intravenous injection of a SP receptor antagonist (Radhakrishnan and Henry, 1991; De Koninck and Henry, 1991). Furthermore, the dorsal horn neurons with stronger nociceptive input were demonstrated to be abundantly innervated by SP-IR varicosities in the cat spinal cord (De Koninck et al., 1992).

However, the fast component of the EPSP was likely to be mediated by a fast-acting excitatory amino acid, such as glutamate or aspartate (Yoshimura and Jessell, 1989), since it is not blocked by non-peptide SP receptor antagonists (De Koninck and Henry, 1991). Experimental evidence indicated that most, if not all, of the primary afferent terminals probably release fast-acting transmitters (Jessell et al., 1986; Yoshimura and Jessell, 1989). Morphologically, glutamate was shown to co-localize with SP in most of SP-IR axonal terminals in the dorsal horn (Battaglia and Rustioni, 1988; De Biasi and Rustioni, 1988; Merighi et al., 1991) and in part with SP and CGRP in DRG cells (Merighi et al., 1991; De Biasi and Rustioni, 1988).

3. Release of SP in the dorsal horn

Following repetitive electrical stimulation of the dorsal roots, an increased calcium-

dependent SP release from the isolated spinal cord of the newborn rat was detected by radioimmunoassay (Otsuka and Konishi, 1976). Capsaicin treatment also increased SP release from the rat spinal cord (Gamse et al., 1979; Theriault et al., 1979).

Release of SP from the spinal cord *in situ* was also detected by various techniques in response to peripheral noxious stimulation, and it was further shown that the release occurred particularly in the superficial dorsal horn. An increased SP release was found in the superfusate from the cat spinal cord after an electrical stimulation of peripheral nerves at a C-fiber, but not an Aδ-fiber, frequency (Yaksh et al., 1980). Furthermore, SP release upon C-fiber stimulation in the dorsal horn was also shown by microdialysis (Brodin et al., 1987). Increased SP release in the substantia gelatinosa of the dorsal horn following noxious mechanical, thermal, and chemical, but not innocuous, stimuli was detected by microelectrode probes coated with anti-SP antibodies (Duggan et al., 1987; Duggan et al., 1988).

III. **Interaction of SP and CGRP**

Calcitonin gene-related peptide (CGRP) is a 37 amino acid-long peptide generated from the calcitonin gene by alternative RNA processing, and is widely distributed in the nervous system (Rosenfeld et al., 1983; Amara et al., 1985). A recent review provided a detailed description of this neuropeptide in the central and peripheral nervous systems (Hökfelt et al., 1992).

A. *Morphological evidence of SP and CGRP interactions*

1. Co-localization of SP and CGRP in primary sensory neurons

CGRP immunoreactive neurons represent the largest peptide-containing population so far observed in the dorsal root and trigeminal ganglia, where they represent more than 50% of all neurons (Gibson et al., 1984). The sizes of CGRP neurons range from small to large, although most of the cells belong to the small size group (Amara et al., 1985). CGRP neurons have a conduction velocity from 0.5 to 28.6 m/sec (McCarthy and Lawson, 1990). A striking feature of CGRP immunoreactivity in sensory systems is its co-localization with immunoreactivities for SP and other neuropeptides. Studies have shown that many of the CGRP-IR neurons also contain SP immunoreactivity (Gibson et al., 1984; Wiesenfeld-Hallin et al., 1984; Gibbins et al., 1985; Lee et al., 1985b; Skofitsch and Jacobowitz, 1985). These studies have led to the assumption that all SP-IR neurons co-localize CGRP immunoreactivity. Subsequently CGRP immunoreactivity was found to co-localize with immunoreactivity for other neuropeptides, such as somatostatin and galanin (Ju et al., 1987; Tuchscherer and Seybold, 1989).

2. Co-localization of SP and CGRP in the dorsal horn

In the superficial laminae of the dorsal horn, CGRP immunoreactivity was detected in high concentration (Kaway et al., 1985; Lee et al., 1985a; Traub et al., 1990). At the ultrastructural level, CGRP immunoreactivity was demonstrated to co-exist with SP immunoreactivity in the same secretory, large dense core vesicles in peripheral and central nerve terminals of primary sensory neurons and in their cell bodies in the dorsal root ganglia (Gulbenkian et al., 1986; Merighi et al., 1988; Merighi et al., 1989; Plenderleith et al., 1990). CGRP immunoreactivity in the dorsal horn originates entirely from the dorsal root ganglia,

a finding which was demonstrated by the almost complete depletion of CGRP immunoreactivity after dorsal rhizotomy (Traub et al., 1989; Chung et al., 1988) and confirmed by the lack of detection of CGRP mRNA in the dorsal horn by *in situ* hybridization (Réthelyi et al., 1989). Hence, it is reasonable to use the co-localization with CGRP immunoreactivity in the dorsal horn as a marker to indicate the primary sensory origin of boutons immunoreactive for peptides such as SP and somatostatin.

B. *Functional evidence of interaction of SP and CGRP in nociception*

The functional role of CGRP in primary sensory neurons is unclear. It is observed that CGRP can excite the dorsal horn neurons (Wiesenfeld-Hallin, 1986b; Woolf and Wiesenfeld-Hallin, 1986; Cridland and Henry, 1988c; Ryu et al., 1988; Morton and Hutchison, 1989; Miletic and Tan, 1988; Kawamura et al., 1989). In behavioral tests, CGRP markedly enhances a scratching and biting behaviour induced by the intrathecal administration of SP (Wiesenfeld-Hallin et al., 1984). Furthermore, CGRP and SP modulate synergistically the nociceptive flexor reflex (Woolf and Wiesenfeld-Hallin, 1986).

C. *Possible mechanisms of CGRP potentiation of SP elicited nociception*

Two possible mechanisms have been suggested for the CGRP potentiation of the nociceptive effects of SP in behavioral tests. The first one is an inhibitory effect of CGRP on an endopeptidase involved in the inactivation of SP (Le Greves et al., 1985; Le Greves et al., 1989). Thus, CGRP would prolong the action of SP by preventing its degradation. The second mechanism involves the capability of CGRP to potentiate the release of SP and fast-

acting excitatory amino acids in the dorsal horn. In agreement with this, CGRP has been shown to enhance the release of SP, glutamate and aspartate from the dorsal horn *in vitro* (Oku et al., 1987; Kangrga and Randic, 1990; Kangrga et al., 1990), due to its ability to increase Ca^{2+} in the sensory afferent terminals in the dorsal horn (Oku et al., 1988). The released SP in turn increases the release of glutamate and aspartate in the dorsal horn (Smullin et al., 1990) and may enhance glutamate-mediated excitatory transmission in the dorsal horn (Randic et al., 1990).

IV. **Interaction of SP and enkephalin**

A. *Distribution of ENK immunoreactivity in the dorsal horn*

Enkephalin (ENK) is an endogenous opioid receptor ligand. Anatomically, both ENK receptor binding sites (Fields et al., 1980; LaMotte et al., 1976) and Met- and Leu-ENK immunoreactivities have been detected in axonal terminals (Hökfelt et al., 1977; Hunt et al., 1981) and cell bodies (Hunt et al., 1981; Glazer and Basbaum, 1983; Miller and Seybold, 1987; Bennett et al., 1982; Del Fiacco and Cuello, 1980) in the dorsal horn, particularly in laminae I and II. Some ENK-IR lamina II cells were identified as stalked cells and islet cells on the basis of their morphology (Bennett et al., 1982). The second region with high concentration of ENK immunoreactivity in the dorsal horn is lamina V (Ruda, 1982).

At the ultrastructural level, ENK-IR axonal terminals were found presynaptic to dendrites and occasionally to neuronal cell bodies (Hunt et al., 1980; Glazer and Basbaum, 1983). In the substantia gelatinosa of the cat spinal cord, some glomerular peripheral profiles with synaptic vesicles were ENK immunoreactive (Bennett et al., 1982; Glazer and

Basbaum, 1983) and in rat evidence that ENK-IR terminals are presynaptic to the central varicosities of glomeruli has been found (Ribeiro-da-Silva et al., 1991b; Ribeiro-da-Silva, 1995). ENK-IR and SP-IR axonal boutons were seen to be presynaptic, separately, to a common dendrite, and SP-IR central boutons in glomeruli were presynaptic to ENK-IR dendrites. However, no morphological evidence has been found for presynaptic interactions of ENK-IR varicosities on SP-IR boutons in rat (Cuello, 1983; Ribeiro-da-Silva et al., 1991b) and cat (Ribeiro-da-Silva et al., 1991a).

B. *Origins of ENK immunoreactivity in the dorsal horn*

ENK immunoreactivity in the dorsal horn has been shown to originate mainly from intrinsic dorsal horn neurons, since transection of the thoracic spinal cord results in a negligible loss of ENK immunoreactivity at lumbar levels (Seybold and Elde, 1982). ENK immunoreactivity in the dorsal horn was suggested to originate from primary sensory afferents, but it was never detected in a significant number of neurons in the dorsal root ganglia (Garry et al., 1989).

SP and ENK immunoreactivities were found to co-localize in a considerable number of dorsal horn neurons and axonal terminals in both rat and cat (Senba et al., 1988; Tashiro et al., 1987; Ribeiro-da-Silva et al., 1991b; Ribeiro-da-Silva et al., 1991a). Indeed, almost all SP-IR neurons in the dorsal horn co-localize ENK immunoreactivity and about 50% of ENK-IR neurons also contained SP immunoreactivity (Senba et al., 1988; Ribeiro-da-Silva et al., 1991b). Therefore, the axonal boutons co-localizing SP and ENK immunoreactivities can be considered as likely to be of intrinsic dorsal horn origin.

C. *Functional evidence of SP and ENK interactions in nociception*

1. Analgesic effects of opiates in nociception

Systemic injection of opiates into spinalized cats or opiate iontophoresis directly into the spinal cord selectively inhibit the response of dorsal horn neurons to peripheral noxious stimulation (LeBars et al., 1976; Zieglgansberger and Bayerl, 1976; Duggan et al., 1976; Duggan et al., 1977; Duggan et al., 1981; Randic and Miletic, 1978). Both δ and μ opiate receptors are believed to mediate the inhibitory actions of ENK on dorsal horn interneurons (Dickenson et al., 1986; Jeftinija, 1988).

2. SP induced ENK release in nociception

In behavioral studies, both the intrathecal administration of SP and noxious cutaneous stimulation in the rat elicit a transient decrease of reaction time in the tail-flick test (Yashpal and Henry, 1983; Cridland and Henry, 1988a). This decrease in reaction time is followed by a rebound overshoot, which can be blocked by naloxone (Yashpal and Henry, 1983), suggesting the activation of an opioid mechanism at the spinal level, due either to SP or to SP-induced activation of spinal nociceptive pathways. Biochemically, SP has been shown to stimulate the release of an endogenous opioid peptide at the spinal (Tang et al., 1983; Iadarola et al., 1986) and supraspinal levels (Naranjo et al., 1986). The involvement of SP receptors in triggering the release of ENK was suggested (Tang et al., 1983).

3. Inhibition of SP release in the dorsal horn by ENK

Opioid receptor binding sites in the substantia gelatinosa were reduced markedly

following dorsal rhizotomy (LaMotte et al., 1976). This finding suggests that a considerable number of opioid receptors is located presynaptically on primary sensory afferents. Biochemically, the release of SP in laminae I and II was induced by noxious stimuli or by high concentration of potassium (Duggan et al., 1987; Yaksh et al., 1980). Opiate analgesics were shown to inhibit SP release from the spinal cord and trigeminal nucleus (Jessell and Iversen, 1977; Yaksh et al., 1980). However, there is no available morphological evidence of ENK-IR axonal terminals presynaptic to SP-IR primary sensory afferents (see above). Thus, it has been hypothesized that endogenous opioid peptides released from the terminals of enkephalinergic interneurons might spread diffusely to exert both presynaptic inhibition on nociceptive afferent terminals and postsynaptic inhibition on dorsal horn neurons (Cuello, 1983; Iversen, 1986).

V. **Interaction of SP and GABA in nociception**

A. *Distribution of GABA immunoreactivity in the dorsal horn*

γ-Amino butyric acid (GABA) is a well established classical inhibitory neurotransmitter in the CNS. GABAergic neurons in the dorsal horn were detected using antibodies generated against GABA itself or the synthesizing enzyme glutamate decarboxylase (GAD). GABAergic neurons are widely distributed in the spinal cord. With respect to the dorsal horn, GABAergic neurons are particularly concentrated in laminae I to III (Magoul et al., 1987; Todd and McKenzie, 1989; Hunt et al., 1981; Barber et al., 1982; Todd and McKenzie, 1989). Both stalked (Barber et al., 1982) and islet cells (Barber et al., 1982; Todd and McKenzie, 1989) were observed to contain GAD or GABA

immunoreactivities. GABA immunoreactivity in the dorsal horn has two sources: intrinsic GABAergic interneurons in the dorsal horn, either from the same or adjacent segments (Carlton and Hayes, 1990), and descending fibres from the medullary raphe nuclei, where GABA has been found in serotonergic cell bodies that project to the spinal cord (Millhorn et al., 1987; Kachidian et al., 1991).

B. *Synaptic arrangements of GABAergic structures in the dorsal horn*

The synaptic arrangements in which GABA-IR elements participate are of particular interest because they provide an anatomical basis for presynaptic and postsynaptic inhibition mediated by GABA. GAD or GABA-IR terminals are presynaptic to the central boutons of glomeruli which are of primary sensory origin (Barber et al., 1978; Basbaum et al., 1986; Magoul et al., 1987; Todd and Lochhead, 1990; Bernardi et al., 1995). GABA-IR profiles have been found presynaptic to the terminals of functionally defined myelinated nociceptors in the monkey and cat spinal cord (Alvarez et al., 1992). These observations serve as morphological substrates for GABA inhibition through a presynaptic mechanism. GABA-IR terminals are also presynaptic to dendritic profiles, which are presumed to serve as postsynaptic inhibition. In addition, most GABA-IR cell bodies and dendrites are postsynaptic to primary sensory afferents (Basbaum et al., 1986; Carlton and Hayes, 1990; Bernardi et al., 1995).

C. *Interaction of SP and GABA*

Morphologically, there is little experimental evidence available as to the interactions

of SP-IR and GABAergic elements in the dorsal horn. A preliminary study using a post-embedding immunogold protocol claimed that GABA-IR axonal boutons were occasionally presynaptic to SP-IR axonal boutons, but no illustration was given (Merighi et al., 1989).

Functionally, bath application of SP was reported to induce a marked increase in the release of GABA from the isolated rat spinal cord (Sakuma et al., 1991). On the other hand, it was reported that the well-known analgesic effects of baclofen (a $GABA_B$ receptor agonist) are probably not mediated by a reduction of the release of SP or CGRP in the dorsal horn from central terminals of primary afferents, based on the results of an *in vivo* study using the antibody microprobe technique (Morton et al., 1992).

VI. **Interactions of SP and NGF**

NGF represents the prototype of a gene family of neurotrophins which are target-derived, retrogradely transported, structurally related and possess neurotrophic effects on certain neuronal populations of the nervous system. This neurotrophin family includes NGF, brain-derived neurotrophic factor (BDNF), neurotrophin-3 (NT-3), and neurotrophin-4/5 (NT-4/5) [for review, see (Ebendal, 1992)]. These neurotrophic factors are produced in small amounts in the target tissues and control the neuron survival and innervation of target tissues during development. Neurotrophic factors also have important functions in the adult nervous system.

Of all neurotrophins, NGF has been the most extensively studied. Its wide range of biological effects upon neural-crest derived sensory neurons and sympathetic neurons, and

the basal forebrain cholinergic neurons have been well characterized and documented [for reviews, see (Thoenen et al., 1987; Purves et al., 1988)]. In primary sensory systems, NGF has been found to interact specifically with a functional group of sensory neurons during embryonic and postnatal periods. This group of sensory cells corresponds mainly to SP and CGRP containing small size neurons which project their thinly myelinated and unmyelinated axonal fibers to both peripheral and central targets [for reviews, see (Johnson, Jr. et al., 1986; Lewin and Mendell, 1993)]. However, the effects of NGF on sensory neurons vary with each of the developmental periods. Here, I will only provide a brief review of the effects of NGF on neuropeptide (SP or CGRP) containing primary sensory neurons at different developmental stages.

A. *The crucial role of NGF in the development of embryonic sensory neurons*

Primary sensory neurons originating from the neural crest have been shown, in both *in vitro* and *in vivo* studies, to be critically dependent on NGF for survival and differentiation during the embryonic period (Levi-Montalcini and Angeletti, 1968; Gorin and Johnson, 1979; Aloe et al., 1981). In these *in vivo* studies, a majority (up to 80%) of primary sensory neurons in early development was killed by deprivation of NGF. Such deprivation has been achieved by either systemically treating animals with high titre antibodies raised against NGF or making auto-immunized animals that will produce antibodies to their own NGF. In recent years, the dependence of embryonic sensory neurons on NGF has been further substantiated by studies using transgenic mouse technology. NGF or its high affinity receptor, trkA, was depleted by homologous recombination in transgenic mice (Crowley et

al., 1994; Smeyne et al., 1994). All or a large portion of small size neuropeptide containing DRG cells died in these transgenic mice, thus leading to a loss or reduction of nociception.

On the other hand, exposure to excess NGF at embryonic stages resulted in excess sensory neurons (Henderson et al., 1994; Albers et al., 1994), elongation of axonal fibers in the spinal cord (Zhang et al., 1994), hyper-innervation of the skin by CGRP-IR fibers (Albers et al., 1994) and consequent hyperalgesia (Davis et al., 1993).

B. *Effects of NGF on primary sensory neurons during the postnatal period*

After birth, the role of NGF on sensory neurons changes from a requirement for survival to the maintenance and modulation of the phenotypes. In the neonatal period, deprivation of NGF results in the death of only a small proportion of the small size sensory neurons (Yip et al., 1984; Hulsebosch et al., 1987; Lewin et al., 1992b), but caused a substantial reduction of SP contents in sensory neurons (Otten et al., 1980). Conversely, exposure of neonatal or mature primary sensory neurons to excess NGF leads to increased SP mRNA expression (Vedder et al., 1993) and protein contents (Otten et al., 1980), and results in a profound behavioral hyperalgesia (Lewin et al., 1993).

In adulthood, the depletion of NGF is unable to cause any neuronal cell death (Gorin and Johnson, 1980), but NGF continually exerts its effects on the maintenance and regulation of the phenotypes of sensory neurons. Experiments have shown that neuropeptides in sensory neurons were differentially regulated by peripheral nerve transection, which deprived sensory neurons of target-derived trophic factors. Transection of a peripheral nerve up-regulated the level of vasoactive intestinal polypeptide and galanin in sensory neurons, and down-

regulated the expression of SP and CGRP [for review see (Hökfelt et al., 1994)]. The reduced levels of SP and CGRP in the lumbar DRG after the section of the sciatic nerve, were reversed by infusion of NGF into the central stumps of the cut nerve in adult rats (Fitzgerald et al., 1985; Wong and Oblinger, 1991; Inaishi et al., 1992) or by a 2 week delayed intrathecal infusion of NGF (Verge et al., 1995). Consistent evidence was obtained from *in vitro* and *in vivo* studies that NGF up-regulated SP and CGRP genes and proteins in cultured adult rat sensory neurons (Lindsay et al., 1989; Lindsay and Harmar, 1989) and that NGF increased SP content and transport in sensory fibers innervating inflamed tissues in the adult rat (Donnerer et al., 1992).

C. NGF and nociception

The role of NGF in nociception was reviewed by Lewin and Mendell (1993). NGF plays an important role in the postnatal development of nociceptors and in mechanisms of nociception occurring in adult animals.

In the early postnatal period (postnatal day 4-11), administration of anti-NGF antibodies caused a possible switch of the Aδ-high threshold mechanical receptor (HTMR) into D-hair type in the skin (Lewin et al., 1992b). This finding implied that sensory neurons might be subject to respecification of their phenotypes by the availability of NGF during early postnatal period. After neonatal anti-NGF antibody treatment (from postnatal days 2 to 14), the numbers of C-mechanothermal fibers in adult rats were reduced by about 60% and the lost fibers seemed to be replaced by a new population of C-fibers that responded exclusively to mechanical stimuli (Lewin and Mendell, 1994). Administration of anti-NGF

antibodies to neonatal animals impaired the ability of Aδ and C-fiber afferents to elicit antidromic vasodilation, suggesting that the sensory neurons which had their phenotypes converted likely mediated the antidromic vasodilation (Lewin et al., 1992a). Conversely, exposure of neonatal animals to excess NGF did not induce dramatic changes in the proportions of Aδ and C-fiber afferents, suggesting that the naturally occurring amount of NGF in the skin is sufficient to ensure the normal development of all the Aδ nociceptors (Lewin et al., 1993).

In adult animals, one systemic injection of NGF led the animal to develop a profound sensitivity to noxious heat and mechanical stimuli (Lewin et al., 1993). A mechanical hyperalgesia was elicited in transgenic mice over-producing NGF in the skin under the control of a K14 keratin promoter (Davis et al., 1993). Therefore, NGF seems to play an important linking role in hyperalgesia and inflammation. This assumption was supported by several lines of evidence. NGF in damaged or inflamed tissues increased many folds above normal levels (Weskamp and Otten, 1987; Aloe et al., 1992). NGF itself is known to cause hyperalgesia (Lewin et al., 1993) through multiple mechanisms, including mast cell degranulation (Stead et al., 1987), nociceptor stimulation following proteolytic cleavage (Miaskowski et al., 1991), and possibly through an effect on the production of peptides by dorsal root ganglion neurons (Donnerer et al., 1992).

VII. **Objectives and rationale of the present thesis project**

A. *Statement of objectives*

As mentioned above, SP is a presumptive neurotransmitter involved in the

transmission of nociception in thinly myelinated and unmyelinated fibers in the dorsal horn. CGRP is likely to potentiate the nociception mediated by SP. The inhibitory neurotransmitters/neuromodulators, ENK and GABA, probably interact with SP in the dorsal horn and thus inhibit SP mediated nociception transmission. In the embryo, SP containing primary afferent neurons are critically dependent on NGF for survival, growth and differentiation. After birth, the phenotypes of SP containing sensory neurons are maintained and modulated by NGF. It is obvious that SP fiber innervation in target tissues is very important for SP to fulfil its roles in nociception. It is of great significance to understand the SP fiber innervation of its central target tissues.

In my thesis work, I investigated the innervation of SP-IR axonal fibers in two different experimental paradigms.

The aim of this thesis work was, therefore, to investigate the innervation by SP-IR axonal terminals of physiologically characterized dorsal horn neurons in a normal experimental condition and, furthermore, to elucidate the innervation by SP-IR axonal terminals of target tissue in the white matter of the CNS in a transgenic mouse model where NGF is over-produced by myelinating oligodendrocytes under the control of myelin basic protein (MBP) promoter.

To achieve these objectives, two hypotheses were formulated and tested in this thesis project.

B. *Statement of hypothesis I*

It is generally thought that functional types of dorsal horn neurons may be

differentiated primarily by their morphology, transmitter/modulator content, and predominant type of apposed boutons. We examined this general concept, by studying the innervation by SP-IR axonal terminals of functionally characterized dorsal horn neurons. A previous study from our group demonstrated that SP-IR axonal boutons abundantly innervated nociceptive dorsal horn neurons, but rarely innervated non-nociceptive neurons (De Koninck et al., 1992). However, these data were collected on a limited sample of neurons. Based on these preliminary results, I specifically tested the following hypotheses in the current thesis project:

There are differences between physiological types of dorsal horn neurons in the innervation by SP-IR axonal fibers and also by other axonal fibers containing other neuropeptides or neurotransmitters involved in nociception, such as CGRP, ENK and GABA.

C. *Statement of rationale to test hypothesis* I

To address hypothesis I, a combination of intracellular electrophysiological recording, intracellular injection of HRP, and ultrastructural immunocytochemistry was used.

1. Functional characterization of dorsal horn neurons

Following electrophysiological recording, the dorsal horn neurons of the cat lumbar spinal cord were functionally classified into three types based on their responses to innocuous or noxious stimuli in the skin. The three types of dorsal horn neurons were nociceptive specific, wide dynamic range and non-nociceptive. Nociceptive neurons, including nociceptive specific and wide dynamic range neurons, exhibited a characteristic

nociceptive response, which was represented by an afterdischarge and a slow, prolonged depolarization after the end the stimuli. This typical nociceptive response was blocked by NK-1 receptor antagonists (Radhakrishnan and Henry, 1991; De Koninck and Henry, 1991). Neurons were classified as nociceptive and non-nociceptive on the basis of the presence or absence of such a nociceptive response. Nociceptive specific neurons responded only to noxious stimuli, while wide dynamic range neurons responded to both noxious and innocuous stimuli. Non-nociceptive cells responded to both noxious and innocuous stimuli with a fast and brief discharge and did not display the typical nociceptive response described above. After functional classification, the cells were injected intracellularly with a tracer, horseradish peroxidase (HRP), so that the cells could be identified using histochemistry. Usually, 1 to 2 cells were injected per animal.

2. Morphological characterization of the dorsal horn neurons

After the intracellular injection of HRP, the animals were further processed for morphological observation. HRP labelled cells were detected after histochemistry, and SP and ENK immunostaining were carried out using a pre-embedding protocol. CGRP and GABA immunoreactivities were demonstrated using a post-embedding immunogold protocol. The detection of ENK immunoreactivity required the use of electron microscopic radioautography. Under the electron microscope, the different markers were easy to differentiate. Neurons filled with an homogenous and dense 3,3'-diaminobenzidine (DAB) reaction product were identified as the intracellularly HRP injected cells. Axonal boutons containing a non-homogeneous and less dense DAB reaction product, which was

preferentially associated with dense core vesicles, were considered as SP immunoreactive. Axonal boutons overlaid by immunogold particles were defined as either CGRP or GABA immunoreactive depending on the antibodies used. Boutons overlaid by silver grains of the radioautographic emulsion were considered as ENK immunoreactive. At the EM level, the quantification of SP-IR, ENK-IR, and CGRP-IR boutons which were apposed to functionally characterized dorsal horn neurons was carried out. The percentages of each type of bouton were determined directly on the EM screen. The densities of each type of bouton was determined with the aid of an image analysis system. The relevant data was compared statistically.

Using these approaches, we found significantly higher numbers of SP-IR boutons and SP+ENK-IR boutons presynaptic to nociceptive neurons than to non-nociceptive neurons. Some of the SP-IR boutons apposed to nociceptive neurons co-localized CGRP, suggesting their primary sensory origin. Most nociceptive neurons contained ENK, but non-nociceptive neurons were never ENK immunoreactive. Although higher numbers of ENK-IR boutons were apposed to nociceptive neurons, considerable numbers of ENK-IR boutons were in contact with non-nociceptive neurons.

Additionally, the interaction of SP and GABA in the superficial dorsal horn of the cat and rat spinal cord was also investigated. The co-localization of SP and GABA immunoreactivities was found in axonal terminals for the first time in the superficial layers of the dorsal horn of the cat, but not rat, spinal cord.

D. Statement of hypothesis II

As mentioned above, during the neonatal and adult periods, SP containing primary sensory neurons are not dependent on NGF for survival, but their phenotypes continue to be modulated by NGF. Since the central target areas of the sensory neurons are very important in nociception transmission and modulation, the SP innervation in the CNS will be definitively modulated by many factors. NGF will be the most suitable candidate to consider. Therefore, I decided to investigate whether SP containing sensory neurons respond to an abnormal NGF over-expression in the white matter of the CNS during the early postnatal period. Based on the available evidence, it was hypothesized that:

SP-IR axonal fibers, originating from NGF-responsive primary sensory neurons innervate specifically target areas in the CNS where NGF is ectopically expressed.

E. *Statement of rationale to test hypothesis II*

To test hypothesis II, the following strategies were taken. A transgenic mouse model was used which bears a chicken NGF cDNA under the control of a MBP promoter. The choice of this animal model was based on the rationale that the MBP promoter would direct NGF transgene expression in the white matter of the CNS and that the transgene expression would be initiated only in the early postnatal period to avoid any developmental defect. NGF mRNA analysis and NGF immunocytochemistry were conducted to examine if the NGF transgene had been over-expressed, at the gene and protein levels, in the CNS of transgenic mice. Since SP and CGRP are sensory neuropeptides contained in most of the NGF responsive primary sensory neurons, SP and CGRP immunoreactivities were used as markers of the effects of NGF over-expression on primary sensory neurons in the white matter of the

CNS. Further electron microscopy was carried out to demonstrate such effects at the ultrastructural level.

We found that SP-IR fibers were present in the white matter of the CNS of both transgenic and control mice from postnatal day 0 to day 2. From day 5 on, however, these SP-IR fibers increased markedly to become ectopic fibers in transgenic mice, but decreased dramatically and finally disappeared in control mice. Ectopic SP-IR fibers in transgenic mice remained throughout adulthood. Capsaicin treatment abolished all the ectopic SP-IR fibers, indicating their primary sensory origin.

CHAPTER II

Quantitative analysis of substance P immunoreactive boutons on physiologically characterized dorsal horn neurons in the cat lumbar spinal cord

Weiya Ma, A. Ribeiro-da-Silva, Y. De Koninck, V. Radhakrishnan, J.L. Henry and A.C. Cuello

ABSTRACT

In the present study, we carried out a quantitative analysis of substance P (SP) immunoreactive (IR) axonal boutons apposed to physiologically characterized dorsal horn neurons in the cat lumbar spinal cord, using a combination of intracellular electrophysiological recording and injection of horseradish peroxidase with ultrastructural immunocytochemistry.

Dorsal horn neurons were classified as nociceptive specific, wide dynamic range and non-nociceptive based on their responses to innocuous and noxious stimuli. All nociceptive neurons (nociceptive specific and wide dynamic range) exhibited a characteristic nociceptive response which was blocked by the selective NK-1 receptor antagonist, CP-99,994.

At the EM level, 3 nociceptive specific, 3 wide dynamic range and 3 non-nociceptive neurons were used for quantitative analysis. The densities of boutons, including SP-IR and non-IR, apposed the cell bodies, proximal and distal dendrites were not significantly different for the three functional types of neurons. The densities of SP-IR boutons apposed to the three regions of nociceptive specific neurons were significantly higher than those of non-nociceptive neurons. When compared with wide dynamic range neurons, nociceptive specific neurons possessed significantly higher densities of SP-IR boutons apposed to the cell bodies and proximal dendrites. The densities of SP-IR boutons apposed to the proximal and distal dendrites of wide dynamic range neurons were significantly higher than those of non-nociceptive neurons.

The percentages of SP-IR boutons apposed to all three regions of nociceptive specific

neurons were significantly higher than those of wide dynamic range and non-nociceptive neurons. Also, the percentages of SP-IR boutons apposed to the three regions of wide dynamic range neurons were significantly higher than those of non-nociceptive neurons. Furthermore, for wide dynamic range neurons, the percentages of SP-IR boutons apposed the distal dendrites which were located in laminae rich in SP immunoreactivity were significantly higher than those of dendrites located in area with sparse immunoreactivity. However, even in areas with intense SP immunoreactivity, the values for the distal dendrites of non-nociceptive neurons remained very low. About 30-45% of SP-IR boutons apposed to nociceptive neurons co-localized CGRP immunoreactivity, a finding indicating that many of the SP-IR boutons were of primary sensory origin. On average, 33.5 % of the SP-IR boutons apposed to the cells, regardless of their functional type, exhibited a synaptic contact.

Our quantitative data provide a direct correlation between the amount of SP-IR input and the functional types of neurons and also indicate a correlation between NK-1 receptor mediated responses and the innervation by SP-IR axonal boutons.

INTRODUCTION

There is an extensive literature indicating that substance P (SP) has a major role in the dorsal horn of the spinal cord as a mediator or modulator of nociceptive transmission [for reviews see (Henry, 1982; Cuello, 1987; Otsuka and Yanagisawa, 1990)] Immunocytochemical studies have shown that SP immunoreactivity occurs in small diameter sensory fibers terminating mainly in lamina I and outer lamina II (Hökfelt et al., 1975a; Cuello et al., 1978), and also in small fiber clusters in lamina V (Ruda et al., 1986). SP specifically excites nociceptive dorsal horn neurons (Henry, 1976; Randic and Miletic, 1977). The type of physiological response that likely corresponds to the effect of SP is a slow, prolonged depolarization that occurs after noxious stimulation, which is blocked by SP receptor (NK-1 receptor) antagonists (Radhakrishnan and Henry, 1991; Radhakrishnan and Henry, 1995; De Koninck and Henry, 1991).

The main objective of the present study was to assess whether there is a direct correlation between the specificity and intensity of the nociceptive response and the number of appositions of SP-immunoreactive (IR) boutons. In our previous study, we showed that neurons which respond to noxious stimuli with a slow, prolonged depolarization after the end of the stimulus receive abundant SP-IR boutons, while non-nociceptive neurons scarcely receive any SP-IR inputs (De Koninck et al., 1992). Although this previous study was indicative of a direct correlation between a nociceptive response and the SP innervation of the cell, the quantitative data were collected on only one cell for each type of physiological response and a comparison was not made between regions of the dendritic tree. Therefore,

we decided to investigate quantitatively the relationship between SP-IR inputs and the three types of dorsal horn neuron. For this purpose, we conducted a quantitative analysis to determine the densities and percentages of SP-IR boutons apposed to the cell bodies, proximal dendrites and distal dendrites of three neurons for each physiological type. To determine the origin of SP-IR boutons apposed to the intracellularly labeled cells, we examined the co-localization of SP and calcitonin gene-related peptide (CGRP) immunoreactivities. Some of the data have been presented in a preliminary communication (Radhakrishnan et al., 1993).

MATERIALS AND METHODS

Electrophysiological recording and intracellular injection of HRP of the dorsal horn neurons

The methods for cat preparation and intracellular recording have been described in detail elsewhere (De Koninck et al., 1993; Radhakrishnan and Henry, 1995). Briefly, adult cats of either sex (3.0 to 4.5 kg) were anesthestized with α-chloralose (60 mg/kg i.v.), artificially ventilated and paralyzed with pancuronium bromide (Pavulon, Organon; 1 mg/kg i.v. and supplemented as necessary). The spinal cord was transected at the L_1 vertebral level to eliminate the influence of supraspinal structures. Glass micropipettes filled with 0.5 M KCl and 4-8 % horseradish peroxidase (HRP; Sigma, Type VI; resistances: 50 to 120 MΩ) were used to record intracellularly from dorsal horn neurons in segments L_5-L_7. A neuron

was studied only if it had a stable resting membrane potential, if its action potential showed an overshoot and if the cell exhibited clear, reproducible responses to natural stimulation of the skin.

Functional classification of the neurons was made based on their responses to natural cutaneous stimulation and to electrical stimulation of afferent nerves following previously described criteria (De Koninck and Henry, 1992; Radhakrishnan and Henry, 1995). The natural stimuli used were movement of hairs, innocuous and noxious pressure, noxious pinch with a serrated forceps and noxious radiant heat. Neurons were thus classified as non-nociceptive, wide dynamic range and nociceptive specific. Nociceptive neurons (i.e. either nociceptive specific or wide dynamic range) were classified as such when they responded to noxious stimulation with a slow, prolonged depolarization following the end of the stimulus. To test whether this response could be blocked by the administration of a SP receptor antagonist, the specific non-peptide NK-1 receptor antagonist CP-99,994 was given intravenously (0.5-1 mg/kg) to three wide dynamic range neurons.

After thorough electrophysiological recording and functional classification, the neuron was injected with HRP by intracellular iontophoresis using 600 ms positive current pulses of 4-8 nA at a frequency of 1 Hz for a duration of 10 to 30 minutes, depending on the type of neuron injected. One to three neurons were injected per cat and a map of the dorsal surface of the spinal cord was drawn to ensure exact localization and identification of the labeled cells.

HRP histochemistry, pre-embedding and post-embedding immunocytochemistry

The morphological approaches are described in detail elsewhere (De Koninck et al., 1993). Following electrophysiological recording and intracellular injection of HRP, the cat was subsequently perfused through the left ventricle with a mixture of 4% paraformaldehyde and 0.5% glutaraldehyde in 0.1M phosphate buffer, pH 7.4, at room temperature. The relevant segment of the spinal cord was removed and postfixed in the same fixative for 90 minutes and then infiltrated overnight in 30% sucrose in 0.1M phosphate buffer. Next day, the spinal cord segment was snap frozen in liquid nitrogen and thawed in 0.1M phosphate buffer at room temperature. Fifty-μm-thick parasagittal sections were cut on a Vibratome, and processed to demonstrate HRP filled cells using HRP histochemistry in which the chromogen, 3, 3'-diaminobenzidine (DAB, Sigma), was intensified by nickel and cobalt (Adams, 1981). Under the light microscope, the HRP labeled neuron was visualized and photographed. The sections containing the labeled cells were further processed to demonstrate SP immunoreactivity in the dorsal horn. The sections were incubated in an anti-SP/anti-HRP bi-specific monoclonal antibody from the rat (Suresh et al., 1986) (coded P4C1; Medicorp, Canada) overnight at 4^{0}C. The following day, the sections were incubated in a solution containing HRP (Sigma type VI, 5μg/ml) at room temperature. The DAB reaction was carried out without intensification.

Subsequently, the tissue was osmicated, dehydrated in ascending alcohols and propylene oxide, and finally flat-embedded in Epon as previously described (Ribeiro-da-Silva et al., 1993). The different parts of the labeled neuron in flat-embedded slices were photographed. The whole morphology of a labeled neuron was reconstructed using a camera lucida. The dendritic tree of a cell was divided into three segments by

imposing three equidistant circles centered on the cell body (Sholl, 1953) on the reconstruction drawing of the whole morphology of the cell. The diameter of each of the circles varied with the size of the dendritic tree. The dendrites located inside the inner circle were considered as the proximal dendrites, while those located in the outer circle represented the distal dendrites. To ensure differentiation between the proximal and distal dendrites, the dendritic segments located in the middle circle were not used for quantitative purposes. Samples from the cell body, proximal dendrites and distal dendrites of the labeled neuron were selected and reembedded in Epon blocks. From re-embedded blocks, 4-μm-thick semithin sections were cut serially, photographed and compared to the original drawing for identification of the parts of the labeled neuron present in each section. The semithin sections were cut then reembedded in Epon block. From these Epon blocks, ultrathin sections were cut on an ultramicrotome and collected onto one slot formvar-coated grids, counterstained with uranyl acetate and lead citrate, and finally observed under a Phillips 410 electron microscope.

Some additional ultrathin sections from three types of neurons were collected onto mesh nickel grids and processed to demonstrate the co-localization of SP and CGRP using a post-embedding immunogold staining protocol described in detail elsewhere (Ribeiro-da-Silva et al., 1993). An anti-human CGRP polyclonal rabbit antibody (Peninsular) was used. The secondary antibody was a gold-conjugated goat anti-rabbit IgG (Biocell). The size of gold particles was 10 nanometers.

Quantitative analysis

Of the cells included in the present study, sections from neurons 207-1, 208-1 and 212-1 have previously been used in two publications (De Koninck et al., 1992; Ribeiro-da-Silva et al., 1992). However, none of the previously used sections was included in the present data.

For each cell, the numbers of SP-IR boutons and non-IR boutons apposed to the cell body, proximal dendrites and distal dendrites were counted directly on the EM screen at the magnification of 13,800 X. After counting, the entire electron microscopic field was photographed at low magnification for the purpose of measuring the length of cell membrane to which the boutons were apposed. On average, 1,370 boutons were counted per cell. Five fields, at least, from each of the three regions of the cell were counted. To analyze the actual synaptic specialization between the two structures in isolated ultrathin sections, the goniometer stage of the electron microscope was used to tilt the grid. Data from each region of the labeled neuron were pooled and the percentages of SP-IR boutons apposed to the cell bodies, proximal dendrites and distal dendrites were determined.

To measure the length of profiles of the cell present in each low magnification electron micrograph, the negative plates were placed on a light box and the image were captured into an image analysis system (MCID-M1 system, Imaging Research Inc., St.Catharines, Ontario, Canada) using a coupled black and white CCD video camera. The density of SP-IR boutons (number of SP-IR boutons per 100 μm of cell membrane length) and the density of the total boutons (number of SP-IR boutons and non-IR boutons/100 μm of membrane length) were obtained from each profile of each labeled neuron. At least, 5 profiles for each region of a cell were used.

For the study of the co-localization of SP and CGRP immunoreactivities, quantitative data were obtained by counting directly from the EM screen the numbers of profiles apposed to the different regions of the cell which were immunostained for SP-only, SP+CGRP and CGRP-only. One cell per physiological type was used for this purpose.

The mean percentages and densities of SP-IR boutons, and the densities of the total boutons, apposed to the cell bodies, proximal dendrites and distal dendrites of the three types of neurons, were statistically compared using one-way analysis of variance (ANOVA) followed by post-hoc Tukey's tests. Statistical significance was set at $P<0.05$.

RESULTS

Electrophysiological and pharmacological characterization of the dorsal horn neurons

Intracellular recordings were obtained from a total of fifty-five neurons, of which 9 cells were included in this study: three nociceptive specific, three wide dynamic range and three non-nociceptive. These nine cells were selected as all of them were thoroughly characterized physiologically through intracellular recording and displayed satisfactory preservation of ultrastructure and immunostaining for SP. On application of noxious stimuli, the nociceptive (nociceptive specific and wide dynamic range) neurons showed an initial depolarization followed by a slow, prolonged depolarization that outlasted the period of stimulation (Fig. 1c,d). This depolarization was usually associated with a period of increased rate of action potential discharge, or *afterdischarge*. Following administration of the NK-1

receptor antagonist, CP-99,994, the late component of the response (the slow, prolonged depolarization and afterdischarge) were considerably reduced, while the initial depolarization was unaffected (Fig. 1e). Responses to non-noxious cutaneous stimulation, such as hair movement, were brief and brisk (Figs. 1a, 2A), and were unaffected by CP-99,994 (Fig. 1b).

Morphological characterization of the dorsal horn neurons

Wide dynamic range neurons

The cell bodies of the three wide dynamic range neurons (276-2; 208-1; 339-1) were located in the laminae II-III border, lamina III and lamina IV respectively (Table 1). All cells displayed identical electrophysiological properties. Representative recordings from one neuron (339-1) are shown in Fig. 1. The morphological properties of two of these cells (208-1 and 339-1) are shown, respectively, in Figs. 3-4 and 5-6. Morphologically, all three neurons were multipolar. One neuron (208-1; Fig. 3A) had an extensive dendritic tree in lamina III and two major dendritic branches extending to outer lamina II and lamina I, an area of intense SP immunoreactivity (Fig. 3B). It is interesting to note that the cell possessed numerous small dendritic spines (Fig. 3A; small arrows). However, the dendritic processes that extended into laminae I-IIo were aspiny (Fig. 3A). These dendrites in laminae I-IIo were the areas of the cell that received the highest number of appositions from SP-IR profiles (Fig. 3B). Even in other areas of the dendritic tree, SP-IR profiles were never seen apposed to dendritic spines. This cell did not have much SP-IR profiles apposed to the cell body area (Fig. 3B-E). Synapses between SP-IR boutons and the cell body were not frequently found (Fig. 3E). A high number of SP-IR boutons apposed to or synapse with the distal dendrites

located in laminae I-IIo (Fig. 4A-D). However, even in this area, SP-IR central varicosities of glomeruli were never found presynaptic to dendrites of the cell (Fig. 4E). Cell 276-2 (not illustrated) was similar to 208-1 in shape, dendritic arborization, dendritic spines and appositions from SP-IR boutons.

Cell 339-1 (Figs. 1 and 5) possessed a cell body that was larger in size and was located in lamina IV (Fig. 5A). Like the other wide dynamic range neurons, appositions and synapses from SP-IR boutons were found infrequently in the cell body region (Fig. 5D,E). Most of the dendrites of the cell branched within the limits of lamina IV and were virtually devoid of spines. One dendrite reached as far as the middle third of lamina II (Fig. 5A), where it received a considerable number of appositions from SP-IR profiles. Some dendrites reached lamina V (Fig. 5A), and branched in the patchy areas rich in SP immunoreactivity characteristic of that lamina (Fig. 6A). These processes received a high number of appositions from SP-IR profiles (Fig. 6C,D).

The synapses established by SP-IR boutons onto the dendrites of the cells were usually clearly asymmetric (see Fig. 6C,D - insets). In the cell body area, synapses were usually symmetric.

Nociceptive specific neurons

All three nociceptive specific neurons had their cell bodies located in Lamina I (Table 1). Two of these cells (271-1, 276-1) were bipolar (fusiform) and oriented parallel to the main axis of the spinal cord, with their dendritic tree branching within the limits of lamina I. Figure 7 illustrates morphological properties of one of these two bipolar cells (271-1).

These cells received numerous synapses from SP-IR bouton profiles in the cell body area and throughout the dendritic branches. Examples of SP-IR boutons apposed to dendrites are illustrated in Fig. 7C,D. A third nociceptive specific neuron (207-1; see Figs. 8 and 9) had the cell body located close to the laminae I-II border (Fig. 8A). This cell was multipolar with a few scarcely branched dendrites. Some of the dendrites of this cell were oriented ventrally and reached as far as the laminae II-III border (Fig. 8A,B). Like the bipolar nociceptive specific cells, this multipolar cell received numerous appositions and synapses from SP-IR profiles, both in the cell body area and in the dendritic tree. Appositions/synapses from SP-IR boutons were abundant both in the proximal (Fig. 8D) and distal (Fig. 9) dendrites. Apparently, appositions were equally abundant no matter whether the dendrites were located in lamina I or inner lamina II.

Non-nociceptive neurons

The somata of all three non-nociceptive neurons (271-2, 212-1 and 258-1) were located in lamina IV. The cells were multipolar, with dendritic arborizations oriented dorsally. As examples, cells 271-2 (Fig. 10; see Fig. 2 for electrophysiological recording from this cell) and 212-1 (Fig. 11) are shown here. The cell bodies gave rise to several thick dendritic trunks that branched extensively mostly in lamina III, but with some distal processes reaching as far dorsally as outer lamina II (Figs. 10A; 11A). The dendritic branches possessed spines, particularly noticeable in cell 212-1 (Fig. 11B). Many of these spines branched at right angles from the dendritic trunks (Fig. 11C; arrows). Under the electron microscope, SP-IR boutons were seldom found in contact with the perikarya or

dendrites of the cells. This scarcity can be noticed in Figs. 10C and 11D. Most of the varicosities that were apposed to non-nociceptive neurons contained small clear round vesicles, although some possessed flattened vesicles. A few dendritic spines were components of synaptic glomeruli (Fig. 11E). It is interesting to note that even in areas of dense SP innervation, such as lamina IIo, the distal dendrites of the non-nociceptive cells were virtually always separated from SP-IR profiles by some distance.

Quantitative results

The quantitative data obtained from each of the cells included in this study are shown in Table 1. Figure 12 shows the mean densities of the total boutons, and the mean densities and percentages of SP-IR boutons apposed to the cell bodies, proximal dendrites and distal dendrites of three types of neurons.

The densities of the total bouton profiles contacting the cell bodies, proximal and distal dendrites, did not differ significantly with the physiological types of cells (Fig. 12A). The densities of SP-IR bouton profiles (Fig. 12B) apposed to the cell bodies, the proximal and the distal dendritic regions of nociceptive specific neurons were significantly higher ($P<0.01$) than those of non-nociceptive neurons. The densities of SP-IR bouton profiles apposed to the cell bodies and the proximal dendrites of nociceptive specific neurons were also significantly higher ($P<0.001$) than those of wide dynamic range neurons, but the values were not significant different in the distal dendrites (Fig. 12B). Compared with non-nociceptive neurons, wide dynamic range neurons showed significantly higher ($P<0.02$) densities of SP-IR boutons apposed to the proximal and the distal dendritic regions, however,

the values were not significantly different in the cell body region (Fig. 12B).

The percentages of SP-IR boutons apposed to the cell bodies, proximal and distal dendrites of nociceptive specific neurons were significantly higher than these of wide dynamic range ($P<0.001$) and non-nociceptive neurons ($P<0.001$) (Fig. 12C). Wide dynamic range neurons had significantly higher percentages of SP-IR boutons apposed to the cell bodies ($P<0.04$), proximal ($P<0.001$) and distal dendrites ($P<0.001$) than non-nociceptive neurons (Fig. 12C). Since the dendritic branches of wide dynamic range neurons and non-nociceptive neurons distributed extensively, it was meaningful to assess the percentages of SP-IR boutons apposed to the distal dendrites located in laminae with intense SP immunoreactivity and located in laminae with sparse SP immunoreactivity. The data in Table 2 showed that, for wide dynamic range neurons, the percentage of SP-IR boutons apposed to the distal dendrites located in laminae rich in SP immunoreactivity was significantly higher ($P<0.001$) than the distal dendrites located in laminae with scarce SP immunoreactivity. However, even in laminae with intense SP immunoreactivity, the value for the distal dendrites of non-nociceptive neurons remained very low (Table 2).

The percentages of SP-IR bouton profiles which established visible synaptic contacts with three types of neurons were virtually identical regardless of the physiological properties of the cells. The ratio of synaptic SP-IR boutons to the total number of SP-IR apposed to the neurons was 33.5± 2.3%, which was virtually identical to the proportion of non-IR boutons that exhibited synapses on the cell (34.0± 3.3%).

Co-localization of SP and CGRP immunoreactivities

Under the electron microscope, SP and CGRP immunoreactivities were observed to co-localize in the same axonal boutons apposed to nociceptive specific and wide dynamic range neurons (Fig. 13). Quantitatively, 43.5 and 30.4 % of the SP-IR bouton profiles apposed, respectively, to nociceptive specific and wide dynamic range neurons co-localized CGRP immunoreactivity. In contrast, virtually all SP-IR boutons apposed to non-nociceptive cells were devoid of CGRP immunoreactivity.

DISCUSSION

In the current study, we presented new direct evidence that spinal nociceptive neurons, which exhibited a slow, prolonged depolarization and afterdischarge blocked by the NK-1 receptor antagonist CP-99,994, received an abundant innervation from SP-IR boutons. Neurons lacking this type of response received limited SP-IR input. Furthermore, our quantitative data revealed that the densities of SP-IR boutons apposed to the cell bodies and the proximal dendrites of nociceptive specific neurons were significantly higher than those of wide dynamic range neurons. These values for the distal dendrites of the two types of nociceptive neurons were not significantly different. Nociceptive specific neurons received significantly higher percentages of SP-IR boutons apposed to the cell bodies, the proximal dendrites and the distal dendrites than did wide dynamic range neurons. In laminae with intense SP immunoreactivity, the percentage of SP-IR boutons apposed to the distal dendrites

of wide dynamic range neurons were significantly higher than that of the distal dendrites located in laminae with scarce SP immunoreactivity. However, the value for the distal dendrites, located in areas of intense SP immunoreactivity, of non-nociceptive neurons remained very low. CGRP immunoreactivity co-localized in the SP-IR boutons apposed to the nociceptive neurons.

Significance of the differences of SP-IR inputs with the cell type

We detected in the present study that approximately one third of SP-IR boutons were presynaptic to three types of the dorsal horn neurons. This result is consistent with a previous study (De Koninck et al., 1992). The ratio in their study has been interpreted as indicating that virtually all varicosities would have had a synaptic specialization if serial sections had been analyzed. Therefore, the percentages of SP-IR boutons apposed to each physiologically characterized dorsal horn neuron can be considered as an indicator of the total number of synapses that the neuron receives from SP-IR boutons.

It is important to stress that all the cells studied received approximately the same densities of appositions from axonal varicosities independently of their neurochemical type. Therefore, the percentage of SP-IR boutons in the total number of varicosities apposed to the cell can represent the relative proportion of SP synaptic inputs to other transmitter/modulator specific synaptic inputs.

It is interesting to note that nociceptive specific cells had a significantly higher number of appositions from SP-IR profiles than either wide dynamic range or non-nociceptive neurons. This result was to be expected, since we had similar finding based on

the quantitative analysis of one cell of each type in a previous study (De Koninck et al., 1992). The present study adds quantitative information about the density and percentage of SP-IR boutons apposed to three regions of nociceptive and non-nociceptive dorsal horn neurons. In the previous study two types of wide dynamic range neurons were studied, but only one type of cells was included in our present study. One of the two wide dynamic range neurons in the previous study, which possessed particularly strong nociceptive responses and had the cell body located in lamina V, was abundantly innervated by SP-IR boutons. However, even this cell was less innervated by SP-IR boutons than the nociceptive specific cell included in that study, particularly in the cell body region (De Koninck et al., 1992). This type of wide dynamic range neuron was not included in the present study, as it is seldom found. The results from the wide dynamic range neuron with moderate nociceptive response in the previous study is comparable to the data obtained in the present study. This type of cell receives minor SP-IR input in the cell body area, where the density of SP-IR boutons was hardly different from non-nociceptive neurons. The data in the current study clearly indicate that this type of wide dynamic range neurons receives most of its SP-IR synaptic input at the distal dendrites, particularly those in areas rich in SP immunoreactivity, such as laminae I-IIo and SP-IR patches of lamina V (Table 2), and at the distal dendritic segment, the density of SP-IR boutons was not significantly different from that of nociceptive specific neurons. In contrast, non-nociceptive cells had weak SP innervation, even in areas of intense SP immunoreactivity, such as lamina IIo (see Table 2).

Substance P receptors

The specific innervation of nociceptive neurons by SP-IR fibers favours a direct synaptic action of SP. Using the same antibody from Vigna et al (1994), several studies have investigated the distribution of NK-1 receptor immunoreactivity in the rat spinal cord (Bleazard et al., 1994; Liu et al., 1994; Littlewood et al., 1995; Brown et al., 1995). All studies showed a conspicuous lack of NK-1 receptor immunoreactivity in cells in lamina II, while considerable immunostaining occurred in lamina I and deeper laminae. Although some NK-1 receptor immunoreactivity was detected in lamina II, it corresponded to the immunostaining of dendrites from neurons, the cell bodies of which were located in other laminae. As it is well known that SP immunoreactivity is abundant in laminae I and II, the lack of immunoreactivity for the receptor in lamina II is unexpected. One of the studies (Liu et al., 1994) using double immunostaining at the ultrastructural level showed that very few SP-IR profiles were presynaptic to NK-1 receptor-IR cells. Both the lack of NK-1 receptor-IR in lamina II and the lack of SP innervation of NK-1 receptor-IR cells were interpreted as that SP might act at a distance from the release site (Liu et al., 1994). A study using another anti-NK-1 receptor polyclonal antibody revealed a comparable distribution of the NK-1 immunoreactivity (Ding et al., 1995). These results are in apparent contradiction with our data, since we found that nociceptive response exhibited by nociceptive neurons is closely associated with the innervation by SP-IR terminals which occurs highly in lamina II, one of the areas rich in SP immunoreactivity. It should be noted that only one of the six nociceptive cells that we studied had the cell body in lamina II. All the others had their cell bodies in lamina I or deeper laminae. However, the scarcity of direct SP innervation of neurons possessing NK-1 receptor immunoreactivity detected in the EM study (Liu et al., 1994)

contrasts with our demonstration of a robust SP-IR innervation of nociceptive cells, but not of non-nociceptive cells. It should be stressed that the lack of NK-1 receptor immunoreactivity in lamina II reported by studies published so far are also in contradiction with SP binding studies, which showed intense binding in both laminae I and II (Yashpal et al., 1990; Gouardères et al., 1993; Bernau et al., 1993). This discrepancy may be due to a limitation of the antibodies used in the above studies, which may recognize only a limited population of the receptor.

SP-IR inputs and nociceptive responses

Our results strongly suggest that SP-IR inputs onto nociceptive neurons are directly related to the nociceptive response. A correlation between the intensity of the nociceptive response and the amount of SP-IR profile innervation of nociceptive neurons is also suggested by our data. We found that all three nociceptive specific neurons possessed a more abundant SP innervation than the three wide-dynamic range cells, both types of nociceptive neurons received a more abundant innervation than non-nociceptive neurons. The wide-dynamic range neurons included in this study had weaker nociceptive responses than the nociceptive specific neurons. Furthermore, in our previous study (De Koninck et al., 1992), we showed that a wide dynamic range neuron (205-1) which responded to noxious pinch with a very strong nociceptive response received a higher number of SP-IR boutons (19% for the cell body and 29% for the distal dendrites) than one (208-1) of the wide dynamic range neurons included in the current study (De Koninck et al., 1992). We did not attempt, however, to further quantify the magnitude of the slow responses. Full

quantification of the magnitude of the slow, prolonged depolarization was precluded by the presence of action potential firing and because recording would have to be performed in the presence of blockers of inhibitory transmission which may contribute to the slow, prolonged response to high intensity stimulation (Urban and Randic, 1984).

It should be stressed that two of the wide dynamic range cells of this study possessed dendritic spines and that SP-IR profiles were never seen synapsing on spines. This observation confirms the finding of our previous study that SP-IR input was always associated with aspiny dendrites or the aspiny portion of mixed dendrites (De Koninck et al., 1992).

The origin of SP-IR boutons

There are three known sources of SP immunoreactivity in the dorsal horn, primary sensory neurons in dorsal root ganglia (Cuello and Kanazawa, 1978; Hökfelt et al., 1975a), intrinsic spinal cord neurons (Hunt et al., 1981; Ljungdahl et al., 1978) and descending fibers from the brainstem (Gilbert et al., 1982; Hökfelt et al., 1978). Therefore, it was important to be able to identify the origin of the SP-IR varicosities apposed to the intracellularly labeled neurons in this study. CGRP immunoreactivity in the dorsal horn of the spinal cord might be exclusively of primary sensory origin, as it appears virtually abolished from the dorsal horn following dorsal rhizotomy (Traub et al., 1989; Chung et al., 1988); and in an *in situ* hybridization study any dorsal horn neurons synthesizing this peptide was not detected (Réthelyi et al., 1989). A high incidence of co-localization of SP and CGRP immunoreactivities has been reported in dorsal root ganglion neurons (Gibson et al., 1984;

Ju et al., 1987; Lee et al., 1985b; Wiesenfeld-Hallin et al., 1984; Garry et al., 1989) and in axon terminals within the superficial dorsal horn of the rat (Plenderleith et al., 1990; Tuchscherer and Seybold, 1989). In the cat, approximately 80% (Garry et al., 1989) or even 100% (Gibson et al., 1984) of SP-IR cells of lumbar dorsal root ganglia were shown to co-localize CGRP immunoreactivity. Therefore, it is reasonable to use the co-localization of CGRP immunoreactivity as a marker to indicate SP-IR boutons of primary sensory origin. Our results revealed that a considerable number of the SP-IR boutons apposed to nociceptive specific and wide dynamic range neurons co-localized CGRP immunoreactivity. The percentages (30-45%) of boutons co-localizing SP and CGRP detected in the current study are conservative because the post-embedding immunogold protocol for CGRP is less sensitive than the preembedding technique for SP (for a discussion, see (Ribeiro-da-Silva et al., 1993). Therefore, it is likely that an even larger proportion of SP-IR boutons is of primary sensory origin. However, some of the SP-IR boutons certainly originate from intrinsic SP-IR neurons in the spinal cord and possibly also from supraspinal sources.

It is also possible that many of the SP-IR boutons that were not CGRP-IR co-localize enkephalin immunoreactivity. In fact, in other studies we have shown that SP and enkephalin immunoreactivities are frequently co-localized in boutons apposed onto the same intracellularly labeled cell (Ribeiro-da-Silva et al., 1991a; Cuello et al., 1993).

Conclusion

The results of the present *in vivo* study in the cat spinal dorsal horn provide further evidence that there is a direct correlation between nociceptive responses of physiologically

characterized neurons and the innervation of SP-IR sensory fibers. In contrast, non-nociceptive neurons were scarcely innervated by SP-IR fibers, even in areas of intense SP immunoreactivity. The specific innervation of nociceptive neurons by SP-IR sensory fibers does not rule out the possibility that SP may also act at receptors away from the release site, as recently suggested by others. However, our data do indicate that the most likely possibility is that SP acts at a very short distance from the release site on cells in direct apposition to the nerve terminals that release the neuropeptide.

Table 1. Percentages and densities of substance P immunoreactive varicosities aposed to each of the neurons studied.

Cell type	Code	Cell body localization	Percentage of SP-IR boutons			Number of SP-IR boutons/100 μm		
			CB	PD	DD	CB	PD	DD
Nociceptive specific	207-1	LI	48.11	51.34	57.53	18.66	23.37	18.99
	271-1	LI	42.75	47.05	49.17	23.12	22.20	12.31
	276-1	LI	41.67	51.62	57.43	18.53	19.12	16.30
Wide dynamic range	276-2	LII-III	17.19	12.79	18.82	7.60	8.40	8.28
	339-1	LIV	6.09	9.76	24.67	5.17	6.33	13.02
	208-1	LIII	11.67	10.83	22.83	4.51	8.23	14.10
Non-nociceptive	271-2	LIV	4.20	3.50	3.99	2.83	3.20	2.60
	212-1	LIV	3.77	5.06	7.40	2.46	2.67	2.86
	258-1	LIV	3.70	4.10	5.46	3.67	1.92	3.14

CB - Cell body region; PD - Proximal dendritic tree; DD - Distal dendritic tree.

Table 2. Comparison of the percentages of SP-IR boutons apposed to the distal dendrites of wide dynamic range, nociceptive specific and non-nociceptive in areas of intense SP immunoreactivity (laminae I-IIo and patches of SP immunoreactivity in lamina V) and areas of sparse SP immunoreactivity (laminae III-IV)

Cell type	Laminae I-IIo and V*	Laminae III-IV
Nociceptive specific	54.33±4.62	N/A
Wide dynamic range	29.15±2.26	5.87±1.34
Non-nociceptive	4.73±1.31	5.47±1.17

* - Values from lamina V were restricted to boutons apposing dendrites located in the patches of intense SP immunoreactivity which are characteristic of lamina V (see text). N/A - Not applicable, as the nociceptive specific cells of this study did not have processes in these two laminae.

Figure 1. Characteristic responses of a wide dynamic range neuron (cell 339-1) to noxious and innocuous natural stimuli and to high intensity electrical stimuli of a sensory nerve. The innocuous stimulus consisted of repetitive movements of hairs in the excitatory receptive field of the neuron; the periods of delivery of the stimulus are indicated by the bars below the records in **a** and **b**. The response to this innocuous stimulus consisted of brief bursts of action potentials to each movement. The noxious stimulus was a pinch to the excitatory receptive field using a serrated forceps; the duration of this stimulus is represented by the bar below the record in **c**. The response to this stimulus consisted of an initial depolarization associated with a high frequency of action potentials throughout the stimulus. This was followed by a small but prolonged depolarization associated with a rate of discharge of action potentials which remained above the pre-stimulus level for greater than one min; the full duration of this prolonged response is not shown. The response to high intensity (5 mA, 1 ms pulses at 20 Hz for 8 s) electrical stimulation of the superficial peroneal nerve (Train) is shown in **d**. This response consisted of an initial depolarization and high frequency of action potentials throughout the stimulus followed by a prolonged depolarization also associated with a high rate of discharge of action potentials. During the recording from this neuron the responses shown in **a** and **d** were tested for the effects of the NK-1 receptor antagonist, CP-99,994, given i.v. at a dose of 0.5 mg/kg. The response to hair movement was unaffected by administration of this antagonist, as shown in **b**, taken 3 min later. In contrast, the response to the high intensity electrical stimulation was depressed by the NK-1 receptor antagonist as shown in **c**; the depolarizations during and following the stimulus were depressed as was the frequency of action potentials during the afterdischarge.

Resting membrane potential -60mV.

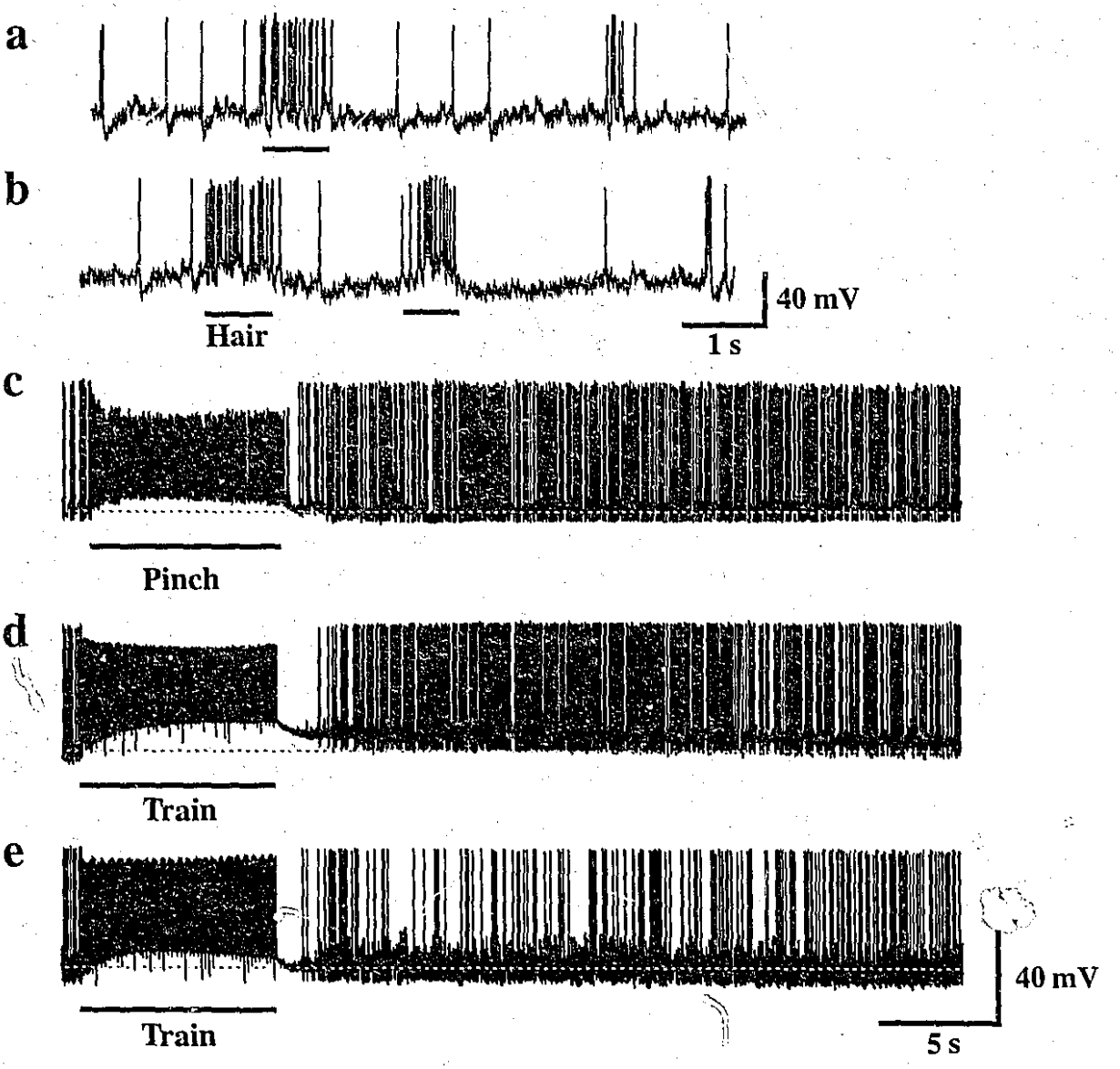
a
b
40 mV
Hair
1 s
c
Pinch
d
Train
e
Train
40 mV
5 s

Figure 2. Effects of noxious and innocuous natural stimuli to the excitatory receptive field of a non-nociceptive neuron (cell 271-2). **A.** Responses to repetitive movements of hairs, as described in Figure 1. **B.** Noxious pinch stimulation of the cutaneous receptive field failed to produce the slow, prolonged depolarization observed with the cell in Figure 1. Rather, the neuron showed only a depolarization and high rate of action potentials only throughout the period of the pinch, consistent with sustained activation of low threshold primary afferents. Effects of noxious pinch stimulation were routinely tested while holding the membrane potential at three different levels to determine whether the slow, prolonged depolarization could have been masked at hyperpolarized potentials (De Koninck and Henry, 1991). In the record in which the membrane was held at -55mV, the stimulus was maintained for a longer period in a further effort to unmask any slow, prolonged depolarization. In the bottom record single, low intensity electrical stimuli were also applied to the superficial peroneal nerve at regular intervals (small triangles below the trace) to provoke action potentials. Resting membrane potential -65 mV.

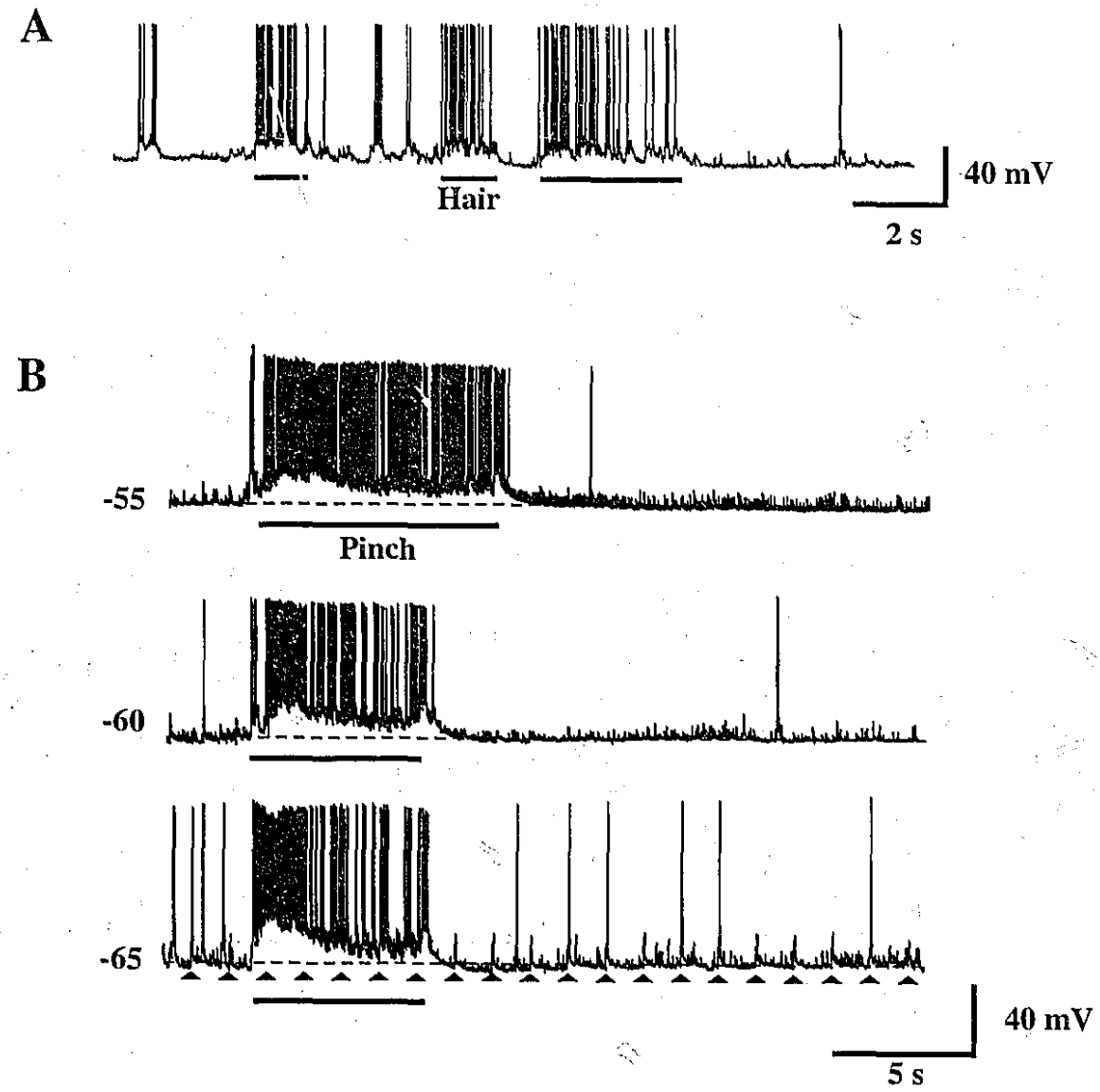
A
Hair
40 mV
2 s
B
-55
Pinch
-60
-65
40 mV
5 s

Figure 3. Morphological properties of a wide dynamic range neuron 208-1 (1). **A.** *Camera lucida* reconstruction of the neuron in the parasagittal plane. The cell, with its cell body located in dorsal lamina III, had an extensive dendritic tree in lamina III and two major dendrites extending to lamina IIo. The latter dendrites branched in lamina IIo, an area of intense SP immunoreactivity. Note the large number of spines on the dendrites in lamina III, some of which are indicated with small arrows (scale bar = 150 μm). **B.** Light micrograph of the neuron in a parasagittal, Epon-embedded 50-μm-thick section; note the intense SP immunoreactivity in laminae I and IIo at the top of the photomicrograph (scale bar =100 μm). **C.** Micrograph from a 4-μm-thick section taken from the section in B, displaying the cell body and segments of dendrites (scale bar = 100 μm). **D.** Low magnification electron micrograph of part of the cell body, obtained from an ultrathin section cut after re-embedding in Epon of the semithin section in C (scale bar =10 μm). **E.** A SP-IR bouton (arrow) is presynaptic to the HRP-filled cell body (scale bar = 0.5 μm).

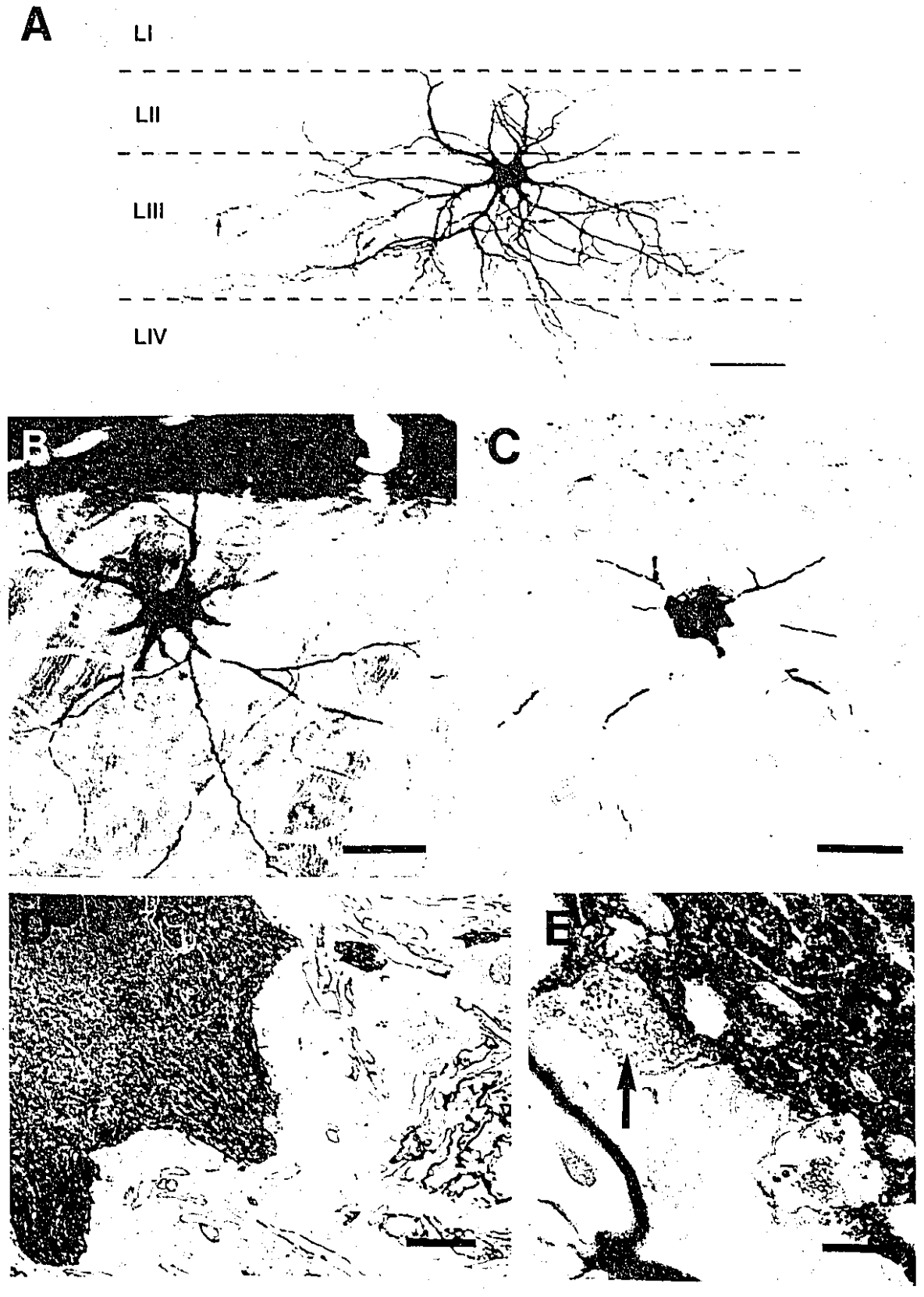
A
LI
LII
LIII
LIV
B
C
D
E

Figure 4. Morphological properties of a wide dynamic range neuron 208-1 (2). **A.** Micrograph from a 4-μm-thick semithin section, showing three segments of dendrites in lamina IIo (upper dendrite) and lamina IIi (two other dendrites). The portions of the dendrites labeled 1, 2 and 3 are illustrated in the electron micrographs in B, C and D, respectively, which were obtained after re-embedding and cutting of this semithin section (scale bar = 25 μm) **B.** A SP-IR bouton (arrow) presynaptic to HRP-filled dendrite (1) in lamina IIo (scale bar = 0.5 μm). **C.** A SP-IR bouton of the glomerular type (arrow) is at a distance from the dendritic profile (2) of the cell. This type of SP-IR profile did not contact this cell or any of the others studied (scale bar = 3 μm). **D, E.** This neuron had dendrites frequently associated with synaptic glomeruli in lamina IIi (**D**) and III (**E**), but these glomeruli always possessed central varicosities (C_{II}) which were not SP-IR. The arrow in **D** points to a SP-IR profile (scale bars = 1 μm).

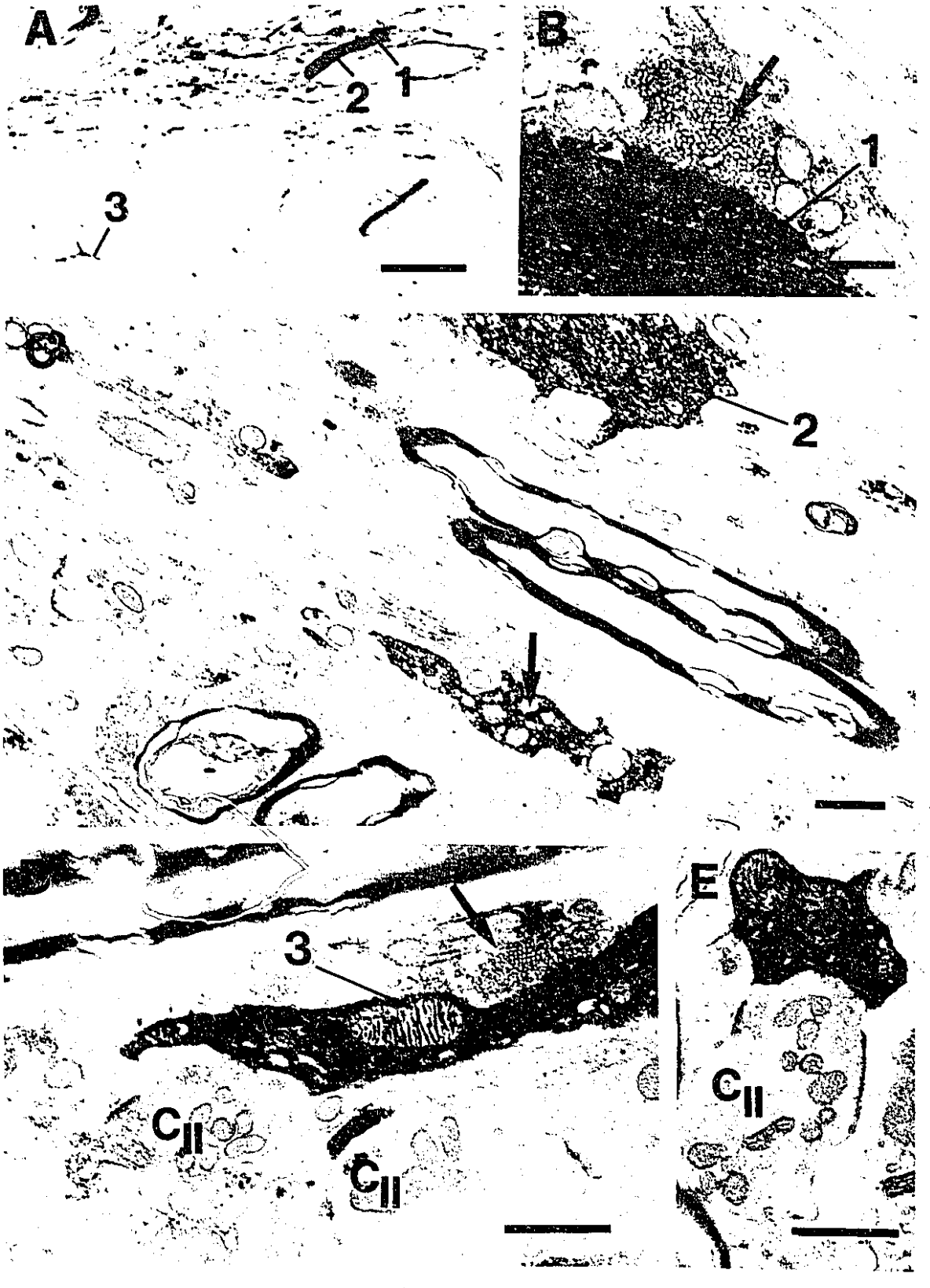
A
1
2
3
B
1
C
2
D
3
CII
CII
E
CII

Figure 5. Morphological properties of wide dynamic range neuron 339-1 (1). **A.** *Camera lucida* reconstruction of the cell in the parasagittal plane. Note that this neuron is almost entirely devoid of dendritic spines, in contrast to the wide dynamic range neuron shown in Figure 3 (scale bar = 50 μm). **B.** Micrograph of part of the cell, obtained from a 50-μm-thick section; open arrow indicates one of the patches of intense SP immunoreactivity which are characteristic of lamina V (scale bar = 50 μm). **C.** Micrograph from a 4-μm-thick section of the cell body region obtained after Epon re-embedding of the 50-μm-thick section from B ; the arrow indicates the location of the SP-IR bouton shown in the EM micrographs (scale bar = 50 μm). **D, E.** Electron micrographs of the cell body area obtained after further re-embedding of the 4-μm-thick section shown in C; arrows indicate a SP-IR bouton; asterisks in E indicate non-IR vesicle-containing profiles apposed to the cell body. Note the relative scarcity of SP-IR boutons apposed to the cell body (scale bars = 10 μm for D and 1 μm for E).

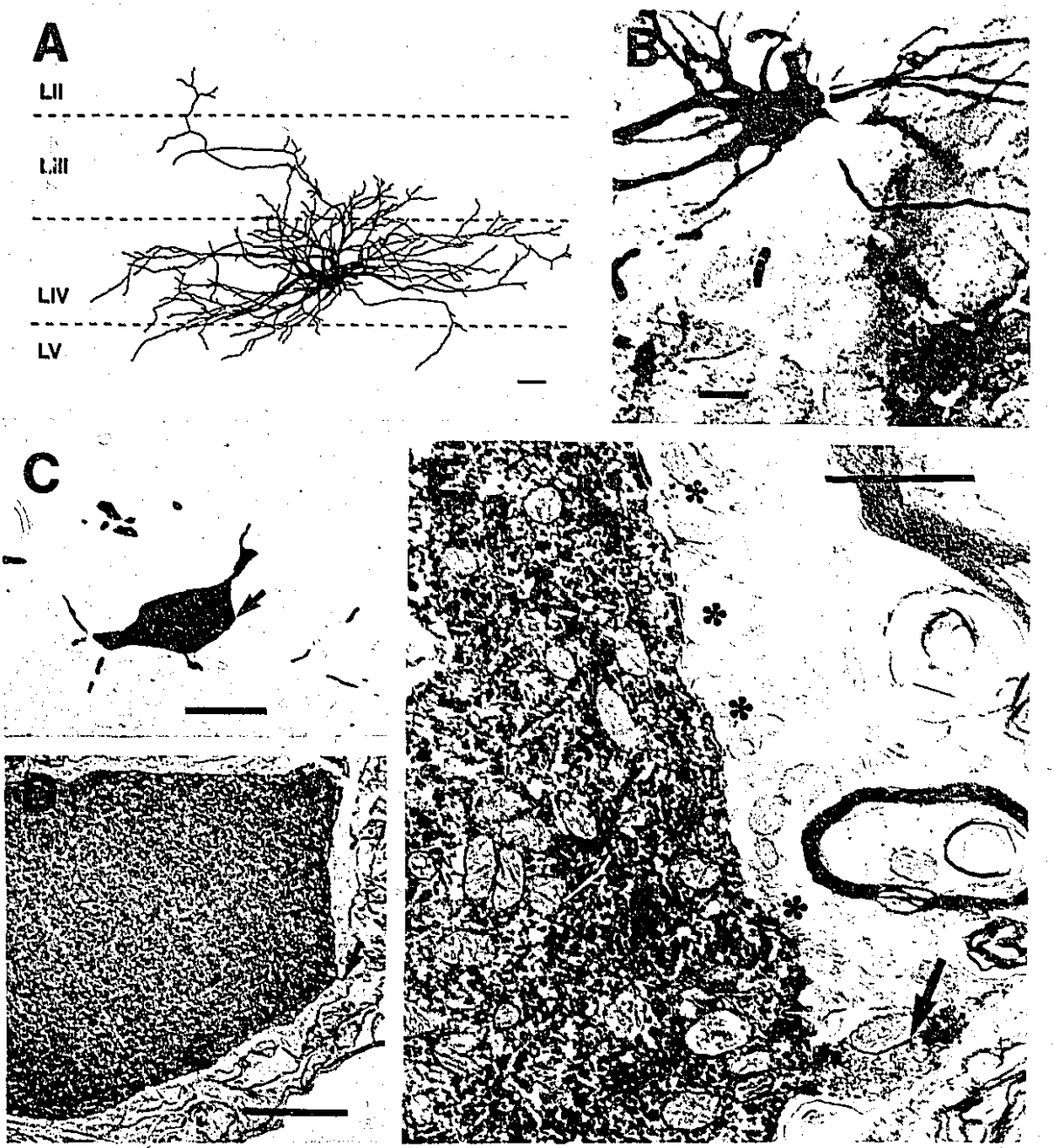
A
LII
LIII
LIV
LV
B
C
D
E

Figure 6. Morphological properties of wide dynamic range neuron 339-1 (2). **A** and **B**. Light micrographs of 50-μm-thick and 4-μm-thick sections, respectively. Open arrows indicate one of the patches of intense SP immunoreactivity in lamina V. Solid arrows indicate the locations in two dendritic branches of the electron micrographs in **C** (upper arrows) and **D** (lower arrows). **C** and **D**. Electron micrographs obtained after Epon re-embedding and ultrathin sectioning of the 4-μm-thick semithin section in **B**; arrows indicate SP-IR boutons apposed to the cell, and arrowheads indicate asymmetric synapses between the SP-IR profiles and the dendritic profiles (areas of synapses are enlarged in the respective insets). The asterisks represent non-IR varicosities. Scale bars = 50 μm (**A** and **B**) and 0.5 μm (**C** and **D**).


A
B
C
D

Figure 7. Morphological properties of nociceptive specific neuron 271-1. **A.** *Camera lucida* reconstruction of the cell (scale bar = 20 µm). **B.** Micrograph from a 4-µm-thick section obtained from the re-embedding and cutting of the 50-µm-thick flat-embedded section (not shown). Note parts of the neuronal cell body and of two dendrites apposed by numerous SP-IR profiles (small arrows). **C, D.** Electron micrographs obtained from an ultrathin section cut after the re-embedding of the section shown in B ; arrows show SP-IR boutons apposed to the dendrites of the cell, and arrowheads indicate synaptic contacts. In **D**, note the asymmetric synapse (arrowhead) of the bouton on the left onto the dendrite of the cell. Scale bars = 20 µm for A and B, and 0.5 µm for C and D.

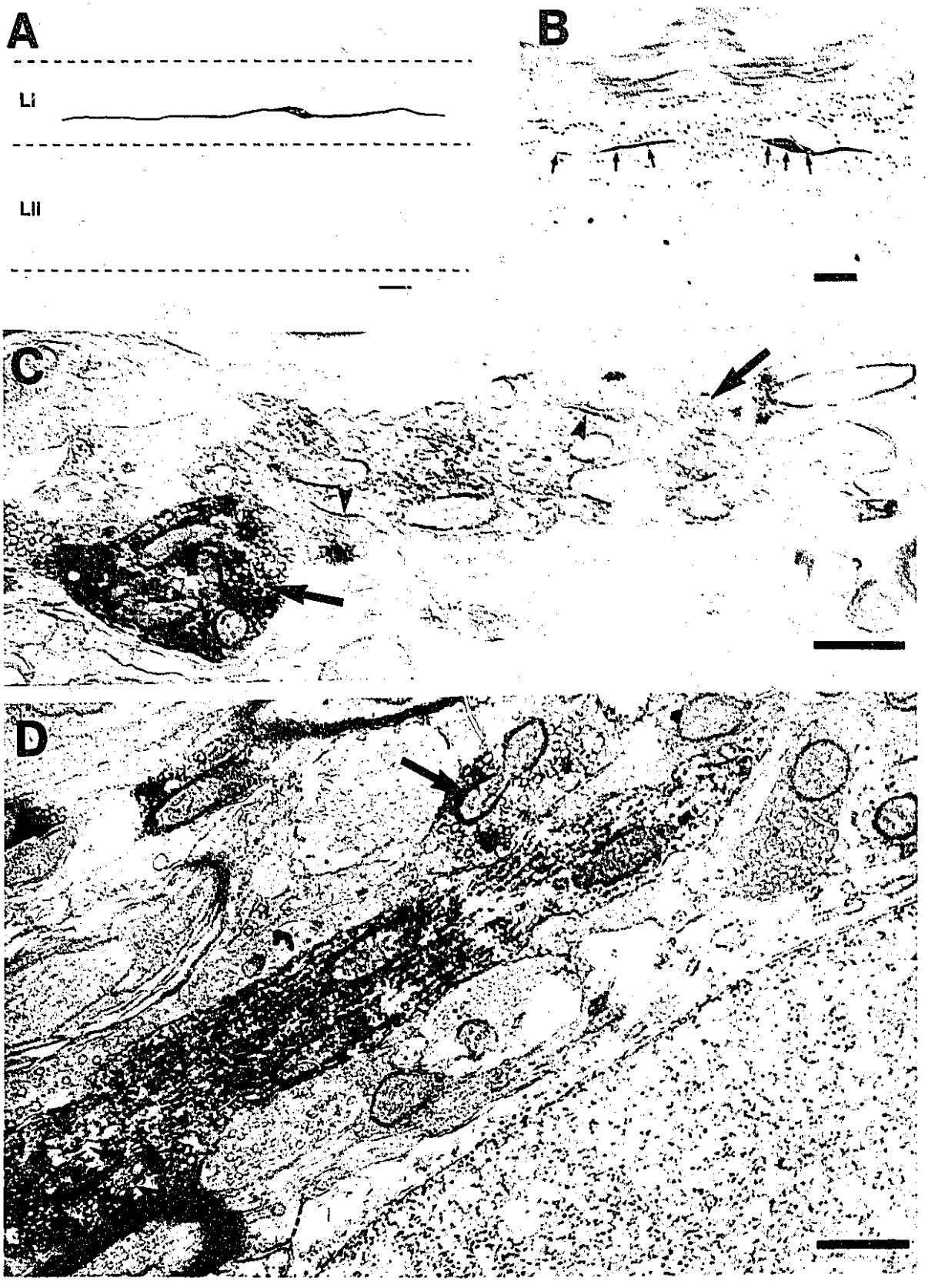
A
LI
LII
B
C
D

Figure 8. Morphological properties of nociceptive specific neuron 207-1 (2). **A.** *Camera lucida* reconstruction of the cell. Note the ventrally oriented dendritic branches reaching inner lamina II. Note also a dorsally oriented primary dendrite with a long branch extending into the white matter (scale bar = 100 μm). **B.** A micrograph of a parasagittal, 50-μm-thick section of the neuron prior to osmication. Note the intense SP immunoreactivity around the cell body and main dendrites (scale bar = 50 μm). **C.** Light micrograph of a 4-μm-thick section cut from the section shown in B after Epon-embedding (scale bar = 20 μm). **D.** Electron micrograph of a proximal dendrite corresponding to the dendrite indicated with an arrow in C . Note the SP-IR varicosities (arrows) apposed to the HRP-filled dendrite (scale bar = 1 μm).

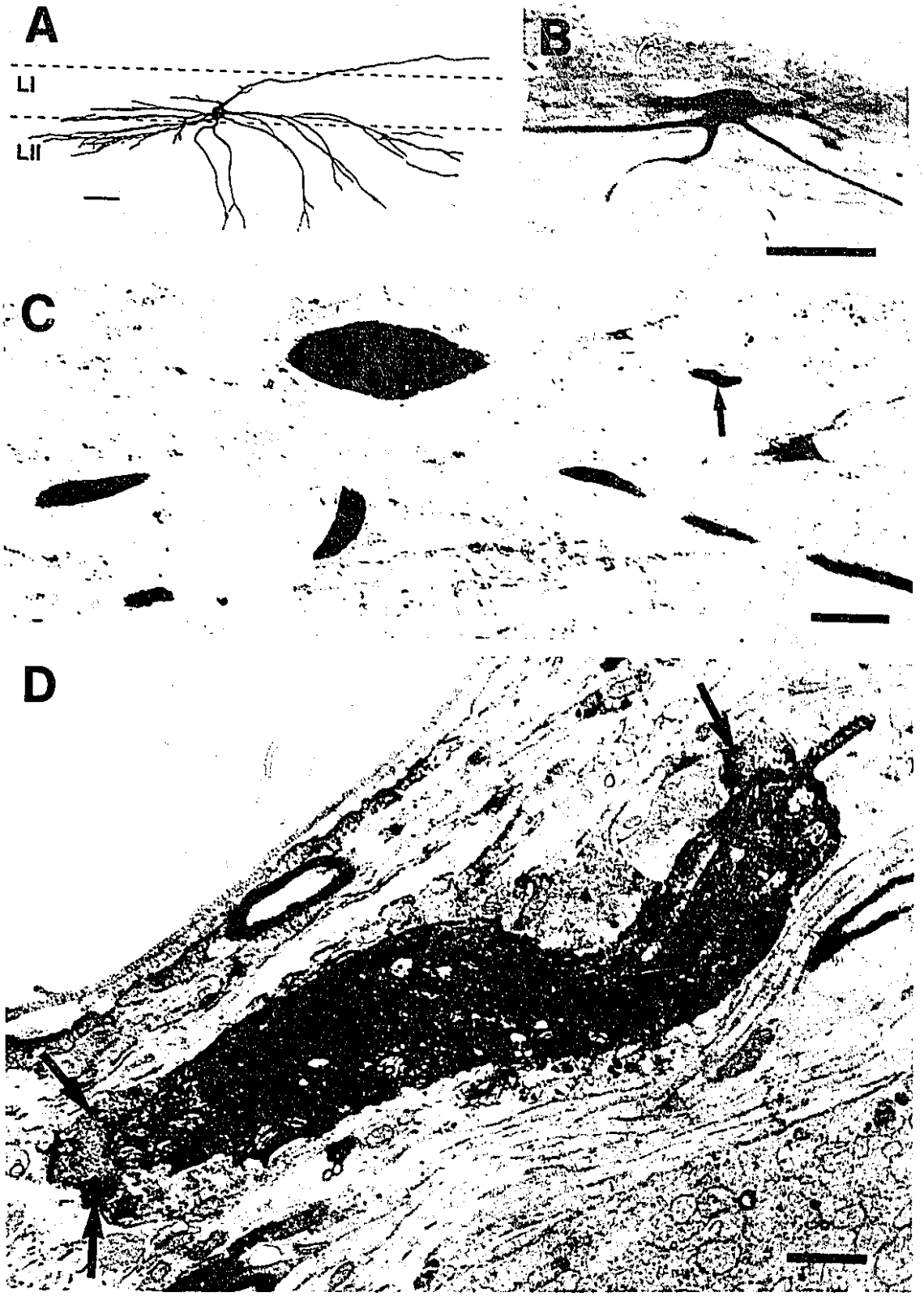
A
LI
LII
B
C
D

Figure 9. Morphological properties of nociceptive specific neuron 207-1 (2). **A.** Light micrograph of a distal dendrite located in lamina II in a 4-μm-thick section. Note the intense SP immunoreactivity. The large arrows point to the HRP-filled dendrite, the short arrows indicate SP-IR varicosities (scale bar = 20 μm). **B.** Electron micrograph of the dendrite indicated with the arrows in **A. C.** An enlargement of the framed area in **B**. The arrows indicate SP-IR axonal varicosities apposed to the HRP-filled dendrite (Scale bars= 20 μm for A , 2 μm for B , and 1 μm for C).

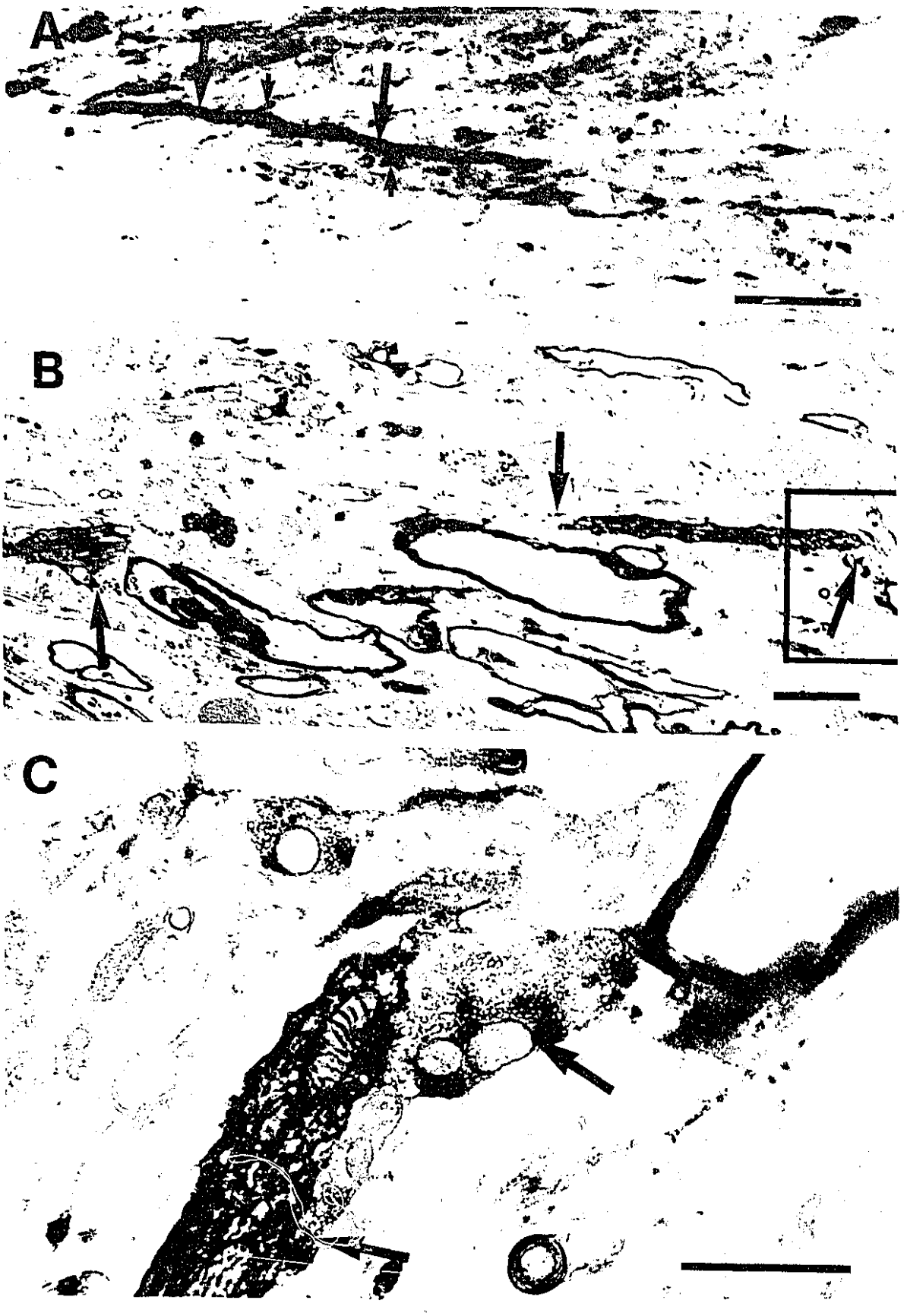
A
B
C

Figure 10. Morphological properties of non-nociceptive neuron 271-2. The electrophysiological recordings of this cell are shown in Figure 2. **A.** *Camera lucida* reconstruction of the cell. Note the extensive arborization in lamina III, a region where abundant hair afferents terminate, and also the spines on the dendrites to the right of the perikaryon (scale bar = 50 μm). **B.** Light micrograph of a 50-μm-thick Epon-embedded section showing the cell body and a portion of dendritic tree. Note the virtual absence of SP-IR fibers in the vicinity of this cell (scale bar = 100 μm). **C** shows an electron micrograph of the portion of the dendrite indicated with an arrow in **B**; note the scarcity of SP-IR boutons apposed to this neuron (arrow indicates a SP-IR bouton; scale bar = 2 μm).

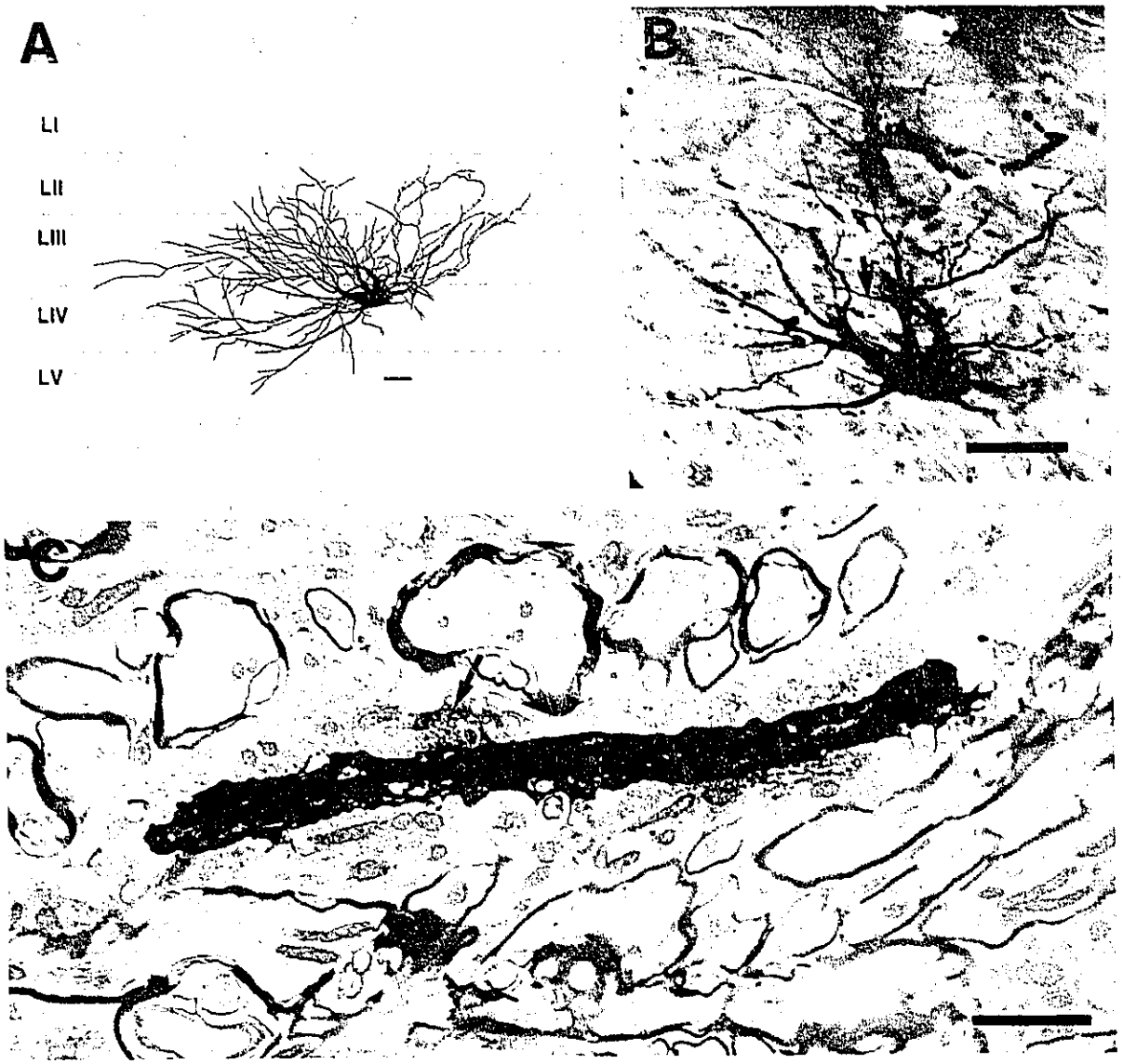
A
LI
LII
LIII
LIV
LV
B
C

Figure 11. Morphological properties of non-nociceptive neuron 212-1. **A.** *Camera lucida* reconstruction of the neuron. The axon of this neuron could be followed into the dorsolateral funiculus (scale bar = 100 μm). **B.** Light micrograph of a 50-μm-thick, Epon-embedded section showing branching of the dendrites of the cell; note that some dendritic branches penetrate the area of intense SP immunoreactivity in lamina IIo (scale bar = 100 μm). **C.** A 4-μm-thick semithin section obtained after re-embedding of the section in **B**; note the axon-like dendritic spines (arrows) originating from the dendrites (scale bar = 25 μm). **D.** Electron micrograph illustrating a dendritic spine (arrow, scale bar = 3 μm). **E.** Electron micrograph showing the participation of a dendritic branch of the cell in a synaptic glomerulus. The glomerular central varicosity (C_{II}) apposed to the dendrite is electron-lucent and rich in mitochondria (scale bar = 1 μm).

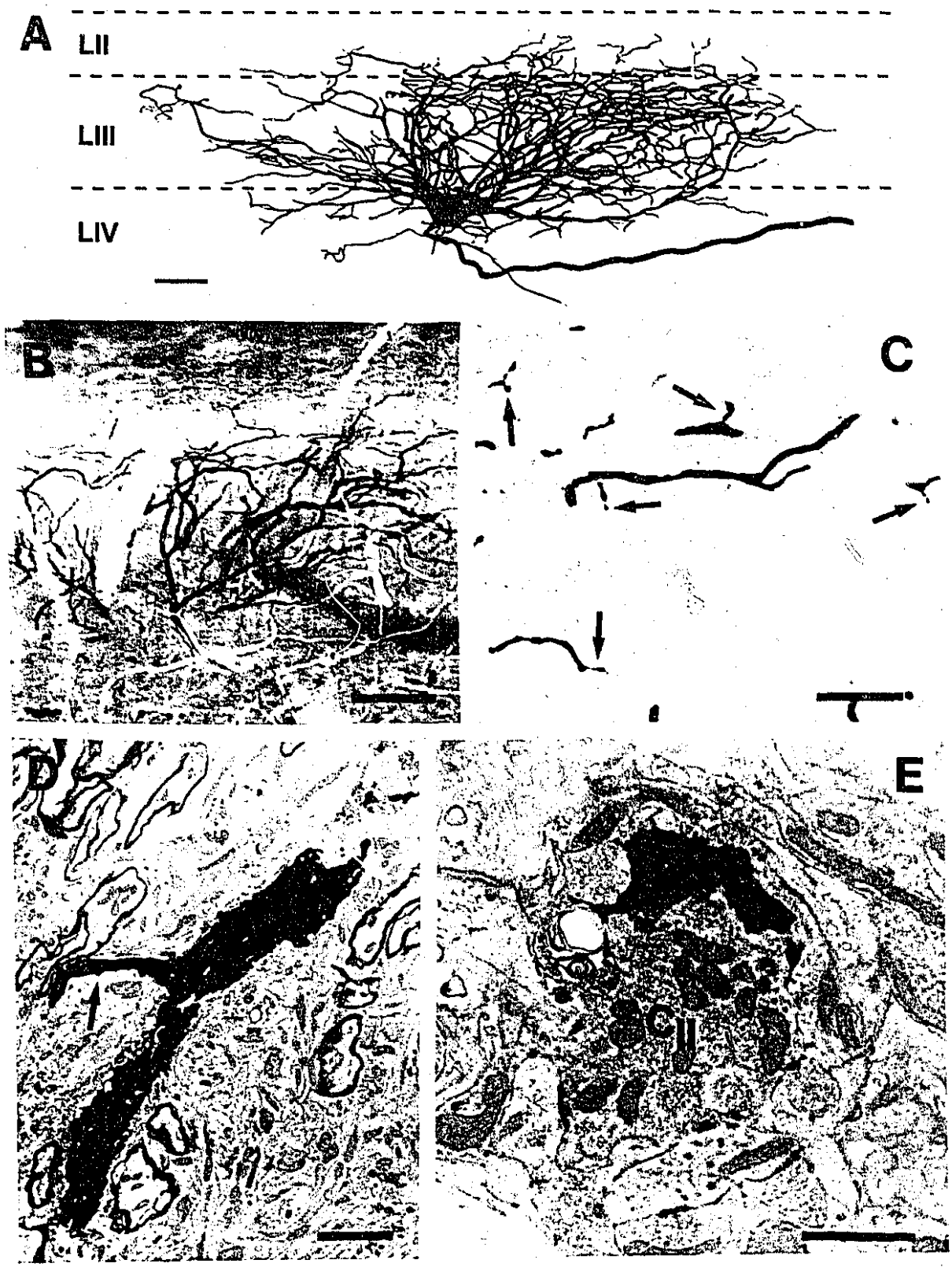
A
LII
LIII
LIV
B
C
D
E
CII

Figure 12. Quantitative analysis of the boutons contacting the physiologically characterized dorsal horn neurons. For statistical comparison, one-way ANOVA followed by post-hoc Tukey test was used. **A.** The densities of total boutons (number of SP-IR and non-IR boutons/100 μm membrane length) apposed to the cell body, proximal and distal dendrites were not significantly different between the three types of neurons ($P=0.5$, mean±.SEM, n=3). In **B**, the densities of SP-IR boutons apposed to the cell bodies and the proximal dendrites of nociceptive specific cells were significantly higher than these of wide dynamic range ($P<0.01$, mean±SEM, n=3), but the values for the distal dendrites were not significantly different between the two types of cells. Compared with non-nociceptive neurons, the densities of SP-IR boutons apposed to the three regions of nociceptive specific neurons were significantly increased ($P<0.01$, mean±SEM, n=3). The densities of SP-IR boutons apposed to the proximal dendrites and the distal dendrites of wide dynamic range neurons were significantly higher than these of non-nociceptive neurons, but no significant differences of the values for the cell body region were detected between the two types of cells. In **C**, the percentages of SP-IR boutons apposed to the three regions of nociceptive specific neurons were significantly higher than these of wide dynamic range and non-nociceptive neurons ($P<0.001$, mean±SEM, n=3). The values for the three regions of wide dynamic range neurons were significantly higher than those of non-nociceptive neurons ($P<0.01$, mean±SEM, n=3).

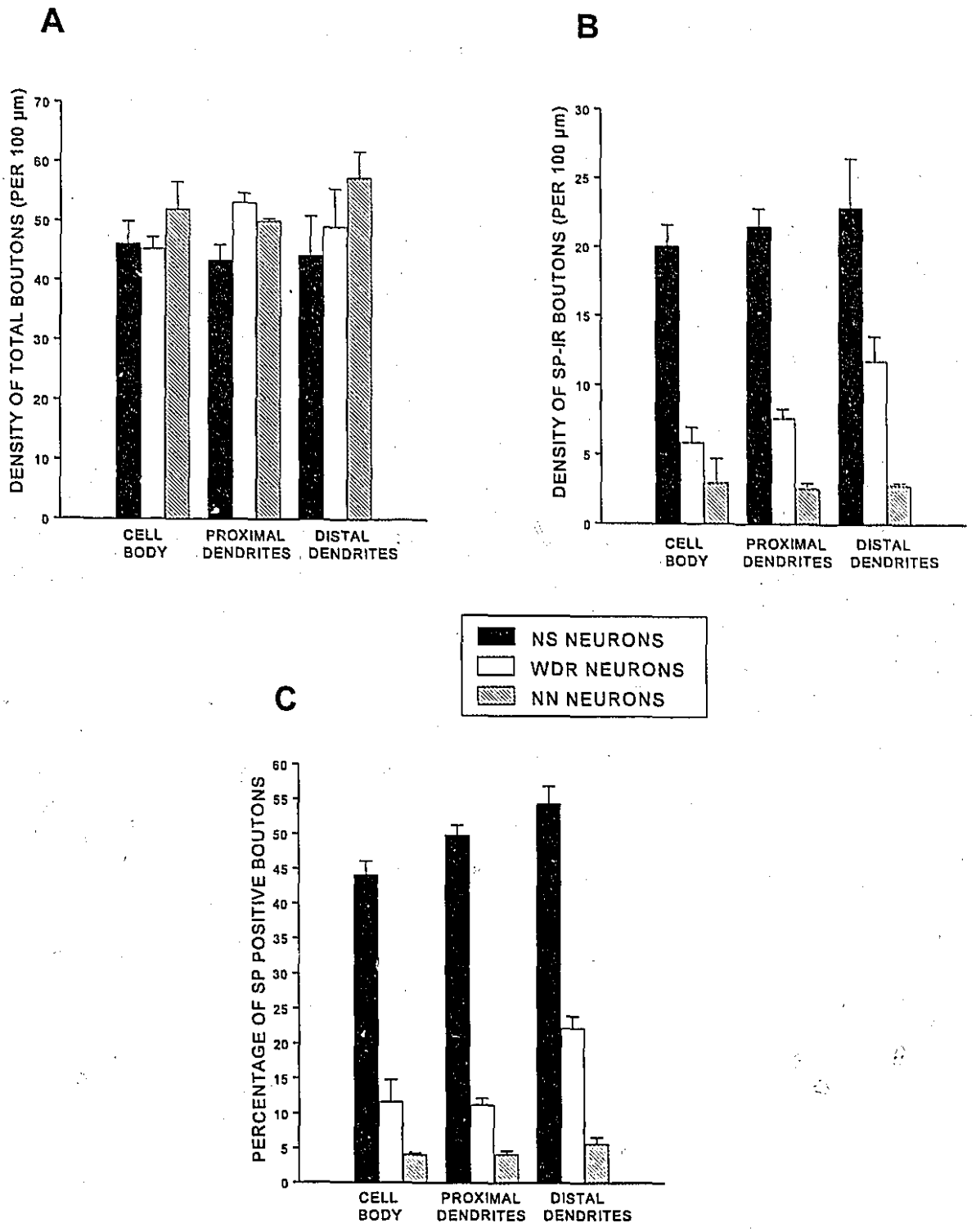
A
DENSITY OF TOTAL BOUTONS (PER 100 µm)
0
10
20
30
40
50
60
70
CELL BODY
PROXIMAL DENDRITES
DISTAL DENDRITES
B
DENSITY OF SP-IR BOUTONS (PER 100 µm)
0
5
10
15
20
25
30
CELL BODY
PROXIMAL DENDRITES
DISTAL DENDRITES
NS NEURONS
WDR NEURONS
NN NEURONS
C
PERCENTAGE OF SP POSITIVE BOUTONS
0
5
10
15
20
25
30
35
40
45
50
55
60
CELL BODY
PROXIMAL DENDRITES
DISTAL DENDRITES

Figure 13. Co-localization of SP and CGRP immunoreactivities in boutons apposed to nociceptive specific neuron in lamina I (cell 276-1). **A.** Distal dendrites (asterisks) in lamina I from this nociceptive specific neuron are innervated by axonal boutons in which SP and CGRP immunoreactivities are co-localized (labeled SP+CGRP). SP immunoreactivity is represented by DAB reaction products and CGRP immunoreactivity by immunogold particles (scale bar = 0.5 μm). **B** shows the framed area in A at higher magnification and printed with lower contrast to allow the easy identification of the gold particles over dense-core vesicles, representing CGRP immunoreactivity (scale bar = 0.5 μm).

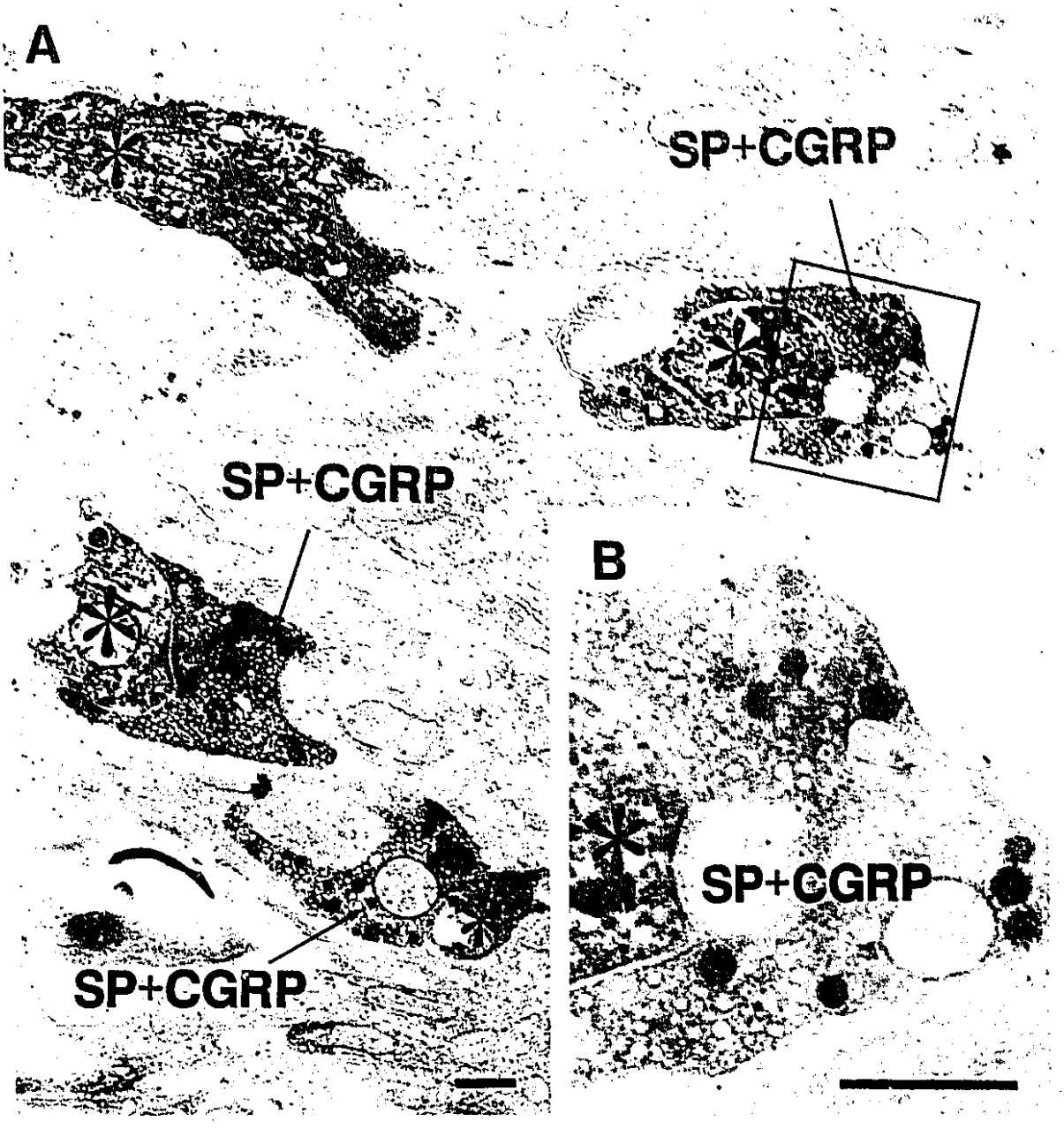
A
SP+CGRP
SP+CGRP
SP+CGRP
B
SP+CGRP

Connecting Text - Chapter II to Chapter III

The study in chapter II demonstrated that nociceptive neurons received significantly higher percentages and densities of appositions from SP-IR boutons in the cell bodies, proximal and distal dendrites than non-nociceptive neurons. Furthermore, nociceptive specific neurons were apposed by significantly higher percentages of SP-IR boutons in the three regions than wide dynamic range neurons. The densities of SP-IR boutons apposed to the cell bodies and the proximal dendrites nociceptive specific neurons were significantly higher than in wide dynamic range neurons, but this difference of the values was not detected in the distal dendritic region. For wide dynamic range neurons, the percentages of SP-IR boutons apposed to these distal dendrites located in laminae with intense SP immunoreactivity were significantly higher than those located in laminae with scarce SP immunoreactivity. Even in laminae with intense SP immunoreactivity, the distal dendrites of non-nociceptive neurons received very low percentages of appositions from SP-IR boutons. About one third SP-IR boutons apposed to nociceptive neurons co-localized CGRP immunoreactivity. Based on the above results, and on those from previous studies, it was proposed that SP-IR boutons apposed to nociceptive neurons might interact with ENK-containing elements involved in the inhibition of nociception.

The experiments presented in the next chapter were designed to test such an hypothesis. In chapter III, the synaptic interactions of SP-IR boutons and ENK-IR boutons in relation to the three functional types of dorsal horn neurons were investigated.

CHAPTER III

Substance P and enkephalin immunoreactivities in axonal boutons presynaptic to physiologically identified dorsal horn neurons. An ultrastructural multiple-labelling study in the cat spinal cord.

Weiya Ma, A. Ribeiro-da-Silva,Y. De Koninck, V. Radhakrishnan, J.L. Henry and A.C. Cuello

ABSTRACT

In the present study, we used a combination of intracellular electrophysiological recording and intracellular injection of horseradish peroxidase with ultrastructural immunocytochemistry to investigate the synaptic inputs from substance P (SP)-, enkephalin (ENK)-, and SP+ENK- immunoreactive (IR) axonal boutons to three types of functionally characterized dorsal horn neurons in the cat spinal cord.

The dorsal horn neurons were classified as nociceptive specific, wide dynamic range and non-nociceptive based on their responses to innocuous and noxious stimuli. At the EM level, we found that most of the nociceptive neurons (either nociceptive specific or wide dynamic range) contained ENK immunoreactivity, but that none of the non-nociceptive neurons was ENK immunoreactive. Furthermore, we observed that SP-IR, ENK-IR and SP+ENK-IR axonal boutons were apposed to the functionally characterized dorsal horn neurons. Our quantitative data revealed that the percentages of SP-IR only boutons apposed to the cell bodies, proximal dendrites and distal dendrites of nociceptive neurons were significantly higher than those of non-nociceptive neurons. Further, the percentages of SP+ENK-IR axonal boutons apposed to the distal dendrites of nociceptive neurons were significantly higher than those of non-nociceptive neurons, the percentages of ENK-IR only boutons apposed to the cell bodies and proximal dendrites of nociceptive neurons were significantly higher than in non-nociceptive neurons. However, no significant differences in the values for the distal dendrites were detected between nociceptive neurons and non-nociceptive neurons. Both ENK-IR only and SP+ENK-IR boutons were never seen

presynaptic to SP-IR only boutons apposed to nociceptive neurons. One third of the axonal boutons exhibited synaptic contacts with the dorsal horn neurons independently of their neurochemical contents and the physiological properties of the apposed neurons.

Our data provide anatomical substrates for the interaction of SP and ENK and support the idea that the modulation of nociception by ENK is mainly through a postsynaptic mechanism.

INTRODUCTION

It is generally accepted that substance P (SP) and enkephalin (ENK) are involved in the transmission/modulation of nociception in the spinal and medullary dorsal horns. The investigation of the interactions of SP and ENK in the spinal dorsal horn has received particular attention in the past two decades. Anatomically, SP and ENK immunoreactivities are similarly localized in the lamina I and II (Cuello et al., 1977b; Hökfelt et al., 1977; Cuello and Kanazawa, 1978; Hunt et al., 1981), and also in lamina V (Ruda, 1982). SP immunoreactive (IR) terminals make synaptic contacts with ENK-IR neurons in the superficial dorsal horn (Cuello, 1983; Ribeiro-da-Silva et al., 1991b). Co-localization of SP and ENK immunoreactivities was found in axonal boutons in the superficial laminae of the dorsal horn of cat (Tashiro et al., 1987) and rat (Senba et al., 1988; Ribeiro-da-Silva et al., 1991b). Biochemically, SP was shown to stimulate the release of endogenous opioid peptides at spinal (Tang et al., 1983; Iadarola et al., 1986) and supraspinal (Naranjo et al., 1986)

levels. Behaviorally, the intrathecal administration of SP in the rat produces a transient decrease in the reaction time in the tail flick test (Yashpal and Henry, 1983; Cridland and Henry, 1988b), followed by a rebound overshoot which is blocked by naloxone (Yashpal and Henry, 1983), suggesting the activation of an opioid mechanism at the spinal level, due either to SP or to SP induced activation of spinal nociceptive pathways. When co-administrated intrathecally, a low dose of SP was shown to potentiate the antinociceptive effects of morphine sulphate at a marginally effective dose in the tail flick test (Kream et al., 1993). The potentiated analgesic response was effectively blocked by the opioid antagonist naloxone, suggesting a convergence of pharmacological effects through opioid-responsive neurons.

However, there is scarce information on anatomical substrates for the functional interactions of SP and ENK. In recent years, we have investigated the direct synaptic interactions of SP and ENK immunoreactive elements in relation to functionally characterized dorsal horn neurons in the cat spinal cord, with the specific aim of providing more convincing anatomical substrates to interpret these functional phenomena. Using a combination of physiological recording, intracellular injection of horseradish peroxidase (HRP) and immunocytochemistry at the electron microscopy level, we previously demonstrated that some nociceptive dorsal horn neurons possessed ENK immunoreactivity, whereas none of the non-nociceptive neurons was ENK immunoreactive (Ribeiro-da-Silva et al., 1992). In the present study we investigated the synaptic interactions of SP-IR and ENK-IR axonal boutons with nociceptive and non-nociceptive neurons in the dorsal horn of the cat spinal cord. Preliminary results were published elsewhere (Cuello et al., 1993).

MATERIALS AND METHODS

Physiological recording and intracellular injection of HRP

Ten adult cats of either sex, with body weights ranging from 3.2 to 4.6 kg, were anesthetized with ∝-chloralose (60 mg/kg i.v.) and paralyzed with pancuronium bromide (Pavulon, Organon; 1 mg/kg i.v.). The cats were ventilated artificially. To minimize the influence of supraspinal structures, the spinal cords were transected at the L_1 vertebral level. Intracellular recording was done with HRP-filled glass micropipettes (resistances: 50 to 120 MΩ) at the L_5-L_7 spinal level. A neuron was processed further only if it exhibited a stable resting membrane potential, an action potential with overshoot and a clear, reproducible response to natural stimulation of the skin.

Functional classification of the neurons was made according to their responses to natural cutaneous stimulation and to electrical stimulation of afferent nerves following previously described criteria (De Koninck et al., 1992). Briefly, the natural stimuli used were: movement of single hair, innocuous and noxious pressure, noxious pinch with a serrated forceps, noxious radiant heat and vibration using a feedback controlled mechanical stimulator. Neurons were categorized as non-nociceptive, wide dynamic range and nociceptive specific. Nociceptive neurons, including both nociceptive specific and wide dynamic range neurons, exhibited a nociceptive response to noxious stimulation characterized by a slow, prolonged depolarization after the end of the stimulus and an afterdischarge. Nociceptive specific neurons responded only to noxious stimuli. Wide dynamic range neurons responded to both innocuous and noxious stimuli. Non-nociceptive

neurons did not display the above type of response after noxious stimulation and exhibited only brisk and brief responses to any kind of stimuli.

Following complete electrophysiological recording and functional identification of the neuron, a tracer, horseradish peroxidase (HRP), was injected by intracellular iontophoresis using 600 ms positive current pulses of 1-5 nA at a frequency of 1 Hz for a duration of 10-30 minutes. The injection times varied with the type of neuron injected. One to three neurons were injected per cat and a map of the dorsal surface of the cord was drawn to ensure exact localization and identification of the labelled cells.

Immunocytochemistry

Subsequently, all cats were perfused intracardially, for 30 minutes, with a mixture of 4% paraformaldehyde and 0.5% glutaraldehyde in 0.1M phosphate buffer (PB) (pH 7.4) at room temperature. The relevant segments of the spinal cord were removed and postfixed in the same fixative for 90 minutes and then infiltrated overnight in 30% sucrose in 0.1M (PB). The following day, the tissue was sectioned parasagittally on a Vibratome at a thickness of 50 μm. After being snap frozen in liquid nitrogen and thawed in 0.1M PB at room temperature to increase the penetration of antibodies, all sections were processed to demonstrate HRP with 3,3'-diaminobenzidine (DAB, Sigma) intensified with cobalt chloride and nickel ammonium sulphate as previously described (Ribeiro-da-Silva et al., 1993) and examined under the light microscope. The sections containing the labelled cells were further processed for pre-embedding immunocytochemistry. The antibodies used were an anti-substance P/anti-HRP bi-specific monoclonal antibody from the rat [coded P4C1; (Suresh

et al., 1986); Medicorp, Canada], and an anti-enkephalin internally radiolabeled monoclonal antibody, prepared from the NOC1 cell line as described elsewhere (Cuello and Côté, 1993). The sections were first incubated in a mixture of P4C1 (1:10) and NOC1 (1:10) antibodies overnight at 4^0C. The following day, all sections were incubated in 5 µg/ml HRP (Sigma, type VI) in phosphate buffered saline (PBS) for 2 hours at room temperature, following thorough rinsing in PBS. A non-intensified DAB reaction was used to show SP immunoreactivity.

Subsequently, all sections were osmicated, dehydrated, and flat-embedded in Epon. The different parts of the HRP labelled neuron, as observed in flat-embedded slices, were photographed and drawn with a *camera lucida*. The whole morphology of the HRP labelled neuron at the light microscopy (LM) level was reconstructed. Using Sholl's concentric circle analysis (Sholl, 1953), the whole neuron was divided into three regions. The dendrites located in the inner circle were considered as the proximal dendrites, while those located in the outer circle represented the distal dendrites. The dendritic segments which were located in the middle circle were not used in order to avoid the overlapping of proximal and distal dendrites. The samples of the different regions of the HRP labelled neuron (cell body, proximal and distal dendrites) were selected and re-embedded in Epon blocks. From re-embedded blocks, 4-µm-thick plastic sections were cut serially, photographed and compared to the original drawings for the identification of the parts of the HRP labelled neuron present in each section. The 4-µm-thick sections were then re-embedded in Epon and sectioned for electron microscopic observation. The ultrathin sections were processed for electron microscopic radioautography as described previously, using the physical fine grain

development (Kopriwa, 1975) or Kodak D19b (Kopriwa, 1973). Exposure time was 3 months. After contrast staining with uranyl acetate and lead citrate, the radioautograms were observed under a Philips 410 electron microscope.

Quantitative analysis

The numbers of SP-IR, ENK-IR, SP+ENK-IR and non-IR boutons apposed to three types of dorsal horn neuron were counted directly on the EM screen. The average percentages of each type of bouton in the total number of boutons apposed to the cell body, proximal and distal dendrites were determined. Three nociceptive specific neurons, 4 wide dynamic range neurons and 3 non-nociceptive neurons were used for quantification. For each cell, at least 5 fields from each of the three regions (cell bodies, proximal dendrites and distal dendrites) were randomly selected and used for the counting of appositions and synapses from neuropeptide-IR and non-IR boutons. The numbers of boutons counted per cell ranged from 155 to 228 for all regions. Profiles were considered as specifically labeled for SP immunoreactivity when at least the dense-core vesicles displayed DAB deposits. Profiles were considered as specifically labelled for ENK immunoreactivity when overlaid by at least 3 silver grains. To decide whether the silver grains were located over the profile, the half distance method was used.

To compare statistically the percentages of SP-IR only, SP+ENK-IR, ENK-IR only and non-IR boutons apposed to the cell body, proximal dendrites and distal dendrites of three types of dorsal horn neuron, one-way analysis of variance (ANOVA) was used followed by post-hoc Tukey test for comparisons of independent samples. Statistical significance was set

at $P<0.05$. For wide dynamic range neurons, only the data from cells 208-1, 258-2 and 276-2 were used for statistical comparisons with other groups. As cell 205-1 was not comparable to the other three in physiological characteristics, this cell was not used for statistical comparisons.

RESULTS

Based on the presence or absence of a slow, prolonged depolarization and afterdischarge after the end of the noxious stimulus, the dorsal horn neurons were classified into nociceptive and non-nociceptive. Of the 12 neurons included in the present study, 3 were nociceptive specific, 5 wide dynamic range and 4 non-nociceptive (Table 1). Approximately one third of the boutons apposed to the intracellularly labelled cells displayed a synaptic contact when observed in an isolated section. This ratio was approximately the same for all boutons independent of their neurochemical characteristics and physiological types of the cells they were apposed to.

Nociceptive specific neurons

All three nociceptive specific neurons (207-1, 271-1, 276-1) had their cell bodies located in lamina I (Table 2). Two of these neurons (271-1 and 276-1) were bipolar and oriented parallel to the main axis of the spinal cord, with their dendritic tree branching within

the limits of lamina I. The third nociceptive specific neuron (207-1) was located close to the laminae I-II border and was a multipolar cell with a few scarcely branched dendrites. Some of the dendrites of this cell radiated ventrally as far as the laminae II-III border. All three nociceptive specific neurons were ENK immunoreactive (Table 1).

Figures 1, 2 and 3 illustrate the morphological properties of nociceptive specific neurons. The cell body (Fig. 3B), proximal dendrites (Figs. 2A and 3A) and distal dendrites (Figs.1B, 2B and 3C) of the cells were overlaid by silver grains indicating ENK immunoreactivity.

Boutons immunoreactive for SP only were observed contacting the cell bodies and dendrites (Figs.2A, 2B and 3A). The synapses formed were almost invariably of the asymmetric type (Fig. 2B).

SP and ENK immunoreactivities were co-localized in a considerable number of the boutons apposed to nociceptive specific neurons (Figs. 1A, 3B and 3C). The synapses formed by such double labelled boutons were of the asymmetric type.

ENK-IR only boutons were also apposed to the cell bodies, proximal and distal dendrites of the nociceptive specific neurons (Figs.1B, 2A, 2B and 3C). Similar to other types of boutons, approximately 32.5% of ENK-IR only boutons established synapses with HRP labelled nociceptive specific neurons. Both ENK-IR only and SP+ENK-IR boutons were never found presynaptic to SP-IR only boutons which were apposed to nociceptive specific neurons.

No obvious morphological differences could be detected in the boutons that were non-immunoreactive when compared to these that were immunoreactive for SP, ENK or

both. However, many of the non-IR boutons did not possess any dense core vesicles, and some established symmetric synapses.

Wide dynamic range neurons

The cell bodies of four wide dynamic range neurons (276-2; 208-1; 258-2; 205-1) were located in the laminae II-III border, lamina III, lamina IV and lamina V, respectively (Table 2). Three of these cells (276-2, 208-1 and 258-2) possessed comparable characteristics. Physiologically, the three neurons responded to noxious stimuli with a moderate nociceptive response. Morphologically, all cells were multipolar neurons. Cell 276-2 had a stellate-shaped cell body, with most of the dendritic tree arborizing within the limits of laminae II and III (Fig. 4A). Some dendrites from this cell penetrated into lamina I where they further arborized into smaller processes which travelled for a short distance along the axis of the spinal cord. Some dendrites in laminae IIi and III were spiny. Cell 208-1 has been described in detail elsewhere (Ma et al., 1995a) and will be described only briefly here. It possessed a stellate-shaped cell body. Its main dendritic trunks radiated in all directions. Most of dendrites were spiny, except those that penetrated lamina IIo and lamina I. Cell 209-1 was similar in localization and morphology to cell 208-1. The cell body of neuron 258-2 had a triangular shape and was continued by the main dendritic trunks. Most of the dendritic branches of the cell extended dorsally to reach laminae III and IIi, a few branches extended ventrally to the deeper laminae (V-VI). This neuron received numerous appositions and synapses from SP-IR boutons in the dendrites located in lamina V, one of the areas with intense SP immunoreactivity.

The physiological properties of cell 205-1 have been described previously (De Koninck et al., 1992). This cell possessed particularly strong nociceptive responses. The cell body of this neuron, located in lamina V, was ovoid and gave rise to four main dendritic trunks. Most of the dendrites were oriented dorsally, with only a few extending to lamina VI. Some of the dorsally oriented dendritic processes were very long and reached as far as the lamina I-II border. The dendrites of this cell were virtually devoid of spines.

Four of the wide dynamic neurons (276-2, 208-1, 258-2 and 205-1) were ENK-IR. However, cell 209-1 was devoid of ENK immunoreactivity. Below, the four wide dynamic range neurons with moderate nociceptive responses are compared with cell 205-1.

Regarding the cells with moderate nociceptive responses, boutons immunoreactive for SP only were apposed to the cell bodies, proximal (Fig. 5C) and distal dendrites (Fig. 5A) of these four cells, particularly to the distal dendrites located in lamina I and II for cells 208-1, 209-1 and 276-2 and in lamina V for cell 258-2. The cell bodies and the proximal dendrites of these cells were innervated by a limited number of SP-IR only boutons. In contrast, cell 205-1 was comparable to the nociceptive specific neurons, in that it received a high number of appositions and synapses from SP-IR only boutons in its cell body, proximal and distal dendrites (Figs. 6A, 6B and 7A).

SP and ENK double labelled boutons were found apposed to all the wide dynamic range neurons. In neurons with moderate nociceptive responses, SP+ENK-IR boutons were more frequently detected in the distal dendritic tree (not shown). In cell 205-1, SP+ENK-IR boutons were rather abundant in both proximal and distal dendrites (Figs.7A, 7B and 7C). Figure 7A shows an asymmetric synapse established by a SP+ENK-IR bouton with cell 205-

1.

Boutons immunoreactive exclusively for ENK were apposed to the cell bodies, proximal and distal dendrites (Fig. 5B) of the four wide dynamic range neurons with moderate nociceptive responses. In comparison, such ENK-IR only profiles were more frequently found apposed to the cell body, proximal dendrites and distal dendrites of cell 205-1 (Figs.6A, 6B and 7B). Both ENK-IR only and SP+ENK-IR boutons were never presynaptic to SP-IR boutons apposed to wide dynamic range neurons.

Non-nociceptive neurons

The cell bodies of the four HRP labelled non-nociceptive neurons (206-2, 212-1, 258-1, 271-2) were located in lamina IV, and were multipolar in shape. As an example, we show the morphological properties of cell 258-1. The body of this cell was ovoid (Fig. 8A), and the dendritic tree branched mostly within the limits of lamina IV. Most of the dendrites of this cell possessed spines (Fig.8A). Cell 206-2 was similar to 258-1, while cells 212-1 and 276-1 possessed dendritic trees which were oriented dorsally and reached outer lamina II. Most of the dendritic processes of these two cells possessed elongated spines.

Under the electron microscope, silver grains, indicating ENK immunoreactivity, were never detected over the cell bodies, proximal dendrites and distal dendrites of cells of this type. SP-IR only boutons were rarely found in contact with any part of this functional type of cells, as previously described (De Koninck et al., 1992; Ma et al., 1995a). Occasionally, an isolated SP-IR bouton was detected presynaptic to these cells. Boutons immunoreactive for both SP and ENK were also infrequently found apposed to this type of the cells. In

contrast, ENK-IR only boutons were rather frequently found apposed to non-nociceptive neurons, in both cell bodies and dendrites (Figs. 8B and 8C).

Quantitative analysis

As described in "Material and Methods", we analyzed quantitatively three nociceptive specific, three wide dynamic range neurons with moderate nociceptive responses and three non-nociceptive neurons (Table 2). For comparison, we also quantitated cell 205-1, a wide dynamic range neuron with particularly strong nociceptive responses. The selection of these cells was based on the quality of the morphological preservation. Table 2 shows the percentages of appositions to each of the cells from SP-IR only, ENK-IR only, SP+ENK-IR and non-IR axonal boutons. The histograms in Figure 9 represent the mean percentages of each type of boutons apposed to the three regions of the three groups of neurons.

Percentages of SP-IR only boutons

When statistically compared, the average percentages of SP-IR only boutons apposed to the cell bodies, proximal dendrites and distal dendrites of nociceptive specific neurons and wide dynamic range neurons were significantly higher than those of non-nociceptive neurons ($P<0.02$, Fig.9A). Nociceptive specific neurons had significantly higher percentages of SP-IR only boutons apposed to their cell bodies and proximal dendrites than wide dynamic range neurons ($P<0.02$, Fig 9A), but not to the distal dendrites.

Percentages of SP+ENK-IR boutons

As shown in Figure 9B, the mean percentages of SP+ENK-IR boutons apposed to the cell bodies and proximal dendrites of nociceptive specific neurons were significantly higher than those of non-nociceptive neurons ($P<0.02$, Fig. 9B), but not in the distal dendritic region. There were no significant differences between the mean percentages of SP+ENK-IR boutons apposed to the cell bodies, proximal dendrites and distal dendrites of nociceptive specific neurons and wide dynamic range neurons (Fig. 9B). Comparing wide dynamic range neurons and non-nociceptive neurons, there were no significant differences between the mean percentages of SP+ENK-IR boutons apposed to the cell bodies and proximal dendrites, but the value for the distal dendrites of wide dynamic range neurons was significantly higher ($P<0.01$, Fig. 9B).

Percentages of ENK-IR only boutons

As shown in Figure 9C, the mean percentages of ENK-IR only boutons apposed to the cell bodies and the proximal dendrites of nociceptive specific neurons were significantly higher than those of non-nociceptive neurons ($P<0.02$), but not in the distal dendritic region. Nociceptive specific neurons had significantly higher average percentages of ENK-IR only boutons apposed to the cell bodies than wide dynamic range neurons ($P<0.02$, Fig. 9C), but not for the proximal and distal dendrites. Wide dynamic range neurons exhibited significantly higher values of appositions from ENK-IR only profiles in the proximal dendrites than non-nociceptive neurons ($P<0.01$, Fig. 9C), but not in the cell bodies and the distal dendrites.

Percentages of non-IR boutons

As shown in Figure 9D, the mean percentages of non-IR boutons apposed to the cell bodies, the proximal dendrites and distal dendrites of nociceptive specific neurons and wide dynamic range neurons were significantly lower than those of non-nociceptive neurons ($P<0.01$, Fig.9D). Compared with wide dynamic range neurons, nociceptive specific neurons had significantly lower mean percentages of non-IR boutons apposed to the cell bodies and proximal dendrites ($P<0.002$, Fig. 9D), but not to the distal dendrites.

DISCUSSION

In the present study, we confirmed that most of the nociceptive dorsal horn neurons (nociceptive specific and wide dynamic range) contained ENK immunoreactivity, whereas none of the non-nociceptive neurons was ENK immunoreactive (Ribeiro-da-Silva et al., 1992). Furthermore, we provide detailed quantitative information on the innervation of nociceptive and non-nociceptive neurons by SP and ENK immunoreactivities. Higher numbers of SP-IR only and SP+ENK-IR axonal boutons were apposed to nociceptive neurons than to non-nociceptive neurons. However, ENK-IR only boutons innervated only the proximal dendritic region of nociceptive neurons in significantly higher numbers than in non-nociceptive neurons. No significant differences of the average percentages of ENK-IR only boutons apposed to the distal dendrites were detected between nociceptive and non-nociceptive neurons. Both ENK-IR only and SP+ENK-IR boutons were never found

presynaptic to SP-IR boutons apposed to nociceptive neurons.

1. Origins of SP-IR only, ENK-IR only, and SP+ENK-IR boutons presynaptic to functionally characterized dorsal horn neurons

Significantly higher numbers of SP-IR only and SP+ENK-IR axonal boutons were detected apposed to nociceptive neurons than to non-nociceptive neurons. In order to interpret the significance of these findings, it is important to identify the origins of SP-IR only and SP+ENK-IR boutons in contact with nociceptive neurons. SP immunoreactivity in the dorsal horn may originate from three sources: primary sensory neurons in the dorsal root ganglion (Hökfelt et al., 1975a; Cuello and Kanazawa, 1978), intrinsic spinal cord interneurons (Hunt et al., 1981; Ljungdahl et al., 1978) and descending fibers from the brainstem (Gilbert et al., 1982; Hökfelt et al., 1978). High incidence of co-localization of SP and calcitonin gene-related peptide (CGRP) was found in dorsal root ganglion cells of rat (Gibson et al., 1984; Ju et al., 1987; Lee et al., 1985b; Wiesenfeld-Hallin et al., 1984; Garry et al., 1989) and cat (Garry et al., 1989; Gibson et al., 1984), and in axonal boutons in the superficial laminae of the rat dorsal horn (Plenderleith et al., 1990; Tuchscherer and Seybold, 1989). Since CGRP immunoreactivity in the dorsal horn is exclusively from primary sensory afferents, a finding confirmed by investigations using multiple dorsal rhizotomies (Traub et al., 1989; Chung et al., 1988) and *in situ* hybridization (Réthelyi et al., 1989), it can thereby be used as a marker for axonal terminals from primary sensory origin. In previous studies (Ribeiro-da-Silva et al., 1992; Ma et al., 1995a), we detected that about 30% of SP-IR boutons apposed to nociceptive neurons also contained CGRP immunoreactivity. These

axonal boutons co-localizing SP and CGRP immunoreactivities were therefore considered to be of primary sensory origin. Thus, some of SP-IR boutons in the current study certainly are primary sensory afferents.

ENK immunoreactivity in the dorsal horn has been shown to originate mainly from intrinsic dorsal horn neurons, since transection of the thoracic spinal cord results in a negligible loss of ENK immunoreactivity in the lumbar spinal cord (Seybold and Elde, 1982). ENK immunoreactivity in the dorsal horn has been suggested to originate from primary sensory afferents, however, ENK has never been detected in a significant number of neurons in the dorsal root ganglia (Garry et al., 1989). SP and ENK immunoreactivities are co-localized in a considerable number of neurons and axonal terminals in the dorsal horn of both rat and cat (Murase et al., 1982; Senba et al., 1988; Tashiro et al., 1987; Ribeiro-da-Silva et al., 1991a; Ribeiro-da-Silva et al., 1991b). It has been shown that almost all SP-IR neurons in the rat dorsal horn co-localize ENK and approximately 50% of ENK-IR neurons co-localize SP (Senba et al., 1988; Ribeiro-da-Silva et al., 1991b). Therefore, the co-localization of SP and ENK in the axonal boutons can be used as a marker to indicate SP-IR axonal boutons of intrinsic origin. Thus, the most likely origin of ENK-IR only and SP+ENK-IR boutons in the current study is from intrinsic spinal cord neurons.

2. Functional implication of SP-IR only, ENK-IR only and SP+ENK-IR axonal boutons in synaptic interactions with nociceptive and non-nociceptive dorsal horn neurons

SP-IR only boutons

In agreement with previous studies (De Koninck et al., 1992; Ma et al., 1995a), we

found that SP-IR only boutons were preferentially associated with nociceptive neurons. This finding further supports the concept of a role of SP as a neurotransmitter or neuromodulator in the first central synapse of nociceptive pathways. Furthermore, the quantitative data in the present study are consistent with those in our previous study (Ma et al., 1995a) where nociceptive specific neurons had significantly higher average percentages of SP-IR only boutons apposed to the cell bodies and proximal dendrites than wide dynamic range neurons. However, in the present study we did not detect a significant difference of SP-IR only boutons apposed to the distal dendritic regions between the two types of cells. This discrepancy is probably due to the different wide dynamic range neurons used in the two studies. The cell (258-2) in this study exhibited a considerably higher percentage of SP-IR boutons apposed to the distal dendrites (Table 2) than the cell (339-1) in the previous study (Ma et al., 1995a). The amount of SP-IR only boutons apposed to nociceptive neurons depends, to a certain degree, on the localization of the dendritic arborization of the cells. The previous study showed that, in wide dynamic range neurons, the average percentages of SP-IR boutons apposed the distal dendrites which were located in laminae with high concentrations of SP immunoreactivity were significantly higher than those apposed to the distal dendrites located in laminae where SP immunoreactivity was scarce (Ma et al., 1995a).

Interestingly, in the present study we found that the mean percentages of SP-IR only boutons apposed to the cell bodies and proximal dendrites of wide dynamic range neurons with moderate nociceptive responses were lower than those for a wide dynamic range neuron (205-1) which exhibited a markedly stronger nociceptive response. The data is indicative that the intensity of nociceptive responses of nociceptive neurons might be associated with the

number of apposed SP-IR boutons.

ENK-IR nociceptive neurons

Most of the nociceptive neurons included in this study were ENK immunoreactive. This result further supports the concept that ENK is mainly associated with the modulation of nociception. In behavioral tests, both intrathecal injection of SP and noxious cutaneous stimulation resulted in a transient decrease of reaction time followed by a rebound overshoot (Yashpal and Henry, 1983; Cridland and Henry, 1988b). The earlier phase of the response was blocked by SP receptor antagonists (Yashpal and Henry, 1983), but the overshoot was blocked by naloxone (Cridland and Henry, 1988b), suggesting the activation of an opioid mechanism at the spinal cord level, due either to SP or to SP-induced activation of spinal nociceptive pathways. In biochemical studies, SP was shown to stimulate the release of endogenous opioid peptides (Naranjo et al., 1986; Tang et al., 1983; Iadarola et al., 1986). The release of endogenous opioid peptides evoked by SP was blocked by a SP antagonist, suggesting that a SP receptor was involved (Tang et al., 1983). Our ENK-IR nociceptive neurons innervated by SP inputs provide an anatomical substrate for the above studies. Interestingly, it has been reported that a low dose of SP caused analgesic effects in behavioral tests, an effect that was blocked by naloxone (Stewart et al., 1976; Kream et al., 1993). These studies suggest that a low dose of SP may trigger the release of endogenous opioids.

ENK-IR only boutons

It has been suggested that an increase in peripheral stimuli activates the intrinsic spinal opioid system, which in turn affects the responsiveness of ascending projection neurons (Basbaum, 1985). ENK-IR axonal boutons were found apposed to spinothalamic neurons in lamina I (Ruda et al., 1984) and in laminae IV to V (Ruda, 1982). Moreover, ENK-IR neurons in laminae I and V have been shown to project to the lateral thalamus (Coffield and Miletic, 1987a) and those in laminae VI and VII to the medial thalamus (Coffield and Miletic, 1987b). In the present study, we found ENK-IR only and SP+ENK-IR boutons apposed to nociceptive neurons in lamina I, III, IV and V. Although we did not investigate the projection sites of our neurons, it is possible that some of the nociceptive neurons included in this study are projection neurons.

As mentioned above, although some of the ENK-IR neurons in the dorsal horn are projection cells, most of these ENK-IR neurons likely represent interneurons. Lamina I neurons with a local axonal arbor may represent a subpopulation of ENK-IR neurons (Bennett et al., 1981). Two types of ENK-IR neurons in lamina II have been identified as stalked cells and ventral lamina II islet cells on the basis of their morphology (Bennett et al., 1982). Our ENK-IR nociceptive neurons were located or possessed dendrites in laminae I, II and V, where both SP and ENK immunoreactivities are concentrated (Cuello et al., 1977b; Hökfelt et al., 1977; Ruda, 1982). Therefore, it is reasonable to speculate that most of ENK-IR boutons innervating nociceptive and non-nociceptive neurons may originate from ENK containing nociceptive neurons. The innervation by ENK-IR boutons of nociceptive neurons is certainly a morphological basis for the inhibition of the responses of nociceptive dorsal horn neurons to peripheral noxious stimulation (LeBars et al., 1976; Zieglgansberger and

Bayerl, 1976; Randic and Miletic, 1978).

In the present study, we also detected ENK-IR boutons innervating non-nociceptive neurons. Quantitatively, although nociceptive neurons had significantly higher percentages of ENK-IR boutons apposed to the cell bodies and proximal dendrites, the values for distal dendrites of three types of cells were not significantly different. This result indicates that the innervation by ENK-IR only boutons of non-nociceptive neurons was considerable. The functional significance of this finding is at present unclear. A previous study showed that the numbers of ENK-IR neurons per unit of volume in lamina I were higher in the thoracic and lower lumbar/sacral cord of rat and cat than at other spinal levels (Miller and Seybold, 1989). The thoracic and lower lumbar/sacral spinal cord receive both visceral and somatic afferent inputs [for review, see (Janig and Morrison, 1986)]. Morphine and other opiate agonists were shown to strongly reduce the response to putative nociceptive visceral stimuli, organ distension and visceral-chemical tests (Brasch and Zetler, 1982). In the present study, both nociceptive and non-nociceptive neurons were located in the dorsal horn of the lower lumbar spinal cord (L5-L7). The innervation of non-nociceptive neurons by ENK-IR boutons in the present study might provide the underlying anatomical substrate for the effects of opioid peptides which are not related to anti-nociception.

SP+ENK-IR boutons

Opposite effects of C- and N-terminal SP metabolites on the release of excitatory amino acid have been reported (Skilling et al., 1990). The reduced release of excitatory amino acids by N-terminal SP metabolites was blocked by naloxone, suggesting that an

opioid receptor was involved. We can speculate that the SP and ENK co-localizing axonal boutons apposed to nociceptive neurons detected in the present study might provide an anatomical substrate to such differential actions of SP metabolites. Certainly, SP+ENK-IR inputs to nociceptive neurons play a role of fine tuning in the transmission and modulation of nociception. Since SP and ENK are frequently co-localized in the dorsal horn of the spinal cord as mentioned above (Senba et al., 1988; Ribeiro-da-Silva et al., 1991b), the possibility exists that the ENK containing nociceptive neurons included in our study might also contain SP. Because of technical limitations, we could not investigate this issue in the present study.

We did not detect any significant differences in the percentages of SP+ENK-IR boutons apposed to the cell bodies, proximal dendrites and distal dendrites between the two types of nociceptive neurons, but the values for the distal dendrites of both nociceptive specific and wide dynamic range neurons were significantly higher than those of non-nociceptive neurons. This result suggests that SP+ENK-IR boutons are associated with the processing of nociception in the spinal cord, thus opening the possibility that besides pure pro-nociceptive (SP) and anti-nociceptive (ENK) messages, a "mixed" peptide message would be part of the rich transmitter coding of spinal cord sensory responses elicited by noxious stimuli originated in the periphery.

It is interesting to note that, in agreement with our previous studies in rat (Cuello, 1983; Ribeiro-da-Silva et al., 1991b), we did not find any ENK-IR only or SP+ENK-IR profiles presynaptic to SP-IR boutons. In contrast, however, our present study showed that both ENK-IR and SP+ENK-IR boutons were more frequently found presynaptic to dorsal horn neurons possessing nociceptive responses than to those not possessing such responses.

This lends further support to the concept that the enkephalinergic modulation of SP-mediated primary sensory information occurs at a postsynaptic site.

Table 1. Physiological and neurochemical properties of the neurons included in this study

Cell type	Code of cell	ENK immunoreactivity of cell
Nociceptive specific	207-1	+
	271-1	+
	276-1	+
Wide dynamic range (regular)	208-1	+
	209-1	-
	258-2	+
	276-2	+
Wide dynamic range (strongly nociceptive)	205-1	+
Non-nociceptive	206-2	-
	212-1	-
	258-1	-
	271-2	-

Table 2. Percentages of neuropeptide-IR varicosities apposed to each of the neurons studied.

Cell type	Code	Cell body	% of SP-IR (non-ENK-IR) boutons			% of SP+ENK-IR boutons			% of ENK-IR (non-SP-IR) boutons			% of non-IR boutons		
			CB	PD	DD	CB	PD	DD	CB	PD	DD	CB	PD	DD
Nociceptive specific	207-1	LI	22.45	20.83	27.27	8.16	20.83	20.00	16.33	19.44	23.64	53.06	38.89	29.09
	271-1	LI	27.59	29.49	31.48	6.90	11.54	14.81	17.24	20.51	14.81	48.28	38.46	38.89
	276-1	LI	27.08	34.38	40.74	7.29	9.38	7.41	14.58	18.75	11.11	51.04	37.5	40.74
Wide dynamic range (regular)	208-1	LIII	12.50	9.38	21.28	4.17	0.00	10.64	10.42	21.88	23.40	72.92	68.75	44.68
	258-2	LIV	11.02	16.33	27.78	1.69	4.08	11.11	8.47	12.24	16.17	78.81	64.35	44.44
	276-2	LII-III	12.50	10.71	25.0	5.00	8.93	16.67	11.25	16.07	20.83	71.25	64.29	37.50
Wide dynamic range (strongly nociceptive)	205-1	LV	23.08	21.33	19.05	15.38	14.67	10.71	19.23	21.33	23.81	42.31	42.67	42.43
Non-nociceptive	206-2	LIV	2.30	3.75	3.39	3.45	0.00	1.69	12.64	5.00	16.95	81.61	91.25	77.97
	212-1	LIV	2.25	1.75	3.66	1.12	3.51	1.22	6.74	7.02	7.32	89.89	87.71	87.80
	258-1	LIV	0.00	3.08	1.64	0.00	4.61	1.64	10.61	9.23	6.56	89.39	83.08	90.16

CB - Cell body region; PD - Proximal dendritic tree; DD - Distal dendritic tree.

Figure 1. Morphological properties of nociceptive specific neurons. **A** shows the *camera lucida* reconstruction of one of the three nociceptive specific neurons (276-1) included in this study. The cell body and most of dendritic branches are within the limits of lamina I. **B** shows an electron micrograph of part of a distal dendrite from this cell in lamina I. Note silver grains representing ENK immunoreactivity over the dendrite. Several ENK-IR boutons are apposed to the dendrite of the cell. A bouton containing DAB reaction products (SP immunoreactivity) is also overlaid by silver grains (SP+ENK). This double labelled bouton is in contact with the dendrite of the cell. Scale bars =20 μm in A, and 0.5 μm in B.

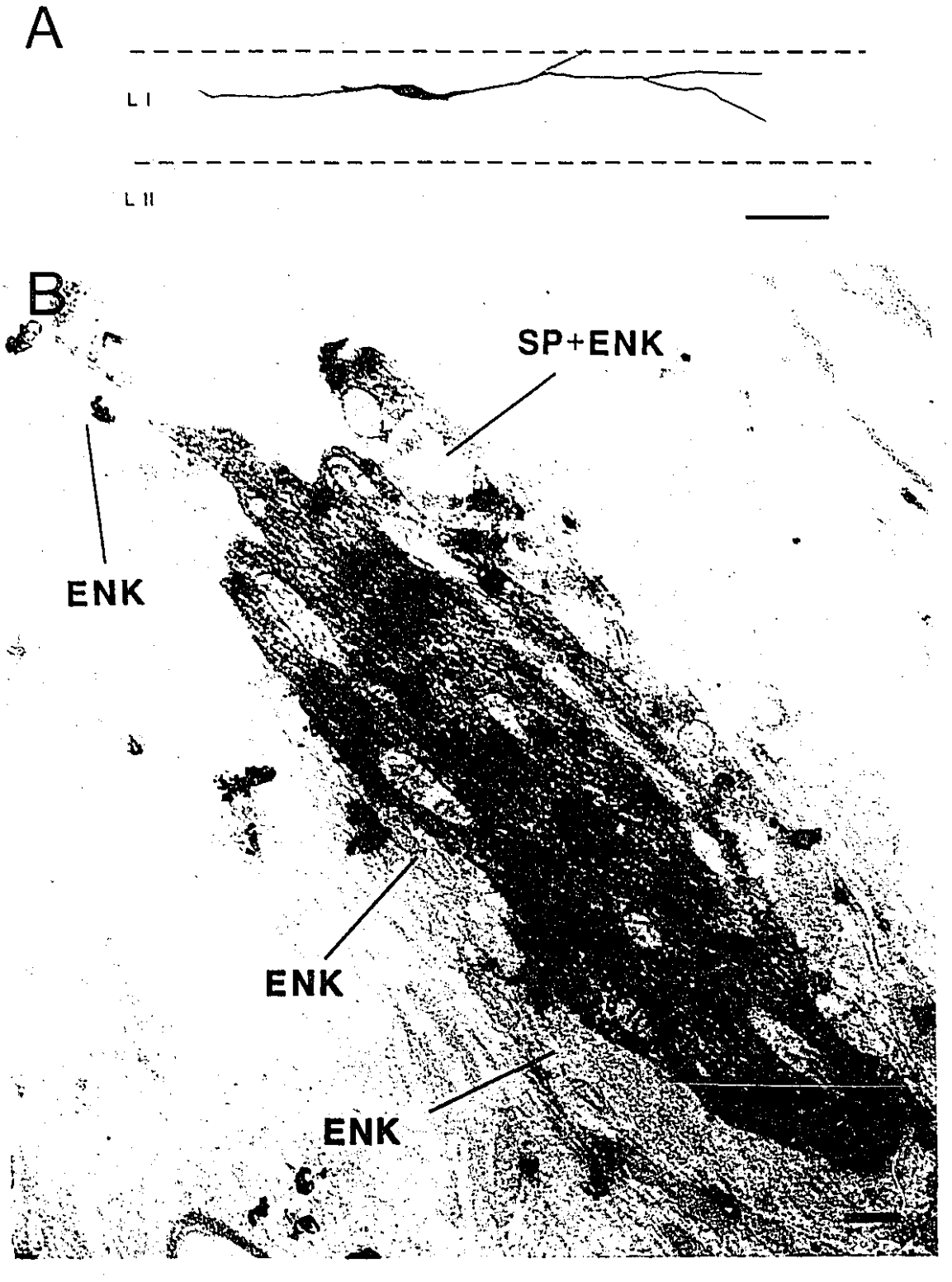
A
L I
L II
B
SP+ENK
ENK
ENK
ENK

Figure 2. Electron micrographs of the proximal and distal dendrites of the cell shown in Figure 1. **A** shows part of a proximal dendrite from the cell. Note one SP-IR bouton and one ENK-IR bouton apposed to this dendrite. Note two double labelled boutons (SP+ENK) which are not in contact with the dendrite of the cell. **B** shows two SP-IR boutons apposed to the dendrite. Note that one of the SP-IR boutons is presynaptic to the dendrite of the cell at an asymmetric synapse (arrowheads). Scale bars = 0.5 μm.

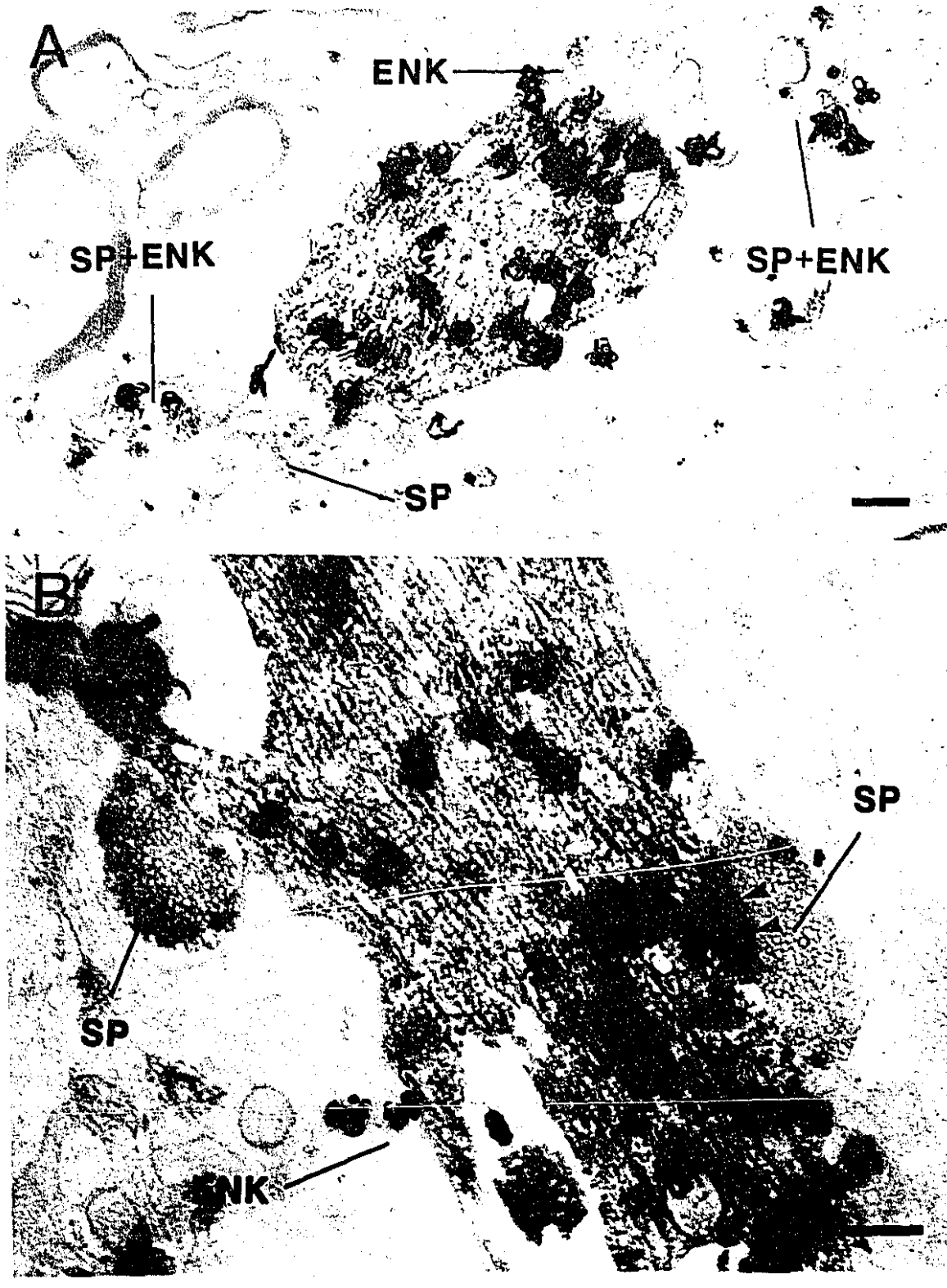
A
ENK
SP+ENK
SP+ENK
SP
B
SP
SP
ENK

Figure 3. Electron micrographs of the cell body, proximal and distal dendrites of one of the nociceptive neurons (207-1). **A** shows part of a proximal dendrite which is overlaid by silver grains (the fine grain developer was used). Note three SP-IR boutons apposed to the dendrite of the cell. **B** illustrates part of the cell body of this cell. A SP+ENK-IR bouton is apposed to the cell body. **C** shows part of a distal dendrite of this cell which is in apposition to three SP+ENK-IR boutons and one ENK-IR bouton. Scale bar = 0.5 μm for all.

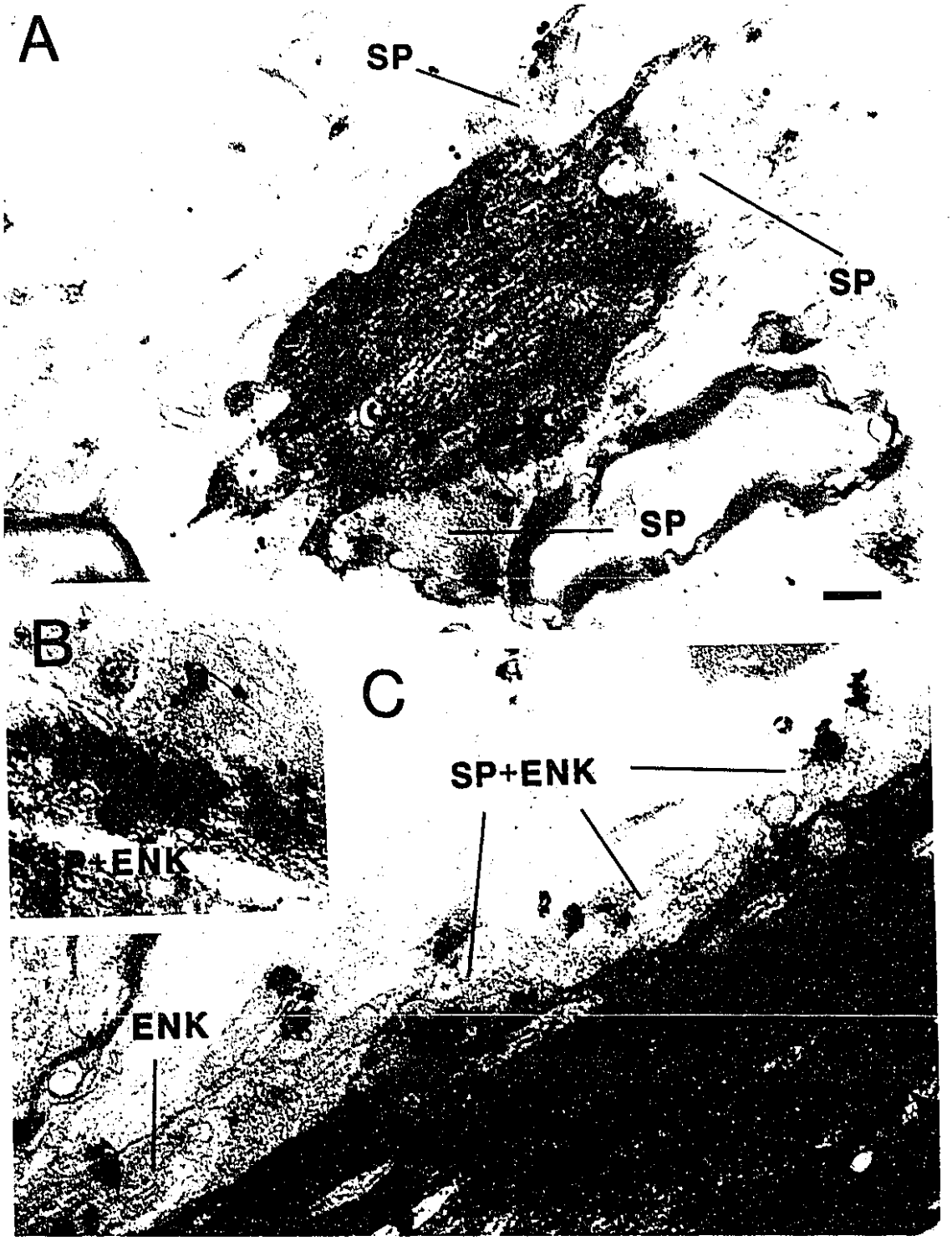
A
SP
SP
SP
B
C
SP+ENK
ENK

Figure 4. Morphological properties of wide dynamic range neurons with moderate nociceptive response. **A** shows the *camera lucida* reconstruction of a wide dynamic range neuron (276-2). Note that the cell body is located at the lamina II-III border. The dendritic tree extend in all directions. Some of the ventrally oriented dendritic branches are spiny. **B** shows an electron micrograph of part of a proximal dendrite of this cell in lamina III. This proximal dendrite is overlaid by silver grains indicating ENK immunoreactivity. Scale bars = 200 μm in A, and 1 μm in B.

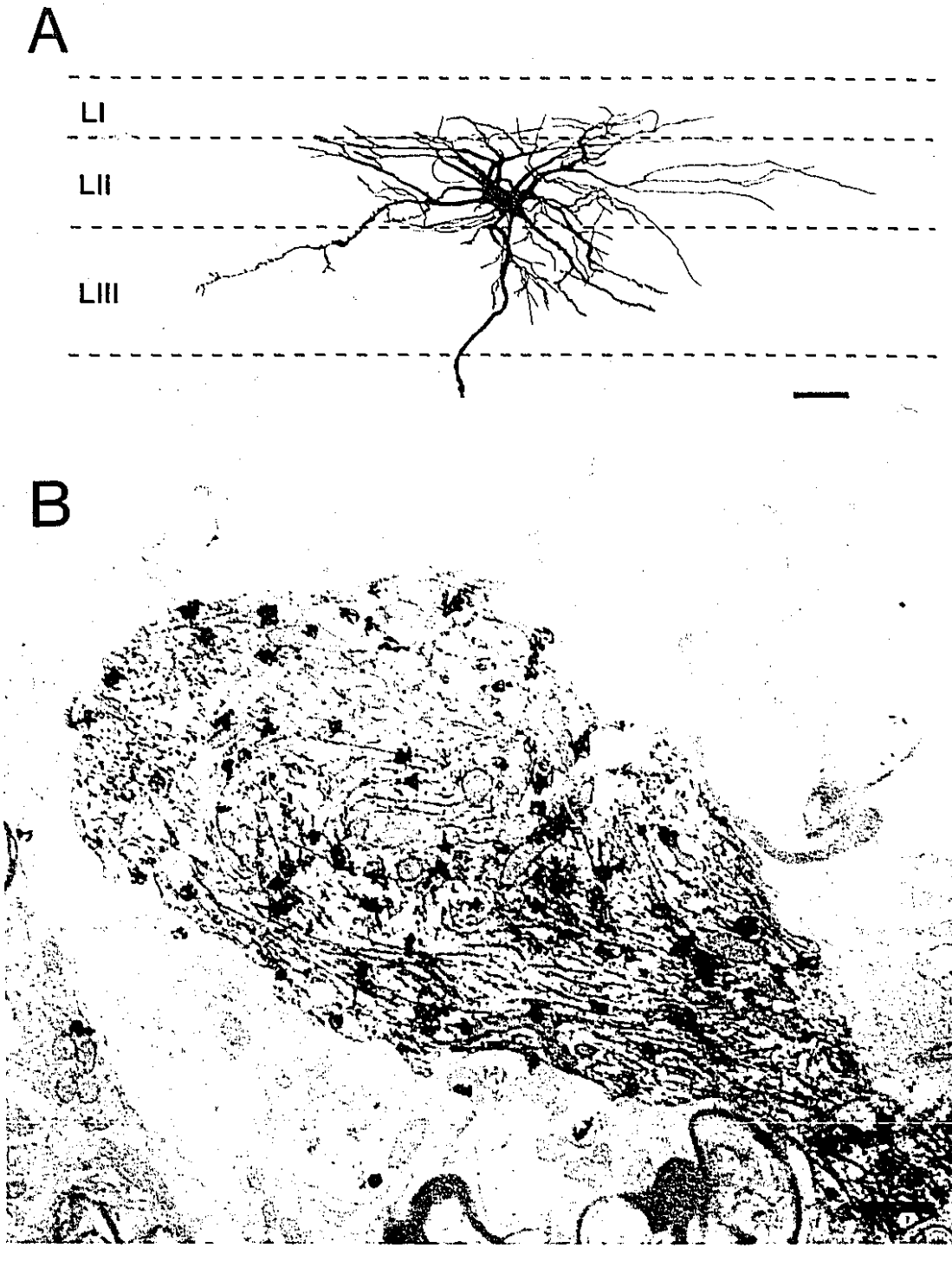
A
LI
LII
LIII
B

Figure 5. Electron micrographs of the proximal and distal dendrites from wide dynamic range neurons with moderate nociceptive response. **A** shows part of an ENK-IR distal dendrite from cell 276-2. Note a SP-IR bouton apposed to the distal dendrite. **B** shows part of an ENK-IR proximal dendrite of cell 208-1. Three ENK-IR boutons are apposed to this proximal dendrite. **C** illustrates part of an ENK-IR distal dendrite from cell 208-1. Note a SP-IR bouton apposed to this distal dendrite. Scale bar = 0.5 μm for all micrographs.

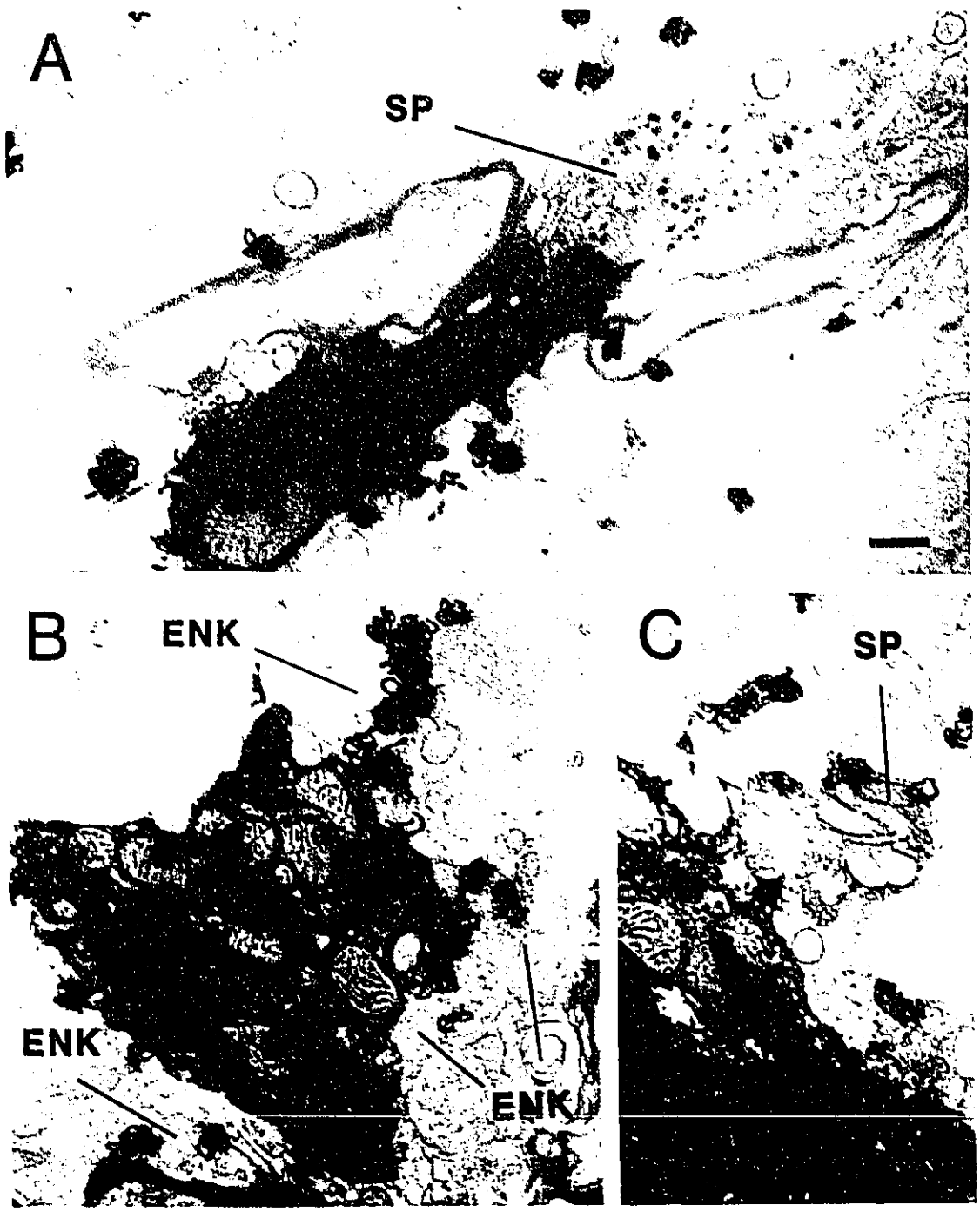
A
SP
B
ENK
ENK
ENK
C
SP

Figure 6. Electron micrographs of part of an ENK-IR distal dendrite from a wide dynamic range neuron (205-1) with strong nociceptive responses. **A** and **B** represent serial ultrathin sections. Note SP-IR and ENK-IR boutons apposed to this distal dendrite. Note that the ENK-IR bouton is presynaptic to the dendrite (arrowheads) in **B**. Lamina IIi. Scale bars = 0.5 μm.

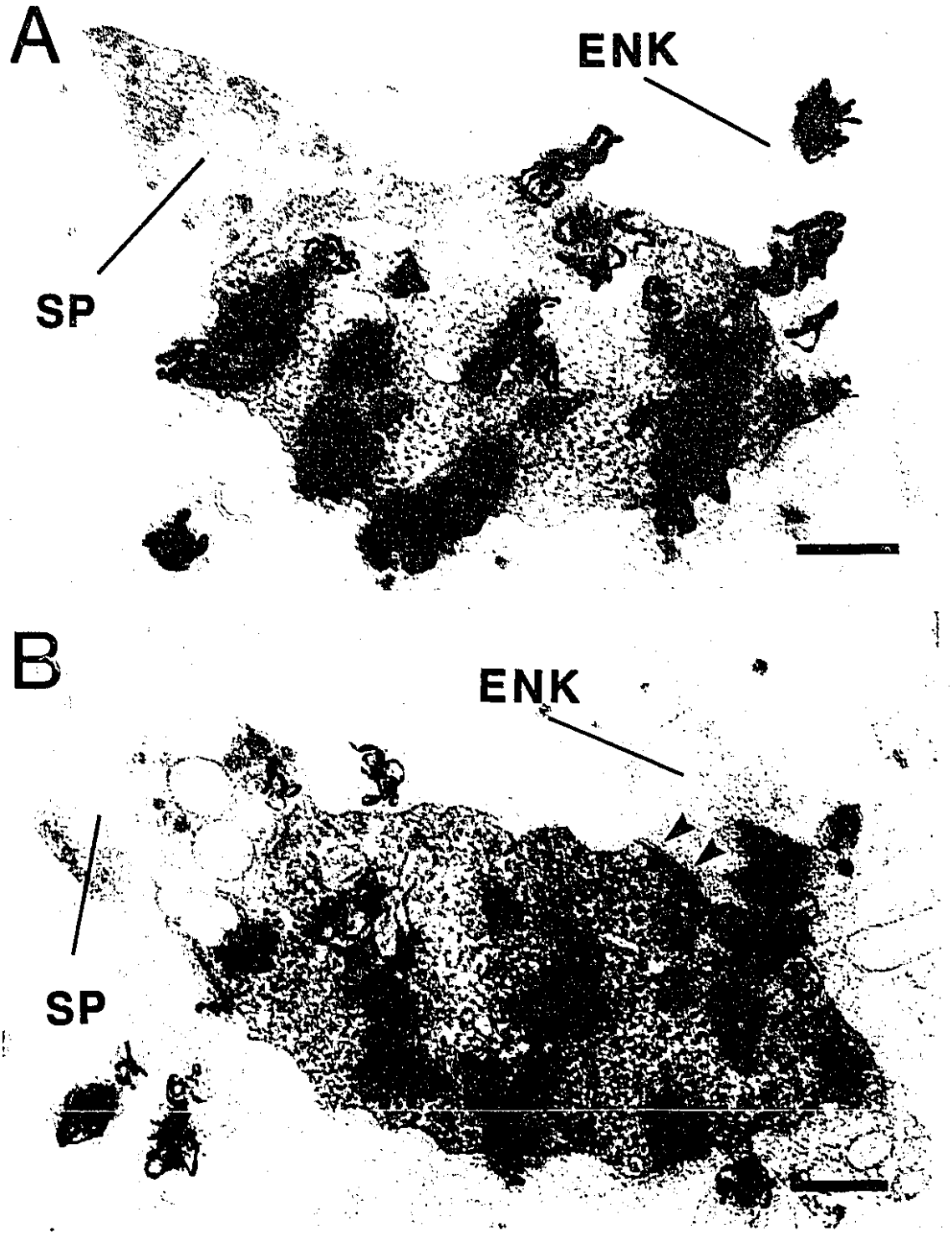
A
ENK
SP
B
ENK
SP

Figure 7. Electron micrographs of the ENK-IR proximal dendrites of a wide dynamic range neuron (205-1). In **A**, note that the dendritic profile receives appositions from both SP-IR and SP+ENK-IR boutons. Note that the SP-IR bouton is presynaptic to the dendrite at an asymmetric synapse (arrowheads). The SP+ENK-IR bouton also establishes a synapse with the dendrite (arrowheads). In **B** and **C**, note SP+ENK-IR boutons apposed to proximal dendrites of the cell. Lamina V. Scale bars = 0.5 μm.

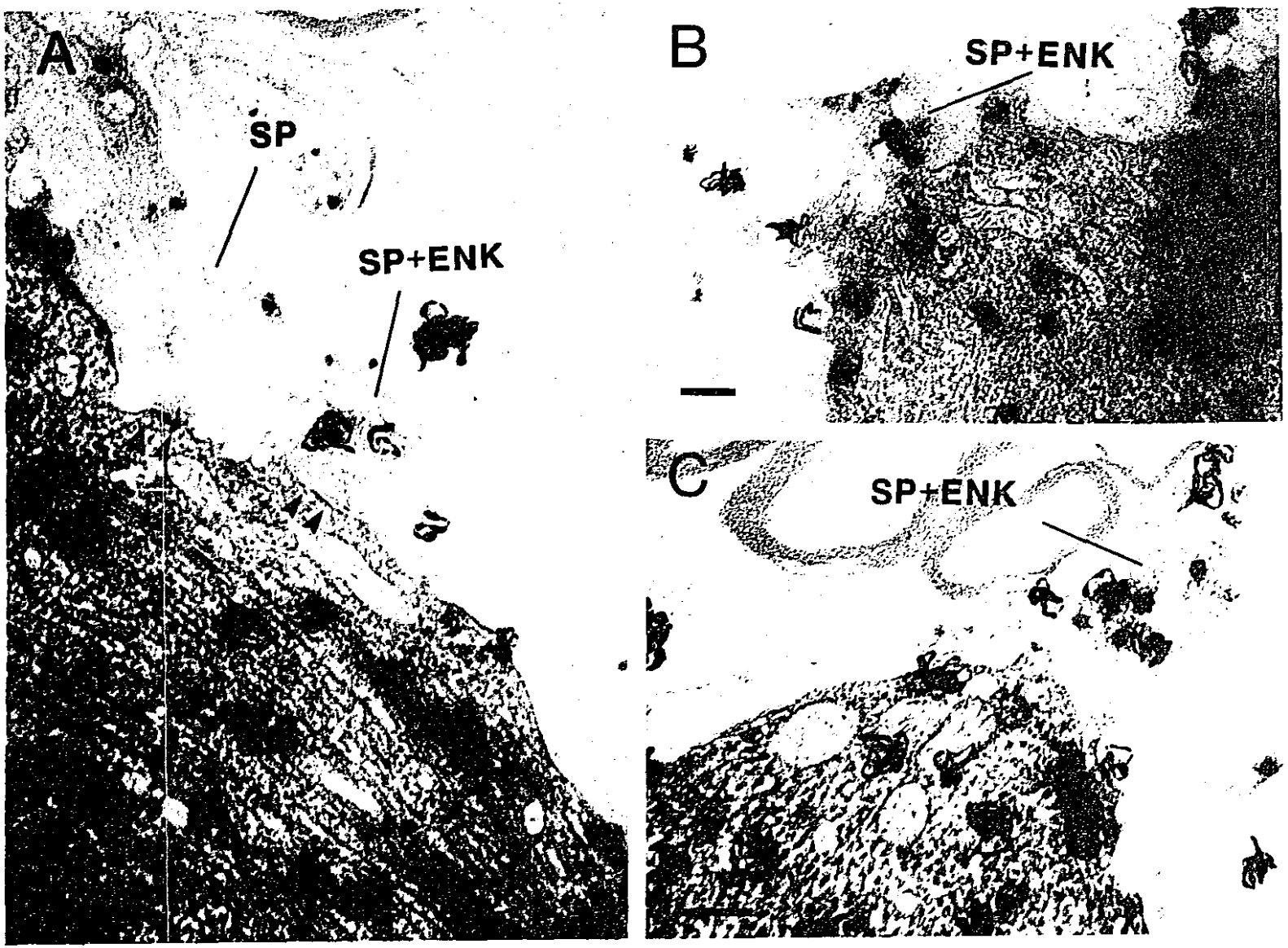
A
SP
SP+ENK
B
SP+ENK
C
SP+ENK

Figure 8. Morphological properties of non-nociceptive neurons. **A** shows the *camera lucida* reconstruction of cell 258-1. The cell body of this neuron is located in lamina IV. The dendritic branches of this cell were mostly located within the limits of lamina IV. Some of the dendritic branches are spiny. Parts of distal dendrites from this non-nociceptive neuron are shown in **B** (lamina IV) and **C** Lamina (III). In **B** and **C**, note the absence of ENK immunoreactivity of the cell, and some ENK-IR boutons apposed to the dendrites of this cell. Scale bars = 200 μm in A, and 0.5 μm in B and C.

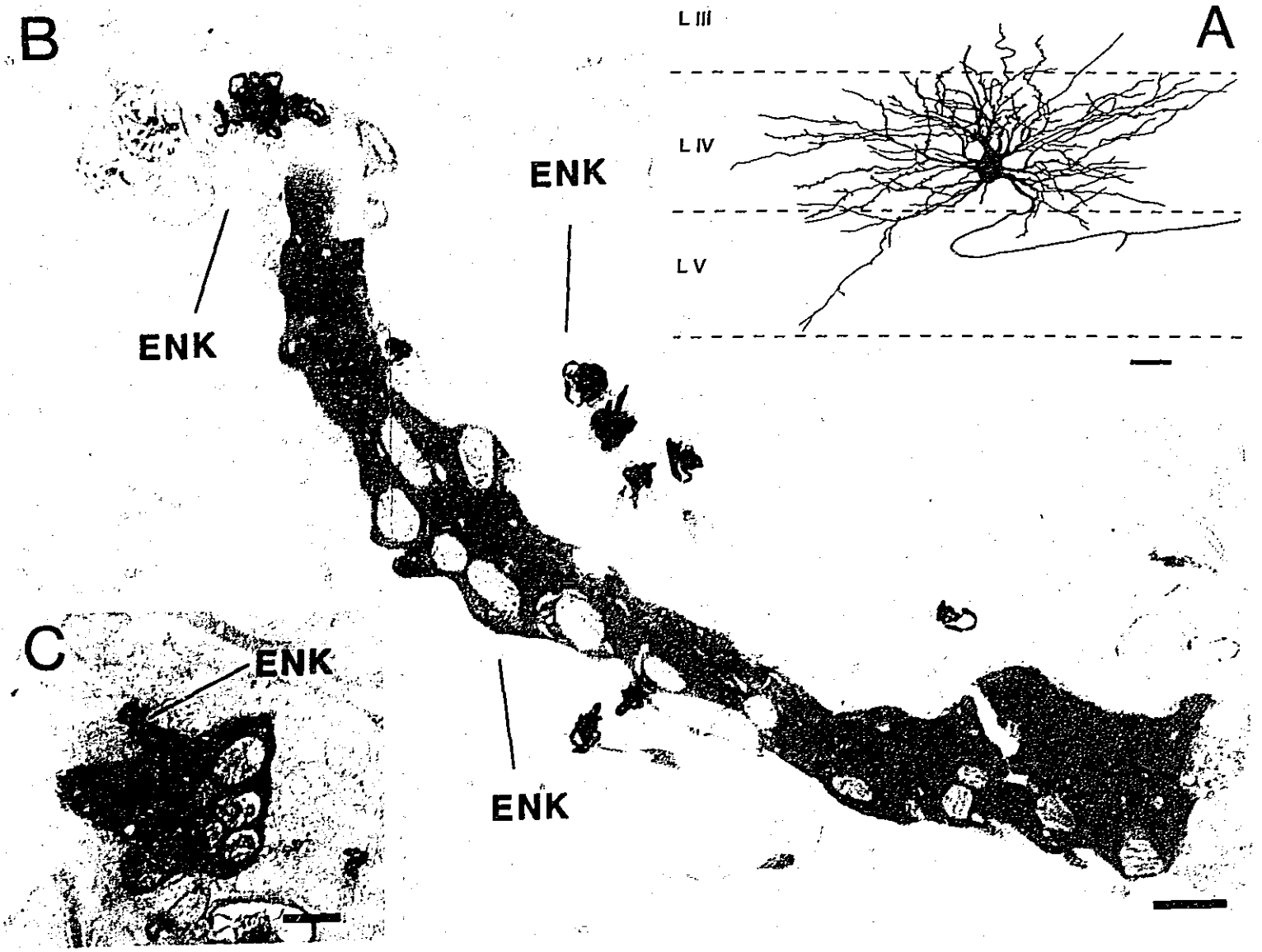
B
A
L III
L IV
L V
ENK
ENK
ENK
C
ENK

Figure 9. Histograms showing the mean percentages (±S.E.M.) of SP-IR only (**A**), SP+ENK-IR (**B**), ENK-IR only (**C**) and non-IR (**D**) boutons apposed to the three regions of the three types of cells. Using one-way ANOVA followed by post-hoc Tukey test, the average percentages of SP-IR only, SP+ENK-IR, ENK-IR only and non-IR boutons apposed to the cell bodies, proximal and distal dendrites among three types of cells were compared. * values for nociceptive specific neurons (NS) significantly different from wide dynamic range neurons (WDR) and non nociceptive neurons (NN). ♦ values for NS significantly different from NN. ● values for WDR significantly different from NS and NN. ◊ values for WDR significantly different from NN.

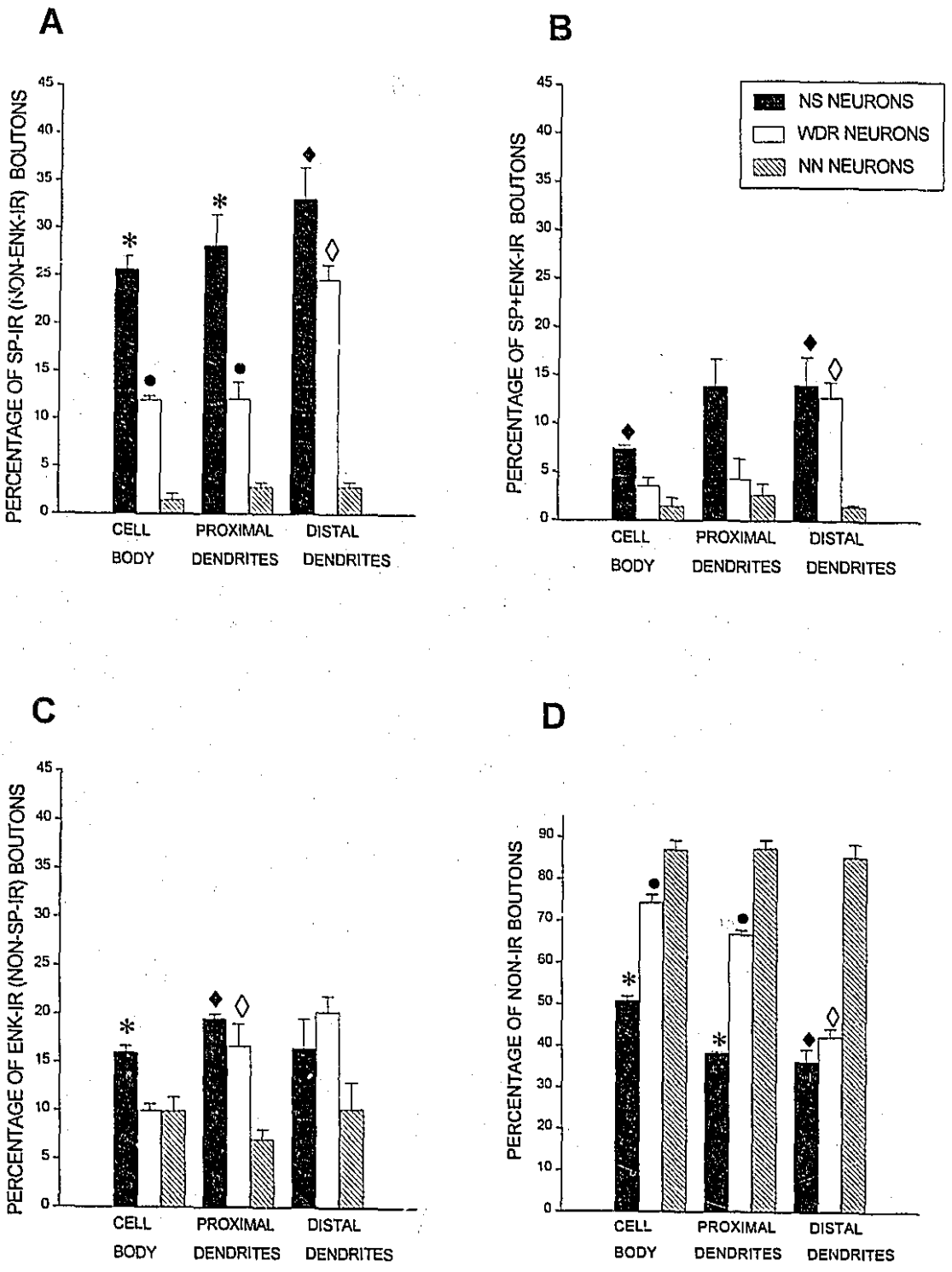
A
PERCENTAGE OF SP-IR (NON-ENK-IR) BOUTONS
CELL BODY
PROXIMAL DENDRITES
DISTAL DENDRITES
B
NS NEURONS
WDR NEURONS
NN NEURONS
PERCENTAGE OF SP+ENK-IR BOUTONS
CELL BODY
PROXIMAL DENDRITES
DISTAL DENDRITES
C
PERCENTAGE OF ENK-IR (NON-SP-IR) BOUTONS
CELL BODY
PROXIMAL DENDRITES
DISTAL DENDRITES
D
PERCENTAGE OF NON-IR BOUTONS
CELL BODY
PROXIMAL DENDRITES
DISTAL DENDRITES

Connecting Text - Chapter III to chapter IV

The study in chapter III demonstrated that most nociceptive neurons in the cat spinal cord were ENK-IR and that nociceptive neurons received significantly higher percentages of SP-IR boutons in the three regions than non-nociceptive neurons. The percentages of SP+ENK-IR boutons apposed to the distal dendritic regions of nociceptive neurons were significantly higher than in non-nociceptive neurons. The percentages of ENK-IR boutons apposed to the cell bodies and proximal dendrites of nociceptive neurons were significantly higher than in non-nociceptive neurons, but no significant differences were detected in the distal dendritic regions.

In addition to ENK, the classic inhibitory neurotransmitter GABA also participates in inhibitory mechanisms in the dorsal horn, as confirmed by ample experimental evidence. Thus, it is of interest to investigate the synaptic interaction of SP-IR boutons with GABA containing elements in the dorsal horn of the spinal cord.

In the next chapter, using a combination of pre-embedding immunocytochemistry and post-embedding immunogold staining, we investigated the interaction of SP-IR elements and GABA-IR elements in the dorsal horn of the cat spinal cord. As we found for the first time a co-localization of SP and GABA immunoreactivities, we decided to investigate whether it also occurred in the rat.

CHAPTER IV

Substance P- and GABA-like immunoreactivities are co-localized in axonal varicosities in the superficial laminae of cat but not rat spinal cord

Weiya Ma and A. Ribeiro-da-Silva

ABSTRACT

In the present study, we applied a combination of pre-embedding peroxidase-based immunocytochemistry and post-embedding immunogold staining to examine the synaptic interactions of substance P (SP) and γ-aminobutyric acid (GABA) in the superficial laminae of the dorsal horn of cat and rat spinal cord. We demonstrate for the first time the co-existence of SP and GABA immunoreactivities in the axonal boutons in laminae I-III of cat spinal dorsal horn. In cat, most SP+GABA immunoreactive (IR) axonal boutons established synapses with SP-IR or non-IR dendrites. These synapses were exclusively symmetric. Quantitative analysis showed that the percentage of SP/GABA double labelled bouton profiles was higher (7%) in lamina I but was considerably lower in laminae IIo, IIi and III. Similarly, the density (number of bouton profiles per 100 μm^2) of SP+GABA-IR bouton profiles was highest in lamina I. However, in agreement with previous studies, the co-localization of SP and GABA immunoreactivities was never detected in the rat dorsal horn. In both species, SP+GABA-IR or GABA-IR axonal bouton profiles were never seen presynaptic to SP-IR boutons. These findings provide a morphological basis for the interaction of excitatory and inhibitory agents in the nociceptive circuits in the dorsal horn of the cat and rat spinal cord.

INTRODUCTION

It has long been known that the superficial layers of the dorsal horn are the first location in the CNS where the nociceptive information originating from the skin and deeper structures is modulated. However, in spite of all the data obtained from studies in various disciplines, little is known concerning the precise neurotransmitter-specific neuronal circuits subserving such modulation. An important issue to be elucidated is how excitatory and inhibitory neurotransmitters interact and are synaptically related to dorsal horn nociceptive neurons. Substantial evidence accumulated during the last two decades indicates that substance P (SP) plays a major role in the transmission of nociceptive information by primary sensory neurons. Briefly, SP can excite dorsal horn nociceptive neurons (Henry, 1976). Substance P immunoreactivity has been detected in small diameter primary afferent fibres (Hökfelt et al., 1975a; Hökfelt et al., 1975b). High concentrations of SP immunoreactivity were revealed in the dorsal horn (Hökfelt et al., 1975b; Hökfelt et al., 1977; Cuello et al., 1977a; Cuello and Kanazawa, 1978), particularly in Rexed's laminae I-II and, to a limited extent, in lamina V, which are the areas where small diameter sensory fibres terminate (Light and Perl, 1979b; Sugiura et al., 1986). SP is released in the spinal cord *in vivo* specifically upon activation of nociceptive sensory fibres (Duggan et al., 1988). SP-mediated responses of dorsal horn nociceptive neurons could be blocked by a NK-1 receptor antagonist (Cridland and Henry, 1988a; Radhakrishnan and Henry, 1991; De Koninck and Henry, 1991), and those nociceptive neurons were shown as being abundantly innervated by SP-

immunoreactive (IR) boutons (De Koninck et al., 1992).

GABA is a well-known inhibitory neurotransmitter in the spinal cord. GABAergic neurons are concentrated in the superficial laminae of the dorsal horn (Ribeiro-da-Silva and Coimbra, 1980; Hunt et al., 1981; Barber et al., 1982; Todd and Sullivan, 1990). Ultrastructural studies using ^{3}H-GABA-uptake or antisera against GAD or GABA have shown that, in rat and cat, GABAergic axons in laminae I-III established mostly symmetrical axodendritic synapses, but were also presynaptic to primary sensory fibres at axoaxonal synapses (Barber et al., 1978; Ribeiro-da-Silva and Coimbra, 1980; Magoul et al., 1987; Maxwell and Noble, 1987; Maxwell et al., 1990). GABA-IR profiles have been found presynaptic to the terminals of functionally defined myelinated nociceptors in the monkey and cat spinal cord (Alvarez et al., 1992).

Despite the progress made in this area, we lack direct information concerning the synaptic interactions of SP-IR and GABA-IR profiles in the spinal dorsal horn. Therefore, the purpose of this study was to address the above issue. To achieve this objective, we applied a combination of pre-embedding DAB-based immunocytochemistry and post-embedding immunogold staining to investigate the distribution of SP and GABA immunoreactivities in the superficial laminae of the dorsal horn of the cat and rat spinal cord. Our results indicate that SP and GABA immunoreactivities are co-localized in some axonal varicosities mainly in laminae I of the cat spinal cord. Consistent with previous studies, however, this co-localization of SP and GABA immunoreactivities was never found in the rat. Furthermore, we never detected GABA-IR profiles presynaptic to SP-IR bouton profiles in either animal

species.

MATERIALS AND METHODS

Four male cats, 3.5 to 4 kg in weight, were anaesthetized with α-chloralose (60mg/kg, i.v.). Four Wistar rats, 250 to 300g in weight, were anaesthetized with Equithesin (3ml/kg, i.p.). All animals were perfused through the left ventricle with a mixture of 4% paraformaldehyde and 0.5% glutaraldehyde in 0.1M phosphate buffer, pH7.4. Spinal cord segments C4-C5 (rat) and L2-L4 (rat and cat) were removed, postfixed in the same fixative mixture for 90 minutes, and infiltrated in 30% sucrose in 0.1M phosphate buffer overnight at 4°C. Before being sectioned, the tissue was snap frozen by immersion in liquid nitrogen and thawed in 0.1M phosphate buffer at 25°C. The spinal cords were sectioned either transversely or parasagittally at 50 μm on a Vibratome. Prior to incubation in the antibody, the sections were treated with 1% sodium borohydride in phosphate-buffered saline (PBS) for 1 hour and washed thoroughly in PBS.

Pre-embedding immunocytochemistry

The antibody used was a bi-specific, anti-substance P/anti-horseradish peroxidase (HRP) monoclonal antibody [coded P4C1 (Suresh et al., 1986); Medicorp, Canada]. Tissue sections were incubated overnight in P4C1 antibody, diluted 1:10, at

4°C. The following day, the sections were incubated for 2 hours at room temperature in PBS containing 5 µg/ml of horseradish peroxidase (HRP; Sigma type VI). After each incubation, sections were washed twice in PBS and reacted for peroxidase with 3,3'-diaminobenzidine tetrahydrochloride (DAB; Sigma) in PBS. After the DAB reaction, the sections were rinsed several times in PBS and immersed for 90 min. in osmium tetroxide in 0.1M phosphate buffer at 4°C. The tissue was then dehydrated in ascending alcohols and flat-embedded in Epon. After selecting the appropriate fields, the sections were trimmed and Epon re-embedded. The selected areas corresponded to the middle third of the mediolateral extent of the superficial dorsal horn, and contained the entire dorsoventral extent of laminae I-III. Ultrathin sections were obtained with a Reichert Ultracut microtome using a diamond knife and collected onto mesh nickel grids.

Post-embedding immunocytochemistry

Post-embedding immunostaining was carried out as described in detail elsewhere (Ribeiro-da-Silva et al., 1993). A well characterized polyclonal anti-GABA antibody (Sigma) raised in rabbit was used. Following washes in Tris-buffered-saline, an anti-rabbit IgG antibody conjugated to 10nm gold (Biocell) was used. After counterstaining with uranyl acetate and lead citrate, the sections were examined under the electron microscope (Philips 410). To assess the specificity of the immunostaining, we carried out preabsorption studies. The antibody against GABA, at the dilution used for immunostaining, was incubated with 1 µM GABA (Sigma) for 24 h at room temperature. GABA immunoreactivity was not detected when the preabsorbed anti-

GABA antibody was used. No specific labelling was obtained when the anti-GABA antibody was replaced by normal rabbit serum.

Quantitative analysis

This analysis was restricted to the cat. For quantitative purposes, two Epon blocks were used from each animal. One section from each block was quantified. At the magnification of X10,200, five non-overlapping fields per laminae were selected at random and photographed (total number of photos=132). The photographic negatives were enlarged X1.5 for a final magnification of X15,300. At this final magnification, the various profiles in the neuropile could be clearly identified. From the micrographs thus obtained, all bouton profiles immunoreactive for SP, GABA and those non-immunoreactive were counted. Profiles were considered as specifically immunostained for GABA when the density of deposited gold particles per square micrometer was at least three times above background. Background levels were measured on capillary lumens. The percentages of SP-, GABA-, SP+GABA-immunoreactive and non-immunoreactive bouton profiles in the total number of bouton profiles were determined for each lamina. In addition, the densities (number of bouton profiles per 100 μm^2) of SP-, GABA-, SP+GABA-immunoreactive, and non-immunoreactive bouton profiles for each lamina were calculated. A total number of 2,431 bouton profiles was counted.

RESULTS

Qualitative results

Under the electron microscope, the two immunocytochemical signals could be easily distinguished. DAB reaction products and immunogold particles represented SP and GABA immunoreactivity, respectively. SP immunoreactivity was associated with dense core vesicles, but also occurred in between the agranular vesicles and on the membranes of mitochondria. Immunogold particles were associated mostly with small agranular vesicles and mitochondria, as described in previous studies(Maxwell et al. 1990; Merighi et al., 1989). SP immunoreactivity was detected in dendrites and axonal terminals, as has been previously described in rat (Chan-Palay and Palay, 1977; Pickel et al., 1977; Barber et al., 1979; Priestley et al., 1982b; Bresnahan et al., 1984; Ribeiro-da-Silva et al., 1989). GABA immunoreactivity was found in axonal boutons, dendrites and also in some neuronal cell bodies (Todd and Sullivan, 1990; Carlton and Hayes, 1991; Powell and Todd, 1992; Alvarez et al., 1992). In this study, we focused on the synaptic interactions of SP- and GABA-IR profiles. To facilitate our description, we will divide such interactions into two types: non-glomerular and glomerular.

Non-glomerular synaptic interactions

The most striking finding in the present study was the detection of boutons double labelled for both SP and GABA immunoreactivities in the dorsal horn of the cat spinal cord (Fig. 1). The double-labelled boutons were more numerous in laminae I than in other laminae. Most of them were apposed to dendrites, although some were in

contact with other axonal boutons or with cell bodies. Usually, double-labelled boutons were presynaptic to other structures, although in some cases no synapses could be detected even after 3-4 serial sections were examined (Fig.1A). A few "en passant" varicosities immunoreactive for both SP and GABA were also detected, particularly in parasagittal sections (Fig. 1B). SP and GABA immunoreactivities were also co-localized in some dendritic profiles in laminae I-IIo (Fig. 2) and occasionally in cell bodies in lamina II (data not shown).

The double labelled boutons participated in several types of synaptic arrangements. The synapses were exclusively of the symmetric type (Fig.1 C and D). The most common postsynaptic element was a dendrite which was either SP immunonegative (Fig.1C) or immunopositive (Fig.1D). Frequently, SP+GABA-IR boutons and boutons immunoreactive for SP or GABA were presynaptic to a common dendrite. In such cases, the synapses formed by SP+GABA- and GABA-IR boutons were symmetric (Fig. 1C and 1D, arrowheads), but the synapses between SP-IR boutons and postsynaptic dendrites were frequently asymmetric (not shown). Occasionally, boutons co-localizing SP and GABA were found apposed to SP immunopositive or immunonegative boutons (data not shown), but no synapses could be detected, even after serial section analysis.

In the rat spinal dorsal horn, SP and GABA immunoreactivities were always seen in separate neuronal profiles as reported previously (Merighi et al., 1989). Rather frequently, GABA-IR boutons were apposed to SP-IR boutons (Fig. 3A and 3C). However, no convincing evidence of GABA-IR boutons presynaptic to SP-IR boutons

could be obtained, in spite of the analysis of serial sections. SP-IR boutons were frequently apposed to (Fig. 3B) or presynaptic to GABA-IR dendrites. Figure 3C shows a frequent synaptic association in which SP-IR and GABA-IR boutons were presynaptic to a common immunonegative dendrite. As in cat, the synapses between the GABA-IR bouton and the dendrite were symmetric (arrowheads in Fig. 3C), in contrast to the asymmetric synapses formed by most of the SP-IR boutons (open arrow in Fig. 3C).

Glomerular synaptic interactions:

Occasionally, in lamina IIo of the cat spinal cord, SP+GABA-IR dendrites were apposed to the central boutons of synaptic glomeruli, although we did not detect any synapses between the two elements (Fig. 2). We also detected SP-GABA-IR boutons which were presynaptic to peripheral dendrites in synaptic glomeruli (Fig. 4). In this type of synaptic association, both the central glomerular bouton and the SP+GABA-IR bouton were presynaptic to a common glomerular dendrite which was immunonegative. The synapses formed by the double labelled bouton were symmetric (Fig. 4, arrowheads), in contrast to the asymmetric synapses formed by the central bouton (Fig. 4, open arrow).

In the superficial layers of the rat dorsal horn, GABA-IR boutons were frequently found as peripheral profiles in synaptic glomeruli, in which the central boutons were SP immunoreactive. Usually, the SP-IR central boutons were presynaptic to GABA-IR dendrites (Fig.5A). Less frequently, GABA-IR boutons were apposed to

SP-IR central boutons, but were never presynaptic to the later element (Fig.5B).

Quantitative results

Figure 6A shows the relative percentages of different types of bouton profiles in the superficial laminae of cat spinal cord. The relative percentage of SP-IR bouton profiles was highest in laminae I and IIo, decreased in lamina IIi and dropped drastically in lamina III. The relative percentage of GABA-IR bouton profiles increased gradually from lamina I to lamina III, where it reached the highest value. SP+GABA-IR bouton profiles were never very abundant. Their relative percentage was highest in laminae I, and decreased drastically in lamina IIo. The percentage of immunonegative bouton profiles remained approximately constant in all laminae, in spite of a small increase in lamina III.

Figure 6B illustrates the densities (number of bouton profiles per 100 μm^2) of different types of bouton profiles in each lamina of cat spinal cord. The density of SP-IR bouton profiles reached its highest value in lamina IIo. Values were slightly lower in laminae I and IIi, and much lower in lamina III. The density of GABA-IR bouton profiles was higher in laminae IIi and III than in laminae I and IIo. The highest density of SP+GABA-IR bouton profiles was detected in lamina I, and the values were considerably lower in laminae IIo, IIi and III. The density of immunonegative bouton profiles was low in lamina I, and increased progressively from laminae IIo to III.

DISCUSSION

The major finding of the present study was the detection of a co-existence of SP and GABA immunoreactivities in axonal boutons of the superficial laminae of the cat spinal dorsal horn. To our knowledge, this is the first time that such co-localization has been reported in this area of the CNS. Such co-localization of SP and GABA immunoreactivities has been reported in cat retina (Pourcho and Goebel, 1988) and in hamster olfactory bulb (Kosaka et al., 1988), at the light microscopic level. In our study, most of the SP+GABA-IR axonal boutons established synapses with SP immunoreactive or immunonegative dendrites. The synapses thus formed were exclusively symmetric. The quantitative analysis indicated that both the percentage and the density of SP+GABA-IR bouton profiles were considerably higher in lamina I than in the other laminae. In contrast, such co-localization was never found in the rat, in agreement with a previous report (Merighi et al., 1989).

We should stress that the quantitative data in this study only serves to provide an idea of how frequent the SP+GABA-IR profiles were, both in absolute numbers and in comparison with others labelled for SP-only and GABA-only in each of the laminae studied. We did not carry out a detailed stereological analysis of bouton numbers per unit of area, but rather counted profile numbers. Therefore, the factor bouton size was not taken into account, and the relative percentages and densities would be affected by possible size differences among the populations of profiles labelled for SP, GABA or SP+GABA. Our values should therefore be considered as approximative. Further work

will be necessary to determine actual terminal numbers.

In some of the double-labelled profiles (see e.g. Fig. 1A), and also in some of those labelled for GABA immunoreactivity only, the gold particles seemed to be more associated with mitochondria than with other structures in the terminal. This association has also been shown in other studies using post-embedding immunostaining for GABA [see e.g. (Valtschanoff et al., 1994)]. The reason why mitochondria should possess more GABA than other components of the terminal is at present unclear.

Origin of SP+GABA-IR axonal boutons

SP immunoreactivity in the dorsal horn originates from small diameter primary sensory fibres (Hökfelt et al., 1975a; Hökfelt et al., 1975b; Cuello et al., 1978), neurons intrinsic to the dorsal horn (Ljungdahl et al., 1978; Hunt et al., 1981) and, to a limited extent, from fibres descending from the raphe nuclei (Menétrey and Basbaum, 1987). GABA immunoreactivity in the dorsal horn has two sources: intrinsic GABAergic interneurons in the dorsal horn, either from the same or adjacent segments (Carlton and Hayes, 1990), and descending fibres from the medullary raphe, where GABA has been co-localized in serotonergic cell bodies that project to the spinal cord (Millhorn et al., 1987; Kachidian et al., 1991). Since GABA has never been identified in dorsal root ganglion neurons, it is very unlikely that SP+GABA-IR boutons might originate from primary sensory afferents. In line with this, in the present study, GABA or GABA+SP immunoreactivity has never been detected in central boutons of synaptic glomeruli, profiles which have been shown to be primary sensory origin in both rat (Coimbra et al.,

1984) and cat (Duncan and Morales, 1978; Murray and Goldberger, 1986). In the present study, SP and GABA immunoreactivities were also co-localized in some dendritic profiles, particularly in lamina IIo, and in cell bodies in lamina II. Together with the above evidence from the literature, this finding indicates that, at least in part, SP+GABA-IR axonal boutons originate from intrinsic spinal dorsal horn neurons located in lamina II. It should be stressed that our study was carried out in the absence of colchicine treatment. It is likely that, after colchicine treatment, SP+GABA-IR neurons and dendritic profiles would be more apparent in the superficial laminae of the dorsal horn of the cat spinal cord.

Functional significance of SP+GABA-IR boutons

The co-existence of SP and GABA in the same axonal boutons in the superficial laminae of the cat spinal cord provides new evidence that excitatory and inhibitory neurotransmitters interact and exert their effects in a more complex manner than previously thought. In a way, this co-localization can be compared to the co-localization of SP and enkephalin (ENK) in axonal boutons in the rat and cat dorsal horn. In previous studies, the co-existence of SP and ENK in axonal boutons has been well described in the superficial laminae of the dorsal horn of cat (Tashiro et al., 1987) and rat (Senba et al., 1988; Ribeiro-da-Silva et al., 1991b). It has been speculated that these SP+ENK-IR dorsal horn neurons are interneurons within the main sensory pathway receiving primary sensory input (likely nociceptive) and transmitting it to projection neurons. Alternatively, some or all of the SP+ENK double-labelled cells may be

interneurons not within the main sensory pathway but parallel to it (Ribeiro-da-Silva et al., 1991b). Neurons co-localizing GABA and SP immunoreactivities might have a similar action to those co-localized by SP and ENK immunoreactivities. It is possible that the former represent a subpopulation of the later. In fact, it is likely that SP+GABA cells also co-localize ENK immunoreactivity.

It is interesting to note that most of the bouton profiles co-localizing SP+GABA immunoreactivities were in lamina I. This lamina contains many neurons which project to the thalamus (Lima and Coimbra, 1988). Some of the lamina I projection neurons are nociceptive (Cervero et al., 1976; Price et al., 1979; Woolf and Fitzgerald, 1983) and some may contain SP (Lima et al., 1993). It is reasonable to postulate that SP+GABA-IR boutons are presynaptic to lamina I projection neurons (SP-IR or non-SP-IR) which are involved in nociception. Moreover, in a preliminary study, we detected some SP+GABA-IR boutons presynaptic to functionally identified and HRP-filled lamina I nociceptive neurons (Ma et al., 1994). This evidence strongly suggests that SP+GABA containing interneurons in the spinal cord play a role in the modulation of nociceptive information.

In the present study, the synaptic contacts established by SP+GABA-IR axonal boutons and their postsynaptic elements (SP immunopositive or immunonegative dendrites) were exclusively symmetric, indicating that an inhibitory signal is transmitted to the postsynaptic element (Uchizono, 1965; Gray, 1969). It is therefore likely that such an inhibitory signal would be mediated by GABA, as the ultrastructural evidence described here suggests.

Consistently, SP-IR, GABA-IR, and SP+GABA-IR boutons were presynaptic to SP immunopositive or immunonegative dendrites. Therefore, it can be speculated that SP containing boutons excite SP-IR dorsal horn neurons that convey nociceptive signals to higher brain regions. GABA-IR inputs would exert their inhibitory effects on the same nociception driven neurons. Although it is not possible to define a precise role for the SP+GABA containing system in the modulation of nociception, neurons co-localizing both immunoreactivities are presumably involved in the fine tuning of nociception modulation in sensory pathways. Thus, the SP+GABA-containing system could regulate their own excitation on postsynaptic targets by means of GABA release (affecting either autoreceptors or postsynaptic receptors). Hence, upon repetitive stimulation of the neuron, an excitatory response elicited by SP could be terminated at pre- or postsynaptic levels by GABA released by neurons co-localizing SP+GABA. Conversely, as GABA is a fast transmitter, SP might modulate the inhibitory response induced by GABA in the postsynaptic neurons.

It should be stressed that the SP+GABA system does not seem to occur in rat, as we did not detect SP+GABA-IR boutons in that species. Although the functional significance of such species difference in SP/GABA interactions is not yet clear, it can be easily predicted that nociception modulation in cat spinal dorsal horn is more complex than in rat.

Interestingly, in both cat and rat spinal dorsal horns, we did not detect GABA-IR boutons presynaptic to SP-IR boutons. Although this type of synaptic arrangement was reported as occasionally seen in a previous preliminary report in the rat dorsal horn,

such finding has not been illustrated (Merighi et al., 1989). In our study, we carried out a detailed search for presynaptic interactions of GABA-IR or SP-IR boutons in serial ultrathin sections. However, GABA-IR boutons were frequently presynaptic to non-immunoreactive vesicle-containing profiles, either axonal boutons or presynaptic dendrites (Ribeiro-da-Silva, 1995). This negative finding suggests that GABA probably might modulate nociceptive information conveyed by SP containing primary sensory fibres through a postsynaptic mechanism. Our finding is also supported by a recent report that the well-known analgesic effects of baclofen are not mediated by a reduction of the release of SP or CGRP in the dorsal horn from central terminals of nociceptive primary afferents, while it could be mediated through the suppression of lumbar dorsal horn neurons (Morton et al., 1992).

Figure 1. Co-localization of SP and GABA immunoreactivities in axonal boutons of lamina I of the dorsal horn of cat spinal cord. Diaminobenzidine reaction product represents SP antigenic sites. Immunogold particles represent GABA immunoreactivity. Micrographs of **A** to **D** show examples of some of the types of profiles detected. **A** shows a bouton co-localizing SP and GABA which did not establish synapses with the surrounding profiles in the four serial sections examined. **B** shows a double-labelled profile which represents an "en passant" varicosity of an axon. **C** illustrates a double-labelled bouton apposed to a varicosity labelled for GABA only; no synapse between the two profiles could be detected, even after serial section analysis. However, SP+GABA-IR bouton is presynaptic to a immunonegative dendrite (d), the synapse thus formed being symmetric (arrowheads). **D** shows a SP+GABA-IR axonal bouton and a GABA-only bouton which are presynaptic to a common SP-IR dendrite, both synapses being symmetric (arrowheads). Scale bars = 0.5 μm.

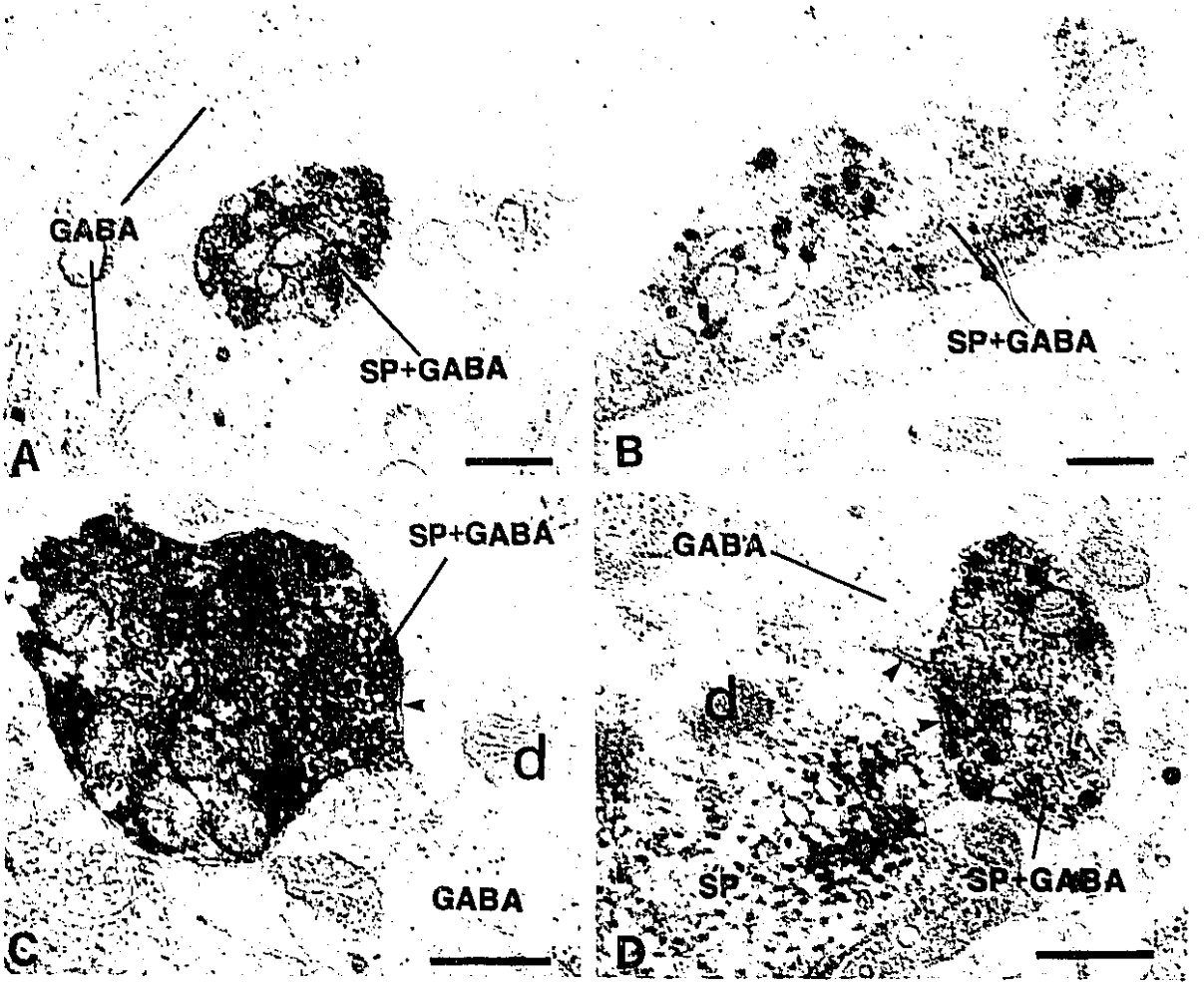
GABA
SP+GABA
A
SP+GABA
B
SP+GABA
d
GABA
C
GABA
d
SP
SP+GABA
D

Figure 2. Co-localization of SP and GABA immunoreactivities in a proximal dendrite in lamina IIo of the cat dorsal horn. The double-labelled dendritic profile (SP+GABA) is apposed to the central element of a synaptic glomerulus (C_1 type; see ref. (Ribeiro-da-Silva, 1995)). The C_1 bouton is presynaptic to other dendrites (d) but not to the double-labelled profile. Scale bar = 0.5 μm.

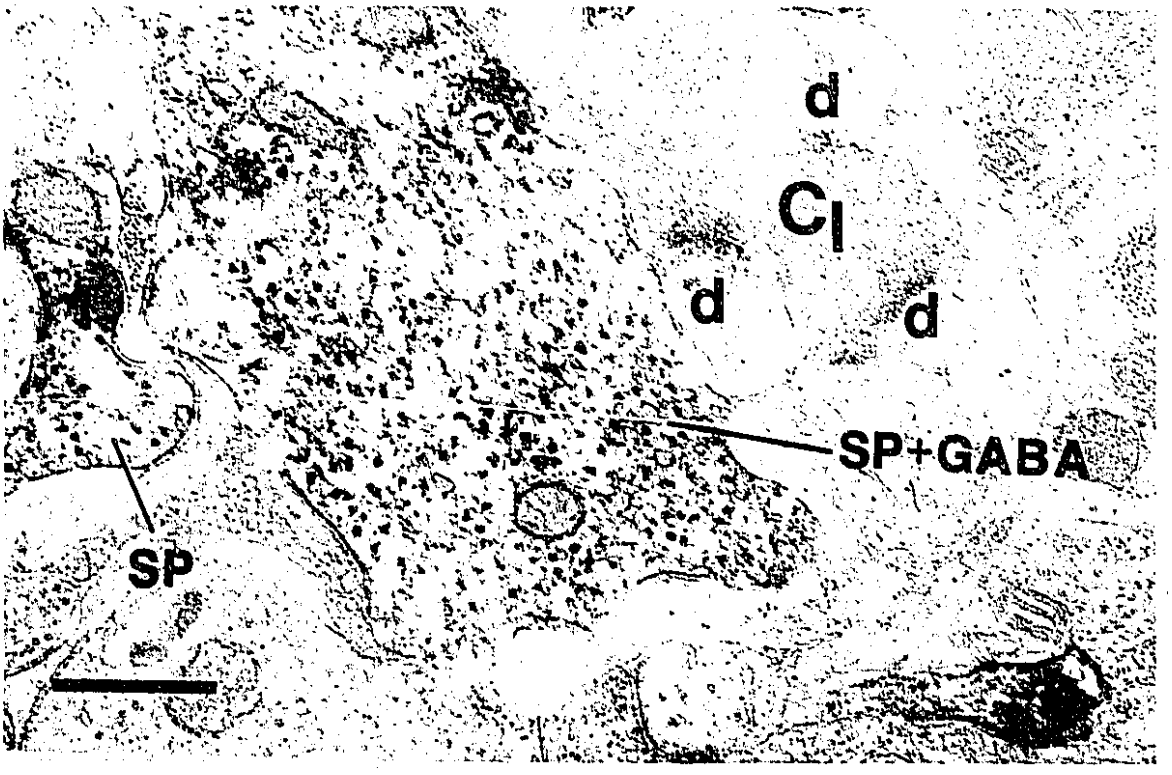
d
Cl
d
d
SP+GABA
SP

Figure 3. Association of SP-IR and GABA-IR boutons in the superficial laminae of the dorsal horn of the rat spinal cord. **A** shows a SP-IR axonal bouton apposed to a GABA-IR axonal boutons in lamina I; no synapses were detected between the two elements after serial section analysis. In **B**, a SP-IR axonal bouton is apposed to a GABA-IR dendrite in lamina I. **C** illustrates a SP-IR axonal bouton and a GABA-IR bouton which are presynaptic to a common dendrite (d) in lamina IIA. The synapse between the SP-IR bouton and the dendrite is asymmetric (open arrow), but the one between the GABA-IR and the dendrite is symmetric (arrowheads). Scale bars = 0.5 μm.

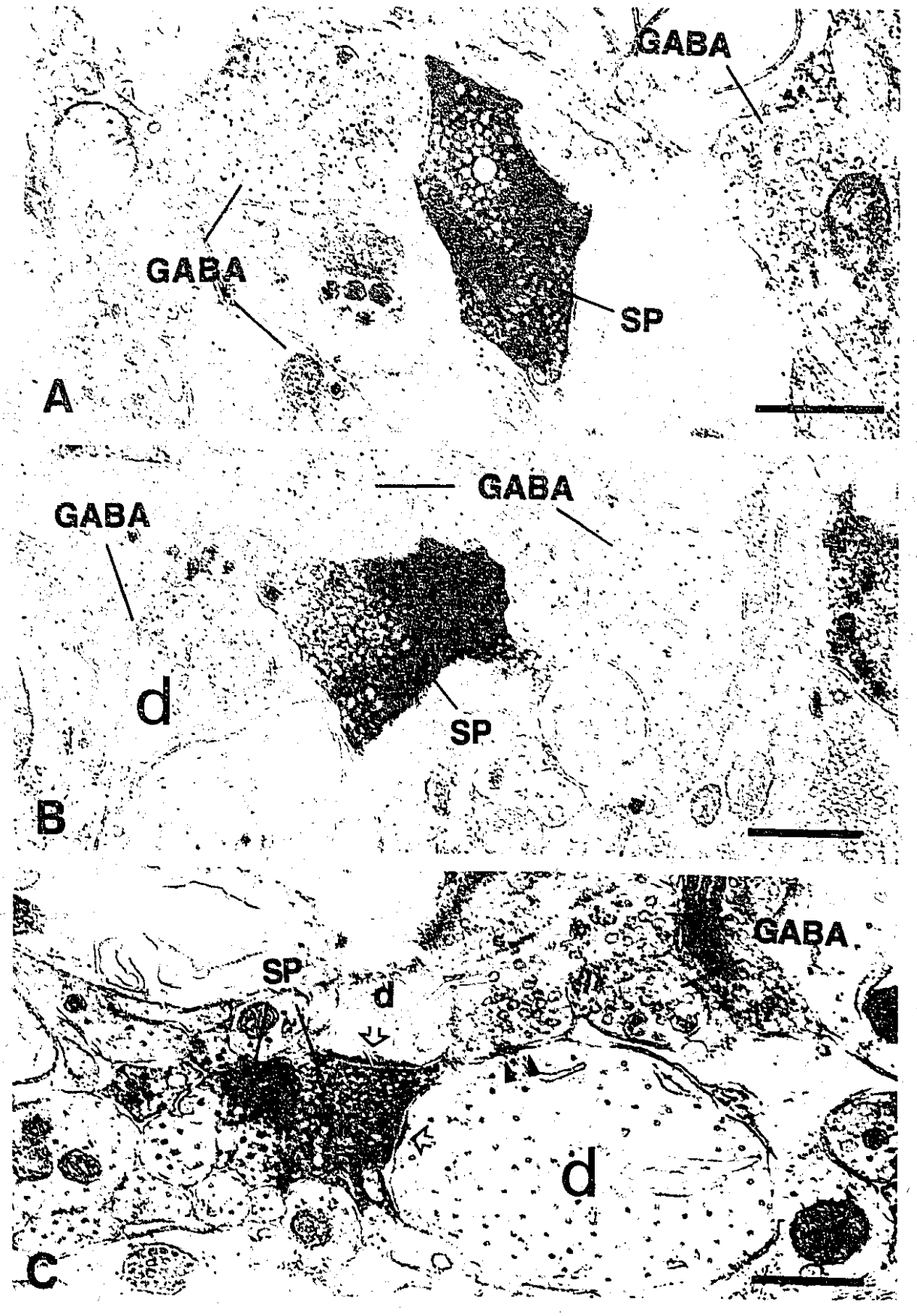
GABA
GABA
SP
A
GABA
GABA
d
SP
B
SP
d
GABA
d
c

Figure 4. Synaptic interactions of SP+GABA-IR axonal boutons and central boutons of synaptic glomeruli in lamina IIo of the cat spinal cord. Note a SP+GABA-IR bouton and an immunonegative central bouton (C_1) which are presynaptic to a common dendrite (d). The synapse between the SP+GABA-IR bouton and the dendrite is symmetric (arrowheads), while the one between the central bouton and the dendrite is asymmetric (open arrow). Scale bars = 0.5 μm.

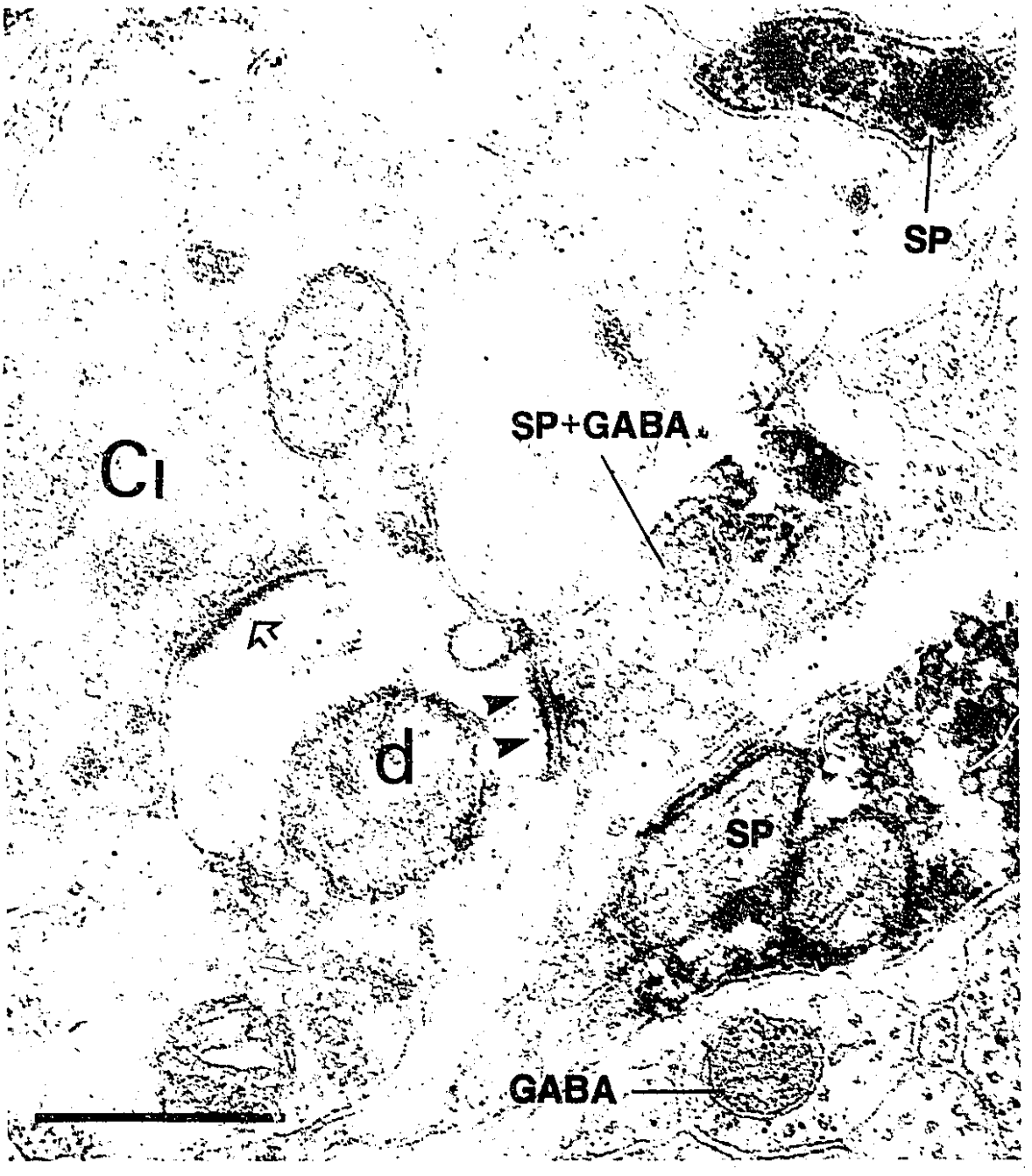
SP
SP+GABA
Ct
d
SP
GABA

Figure 5. Synaptic interactions of SP-IR central boutons of synaptic glomeruli and GABA-IR profiles in the superficial laminae of the rat spinal dorsal horn. In **A**, a SP-IR glomerular central bouton (C_1 type) is presynaptic to GABA-IR or non-IR dendrites in lamina IIA. Although the dendrites appear lightly labelled for GABA immunoreactivity, it was considered specific as it is over 5 times above background levels. The synapses are asymmetric (open arrows). In **B**, a GABA-IR bouton is apposed to a SP-IR central terminal (C_1) in lamina IIB, no synapses were observed between these two elements, even after analysis of adjacent sections. Scale bars = 0.5 μm.

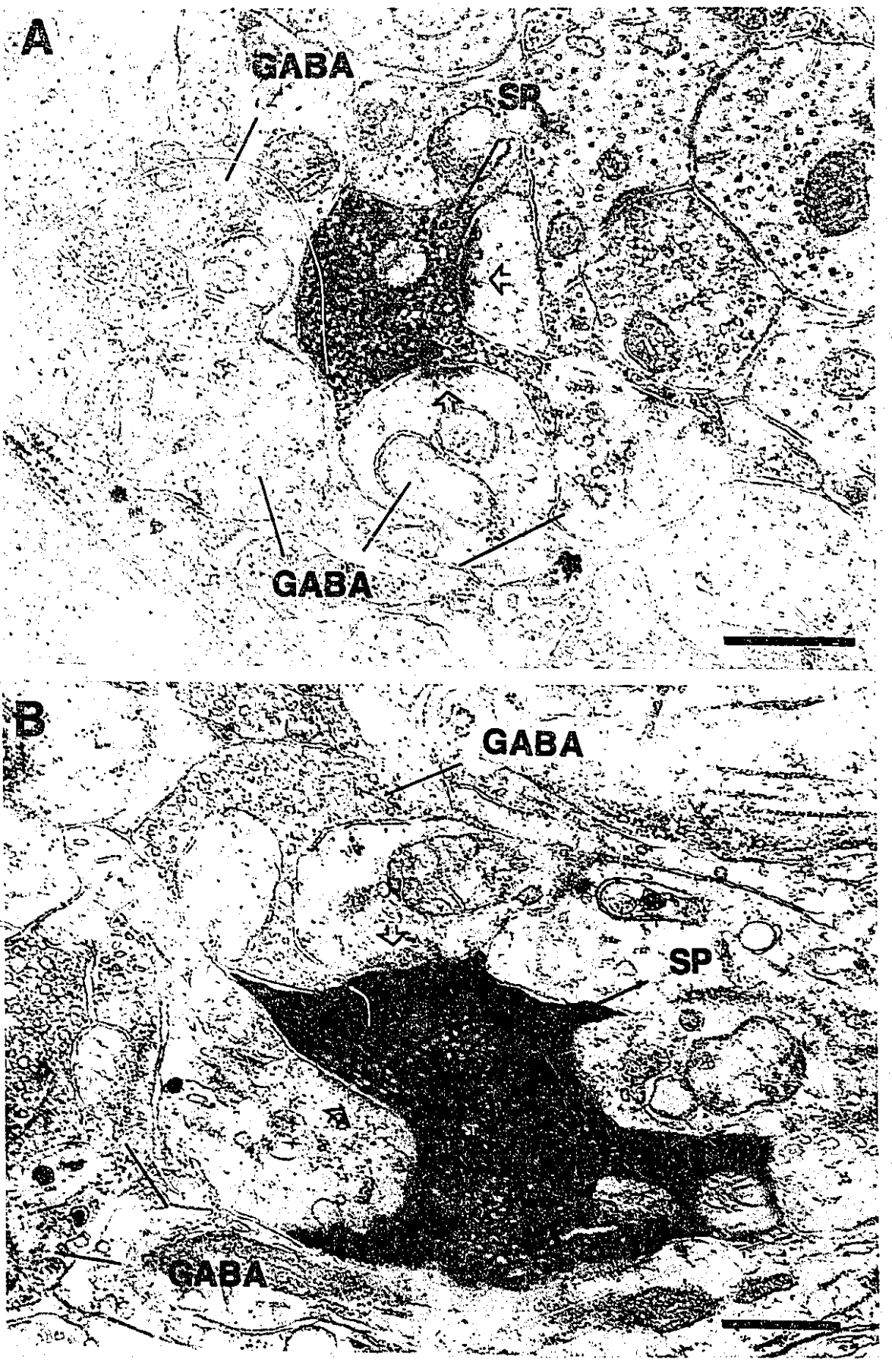
A
GABA
SR
GABA
B
GABA
SP
GABA

Figure 6. Quantification of SP-, GABA- and SP+GABA-IR axonal bouton profiles in laminae I-III of the dorsal horn of cat spinal cord. **A** represents the relative percentage of each neurochemical type of axonal varicosity profile in each lamina. **B** represents the density per 100 μm^2 of each neurochemical type of bouton profile per lamina. Note that bouton profiles co-localizing SP and GABA immunoreactivities were never very abundant, although in lamina I they represented 7% of the total number of bouton profiles in the lamina. Total number of varicosity profiles counted = 2,431.

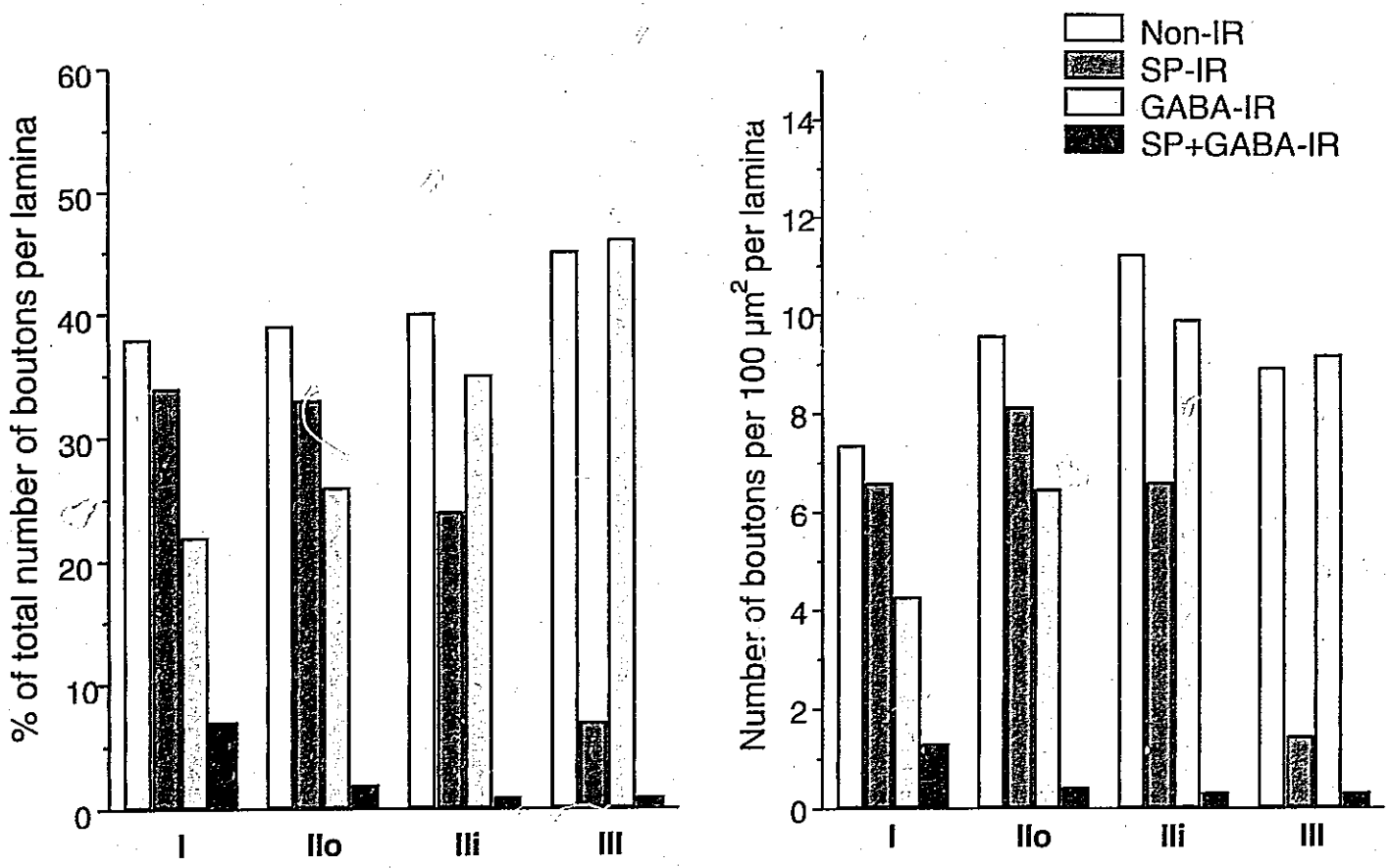
% of total number of boutons per lamina
60
50
40
30
20
10
0
I
IIo
IIi
III
Number of boutons per 100 µm² per lamina
14
12
10
8
6
4
2
0
I
IIo
IIi
III
Non-IR
SP-IR
GABA-IR
SP+GABA-IR

Connecting Text - Chapter IV to Chapter V

In the study of chapter IV, we observed for the first time that SP and GABA immunoreactivities were colocalized in the same axonal boutons in the dorsal horn of cat, but not rat, spinal cord. The percentages and densities of SP+GABA-IR boutons were higher in lamina I than in other laminae. SP+GABA-IR boutons were presynaptic to both SP-IR dendrites or non-immunoreactive dendrites. The synapses thus formed were always symmetric.

In chapter II, III and IV, we investigated the innervation of SP-IR axonal terminals in the first experimental model, namely, under the normal physiological condition. As the innervation by SP-IR fibers might be altered under an abnormal developmental environment, we decided to investigate such possibility. To address this issue, we used a transgenic mouse model which over-expressed NGF in myelinating oligodendrocytes under the control of MBP promoter. In Chapters V and VI, we investigated the over-expression of NGF in myelinating oligodendrocytes in the CNS and the SP-IR sensory fiber innervation in central target tissues of transgenic mice.

CHAPTER V

Ectopic substance P and calcitonin gene-related peptide immunoreactive fibers in the spinal cord of transgenic mice over-expressing nerve growth factor

Weiya Ma, A. Ribeiro-da-Silva, G. Noel, J.-P. Julien and A. Claudio Cuello

ABSTRACT

The aim of the present study was to investigate the *in vivo* effects of the CNS over-expression of nerve growth factor (NGF) on primary sensory neurons. To achieve this objective, a transgenic mouse model was generated which bears a chick NGF gene driven by the myelin basic protein (MBP) promoter. Northern blot analysis demonstrated that high levels of NGF mRNA were detected in the spinal cord of adult transgenic mice. By using immunocytochemistry, NGF immunoreactive (IR) oligodendrocytes were observed throughout the white matter. Furthermore, numerous ectopic substance P (SP)- and calcitonin gene-related peptide (CGRP)-IR fibers were detected in the white matter of the spinal cord of transgenic mice. NGF-IR oligodendrocytes and ectopic SP- and CGRP- fibers were entirely absent from control mice. In the cervical and lumbar dorsal root ganglia, the percentages of SP-IR neurons were significantly higher in transgenic mice when compared to controls. At the EM level, ectopic SP- and CGRP-IR fibers were characterized as unmyelinated axons and axonal boutons. SP co-localized with CGRP in some of those axonal boutons and fibers. Capsaicin treatment of adult mice completely abolished those ectopic SP-IR fibers, confirming their primary sensory origin. Our results indicate that primary sensory neurons are responsive to NGF over-expression in CNS. Ectopic SP- and CGRP-IR fibers in the white matter likely represent collateral sprouts of the central processes of the dorsal root ganglion cells, which were triggered by NGF over-expressed in the myelinating oligodendrocytes in the spinal cord of transgenic mice.

INTRODUCTION

Nerve growth factor (NGF) represents the prototype of target-derived, retrogradely transported trophic molecules. A wide range of functions of NGF in the nervous system have been well characterized and documented [for reviews see (Thoenen et al., 1987; Purves et al., 1988)]. Briefly, NGF was found to be essential to the growth, differentiation and survival of neurons in the autonomic and sensory nervous systems during early development (Levi-Montalcini and Angeletti, 1968; Gorin and Johnson, 1979; Aloe et al., 1981). In adult animals, sympathetic (Purves et al., 1988; Ruit et al., 1990), some sensory (Yip et al., 1984), and cholinergic basal forebrain [for review see (Hefti et al., 1989)] neurons remain responsive to NGF when damaged or in their normal state.

In sensory systems, NGF is specifically taken up along the length of both peripheral and central processes of sensory neurons (Richardson and Riopelle, 1983) and is transported retrogradely to the neuronal perikaryon (Stöckel et al., 1975). Approximately 40% of the neurons in the adult dorsal root ganglion (DRG) display high-affinity NGF receptors, which are thought to be responsible for the transport of NGF (Richardson et al., 1986; Verge et al., 1989b). Subsequently, *trkA* protein has been proven to be an essential component of the high-affinity NGF receptor in some adult small and medium-sized sensory neurons (Verge et al., 1992). Moreover, continuous infusion of NGF to the proximal stump of a transected sciatic nerve mitigates some of

the morphological, biochemical, and electrophysiological alterations in axotomized dorsal root ganglion neuronal perikarya (Schwartz et al., 1982; Fitzgerald et al., 1985; Otto et al., 1987; Rich et al., 1987). In addition, the dramatic reduction in the number of high-affinity NGF receptors on sensory neurons following axotomy can be prevented by administration of NGF to the proximal stump (Verge et al., 1989b). Taken together, these findings suggest that NGF continues to act on intact adult (mature) sensory nerves.

Substance P (SP) and calcitonin gene-related peptide (CGRP) are both present in small diameter DRG neurons (Hökfelt et al., 1975b; Hökfelt et al., 1976; Gibson et al., 1984) and their thinly myelinated and unmyelinated central and peripheral processes (Cuello et al., 1978; Lee et al., 1985b). These small diameter cells are the most conspicuous NGF-sensitive elements among primary sensory neurons. Thus, it has been reported that NGF modulates the gene expression and content of SP and CGRP in these DRG neurons (Lindsay and Harmar, 1989; Rich et al., 1987; Verge et al., 1992). However, the above studies, and others using transgenic models (Hoyle et al., 1993; Albers et al., 1994), are focused on the effects of NGF when supplied directly to cell somata or to the peripheral nervous system. Therefore, there are no studies on the *in vivo* effects upon neural crest-derived primary sensory neurons of endogenous over-expression of NGF within the CNS boundaries. A transgenic mouse model with a chick NGF gene driven by the myelin basic protein (MBP) promoter was generated to induce such a condition. NGF was expected to be over-expressed in the myelinating oligodendrocytes of the white matter of the CNS in these transgenic mice. Interestingly, one NGF transgenic line (414) was found to express elevated levels of NGF in the

abundant white matter of the spinal cord.

Based on the above, SP and CGRP immunoreactivities were used as markers to detect whether thinly myelinated and unmyelinated nociceptive fibers originating from the DRG were responsive to the endogenous over-expression of NGF in the CNS. Examination of SP and CGRP immunoreactivities were undertaken in the spinal cord of those transgenic mice and controls at both LM and EM levels. In addition, SP immunoreactivities of the dorsal root ganglia and the lower lip skin of transgenic mice and controls were also examined.

MATERIALS AND METHODS

Making of the MBP/NGF construct

A HindIII/SmaI fragment (884 bp) of DNA including the partial chicken NGF cDNA cloned into pGEM1 (cloned by Dr. Heumann and kindly provided from Dr. M. Saarma, Helsinki) was blunt-ended with Klenow and subcloned into the ScaI site of the pSVsec plasmid in frame with the proopiomelanocortin (POMC) signal peptide sequences (Lemay et al., 1989). A PvuI/SmaI fusion POMC/NGF fragment of 1.1 kb was then subcloned into the BspM2 site of the pM2 vector (kindly provided from Dr. A. Roach, Toronto) that includes the 5' and 3' sequences of the mouse MBP gene (Readhead et al., 1987). The cloning site is located 10 bp upstream of the initiation AUG codon of the MBP gene. A 4.5 BglII fragment comprising 1.3 kb of 5' MBP

sequences, 1.1 kb of the POMC/NGF fusion gene and 2.1 kb of the 3' MBP regions was isolated and used to generate transgenic mice.

Production of transgenic mice

Microinjection into one-cell embryos of the linearized MBP/NGF construct was performed as described by Brinster et al. (1981). Mouse strain C3B6S1, derived from a cross of strain C3H with strain C57BL/6, was used. Integration of the transgene into the mouse genome was assessed by Southern blot analysis of genomic DNA isolated from the mouse tail. Eight transgenic founders have been derived bearing various copies of the MBP/NGF transgene. However, only one founder (line 414) showed detectable levels of chick NGF expression in the nervous system.

RNA analysis

Mice were sacrificed by cervical dislocation. Total RNA was isolated by homogenization in guanidinium thiocyanate and ultracentrifugation through a CsCl cushion (Chirgwin et al., 1977). Each RNA sample (20 µg) was fractionated on a 1% agarose-formaldehyde gel (Sambrook et al., 1989) prior to blotting. The filter was hybridized at high stringency as descibed in Sambrook et al. (1989) using a ^{32}P-labeled PstI/SmaI fragment of the chick NGF cDNA.

Immunocytochemical procedures

Light Microscopy

A) NGF immunostaining

Ten transgenic mice of either sex from line 414, and ten age-matched controls from the same strain were used. The ages of animals were 20 days and 2 months. All animals were anesthetized with Equithesin (4 ml/kg, i.p.) and perfused transcardially with a mixture of 2% paraformaldehyde and 0.2% benzoquinone in 0.075M phosphate buffer (pH 7.4) for 30 minutes. The spinal cords were removed, postfixed in the same fixative for 2 hours and then infiltrated in 30% sucrose in 0.1M phoshate buffer at 4°C. Spinal cord segments were cut on a cryostat at the thickness of 50 µm and collected as free-floating in phosphate buffered saline with 0.2% Triton X-100 (PBS+T). After washes in PBS+T, sections were incubated in an anti-mouse NGF antibody (1:1000) (kindly provided by Dr. J. Conner, San Diego) for 72 hours. An ABC kit (Vector) was subsequently used according to manufacturer's instructions. After being thoroughly rinsed in PBS, the free-floating sections were mounted onto gelatin-subbed slides. All sections were further dehydrated in ascending alcohols, cleared in xylene, and cover slipped with Entellan (E. Merck).

B) SP and CGRP immunostaining

Five adult transgenic mice, male and female, from line 414 were anesthetized with Equithesin (3 ml/kg, i.p.) and perfused through the ascending aorta with a fixative containing 3% paraformaldehyde, 0.1% glutaraldehyde and 15% saturated picric acid (v/v) in 0.1 M phosphate buffer, pH 7.4, for 30 minutes followed by perfusion with the same fixative mixture devoid of glutaraldehyde, and finally by 10% sucrose in 0.1 M

phosphate buffer, for 30 minutes each (Garofalo et al., 1992). Five non-transgenic mice of the same age and from the same strain were used as controls. The cervical, thoracic and lumbar spinal cords, the cervical and lumbar dorsal root ganglion and the skin of the lower lip were removed and infiltrated overnight in 30% sucrose in 0.1 M phosphate buffer. Ten µm-thick sections of the dorsal root ganglia (DRG) were obtained in a cryostat, collected onto gelatin-subbed slides and processed for SP immunostaining only. Fifty µm-thick transverse and parasagittal sections of the cervical, thoracic, lumbar spinal cords and the skin of lower lip were obtained with a sledge freezing microtome, immersed in 0.5% H_2O_2 in phosphate-buffered saline (PBS) for 15 min, and washed extensively in PBS+T. Subsequently, half of the spinal cord sections and all sections from lower lip skin were processed for the demonstration of SP and the other half of the spinal cord sections for CGRP immunoreactivity. For SP immunostaining, the sections were incubated with a bi-specific anti-SP/anti-horseradish peroxidase (HRP) monoclonal antibody [code P4C1; (Suresh et al., 1986); Medicorp, Canada]. For CGRP immunostaining, an anti-human CGRP rabbit polyclonal antibody (Peninsula) was used, diluted in PBS+T. All sections were incubated overnight at 4°C. All subsequent incubations were performed at room temperature. After two washes in PBS+T, the sections for CGRP immunostaining were incubated for 1 hour in an anti-rabbit/IgG anti-HRP bi-specific monoclonal antibody [Code McC8; (Kenigsberg et al., 1990); Medicorp, Canada]. Following two washes (15 min each) in PBS+T, all sections were incubated in 5 µg/ml of Sigma type VI HRP dissolved in PBS+T, rinsed three times in PBS+T, and reacted with 3,3'-diaminobenzidine tetrahydrochloride (DAB;

Sigma) in PBS. Subsequently, the sections were mounted on subbed slides, dehydrated and cover slipped as described above. Half of the cervical and lumbar DRG sections were counterstained with 1% cresyl violet for the purpose of quantification.

Electron Microscopy

Segments (C4-C7) of the cervical spinal cord from both transgenic mice and controls fixed were quickly frozen by immersion in liquid nitrogen, and thawed in 0.1 M phosphate buffer at 25^{0}C. Fifty µm-thick sections were obtained with a Vibratome, treated for 30 min in 1% sodium borohydride in PBS and then rinsed several times in PBS until all bubbles disappeared (Kosaka et al., 1986). The sections were incubated overnight at 4^{0}C in anti-SP/anti-HRP bi-specific monoclonal antibody, followed by 5µg/ml of HRP in PBS. After several washes in PBS, the DAB reaction was carried out with double intensification (Adams, 1981). Triton X-100 was omitted from all steps. After the DAB reaction, the tissue was rinsed several times with PBS and then osmicated for 1 hour in 1% osmium tetroxide in 0.1 M phosphate buffer at 4^{0}C. Subsequently, the osmicated sections were washed twice with distilled water, dehydrated in ascending concentrations of alcohol and flat embedded in Epon between thick acetate foil and a plastic cover slip. After polymerization of the Epon, the sections were examined by light microscopy. The selected fields of the superficial layers of the dorsal horn and the dorsolateral funiculus were trimmed and re-embedded for electron microscopic examination. The ultrathin sections were counterstained with uranyl acetate and observed with an electron microscope (Philips 410). For the detection of the co-

localization of SP and CGRP at EM level, a post-embedding immunogold technique was used to detect CGRP antigenic sites in ultrathin sections previously processed for SP immunocytochemistry as described above. Ultrathin sections were collected onto formvar-coated nickel grids and were incubated in the primary antibody overnight at room temperature in a humid chamber. The primary antibody was a rabbit antibody against rat CGRP (Peninsula). Subsequently, sections were incubated in the secondary antibody for 1 hour at room temperature. The secondary antibody was a gold-conjugated goat anti-rabbit IgG (Biocell). The size of gold particles was 10 nanometers. Subsequently, sections were rinsed thoroughly in BSA-Tris and distilled water, contrast stained with uranyl acetate and lead citrate, and examined under the EM.

Capsaicin treatment

Four 3-month-old male transgenic mice from line 414 and 4 control mice were used. All animals were anesthetized before capsaicin treatment with an intramuscular injection of ketamine (100 mg/kg) and acepromazine (2.5 mg/kg). Atropine (0.04 mg/kg) was administrated subcutaneously 15 minutes prior to capsaicin. Three transgenic mice were injected subcutaneouslly with capsaicin (50 mg/kg, Sigma) and one mouse was injected with solvent only to serve as control. Five days later, the second injection of capsaicin was carried out in the same way and at the same dose as the first one. Ten days after first injection of capsaicin, all animals were anesthetized with Equithesin and perfused through the ascending aorta with 4% paraformaldehyde in 0.1M phosphate buffer, pH 7.4. The spinal cords were removed and postfixed in the

same fixative for 2 hours and infiltrated overnight in 30% sucrose in 0.1M phosphate buffer at 4°C. Subsequently, spinal cord segments were cut transversely on a cryostat at the thickness of 50 µm. The free-floating sections were incubated overnight at 4°C in anti-SP/anti-HRP bi-specific monoclonal antibody and processed for the demonstration of SP immunoreactivity as described above.

Quantitative analysis

The following parameters were analyzed quantitatively in sections processed for light microscopy: 1) the relative optical density of SP and CGRP immunoreactivities in laminae I-II of the dorsal horn of the spinal cord , and 2) the percentage of the area occupied by ectopic SP and CGRP immunoreactive fibres in the dorsolateral funiculus of the spinal cord. Quantification of immunostaining was carried out by means of an automated image analysis system (M1, Imaging Research Inc., St. Catharines, Ontario, Canada), with the help of a light microscope (Olympus) coupled to a black and white CCD camera. The intensity of the immunostaining was assessed by measuring the relative optical density in laminae I-II of the dorsal horn of the spinal cord within a rectangular area with 18.52 µm in length and 1.85 µm in width. The measuring rectangle was placed with the upper edge in contact with the dorsal column, equidistant from both the lateral and medial edges of the dorsal horn. For the quantification of the SP and CGRP immunoreactive fiber network in the lateral columns, the percentage of the area occupied by SP and CGRP immunoreactive fibers was measured using a sample window of 220.37 µm X 287.04 µm, which was placed in the dorsolateral

funiculus.

Cresyl violet counterstained cervical and lumbar DRG sections were used to determine the percentage of SP-IR cells in the total number of DRG cells per section. All DRG cells per section were counted directly under the light microscope. For each animal, counts were carried out on 12 sections of cervical and lumbar DRG, respectively. DRGs from 4 transgenic and 4 control mice were used.

Statistical comparisons were carried out by means of Student's t-tests. The significance level was set at $P<0.05$.

RESULTS

Expression of a MBP/NGF construct in a transgenic mouse line

A partial chick NGF cDNA of 884 bp corresponding to the third exon of the gene was subcloned in frame with the POMC signal sequence of the pSVsec vector (Lemay et al., 1989) to allow secretion of NGF in expressing cells. The chicken NGF cDNA contained all coding sequences but was missing the sequences for the signal peptide. The POMC/NGF fragment was then subcloned into the MBP expression vector (Readhead et al., 1987) called pM2 (kindly provided by Dr. A. Roach, Toronto). Before generating transgenic mice, the POMC/NGF fusion construct under the SV40 promoter was tested in transient assays in COS cells. Conditioned medium from transfected cells with the POMC/NGF construct promoted neurite extension from PC12 cells indicating

that the precursor molecules were correctly synthesized and processed to the secretory pathway of COS cells to produce a functional NGF product.

Transgenic mice were generated by the microinjection of a 4.5 kb DNA fragment comprising the POMC/NGF fusion gene flanked by 1.3 kb of 5' and 2.1 kb of 3' sequences from the MBP gene (Fig.1A). The choice of this promoter was based on the hope that the MBP regulatory elements would direct substantial levels of transgene expression throughout the nervous system and that expression would be restricted to the postnatal period to avoid developmental defects.

Eight NGF transgenic lines were generated. Northern blot analysis was carried out on 20 μg of total RNA obtained from different tissues of F1 offspring (2 months old). Only one NGF transgenic line (line 414) showed detectable levels of NGF mRNA in the adult nervous system. As shown in Figure 1B, these transgenics express NGF mRNA at high levels in the spinal cord and low levels in the brain stem. However, no detectable level of NGF mRNA was observed in the kidney.

NGF, SP and CGRP immunoreactivities

The results obtained using immunocytochemistry for NGF or neuropeptides SP and CGRP were identical in homozygous and heterozygous transgenic mice and differed from those in controls. Therefore, the results reported below were obtained using both homozygous and heterozygous animals.

NGF immunoreactivity in the spinal cord

NGF immunoreactive cells were observed throughout the white matter of the spinal cord of both 20-day-old and 2-month-old transgenic mice (Fig. 2B and 2D). These NGF immunoreactive cells in the white matter possessed the morphological characteristics of oligodendrocytes. In logitudinal sections, they were aligned in rows in between the nerve fibers. A few NGF immunoreactive oligodendrocytes were found in the gray matter (Fig. 2B). In short, these cells showed few processes radiating from a spherical or polygonal cell body. These processes were more delicate and thinner than those of astrocytes and neurons, and never formed the vascular feet typical of astrocytes. No NGF immunoreactive oligodendrocytes were detected either in the gray or white matter of the spinal cords from age-matched control mice (Fig. 2A and 2C).

SP AND CGRP immunoreactivities in the spinal cord

Intense SP and CGRP immunoreactivities were observed in laminae I-II of dorsal horn of the spinal cord of transgenic mice and their age-matched controls (Figs. 3 and 4). Some scattered SP and CGRP immunoreactive fibres could be detected in the area around the central canal. The well-known staining of CGRP of some motoneurons was also visualized (Figs. 4A and 4B). No apparent transgenic vs. control differences in the immunoreactivities for both peptides were detected in the gray matter.

However, striking changes in the immunostaining patterns for both peptides were detected in the white matter. Particularly in the lateral columns, but also in the ventral and dorsal columns, ectopic SP and CGRP immunoreactive fiber bundles were

detected in transgenic mice (Figs. 3B and 4B). The orientation of the fiber bundles was mainly parallel to the main axis of the spinal cord (Fig. 5B). Such fiber bundles were entirely absent from controls (Figs. 3A and 4A), which possessed only isolated fibers in the white matter (and almost exclusively in the dorsal columns).

At high magnification, ectopic SP and CGRP immunoreactive fibers were visualized as fiber bundles in the white matter of the transgenic mouse spinal cord (Figs. 3D and 4D). Some particularly long ectopic SP and CGRP immunoreactive fibers were found to penetrate transversely toward the gray matter or to travel around the edge of the gray matter (Figs.3B and 4B). Many varicosities could be found along these long CGRP immunoreactive fibers.

SP immunoreactivity in the spinal cord after capsaicin treatment

Figure 6 illustrates SP immunostaining of spinal cord sections from vehicle-treated (6A and 6C) and capsaicin-treated (6B and 6D) transgenic mice. SP immunoreactivity in laminae I-II was remarkedly reduced in capsaicin-treated transgenic mice (Fig. 6B) compared to the vehicle-treated mouse (Fig. 6A). In capsaicin-treated animals, no ectopic SP immunoreactive fibers could be detected (Fig. 6B and 6D). No changes in the pattern of ectopic SP immunoreactive fibers were observed throughout the white matter of the spinal cord of vehicle-treated transgenic mice (Fig. 6A and 6C).

SP immunoreactivity in the dorsal root ganglion cells, sciatic nerve and lower lip skin

Cervical and lumbar SP-IR DRG cells were usually darker in transgenic than in control mice (Figs. 7A and 7B). Quantification of DRG cells revealed that the percentages of both cervical and lumbar SP-IR DRG cells were significantly higher in transgenic mice than in controls (Fig. 8). In the skin of the lower lip, SP-IR fibres were visualized around blood vessels, glands, hair follicles, and in the epidermis itself as described by previous researchers (Hökfelt et al., 1977; Cuello et al., 1978). Although fibers were not quantified, there were no obvious transgenic vs. control differences in the number, intensity of staining and distribution pattern of SP immunoreactive fibers in the lower lip skin (Figs. 7C and 7D).

SP and CGRP immunoreactivities at the EM level

SP immunoreactivity was present in unmyelinated and some thinly myelinated axonal profiles of laminae I to II and Lissauer's tract. SP-IR axonal varicosities contained numerous agranular round synaptic vesicles and a variable number of larger dense core vesicles. Occasionally, synaptic glomeruli with central profiles immunoreactive for SP were found mainly in the outer two-thirds of lamina II. In the double-stained sections, SP and CGRP immunoreactivities were co-localized in some boutons in the superficial dorsal horn of both transgenic mice and controls. Immunogold particles representing CGRP immunoreactivities were detected primarily overlying dense-core vesicles. Some boutons were CGRP immunoreactive only. From two transgenic and two control mice, the numbers of SP- and CGRP-IR boutons were counted on photographic enlargements of 10 low power electron micrographs obtained

at random from lamina I and outer lamina II. The counting of the numbers of immunoreactive boutons did not reveal any significant difference in SP and CGRP immunoreactivities between transgenic mice and controls. In the area of the white matter where the dorsolateral funiculus is located, SP-IR ectopic fibers were visualized among many small unmyelinated fibers in small groups, surrounded by thickly-myelinated fibers (Fig.9). In some fields, SP-IR fibers occurred in isolation (Figs. 10A and 10B), while in other fields they formed clusters (Figs. 9C, 9D and 10C). All ectopic fibers were unmyelinated and of varied diameters. Some SP-IR terminals or varicosities could be found containing large dense-core vesicles and small clear vesicles (Figs. 10A and 10B). DAB-reaction product was mainly deposited in large dense-core vesicles and in cytoplasm between small clear vesicles. Some SP-IR boutons could be seen establishing synapses with dendritic profiles which were SP immunonegative (Figs. 10B). In the post-embedding immunogold stained sections, CGRP was found to co-localize with SP in the same boutons or varicosities in almost half of the SP-IR profiles. As in the double-stained boutons in the substantia gelatinosa, immunogold particles representing CGRP antigenicity were visualized mostly in the dense core vesicles where SP immunoreactivity was also detected (Figs. 10D and 10E). Some boutons co-localizing SP and CGRP formed synaptic specializations with immunonegative dendritic profiles (Fig. 10E). CGRP/SP co-localization was also detected in unmyelinated axons (Fig. 10C).

In the dorsolateral funiculus of the spinal cord from control mice, no such ectopic SP-IR fibers and boutons could be found. In the double-stained sections, no

CGRP- and/or SP-IR boutons or varicosities could be visualized in the white matter of control mice.

Quantitative results

Fields from laminae I-II of the dorsal horn and lateral funiculus of 125 sections were measured bilaterally in 5 transgenic mice and 5 controls. The relative optical density of SP and CGRP immunoreactivities in the laminae I-II of the dorsal horn of the cervical spinal cord of transgenic mice were not significantly different from controls. The percentages of the area occupied by CGRP- and SP-IR fibers in the dorsolateral funiculus of the transgenic mouse spinal cord were 24.34±1.4% and 4.97±0.7% respectively. The values were significantly higher ($P<0.001$) than those obtained from control mice (0.08±0.04% and 0.28±0.1%, respectively)

DISCUSSION

In the present study, high levels of NGF mRNA were detected in the spinal cord of adult transgenic mice (2 month old) from line 414 in Northern blot analysis. Furthermore, NGF-IR oligodendrocytes were revealed throughout the white matter of the spinal cord of transgenic mice from this line at ages of 20 days and 2 months by immunocytochemistry. Those transgenic mice possessed ectopic SP- and CGRP-IR fibers throughout the white matter of the spinal cord. After capsaicin treatment of adult animals, peptide immunoreactivity was virtually entirely abolished from the white

matter. At EM level, those ectopic SP- and CGRP-IR fibers were characterized as unmyelinated axons and axonal terminals. SP was found to co-localize with CGRP in some of those axons and axonal terminals.

Anatomical origin of ectopic SP and CGRP immunoreactive fibers

Substance P immunoreactivity in the spinal cord originates from three sources: dorsal root ganglia cells (Hökfelt et al., 1975b; Hökfelt et al., 1976), intrinsic spinal cord neurons in laminae I and II (Ljungdahl et al., 1978) and descending fibers from supraspinal structures (Hökfelt et al., 1978). The high incidence of the co-existence of SP and CGRP immunoreactivities has been reported in somata of the dorsal root ganglion (Gibson et al., 1984; Lee et al., 1985b), and in axon terminals within the superficial dorsal horn of the rat (Plenderleith et al., 1990). The axon terminals co-localizing SP and CGRP immunoreactivites in the superficial layers of the dorsal horn should be virtually all of primary sensory origin, because CGRP immunoreactivity is abolished from the dorsal horn following dorsal rhizotomy (Chung et al., 1988; Traub et al., 1989). Therefore, for most ectopic CGRP-IR fibers and some ectopic SP-IR fibers, the most likely origin is the dorsal root ganglion cells. SP- and CGRP-IR dorsal root ganglion neurons in the adult rat are responsive to NGF, as shown by *in vitro* and *in vivo* studies (Lindsay and Harmar, 1989; Verge et al., 1989b; Inaishi et al., 1992; Donnerer et al., 1992; Tuszynski et al., 1994). In our present study, we detected a higher number of SP-IR neurons in DRGs from transgenic mice than in those from controls. Additionally, SP-IR DRG neurons were more intensely stained in transgenic mice than

in controls. Those findings strongly suggested that DRG cells were influenced by the over-expression of NGF in the white matter of the spinal cord of transgenic mice. To identify the origin of ectopic SP-IR fibers, we carried out capsaicin treatment for adult transgenic mice. Capsaicin is a neurotoxin which is specific for a certain population of sensory neurons and does not directly affect neurons intrinsic to the CNS [for review see (Holzer, 1988)], and which can deplete substance P from primary sensory fibers in the spinal cord (Jessell et al., 1978). In our present study, ectopic SP-IR fibers were no longer detected after capsaicin treatment, confirming that those ectopic fibers are of primary sensory origin.

Formation of ectopic SP and CGRP immunoreactive fibers

An important issue is how those ectopic SP- and CGRP-IR fibers were formed in transgenic mice. It is well documented in earlier experiments (Levi-Montalcini and Angeletti, 1968; Gundersen and Barrett, 1979; Campenot, 1982) that one of the important properties of NGF is its ability to direct growth or regeneration of sensory and sympathetic axons along a concentration gradient. Intact nociceptive fibers (Diamond et al., 1992), sympathetic axons (Kuchel et al., 1992) and axons of septo-hippocampal neurons (Van der Zee et al., 1992) of adult rat have been shown to sprout collateral branches into denervated target tissues where an up-regulation of NGF expression probably occurs. Furthermore, NGF was also demonstrated to induce collateral sprouting of mature, uninjured sensory (Diamond et al., 1992) and sympathetic (Isaacson et al., 1992) axons in adult rats and aged rats as well (Andrews and Cowen,

1994). NGF was demonstrated to increase the content and transport of substance P and CGRP in sensory nerves innervating inflamed tissue (Donnerer et al., 1992). The exogenous administration of NGF to the spinal cord by means of the grafting of genetically engineered fibroblasts has been shown to exert a neurotropic action on primary sensory fibers in adult animals (Tuszynski et al., 1994). Our present results support their observation and suggest that neurotrophins have the capability of overuling the known inhibitory influences of oligodendrocytes in CNS regeneration (Schnell and Schwab, 1990).

Other transgenic mouse models have been generated which over-express NGF under the control of different promoters. In DBH-NGF transgenic mice (Hoyle et al., 1993), over-expression of NGF in sympathetic neurons caused excessive axon outgrowth from ganglia, although no terminal hyperinnervation, but rather an hypoinnervation of tissues, was detected. Recently, Albers et al. (1994) have observed that overexpression of NGF in the epidermis of transgenic mice caused an hyper-innervation of the skin by CGRP immunoreactive fibers.

In the present study, the over-expression of NGF was predicted to be restricted to the white matter in the transgenic animals due to the nature of the transgene promotor. In fact, all MBP promoter fragments used so far have failed to direct Schwann cell specific transcription in transgenic mice [see e.g. (Gow et al., 1992)]. In agreement with this, we did not detect any NGF-IR cells in peripheral nerves in our transgenic mice (data not shown). Only oligodendrocytes in the white matter of CNS of transgenic animals were detected as NGF immunoreactive. As the white matter

represents the area of highest NGF concentration, NGF over-expression in the white matter presumably induced the growth of collateral sprouts of the dorsal root axons. Although no individual fibers were followed to their termination point, the observation of numerous SP-IR boutons in the white matter indicates that many of them probably end in the white matter.

When compared to controls, no increases of SP and CGRP immunoreactivities could be detected in the substantia gelatinosa of transgenic mice, where most thinly myelinated and unmyelinated primary afferents terminate. The most likely interpretation is the absence of over-produced NGF in transgenic dorsal horn demonstrated in NGF immunostaining. Moreover, SP immunoreactivity in the lower lip skin of transgenic mice did not differ from controls, which also could be explained by the absence of NGF over-expression in peripheral target tissues.

Taken together, all these lines of evidence support our hypothesis that the collateral sprouting of sensory fibers into the white matter is induced by NGF over-expressed in the oligodendrocytes.

These NGF immunoreactive oligodendrocytes could be detected, from postnatal day 0 to 2 month, in the white matter of the spinal cord as well as in other brain regions, such as in the white matter of lower brainstem and cerebellum (Ma et al., unpublished observations). The expression pattern of NGF positive oligodendrocytes in the CNS was consistent with the expressions of reporter genes driven by MBP gene promoters of various sizes as defined in previous studies (Foran and Peterson, 1992; Goujet-Zalc et al., 1993). Ectopic SP-IR fibers were first detected by the day of birth

and persisted throughout adulthood in transgenic mice (Ma et al., unpublished observations).

Possible significance of ectopic SP and CGRP immunoreactive fibers

Depletion of NGF by its antisera in a critical period (postnatal days 4 to 11) could switch developing afferents from high-threshold mechanoreceptors (HTMRs) into D-hairs and increased the mechanical thresholds of those HTMRs that remained (Lewin et al., 1992b). NGF could induce heat and mechanical hyperalgesia in adult rats (Lewin and Mendell, 1992). It is clear that NGF can still modulate phenotypic expression of nociceptors after birth. In our experiments, ectopic SP- and CGRP-IR fibers induced by overexpression of NGF in the white matter of the transgenic spinal cord likely represent the collateral sprouting of thinly myelinated and unmyelinated primary afferents which convey nociceptive information. Therefore, an interesting question is whether this transgenic mouse model will display altered patterns of physiological and behavioral responses to noxious stimulation. Further physiological and behavioral experiments will clarify this issue.

Figure 1. A Schematic representation of the MBP/NGF transgene. A chick NGF cDNA fragment (NGF) was fused in frame to the POMC (P) signal peptide sequence. The microinjected DNA fragment contained the POMC/NGF construct (1.1 kb) flanked by 1.3 of 5' and 2.1 kb of 3' sequences from the MBP gene. **B.** High-level expression of NGF mRNA in the spinal cord of transgenic mice. Note the dense band corresponding to 1.1 kb on line 4 from the spinal cord of a transgenic mouse. Northern blot analysis was carried out using total RNA (20μg) isolated from the cortex (lanes 1 and 6), cerebellum (lanes 2 and 7), brain stem (lanes 3 and 8), spinal cord (lanes 4 and 9) and kidney (lanes 5 and 10) of a transgenic mouse from line 414 (lanes 1-5) and from a normal mouse (lanes 6-10). The membrane was hybridized at high stringency with a chick NGF ^{32}P-labeled cDNA probe.

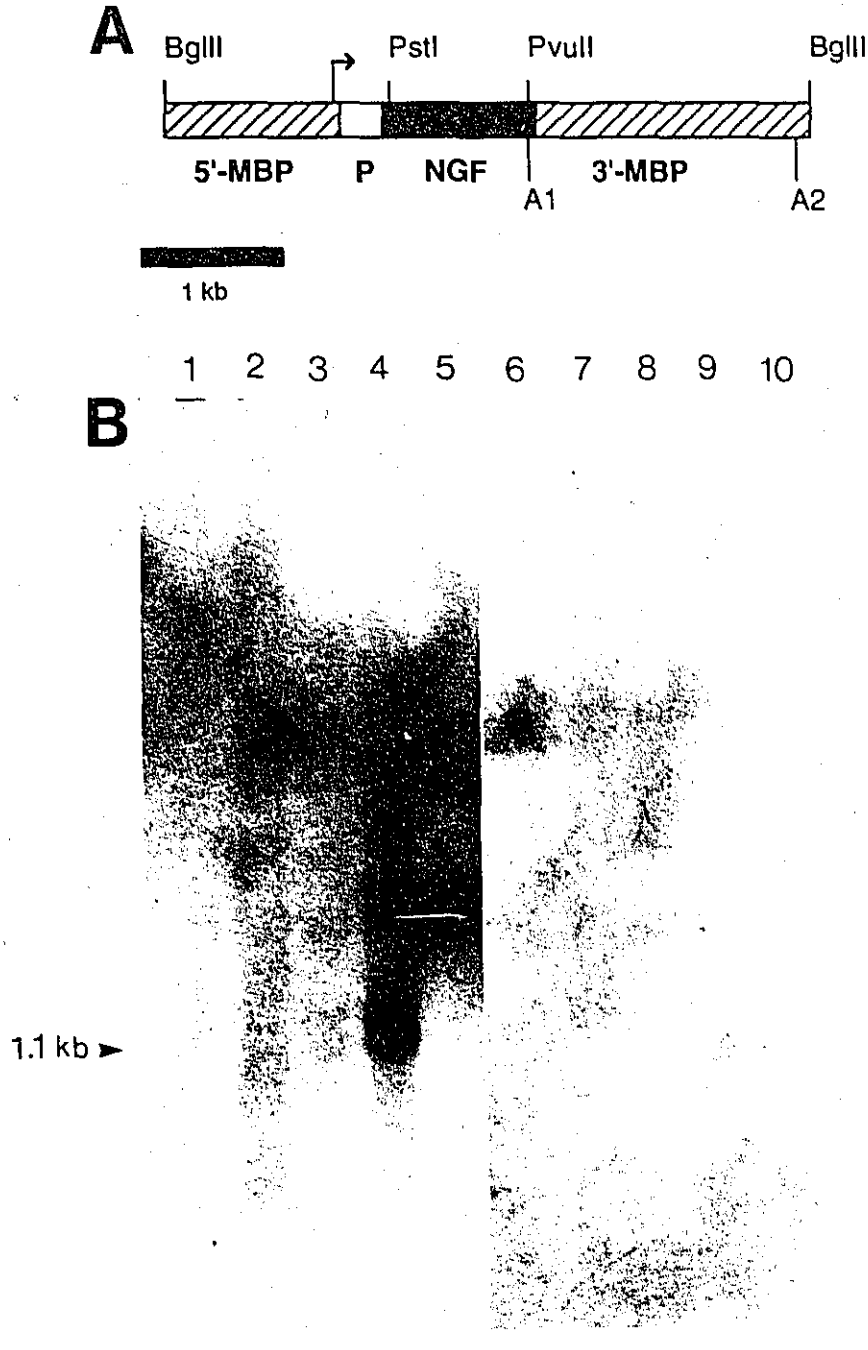
A
BglII
PstI
PvuII
BglII
5'-MBP
P
NGF
3'-MBP
A1
A2
1 kb
1 2 3 4 5 6 7 8 9 10
B
1.1 kb

Figure 2. NGF immunostaining in the cervical spinal cord (C5 level) of control (**A**) and 20-day-old transgenic mice over-expressing NGF (**B**). The framed areas in **A** and **B** are illustrated at higher magnification in **C** and **D** respectively. In **B**, observe numerous NGF immunoreactive oligodendrocytes in the white matter, and very few in the gray matter, of the spinal cord of transgenic mice. In **D**, note that the NGF immunoreactive cells displayed the morphological characteritics of oligodendrocytes, as they possess spherical or polygonal cell body and a few short processes with right-angled branching (arrows), and never formed the vascular feet typical of astrocytes. No NGF immunoreactive oligodendrocytes could be detected in the spinal cord of control mice (**A** and **C**). Scale bars=200 μm in A and B, and 50 μm in C and D

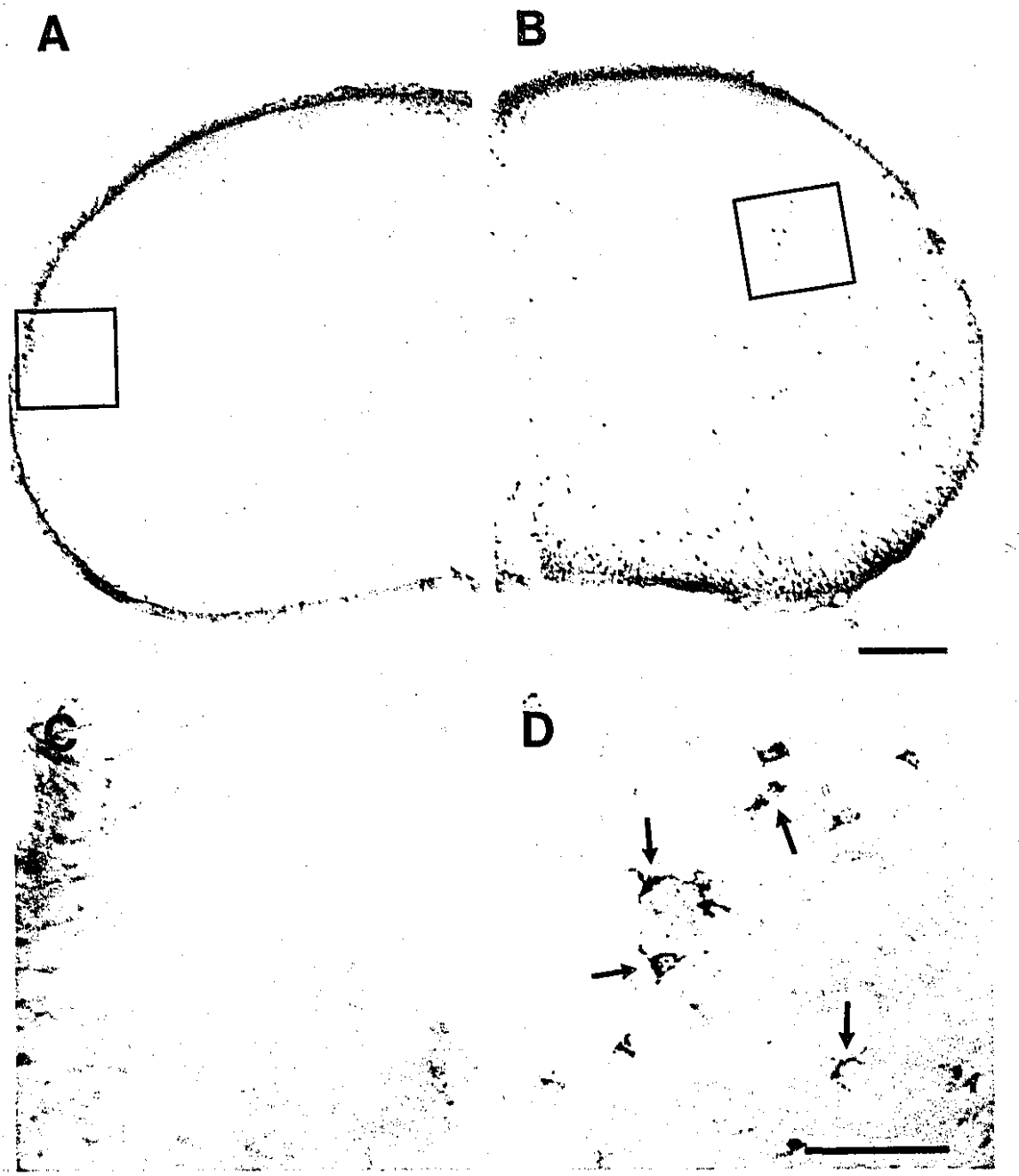
A
B
C
D

Figure 3. SP immunoreactivity in the cervical spinal cord (C5 level) of control (**A**) and transgenic mice over-expressing NGF (**B**). The framed areas in **A** and **B** are shown at higher magnification in **C** and **D** respectively. SP immunoreactivity was intense in Laminae I and II of the dorsal horn in both control (**A**) and transgenic mice (**B**). In **B**, note ectopic SP-IR fibers in the anterior, lateral and dorsal columns of spinal cord of transgenic mouse. Arrows indicate ectopic SP-IR fibers in the dorsolateral funiculus. In **A** and **C**, no such ectopic SP-IR fibers could be detected in the spinal cord from a control mouse. Scale bar =200 μm in A and B, =50 μm in C and D.

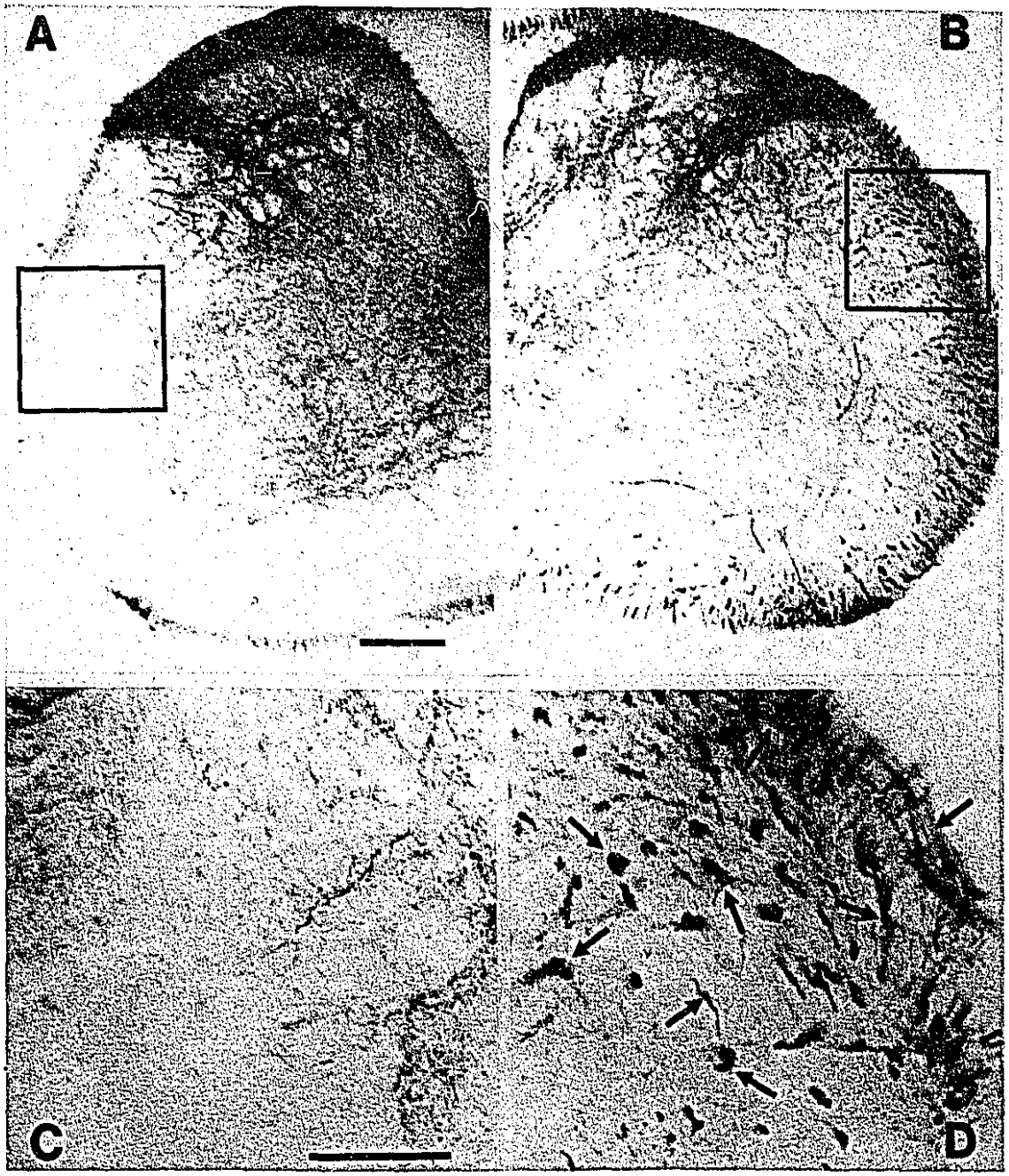
A
B
C
D

Figure 4. CGRP immunostaining in the cervical spinal cord (C5 level) of control (**A**) and transgenic mice (**B**). The framed areas in **A** and **B** are shown at higher magnification in **C** and **D** respectively. Observe the intense immunostaining in the superficial layers (LI-LII) of the dorsal horns from both control (A) and transgenic (**B**) mice. However, in **B**, ectopic CGRP-IR fibers were found in the anterior, lateral and dorsal columns. In **D**, observe the details of ectopic CGRP-IR fibers in the dorsolateral funiculus (arrows); some long ectopic CGRP-IR fibers (arrowheads) could be seen to originate from the white matter and to course transversely toward the gray matter. No such CGRP-IR fibers could be detected in the white matter of control mice. CGRP-IR ventral horn neurons could be found in both control and transgenic mouse spinal cords (open arrows). Scale bars = 200μm in A and B, =100 μm in C and D.

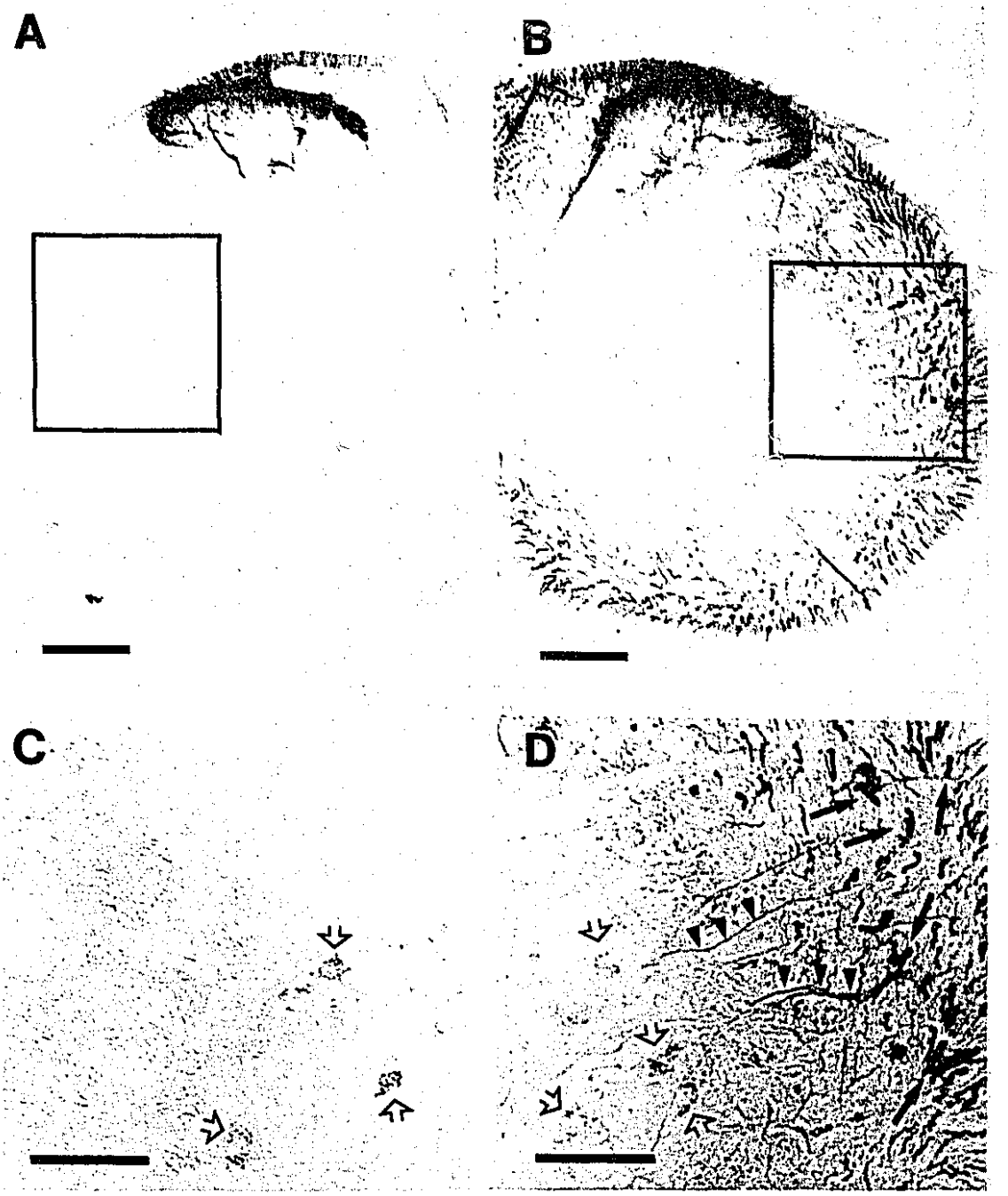
A
B
C
D

Figure 5. SP immunoreactivities in the dorsolateral funiculus as observed in the parasagittal sections from control (**A**) and transgenic (**B**) mice. In **B**, ectopic SP-IR fibers (arrows) travel in the dorsolateral funiculus parallel to the axis of the spinal cord. No such longitudinally orientated ectopic SP-IR fibers can be found in the white matter of the spinal cord of control mice (**A**). Scale bar = 50 μm.

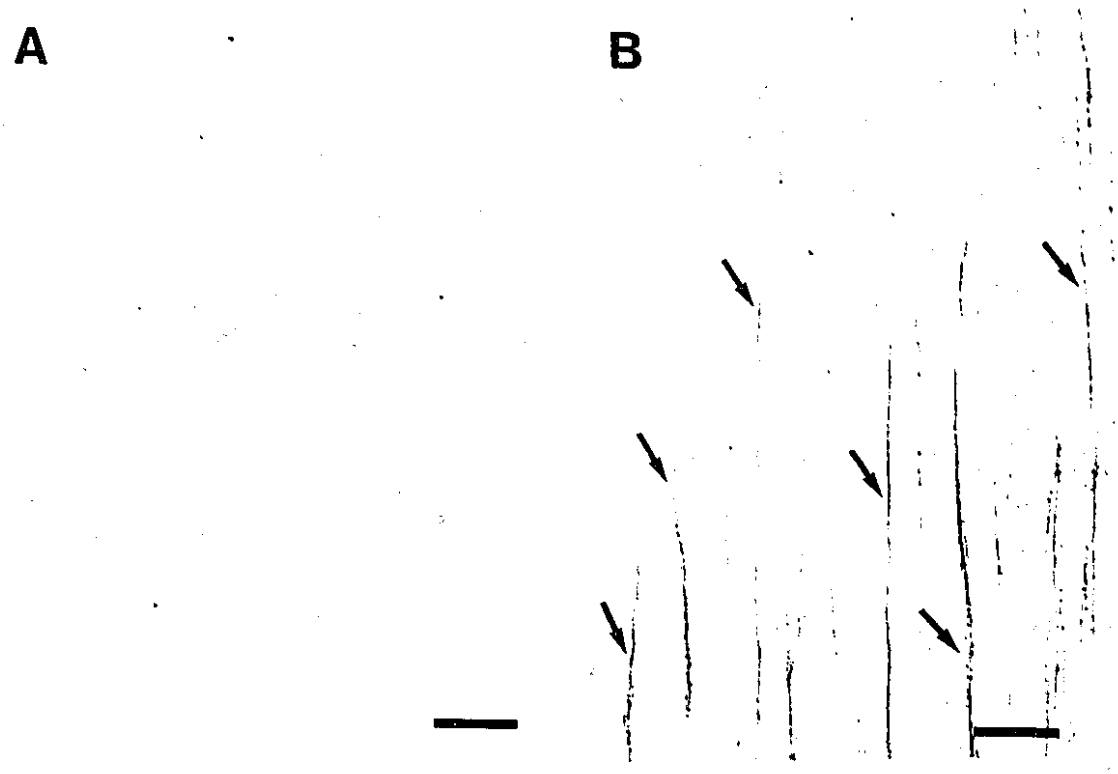
A
B

Figure 6. SP immunoreactivities in the cervical spinal cord (C4 level) of vehicle-treated (**A**) and capsaicin-treated (**B**) transgenic mice. The framed areas in **A** and **B** are shown at higher magnification in **C** and **D** respectively. SP immunoreactivity was intense in Laminae I and II of the dorsal horn in the vehicle-treated animal (**A**) and drastically reduced in the capsaicin-treated mouse (**B**). In B and D, note that ectopic SP-IR fibers were not detected in the white matter of the spinal cord of capsaicin-treated transgenic mouse. However, those ectopic SP-IR fibers were present in vehicle-treated transgenic mouse (**A** and **C**). Scale bars = 200 μm in A and B, and 50 μm in C and D

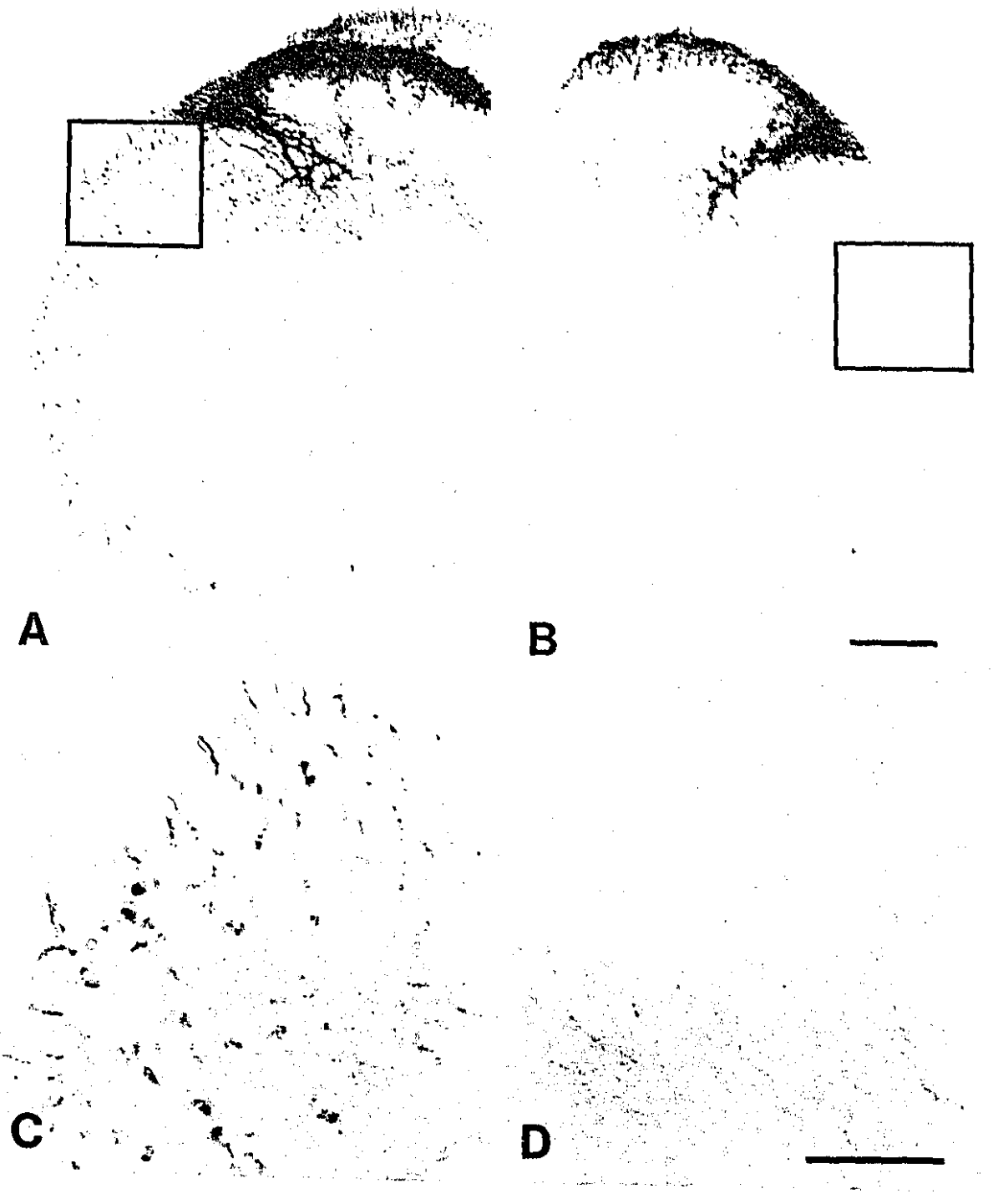
A
B
C
D

Figure 7. SP immunoreactivity in cervical dorsal root ganglia and in the skin of the lower lip in control (**A** and **C**) and transgenic mice (**B** and **D**). Note that the SP-IR DRG cells in the transgenic mouse specimen (**B**, arrows) were almost all intensely immunostained, in contrast with the wide variation in the intensity of SP immunoreactivity detected in the neurons of the control DRG (**A**, arrows). No significant differences in the size of DRG cells could be detected between controls and transgenic mice. However, In the skin of the lower lip, no apparent differences in SP-IR fibers were detected between control (**C**) and transgenic (**D**) mice. Scale bar = 50 μm.

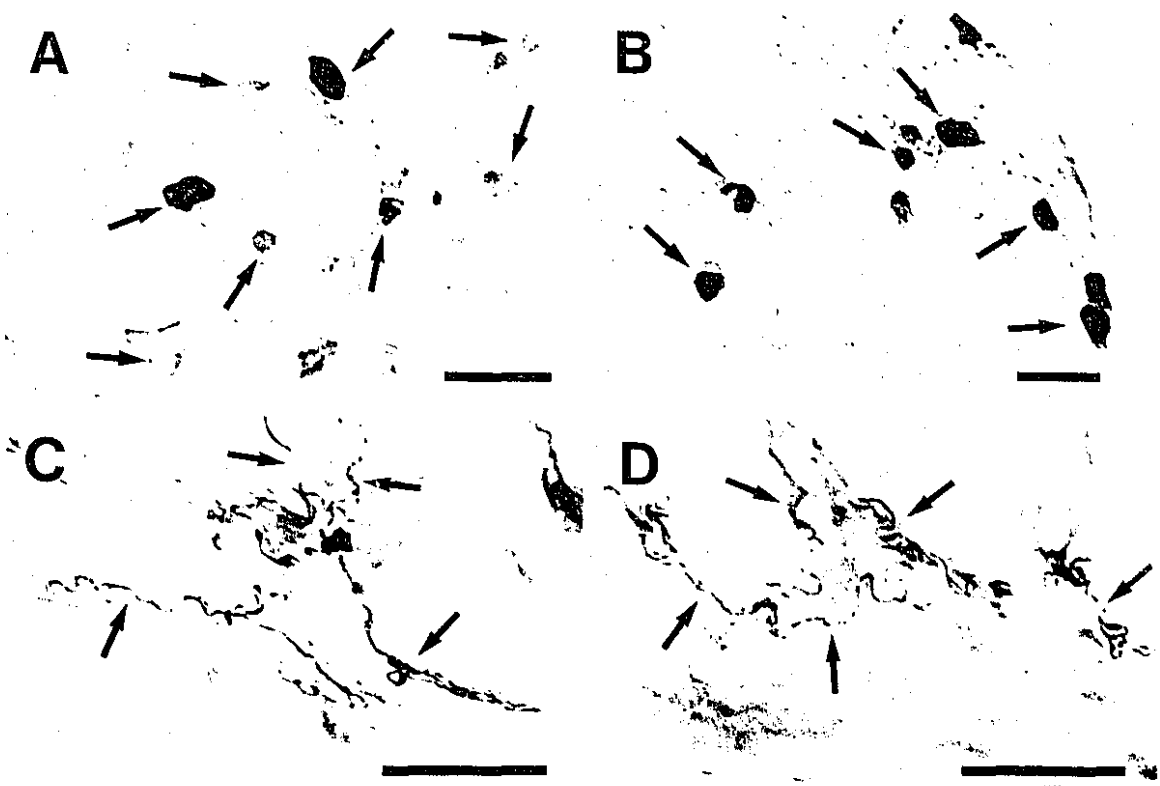
A
B
C
D

Figure 8. Quantification of DRG neurons in transgenic mice and controls. Cresyl violet counterstained sections from cervical and lumbar DRG of transgenic mice and controls were used for quantification. Both SP positive and negative DRG cells were counted directly under the light microscope. The percentages of SP-IR DRG neurons in the total number of DRG neurons per section were determined for transgenic mouse specimens and controls. The percentages of both cervical and lumbar SP-IR DRG cells were significantly higher in transgenic mice than in controls ($P<0.01$, $n=4$, Student's t-test).

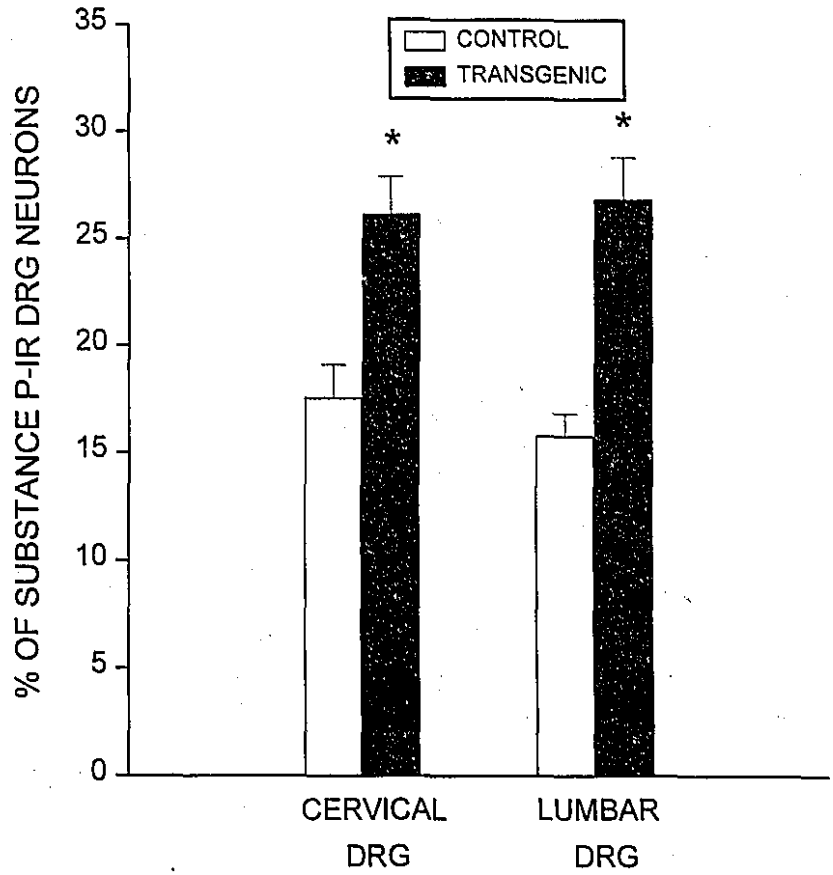
CONTROL
TRANSGENIC
% OF SUBSTANCE P-IR DRG NEURONS
35
30
25
20
15
10
5
0
*
*
CERVICAL DRG
LUMBAR DRG

Figure 9. Electron micrograph of SP immunoreactivity in the white matter of the dorsolateral funiculus in control (**A** and **B**) and transgenic (**C** and **D**) mice. In **C**, observe ectopic SP-IR fibers (arrows). Such fibers were part of bundles of unmyelinated axons in between the myelinated fibers. **D** shows at higher magnification the area framed in **C** . Such groups of unmyelinated SP-IR axons were absent from controls (**A**). **B** represents an enlargment of the framed area in **A** and shows one of the few axonal boutons which forms a synapse on a dendritic profile (curved arrow) in the white matter of controls. Scale bar = 1 μm for A and C, =0.5 μm for B and D.

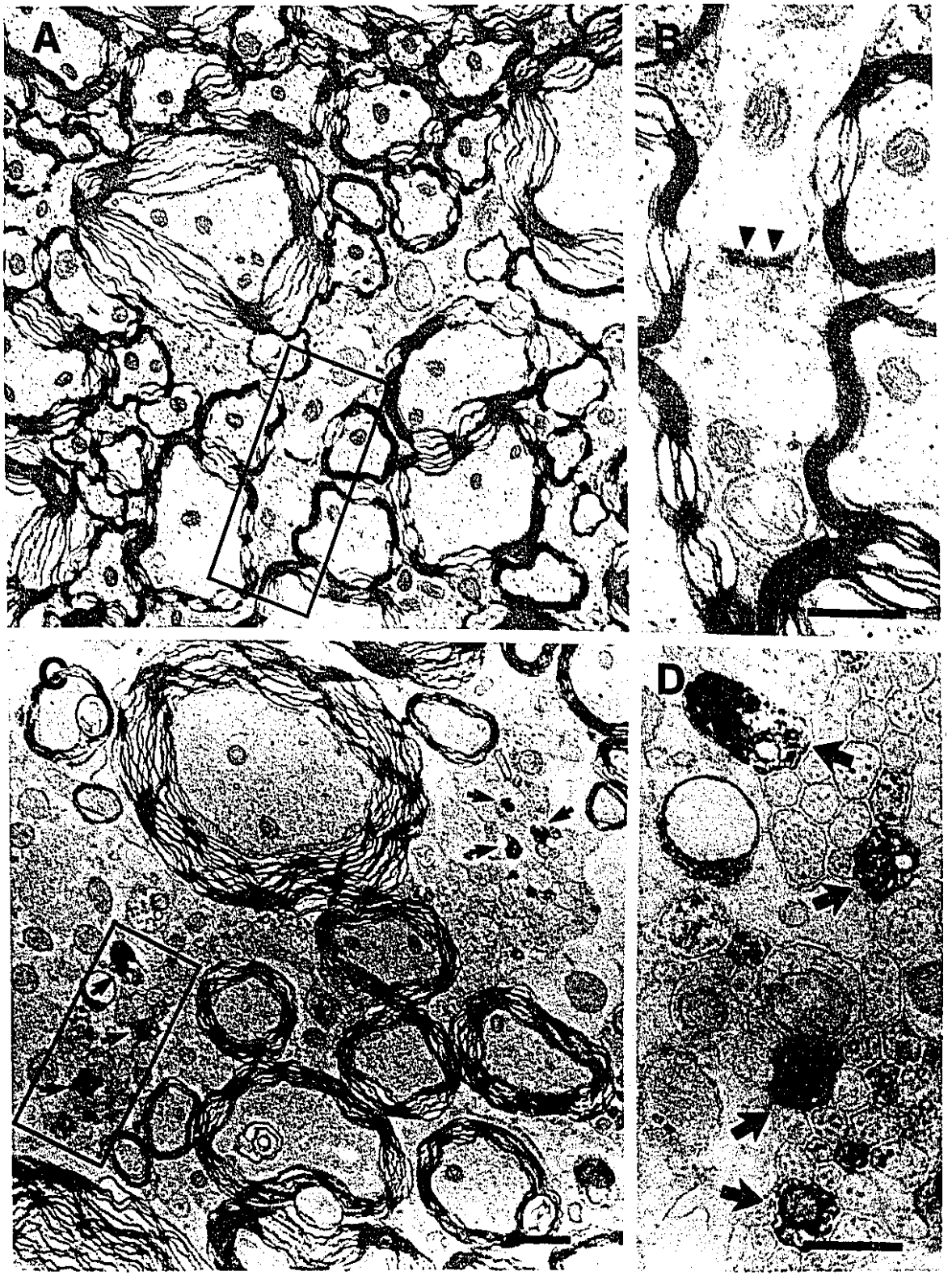
A
B
C
D

Figure 10. Electron micrograph of ectopic SP- and CGRP-LI axon and axonal boutons in the dorsolateral funiculus of the spinal cord of transgenic mice. **A** shows a SP-IR bouton containing dense core vesicles (arrows). **B** shows a SP-IR bouton containing small agranular vesicles (arrows), which is presynaptic (curved arrow) to a dendritic profile. **C**, **D** and **E** represent electron micrographs from a double staining for SP (electron-dense immunoprecipitates) and CGRP (gold particles). **D** and **E** show double-labeled boutons and **C** illustrate double-labeled axons. Immunogold particles, representing CGRP immunoreactivity, were localized over the dense core vesicles. In **E**, a bouton co-localizing by SP and CGRP immunoreactivities establishes a synapse (curved arrow) with a dendritic profile. Scale bar = 0.5 μm.

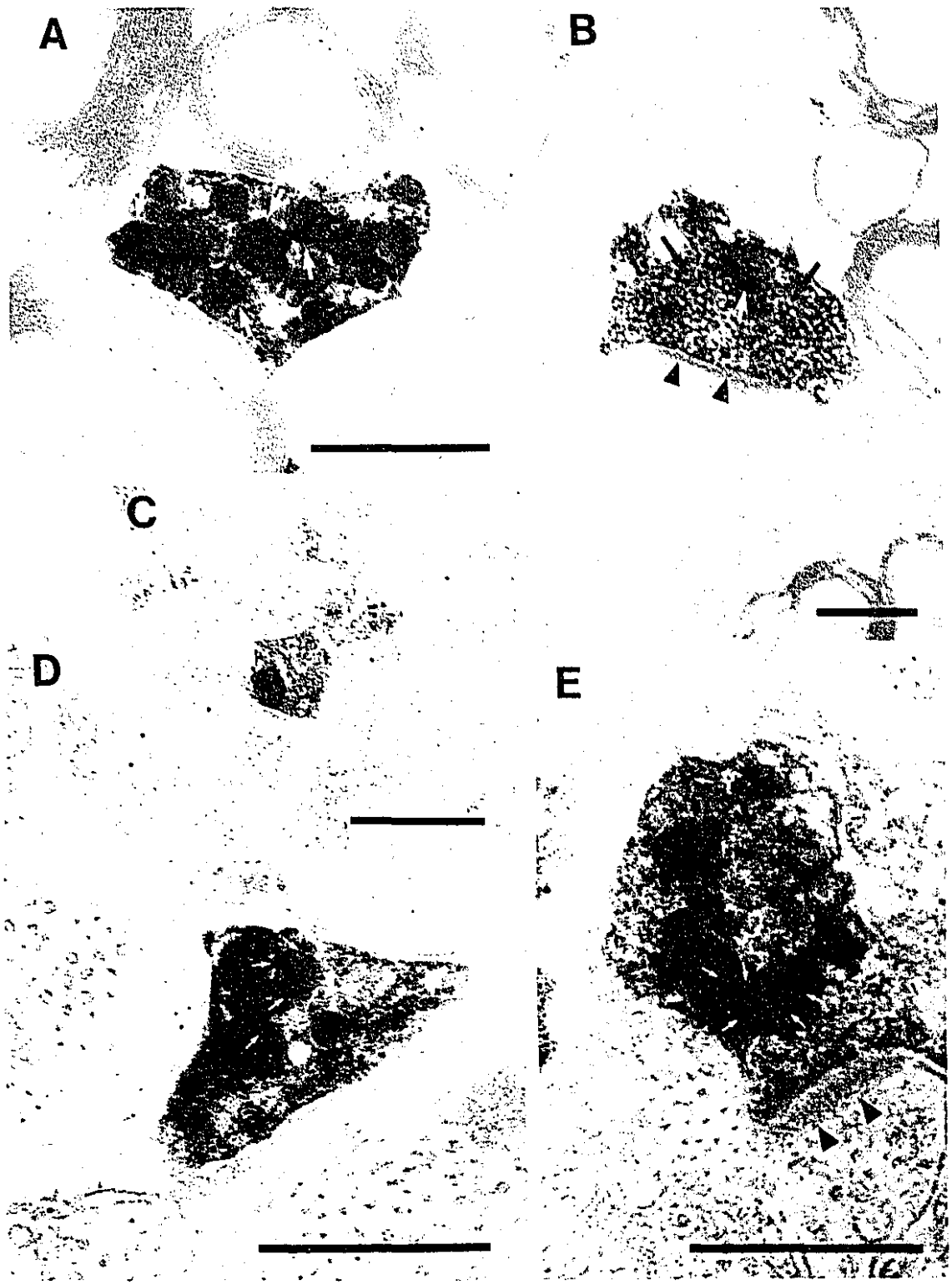
A
B
C
D
E

Connecting Text - Chapter V to VI

In the study of chapter V, we demonstrated that NGF-IR oligodendrocytes and ectopic SP-IR and CGRP-IR fibers were present in the white matter of the spinal cord of 20-day-old and 2-month-old transgenic mice. These ectopic SP-IR fibers disappeared following capsaicin treatment. Under the EM, these ectopic SP-IR fibers were characterized as fiber bundles, consisting of unmyelinated axons. Some ectopic SP-IR boutons co-localized CGRP and were presynaptic to dendrites. The numbers of SP-IR neurons in the cervical and thoracic DRG of transgenic mice were increased compared to controls. In chapter VI, we studied developmentally and topographically the expression of the NGF transgene in myelinating oligodendrocytes and the distribution of ectopic SP-IR fibers in the white matter of the CNS of transgenic mice.

CHAPTER VI

Topographic and time course studies of ectopic substance P immunoreactive fibers in the CNS of transgenic mice which over-express nerve growth factor in myelinating oligodendrocytes

Weiya Ma, A. Ribeiro-da-Silva, J.-P. Julien and A. C. Cuello

ABSTRACT

To examine the *in vivo* biological effects of the over-expression of nerve growth factor (NGF) in the CNS upon neuropeptides containing primary sensory neurons, we used transgenic mice which bear chicken NGF cDNA driven by a 1.3 kb myelin basic protein (MBP) promoter fragment. Using immunocytochemistry, we demonstrated in a previous study (see chapter V) that NGF immunoreactive (IR) oligodendrocytes occurred in the white matter of the spinal cord of adult transgenic mice. Consistently, substance P (SP)- and calcitonin gene-related peptide (CGRP)-IR ectopic fibers of sensory origin were observed in the white matter of the transgenic spinal cord. The aim of the present study was to investigate, spatially and temporally, the expression of NGF-IR oligodendrocytes and the occurrence of ectopic SP-IR fibers in the CNS of transgenic mice. Our data show that NGF-IR oligodendrocytes occurred in the white matter of CNS from postnatal day 0 (the earliest day examined) to 2 months. At day 20, NGF-IR oligodendrocytes were present in the caudate-putamen, corpus callosum, reticular nuclei of thalamus, reticular nuclei of pons and medulla, trigeminal spinal tract, cochlear nuclei, pyramidal tract, and white matter of cerebellum and spinal cord. No NGF-IR oligodendrocytes were detected in the CNS of control mice at any age. NGF-IR fiber- like structures were observed in the white matter of the cerebellum, pons, medulla oblongata and spinal cord of transgenic mice aged from day 0 to day 5. By day 15, these NGF-IR fiber-like structures were no longer detected. Under the electron microscope, these NGF-IR fiber-like structures were characterized as NGF immunoreactivity around

small unmyelinated fibers. Some of these small unmyelinated fibers which were surrounded by NGF immunoreactivity contained SP and CGRP immunoreactivities. Interestingly, in both transgenic and control mice from postnatal day 0 to day 10, numerous NGF-IR glia-like cells were observed in the ventral part of the forebrain as well as in the brainstem, cerebellum and spinal cord. These glia-like cells were considerably smaller than the NGF-IR oligodendrocytes. From day 5 on, these NGF-IR glia-like cells decreased markedly in number, and by day 15 could not be detected. Numerous SP-IR fibers were found in the white matter of the spinal cord, medulla oblongata, pons and cerebellum of both transgenic mice and controls from postnatal day 0 to day 2. By day 5, the SP-IR fibers in the white matter had decreased dramatically in controls, but increased markedly in transgenic mice. In these animals, from day 5 on, SP-IR fibers in the white matter (ectopic) increased to adult level by day 20, at which they persisted throughout adulthood. The percentages of SP-IR cells in the cervical and lumbar dorsal root ganglia, and in the trigeminal ganglia were significantly higher in transgenic mice than in controls. Moreover, SP-IR sensory ganglion cells in transgenic mice were more intensely stained than in controls. Therefore, we conclude that neuropeptide containing sensory neurons responded to the over-expression of NGF in the myelinating oligodendrocytes in the CNS of transgenic mice. Our results also suggest that the SP-IR fibers which normally occurred in the white matter of the CNS during early development were induced to sprout by the over-expression of NGF during the postnatal period, thus becoming ectopic fibers in transgenic mice. In adulthood, the maintenance of these ectopic fibers was independent of NGF over-expression.

INTRODUCTION

It has been noted that nerve growth factor (NGF) interacts specifically with substance P (SP) and calcitonin gene-related peptide (CGRP) containing small and medium size sensory neurons during embryonic development and in the postnatal period [for review, see (Lewin and Mendell, 1993)]. However, the effects of NGF on sensory neurons vary with different developmental stages. In embryos, sensory neurons, particularly those which contain SP and CGRP, are critically dependent on NGF for survival and differentiation. This NGF dependence was evidenced by classical studies in which primary sensory neurons were deprived of NGF, through either systemic administration of anti-NGF antibodies or autoimmunization (Levi-Montalcini and Angeletti, 1968; Gorin and Johnson, 1979; Aloe et al., 1981). More recently, this critical NGF dependence of the developing sensory neurons has been substantiated by studies which, using homologous recombination, depleted NGF (Crowley et al., 1994) or the high affinity NGF receptor, trkA (Smeyne et al., 1994) in transgenic mice. All these studies have shown that deprivation of NGF or its receptors at an embryonic stage abolished all, or a large portion, of the small size neuropeptide-containing sensory neurons and led to the loss or reduction of nociception. Conversely, the over-availability of NGF at embryonic stages resulted in excess of sensory neurons (Henderson et al., 1994; Albers et al., 1994), hyperinnervation of CGRP-immunoreactive (IR) fibers in the

skin (Albers et al., 1994) and consequent hyperalgesia (Davis et al., 1993).

In the neonatal period, deprivation of NGF results only in the death of a small number of the small size sensory neurons (Yip et al., 1984; Hulsebosch et al., 1987; Lewin et al., 1992b), and in a reduction of SP contents of sensory neurons (Otten et al., 1980). Administration of excess NGF to neonatal or mature animals increased SP contents (Otten et al., 1980) and gene expression (Vedder et al., 1993), and brought about a profound behavioral hyperalgesia (Lewin et al., 1993). These lines of evidence indicate that NGF modulates the phenotypes of sensory neurons after birth.

We recently communicated that the endogenous over-expression of NGF in the white matter of transgenic mice resulted in an abnormal termination pattern of primary sensory fibers in the CNS (Ma et al., 1995b). For the generation of this transgenic mouse model, fragments of 1.3 kb of 5' and 2.1 kb of the 3' sequences from the myelin basic protein (MBP) gene were chosen as the regulatory element to promote chicken NGF cDNA expression throughout the CNS. Because of the nature of the promoter, the expression of chicken NGF was restricted to the postnatal period to avoid developmental defects. In these transgenic mice, NGF immunoreactivity was detected in myelinating oligodendrocytes throughout the white matter of the spinal cord of 20-day-old and 2-month-old animals (Ma et al., 1995b). Moreover, we also observed ectopic SP- and CGRP-IR sensory fibers in the white matter of the spinal cord. In the present study we investigated the temporal and spatial expression of NGF immunoreactivity in myelinating oligodendrocytes in the CNS of this transgenic mouse model to assess the *in vivo* effects of NGF over-expression on sensory neurons in the

CNS in the early postnatal stages. We extended our investigation by studying the time course and distribution patterns of NGF-IR oligodendrocytes and ectopic SP-IR fibers in the CNS of these transgenic mice.

MATERIALS AND METHODS

NGF and SP immunostaining in the CNS of transgenic and control mice

All animals were from mouse strain C3B6S1. Forty-five homozygous and heterozygous transgenic mice of either sex from line 414 were used. The ages of transgenic mice were postnatal day 0, day 5, day 10, day 15, day 20, 2 months, 4 months, 6 months and 12 months. Age-matched non-transgenic mice were employed as controls. All animals were anesthetized with Equithesin (4 ml/kg, i.p.) and perfused transcardially with a mixture of 2% paraformaldehyde and 0.2% p-benzoquinone in 0.075M phosphate buffer (PB) (pH 7.4) for 30 minutes. The whole brain and the spinal cord were removed, postfixed in the same fixative for 2 hours and then infiltrated overnight in 30% sucrose in 0.1M PB at 4°C. Most of the brain and the spinal cord segments from cervical, thoracic and lumbar levels were cut on a cryostat transversely, 50 μm thick, and collected as free-floating sections in phosphate-buffered saline with 0.2% Triton X-100 (PBS+T). Some of the brain and the spinal cord segments were cut parasagitally; one half of the sections was processed for NGF immunostaining, while

the other half was used for SP immunostaining.

For NGF immunostaining, sections were first incubated in 1.5% normal goat serum in PBS+T for 30 minutes to block non-specific staining. Then sections were incubated in an anti-mouse NGF antibody (1:1000, kindly provided by Dr. J. Conner, San Diego) for 72 hours. An Elite ABC kit (Vector) was subsequently used according to the manufacturer's instructions. In short, sections were incubated in biotinylated goat anti-rabbit antibody (1:200) and ABC complex (1:50) for one hour each, at room temperature. Finally, sections were reacted with 0.06% 3,3'-diaminobenzidine tetrahydrochloride (DAB, Sigma) and 0.03% hydrogen peroxide dissolved in PBS+T. Between incubations, sections were extensively rinsed in PBS+T.

For SP immunostaining, a bi-specific monoclonal antibody, anti-SP/anti-horseradish peroxidase [code P4C1; (Suresh et al., 1986); Medicorp, Canada] was used. This antibody recognized both the antigen, SP, and the marker, horseradish peroxidase (HRP). Sections were incubated in P4C1 overnight at 4°C. Subsequent incubations were performed at room temperature. Following two washes in PBS+T, all sections were incubated in 5 µg/ml of HRP (Sigma type VI) in PBS+T for one hour. Subsequently, sections were rinsed in PBS+T and reacted with DAB in PBS+T. Finally, the free-floating sections were mounted on gelatin-subbed slides. All sections were further dehydrated in ascending alcohols, cleared in xylene, and cover slipped with Entellan (E. Merck).

SP immunostaining of cells in primary sensory ganglia

Four male homozygous and heterozygous transgenic and 4 male control mice, 3 months old, were anesthetized with Equithesin (4ml/kg, i.p.) and perfused with 4% paraformaldehyde in 0.1M phosphate buffer for 30 minutes. The cervical and lumbar dorsal root ganglia (DRG), and the trigeminal ganglia from both transgenic and control mice were removed and postfixed in the same fixative for 2 hours. Subsequently, all specimens were infiltrated in 30% sucrose in 0.1M PB at 4^{0}C. All the DRG and the trigeminal ganglia were cut serially on a cryostat at a thickness of 10 μm. Sections were mounted alternately on two sets of gelatin-subbed slides. The mounted sections were air dried and thoroughly washed in PBS+T. Sections underwent SP immunostaining as mentioned above with the anti-SP/anti-HRP bi-specific monoclonal antibody. After SP immunostaining, one of the sets of serial sections was counter-stained with 1% cresyl violet. All sections were dehydrated in ascending alcohols, cleared in xylene, and cover slipped as described above.

Capsaicin treatment

Four 3-month-old male homozygous transgenic mice from line 414 and 4 control mice were used. Before capsaicin treatment, all animals were anesthetized with an intramuscular injection of ketamine (100 mg/kg) and acepromazine (2.5 mg/kg). Atropine (0.04 mg/kg) was administrated subcutaneously 15 minutes prior to the capsaicin. Three transgenic and control mice were injected subcutaneously with capsaicin (50 mg/kg, Sigma) and one mouse of each type was injected with solvent only to serve as control. Five days later, this procedure was repeated. Ten days after the first

injection, all animals were anesthetized with Equithesin and perfused intracardially with 4% paraformaldehyde in 0.1M PB (pH 7.4) and the brainstem, cerebellum, spinal cords and the trigeminal ganglia were removed. All tissues were postfixed in the same fixative for 2 hours and infiltrated overnight in 30% sucrose in 0.1M PB at 4°C. Subsequently, the brainstem, the cerebellum and the spinal cord segments were cut transversely on a cryostat at a thickness of 50 µm. Forty-µm-thick sections were cut for the trigeminal ganglia. The free-floating sections were incubated overnight at 4°C in an anti-SP/anti-HRP bi-specific monoclonal antibody and processed for the demonstration of SP immunoreactivity as described above.

NGF immunostaining for electron microscopic observation

Two male transgenic mice, at the age of postnatal day 5, were anesthetized with Equithesin (3 ml/kg, i.p.) and perfused with a fixative containing 3% paraformaldehyde, 0.1% glutaraldehyde and 15% saturated picric acid (v/v) in 0.1 M PB (pH 7.4) for 30 minutes, followed by perfusion with the same fixative mixture without glutaraldehyde, and finally with 10% sucrose in 0.1 M PB, for 30 minutes each (Ribeiro-da-Silva et al., 1993). The cervical spinal cord was removed and cryoprotected in 30% sucrose in 0.1M PB. The following day, segments C4-C7 of the cervical spinal cord were snap frozen by immersion in liquid nitrogen, and thawed in 0.1 M PB at 25°C. Fifty µm-thick sections were cut on a Vibratome, treated for 30 minutes in 1% sodium borohydride in phosphate-buffered saline (PBS) and then rinsed several times in PBS until all bubbles disappeared (Kosaka et al., 1986). The sections were incubated in the anti-mouse NGF

antibody mentioned above at the dilution of 1:1000 for 72 hours. An Elite ABC kit (Vector) was used according to the manufacturer's instructions. Finally, the DAB reaction was carried out with double intensification (Adams, 1981). Triton X-100 was omitted from all steps. After the DAB reaction, the tissue was rinsed several times with PBS and then osmicated for 1 hour in 1% osmium tetroxide in 0.1 M PB at 4^0C. Subsequently, the sections were washed twice with distilled water, dehydrated in ascending concentrations of alcohol, and flat embedded in Epon between thick acetate foil and plastic cover slips. After polymerization of the Epon, the sections were examined by light microscopy. The selected fields of the white matter of the ventral and lateral columns of the spinal cord were trimmed and re-embedded for ultrastructural examination. The non-counterstained ultrathin sections were observed with an electron microscope (Philips 410).

For the detection of SP and CGRP immunoreactivities at the electron microscopy level, a post-embedding immunogold protocol was used for ultrathin sections previously processed for NGF immunocytochemistry as described above. Ultrathin sections were collected onto formvar-coated nickel grids and incubated in the primary antibody overnight at room temperature in a humid chamber. The primary antibody was either a rabbit antibody against rat CGRP (1:2000, Peninsula) or a rat monoclonal antibody against SP (1:10, (Cuello et al., 1979)). Subsequently, sections were incubated in the secondary antibody for 1 hour at room temperature. The secondary antibody was either a gold-conjugated goat anti-rabbit IgG (1:20, Biocell) or a gold-conjugated goat anti-rat IgG (1:20, Biocell). The size of the gold particles was

10 nm. Subsequently, sections were rinsed thoroughly in BSA-Tris and distilled water, contrast stained with uranyl acetate and lead citrate, and examined under the electron microscope.

Quantitative analysis

A) Number of NGF-IR oligodendrocytes in the white matter of the spinal cord

The numbers of NGF-IR oligodendrocytes were counted directly under the light microscope in both cervical and thoracic spinal cord sections from transgenic mice aged from postnatal day 0 to 6 months. Ten sections from the cervical region and 10 from the thoracic were counted, respectively, for each animal. Five transgenic and five control mice were used for each age group. The mean numbers of NGF-IR oligodendrocytes per section were determined for each age group.

B) Number of intersections of ectopic SP-IR fibers in the white matter of the spinal cord

Quantification was carried out by counting directly the total numbers of intersections of SP-IR fibers with a line drawn along the periphery of the spinal cord. Sections obtained from transgenic mice aged from postnatal day 0 to 12 months and control mice aged from postnatal day 0 to day 10 were used for this quantification. The counting was done for 10 cervical and 10 thoracic sections, respectively, from each animal. Five transgenic mice and five control mice were used in each age group. The mean number of intersections per section of ectopic SP-IR fibers were determined for each age group. Statistical comparisons of the mean number of intersections per section

between transgenic mice and controls was carried out using Student's t-test. The significance level was set at $P<0.05$.

C) Percentages of SP-IR neurons in the total number of neurons in primary sensory ganglia

SP-IR and non-immunoreactive cells were counted directly under the light microscope in sections from the cervical and lumbar DRG, and from the trigeminal ganglion of four transgenic and four control mice. Two cervical and two lumbar DRG from each animal were used for counting. Six sections were counted for each ganglion. Sections from one trigeminal ganglion from each animal were counted. The percentages of SP-IR neurons in the total number of neurons per section were thus determined. The mean percentages of SP-IR neurons in the cervical and lumbar DRG and in the trigeminal ganglia from transgenic mice and controls were compared, using Student's t-test. The significance level was set at $P<0.05$.

D) Size frequency distribution of SP-IR neurons in primary sensory ganglia

The soma areas and average soma diameters were measured for SP-IR neurons from the cervical and lumbar DRG and the trigeminal ganglia of transgenic mice and controls. The measurements were made using an image analysis system (M1, Imaging Research Inc., St. Catharines, Ontario, Canada), with the aid of a light microscope (Olympus) coupled to a black and white CCD camera. One hundred SP-IR cells from each of the cervical and lumbar DRG and the trigeminal ganglia were measured for each

animal. Four transgenic animals and four controls were used. Cells were considered as small size neurons when their average soma diameters were below 15 μm. Medium size neurons had average soma diameters from 15 to 25 μm. Large size neurons had average soma diameters larger than 25 μm. The mean percentages of SP-IR cells in different ranges of average soma diameter were compared between transgenic mice and controls using Student's t-test. Significance level was set at $P<0.05$.

RESULTS

The generation and expression of the NGF transgene, and the phenotypic effects in the adult transgenic mice of this line have been reported previously (Ma et al., 1995). In this study, we addressed developmentally the *in vivo* NGF transgene expression and the consequences of this expression on NGF responsive sensory neurons. On gross examination, we did not detect any differences in the appearances of the brain, the spinal cord, the trigeminal ganglia and the dorsal root ganglia between transgenic and control mice.

The spatial and temporal expression of the chicken NGF transgene in myelinating oligodendrocytes in the CNS of transgenic mice

At ages from postnatal day 0 to 2 months, numerous NGF-IR oligodendrocyte like cells were observed in certain specific areas in the CNS of line A414 transgenic

mice. In sharp contrast, no such NGF-IR oligodendrocytes could be detected in any CNS region in control mice in any age group. Most of the NGF-IR oligodendrocytes were located in the white matter of the CNS. Some of the NGF-IR oligodendrocytes could be found in the white matter within certain nuclei. The topographic distribution of the NGF-IR oligodendrocytes is shown in Figure 1. In the forebrain of postnatal day 10 to day 20 transgenic mice, NGF-IR oligodendrocytes were found in the corpus callosum, caudate-putamen and the internal capsule. At the brainstem level, NGF-IR oligodendrocytes were observed in the reticular thalamic nucleus, in the reticular formation, pyramidal tract, spinal trigeminal tract and cochlear nuclei. NGF-IR oligodendrocytes were also detected in the central white matter of the cerebellum, the cerebellar cortex and throughout the white matter of the spinal cord. NGF-IR oligodendrocytes in these areas of the CNS exhibited the typical morphological characteristics of oligodendrocytes, e.g. a few delicate and thin processes radiating from a spherical or polygonal cell body (Fig. 2, arrows).

Temporally, NGF-IR oligodendrocytes occurred in a caudo-rostral gradient in parallel with the postnatal progression of myelination by oligodendrocytes in the CNS (Table 1). By postnatal day 0, NGF-IR oligodendrocytes could be found only in the white matter of the spinal cord and certain regions in the pons and the medulla oblongata. By postnatal day 2, NGF-IR oligodendrocytes were also detected in the central white matter of the cerebellum and the cerebellar cortex. By postnatal day 10, NGF-IR oligodendrocytes could be detected in the caudate-putamen in some transgenic mice. At day 20, NGF-IR oligodendrocytes were seen in all these regions in all the

transgenic mice examined, as illustrated in Figure 1. By postnatal day 60, however, NGF-IR oligodendrocytes were dramatically decreased in number in the white matter of the spinal cord, medulla oblongata, pons and cerebellum, and could no longer be found at the forebrain level. Quantitatively, as shown in Figure 3, the numbers of NGF-IR oligodendrocytes in the white matter of both the cervical and thoracic regions of the spinal cord of transgenic mice increased considerably during the early postnatal period and reached a plateau by day 10. After day 20, they declined gradually and completely disappeared by the age of 6 months (Fig.3, Table 1).

Interestingly, in transgenic mice from postnatal day 0 to day 5, we observed not only NGF-IR oligodendrocytes, but also NGF-IR fiber-like structures in the white matter of the spinal cord, medulla oblongata, pons and cerebellum (Fig.4 and 5). NGF-IR oligodendrocytes were scattered within the networks formed by NGF-IR fiber-like structures. Some of the NGF-IR fiber-like structures were very long, extruding branches into surrounding white matter (Fig. 5, arrows). In the spinal cord, some of those fiber-like structures were seen in the ventral roots. Others travelled transversely in the ventral and lateral columns of the white matter of the spinal cord (Fig.5E and 5F), and some extended into the gray matter (Fig.5E and 5F). No NGF-IR cell profiles were present in the ventral roots (Fig. 5E and 5F, curved arrows). However, at postnatal day 0, the NGF-IR fiber-like structures were present only in the ventral part of the spinal cord. They were absent in the dorsal columns despite the occurrence of numerous NGF-IR oligodendrocytes there. By postnatal 5, both NGF-IR oligodendrocytes and fiber-like structures were seen in the dorsal columns of the spinal cord. These NGF-IR fiber-like

structures were still visible in some specimens from 10-day-old mice, although they were harder to detect than in 5-day-old animals. By postnatal day 15, the NGF-IR fiber-like structures were no longer detected in any of the areas where NGF-IR oligodendrocytes occurred.

At day 5, the thickness and length of NGF-IR fiber-like structures and of ectopic SP-IR fibers (described below) were similar in the cerebellar cortex (Fig. 6A and 6B) and in the white matter of the spinal cord (Fig. 6C and 6D). However, this similarity was not observed in specimens from day 0 and day 2 mice, in which NGF-IR fiber-like structures were thicker and longer than SP-IR fibers.

Under the electron microscope, NGF-IR oligodendrocytes were identified in the white matter of the spinal cord (Fig. 7). In the cytoplasm of oligodendrocytes, NGF immunoreactivity was particularly associated with the Golgi apparatus and multivesicular bodies. The NGF-IR fiber-like structures seen under the light microscope corresponded to NGF immunoprecipitates around bundles of unmyelinated axon-like processes (Fig. 8 A, B and C). In the double-stained ultrathin sections, immunogold particles, representing SP and CGRP immunoreactivities (respectively in Figures 8B and 8C) were detected in some of these small diameter unmyelinated axon-like processes.

The topographic and temporal occurrence of ectopic SP-IR fibers in the CNS of NGF over-expressing transgenic mice

In adult transgenic mice, ectopic SP-IR fibers were seen in the pyramidal tracts,

reticular formation and cochlear nuclei at the brainstem level; in the central white matter of the cerebellum and the cerebellar cortex; and in the white matter of the spinal cord (Fig. 9). Ectopic fibers always occurred in bundles which consisted of thin fibers possessing numerous tiny varicosities, which could be detected clearly at higher magnifications (see Fig. 10B). These thin fibers were characterized as unmyelinated fibers under the electron microscope in a previous study in the spinal cord (Ma et al., 1995). In fact, ectopic fibers were detected only in the areas where NGF-IR oligodendrocytes were also seen. However, no ectopic SP-IR fibers were observed in the forebrain (Fig. 9). Figure 10 shows the ectopic SP-IR fibers in certain regions of the CNS of the transgenic mice. In the central white matter of the cerebellum, ectopic fibers extended at random with no specific orientation (Fig. 10A). Some ectopic fibers penetrated into the white matter of the paraflocculus. In the cortex of the cerebellum, the ectopic fibers formed bundles which penetrated externally to the surface (Fig. 10A); the varicosities in these fiber bundles were usually larger and more apparent (Fig. 10B) than other regions of the CNS. In the pons, ectopic SP-IR fibers travelled transversely along the margin of the pons (Fig. 10C). In the medulla oblongata, ectopic SP-IR fibers entered the white matter longitudinally or obliquely (Fig. 10D).

In the time course study, from postnatal day 0 to day 5, we detected a widespread SP-IR fiber network in the gray and white matter of the pons, medulla oblongata and spinal cord of both transgenic mice and controls. However, SP immunostaining was more intense in specimens from transgenic mice than from controls. SP-IR fibers formed thin bundles, from postnatal day 0 to day 2, not only in

the white matter of the pons, medulla oblongata and the spinal cord of transgenic mice, but also in the white matter of the same regions in control mice. Figure 11 shows the extensive SP-IR fiber network in the cervical spinal cord of transgenic and control mice from day 0 to day 5. Interestingly, from day 0 to day 5, these thin SP-IR fiber bundles increased dramatically in number and thickness in transgenic specimens (Fig. 11B, 11D and 11F), while decreasing markedly to an almost undetectable level in control animals (Fig 11A, 11C and 11E). There were no statistically significant differences in the numbers of intersections of SP-IR fiber bundles in the white matter of the cervical and thoracic spinal cord between transgenic mice and controls at the ages of postnatal day 0 and day 2, in contrast to postnatal day 5 and day 10 where those found in transgenic mice were significantly higher (Fig. 12).

By postnatal day 5, SP-IR fibers in the white matter of transgenic mice were more numerous and formed thicker bundles than at earlier ages. As very few SP-IR fibers were detected in the white matter of control mice older than day 5, we considered these thick SP-IR fiber bundles in the white matter of similar transgenic mice older than 5 days as ectopic fibers.

Quantitatively SP-IR fibers in the white matter of the cervical and thoracic spinal cord increased significantly after birth and reached adult levels by day 20 (Fig. 13). Then, the number of ectopic SP-IR fibers remained constant until 12 months, the oldest age studied. The ectopic SP-IR fiber bundles grew in the thickness, reaching their thickest point between 2 to 4 months, after which they progressively thinned upto the final time point studied (12 months).

Increased numbers of SP-IR cells in primary sensory ganglia of transgenic mice

SP-IR cells in the cervical and lumbar DRG and the trigeminal ganglia of transgenic mice (Fig. 14B and 14D) were more intensely stained and more numerous than in controls (Fig.14A and 14C). Quantitative analysis revealed that the percentages of SP-IR cells increased significantly in the cervical and lumbar DRG and the trigeminal ganglia of transgenic mice, when compared with controls (Fig. 15). Size frequency distribution analysis did not detect any significant difference in SP-IR neurons in the cervical and lumbar DRG and the trigeminal ganglia between transgenic mice and controls (Fig.16). Most of the SP-IR ganglion cells were within the small size range; only a small proportion of the cells were within the medium size range (Fig.16).

Effects of capsaicin treatment

Following capsaicin treatment, ectopic SP-IR fibers were no longer detected in the cerebellum, pons, medulla oblongata (Fig. 17B and 17D) and spinal cord of transgenic mice; vehicle-treated animals were not similarly affected (Fig. 17A and 17C). Furthermore, capsaicin treatment decreased markedly the numbers of SP-IR cells in the trigeminal ganglia of transgenic mice (Fig. 17F), compared to vehicle-treated transgenic animals (Fig. 17E). In capsaicin-treated transgenic and in control specimens, the SP immunoreactivities in the dorsal horn of the spinal cord and of the trigeminal nucleus caudalis were reduced, as previously reported (Jessell et al., 1978; Nagy et al., 1980; Jancsó et al., 1981; Priestley et al., 1982a).

Detection of NGF-IR small glia-like cells in the CNS of both transgenic and control mice during neonatal period

In the specimens from both transgenic and control mice aged from day 0 to day 10, NGF-IR small glia-like cells were detected in the gray matter and white matter of the ventral part of the forebrain, as well as in the brainstem, cerebellum and spinal cord. These cells possessed a small cell body and a few processes giving rise to several multiple short branches (Fig. 18), and were considerably smaller than the NGF-IR oligodendrocytes (Fig. 18D). At postnatal day 0, these cells were most apparent in all of the above regions, progressively decreasing in quantity by day 10, and disappearing entirely by day 15 in all regions of the CNS of both transgenic and control mice.

DISCUSSION

Topographic and temporal expression of the NGF transgene

We demonstrated in the present study that, under the control of the 1.3 kb 5' and 2.1 kb 3' sequences of the MBP promoter, NGF was expressed in oligodendrocytes located in the caudate-putamen, corpus callosum, reticular nucleus of the thalamus, central white matter of the cerebellum, cerebellar cortex, trigeminal tracts, pyramidal tracts, cochlear nuclei, reticular formation of the brainstem, and white matter of the spinal cord. The expression of chick NGF immunoreactivity in this study was tissue and cell specific, since NGF immunoreactivity was restricted to the oligodendrocytes in the

white matter of the CNS of transgenic mice. This tissue and cell specific expression of NGF immunoreactivity was likely determined by the nature of the MBP promoter.

Previous studies using 0.63 kb to 4.2 kb MBP promoter fragments all failed to direct Schwann cell specific transcription in transgenic mice (Readhead et al., 1987; Gow et al., 1992; Foran and Peterson, 1992; Goujet-Zalc et al., 1993). Oligodendrocytes normally expressed MBP at levels several fold higher than that expressed by Schwann cells. The promoter used in this study lacks upstream regulatory elements which might be required for MBP expression in Schwann cell. This may explain the lack of NGF expression in Schwann cells in peripheral nervous tissues. Indeed, our NGF immunostaining failed to detect any NGF-IR cells in peripheral nerves. Thus, NGF expression was restricted exclusively to the CNS. Although immunostaining of oligodendrocyte-specific markers was not carried out, we presume that the numerous cells with intense NGF immunoreactivity were oligodendrocytes, based on their morphological characteristics and distribution pattern. In our study, NGF-IR oligodendrocytes appeared only in the white matter of several regions in the CNS of transgenic mice. This spatial specificity of transgene expression is also consistent with several reports of expression in oligodendrocytes of a bacterial reporter gene (β-galactosidase) under different fragments of the MBP promoter, varying from 0.63 kb to 3.2 kb in size, in transgenic models (Miskimins et al., 1992; Gow et al., 1992; Foran and Peterson, 1992; Goujet-Zalc et al., 1993).

In the present study, the developmental expression of NGF immunoreactivity in the CNS of transgenic mice followed a caudo-rostral gradient. At birth, NGF-IR

oligodendrocytes appeared in the white matter of the spinal cord, medulla oblongata and pons. By day 2, they began to appear in the central white matter of cerebellum and the cerebellar cortex. By day 10, NGF-IR oligodendrocytes could be detected in the the caudate-putamen of some transgenic mice. This pattern of development is in agreement with previous studies of transgenic mice using MBP promoters of various gene sizes (Foran and Peterson, 1992; Goujet-Zalc et al., 1993). Although we did not examine transgenic mice at embryonic stages, we have detected NGF-IR oligodendrocytes as early as postnatal day 0 in the white matter of the spinal cord, medulla oblongata and pons. This is consistent with previous studies (Foran and Peterson, 1992; Goujet-Zalc et al., 1993) in which the bacterial reporter gene expression in oligodendrocytes started perinatally. In our transgenic mice, it is likely that oligodendrocytes begin to produce NGF shortly before birth, because of the nature of MBP promoter. At birth, NGF-IR oligodendrocytes and fibers in the white matter of the CNS were present in only limited numbers; after birth, more oligodendrocytes were driven to produce NGF by the MBP promoter, to reach a plateau level on day 10.

Interestingly, in addition to NGF-IR oligodendrocytes, we also detected NGF-IR fiber-like structures in several CNS regions in transgenic mice from postnatal day 0 to 5, which were absent in controls. Surprisingly, such fiber-like structures displayed a continuous immunostaining for considerable distances, as if they represented bundles of immunostained axons rather than processes of immunostained oligodendrocytes. Such structures were investigated by electron microscopy at postnatal day 5 and were shown to represent immunoprecipitates in between and on the membranes of profiles

that apparently corresponded to unmyelinated fibers organized in bundles. Because less than ideal conditions of fixation had to be used to allow the demonstration of NGF immunoreactivity at the ultrastructural level, the morphological preservation of the tissue was not sufficient to allow us to identify whether the staining around the fibers was intracellular, presumably in oligodendrocyte processes, or extracellular. It is likely that part of the NGF immunoreactivity corresponded to extracellular NGF released from nearby oligodendrocyte processes. However, part of the staining was detected on the membranes of the unmyelinated fibers themselves. We can conclude that the NGF-IR fiber-like structures seen under light microscopy correspond to NGF immunostaining on and around unmyelinated fibers.

As the light microscopic appearance of both NGF fiber-like structures and of SP-IR fiber bundles in the white matter was fairly similar at postnatal day 5, but not at earlier ages, we decided to carry out a double-labeling study at the ultrastructural level. This revealed that, in the lateral funiculus, some of the unmyelinated fibers surrounded by NGF immunoreactivity, were themselves immunoreactive for SP or CGRP. Although we were only able to detect a few such fibers, this observation clearly demonstrates that some of the NGF-IR fiber-like structures seen under light microscopy are equivalent to the SP-IR ectopic fiber bundles. This finding is important as almost all SP-IR and most of the CGRP-IR DRG neurons express high affinity NGF receptors (Verge et al., 1989a). As the ectopic SP-IR fibers were abolished by capsaicin treatment (see Results), they are likely of sensory origin (Holzer, 1988). It is tempting to speculate that the NGF immunoreactivity around SP-IR fibers represents NGF released

from nearby oligodendrocyte processes and that the NGF immunostaining on the membranes of such SP-IR fibers represents NGF bound to NGF receptors, prior to internalization and retrograde transport to the cell body in the DRG. The reason why such NGF-IR fiber-like structures are hard to detect after day 10 is at present unclear, but we can speculate that it may result from a faster uptake of NGF by slightly more mature fibers, preventing the accumulation of NGF at levels detectable by immunocytochemistry.

The observation of NGF-immunoreactivity around some unmyelinated fibers which were immunoreactive for sensory neuropeptides at postnatal day 5 is very important, as these arrangements may indicate sites of active sprouting of sensory fibers attracted to areas of higher NGF concentration. Such NGF accumulations in the white matter of transgenic mice might induce normally occurring, isolated SP-IR fibers to sprout into bundles of ectopic fibers. In contrast, SP-IR fibers quickly disappeared in the early postnatal period from the white matter of control mice, due to the lack of NGF over-availability. This issue is discussed in detail in the following section.

Certainly, some of the NGF fiber-like structures may not be related to sensory fibers, since neuropeptide immunostaining was restricted to a limited number of unmyelinated fibers. NGF-IR fiber-like structures were located primarily in the ventral columns at postnatal days 0 and 2 and did not correlate with the SP-IR fibers. A possible explanation is that part of the NGF-IR fiber like structures correspond to immunostaining associated with oligodendrocyte processes surrounding fiber bundles that will be finally myelinated.

from nearby oligodendrocyte processes and that the NGF immunostaining on the membranes of such SP-IR fibers represents NGF bound to NGF receptors, prior to internalization and retrograde transport to the cell body in the DRG. The reason why such NGF-IR fiber-like structures are hard to detect after day 10 is at present unclear, but we can speculate that it may result from a faster uptake of NGF by slightly more mature fibers, preventing the accumulation of NGF at levels detectable by immunocytochemistry.

The observation of NGF-immunoreactivity around some unmyelinated fibers which were immunoreactive for sensory neuropeptides at postnatal day 5 is very important, as these arrangements may indicate sites of active sprouting of sensory fibers attracted to areas of higher NGF concentration. Such NGF accumulations in the white matter of transgenic mice might induce normally occurring, isolated SP-IR fibers to sprout into bundles of ectopic fibers. In contrast, SP-IR fibers quickly disappeared in the early postnatal period from the white matter of control mice, due to the lack of NGF over-availability. This issue is discussed in detail in the following section.

Certainly, some of the NGF fiber-like structures may not be related to sensory fibers, since neuropeptide immunostaining was restricted to a limited number of unmyelinated fibers. NGF-IR fiber-like structures were located primarily in the ventral columns at postnatal days 0 and 2 and did not correlate with the SP-IR fibers. A possible explanation is that part of the NGF-IR fiber like structures correspond to immunostaining associated with oligodendrocyte processes surrounding fiber bundles that will be finally myelinated.

Reponse of SP containing primary sensory ganglion cells to NGF expression in myelinating oligodendrocytes

In a previous study (Ma et al., 1995), we described ectopic SP- and CGRP-IR fibers in the white matter of the spinal cord of adult transgenic mice. At the EM level, the SP-IR fibers were characterized as unmyelinated fibers occurring in bundles. After capsaicin treatment, the ectopic SP-IR fibers disappeared from the spinal cord, confirming their primary sensory origin. Here, we report that there are also ectopic SP-IR fibers in other areas of the CNS of transgenic mice. SP-IR fibers were observed in the white matter of the spinal cord, medulla oblongata, pons and cerebellum of transgenic mice from postnatal day 0 to 1 year of age. After capsaicin treatment, these ectopic fibers were abolished from the white matter of these regions, confirming their sensory origin. No such fibers were found in the forebrain of transgenic mice.

A. SP-IR fibers in the white matter of the CNS in neonatal transgenic and control mice

Unexpectedly, SP-IR fibers were also found in the white matter of the CNS of control mice from postnatal day 0 to day 2. The distribution pattern was similar to that observed in transgenic mice. SP-IR fibers in the white matter of control mice decreased markedly from day 2 to day 5. By day 10, no obvious SP-IR fibers could be detected in the white matter of controls, except for those crossing from the dorsal roots and localized in Lissauer's tracts. An earlier study (Pickel et al., 1982) showed that longitudinal SP-IR fibers were present in the white matter of medulla and spinal cord

of the fetal rat (E15-18), but not in adult animals. Therefore, these SP-IR fibers in the white matter of neonatal transgenic and control mice are likely present before birth. These fibers might constitute redundant elements which are probably eliminated during the early postnatal stage, an issue which requires further investigation.

The occurrence of SP-IR fibers in the white matter of both transgenic mice and controls is closely related to NGF, given the known sensitivity of SP containing sensory neurons to NGF during early development (Otten et al., 1980; Kessler and Black, 1980; Otten and Lorez, 1983). More importantly, during the early postnatal period, NGF was shown to up-regulate SP gene expression and protein biosynthesis in rat sensory neurons *in vitro* and *in vivo* (Vedder et al., 1993). But where in the CNS is NGF produced at this stage? Interestingly enough, we did find NGF-IR small glia-like cells throughout the spinal cord, brainstem, cerebellum and ventral part of forebrain from postnatal day 0 to 10 in both control and transgenic mice. Such cells were particularly abundant at postnatal day 0 to day 2. These NGF-IR small cells possessed glial characteristics, and were considerably smaller than NGF-IR oligodendrocytes. The characterization of these cells is beyond the scope of this study. A previous study described NGF immunoreactivity in the gray matter and white matter of the spinal cord, medullary fiber tract and cerebellum of E15 and 16 day mouse CNS (Finn et al., 1987). This study is consistent with our observation. *In vitro* and *in vivo* studies (Lu et al., 1991) also suggested that glial NGF gene expression and protein synthesis may be restricted to the active growth phase that normally occurs during early development. In light of these studies, we propose that the occurrence of SP-IR fibers in the white

matter of the spinal cord, brainstem and cerebellum of both transgenic and control mice was probably a consequence of high levels of NGF released by NGF-IR non-neuronal cells in the above regions.

The functional implication of SP-IR fiber growth and sprouting during early development is unknown, but it is indicative that SP containing sensory neurons are extremely sensitive to NGF at this stage. A previous study showed that transection of the infraorbital nerve in neonatal rats resulted in a selective survival of SP containing trigeminal ganglion cells (Enfiejian et al., 1989). It is possible that SP containing trigeminal cells could obtain NGF from NGF releasing glial cells through the sprouting of their central terminals in the CNS, thus being spared from neuronal death.

B. Ectopic SP-IR fibers in the white matter of the CNS of adult transgenic mice

The up-regulation of SP in sensory neurons by NGF has been confirmed by numerous studies (Otten et al., 1980; Lindsay et al., 1989; Lindsay and Harmar, 1989; Donnerer et al., 1992; Vedder et al., 1993). Therefore, the over-availability of NGF in the CNS of transgenic mice may explain why we detected more SP-IR neurons in primary sensory ganglia in these animals and why these SP-IR cells were more intensely stained than in control mice. This would be the consequence of higher production of SP in primary sensory neurons. The increased thickness and number of SP-IR fiber bundles which were observed in transgenic mice after day 5 probably results from the sprouting of SP-IR fibers which normally occur in the white matter only in the early postnatal period. This was likely induced by the over-availability of NGF produced by

oligodendrocytes. In control mice, as no NGF over-producing oligodendrocytes exist in the CNS, these SP-IR fibers in the white matter withdraw after day 5, due to the down-regulation of NGF in the CNS which normally occurs postnatally.

By the age of two months, NGF expression in myelinating oligodendrocytes in transgenic mice is probably turned off because of the nature of MBP gene expression [for review, see (Campaghoni, 1988)]. Gradual down-regulation of MBP gene expression after postnatal 1 month may explain why no NGF-IR oligodendrocytes were detected after two months of age. However, ectopic SP-IR fibers persisted in the white matter of the CNS, independently of NGF over-expression until the age of 12 months. It is likely that they persist for longer, but no older animals were studied. Since ectopic SP-IR fiber bundles in 12-month-old transgenic mice were much thinner than those in 2-month-old animals, it is possible that at this age the production of SP was down-regulated to a level at which fewer individual SP-IR fibers were visible in the bundles, due to the lack of expression of the transgene in the CNS.

As mentioned above, ectopic SP-IR fibers were not detected in the forebrain. The reason is not known. It may be simply because the forebrain is far away from the central targets of NGF responsive primary sensory neurons in the trigeminal ganglia and DRG. Such distance is probably excessive for prospective SP containing sensory fibers to reach, although NGF-IR oligodendrocytes were observed in certain forebrain regions.

Table 1. Postnatal distribution of NGF-IR oligodendrocytes in the CNS of transgenic mice

Postnatal day	Forebrain			Brainstem					Cerebellum	Spinal cord
	CCA	CPu	CAI	TR	RF	P	STV	CN		
0	-	-	-	-	++	-	++	++	-	+++
2	-	-	-	-	++	-	++	++	++	+++
5	-	-	-	-	+++	-	+++	+++	+++	++++
10	-	++	-	-	++++	++	++++	++++	+++	+++++
15	++	+++	++	++	++++	++	++++	++++	+++	++++
20	+++	++++	+++	+++	+++	++	+++	+++	++	+++
60	-	-	-	-	+	+	++	++	+	++
180	-	-	-	-	-	-	-	-	-	-

CCA - corpus callosum; CPu - caudate-putamen; CAI - internal capsule; tr - reticular thalamic nucleus; RF - Brainstem reticular formation; P - pyramidal tract; STV - spinal trigeminal tract; CN - cochlear nuclei.
The density of NGF-IR oligodendrocytes was quantitatively assessed. Results are expressed in a scale from -, not found, to +++++, the highest density observed (approximately 15 cells per 10,000 μm^2).

Figure 1. Topographic distribution of NGF-IR oligodendrocytes in the CNS of 20-day-old transgenic mice. At the forebrain level, NGF-IR oligodendrocytes were found in the corpus callosum (CCA), caudate-putamen (CPu), and internal capsule (CAI). At the brainstem level, NGF-IR oligodendrocytes appeared in the reticular thalamic nucleus (tr), reticular formation (RF), pyramidal tracts (P), spinal trigeminal tract (STV) and cochlear nuclei. Numerous NGF-IR oligodendrocytes were present in the cerebellar cortex, the central white matter of the cerebellum and the spinal cord. One circle represents 4 cells counted.

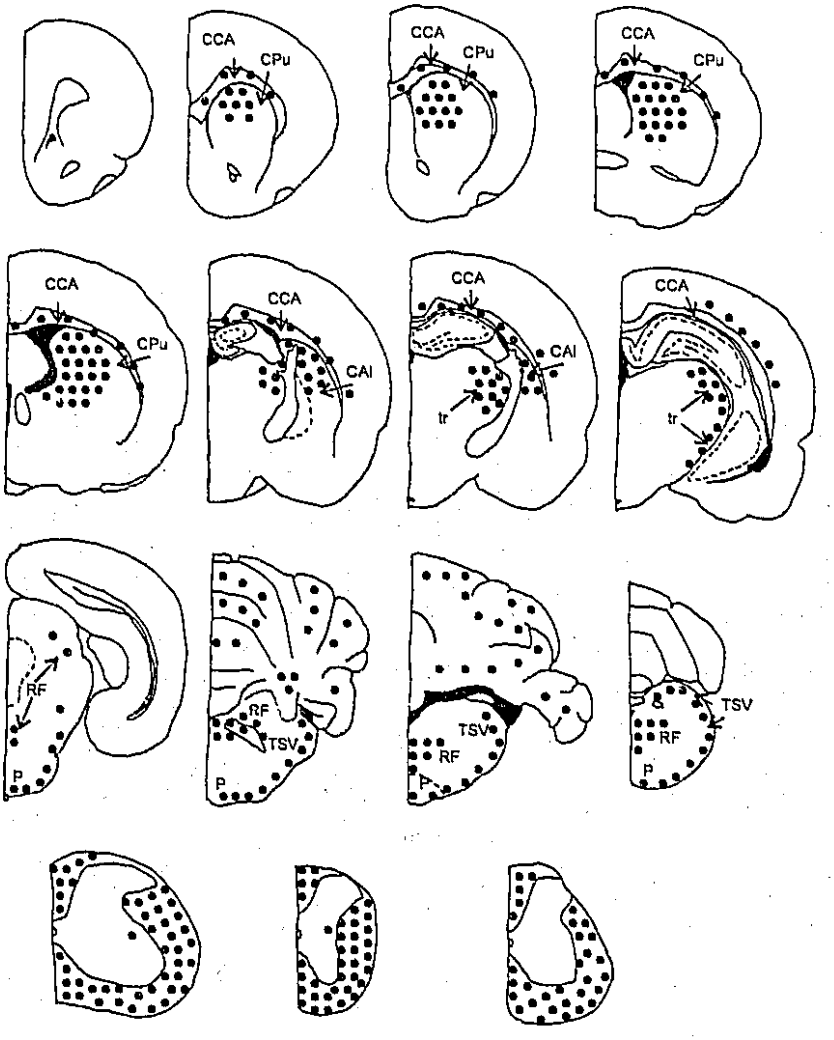
CCA
CPu
CCA
CPu
CCA
CPu
CCA
CPu
CCA
CAl
CCA
CAl
tr
CCA
tr
RF
P
RF
TSV
P
TSV
RF
P
TSV
RF
P

Figure 2. NGF-IR oligodendrocytes in various areas of the CNS of 20-day-old transgenic mice. NGF-IR oligodendrocytes were detected in the caudate-putamen (**A**), pyramidal tract at the pons level (**B**), the central white matter of the cerebellum (**C**), trigeminal tract (**D**), brainstem reticular formation (**E**) and the white matter of the spinal cord (**F**). Note that the NGF-IR cells indicated by arrows exhibit the typical morphological characteristics of oligodendrocytes. Scale bars =25 μm.

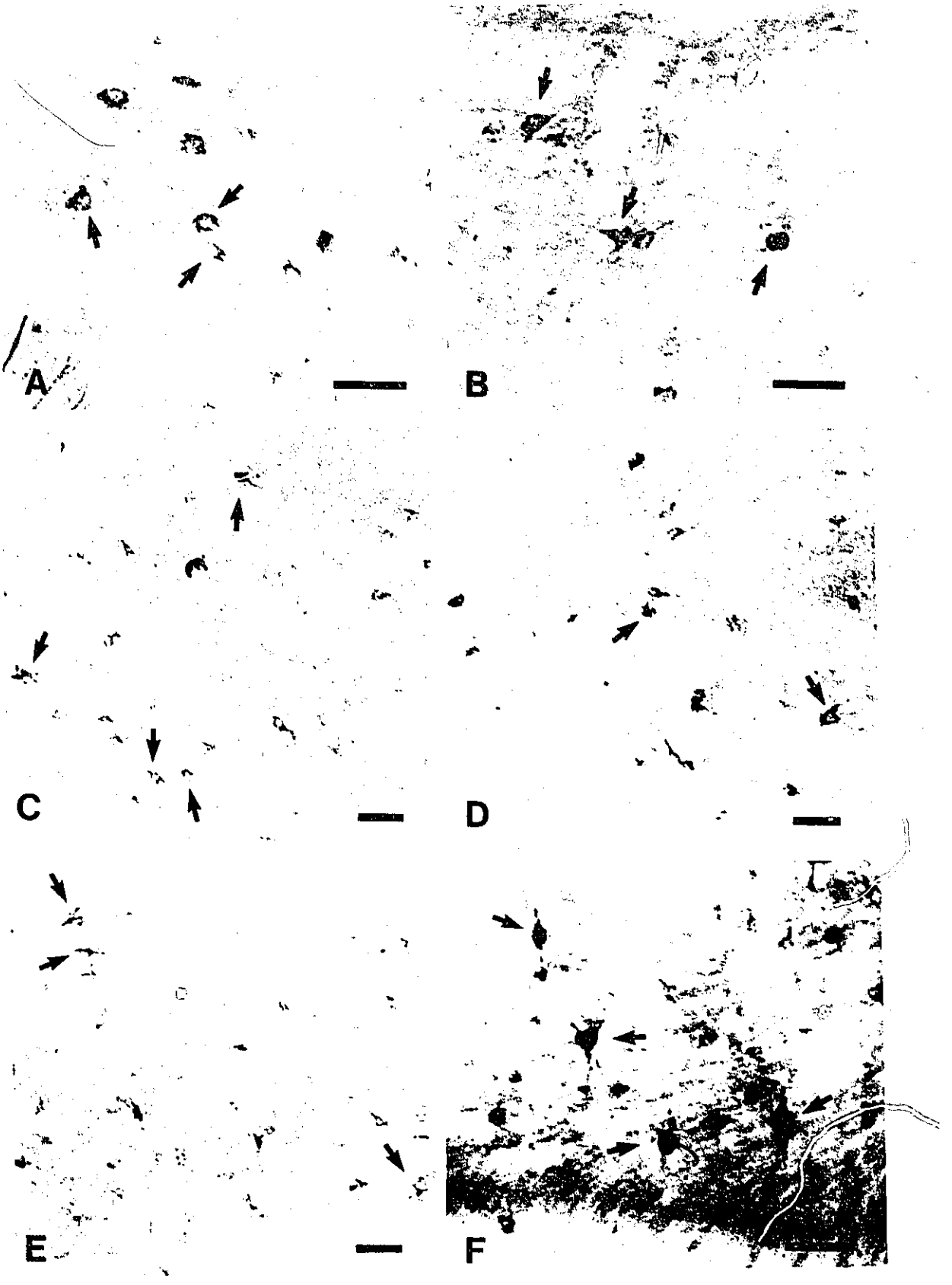
A
B
C
D
E
F

Figure 3. Number of NGF-IR oligodendrocytes (mean±SEM, n=5) in the cervical and thoracic spinal cords of transgenic mice at different postnatal ages. NGF-IR oligodendrocytes were detected by postnatal day 0, and reached the maximum at day 10. After day 20, NGF-IR oligodendrocytes decreased gradually in number and disappeared completely by the age of postnatal 6 months.

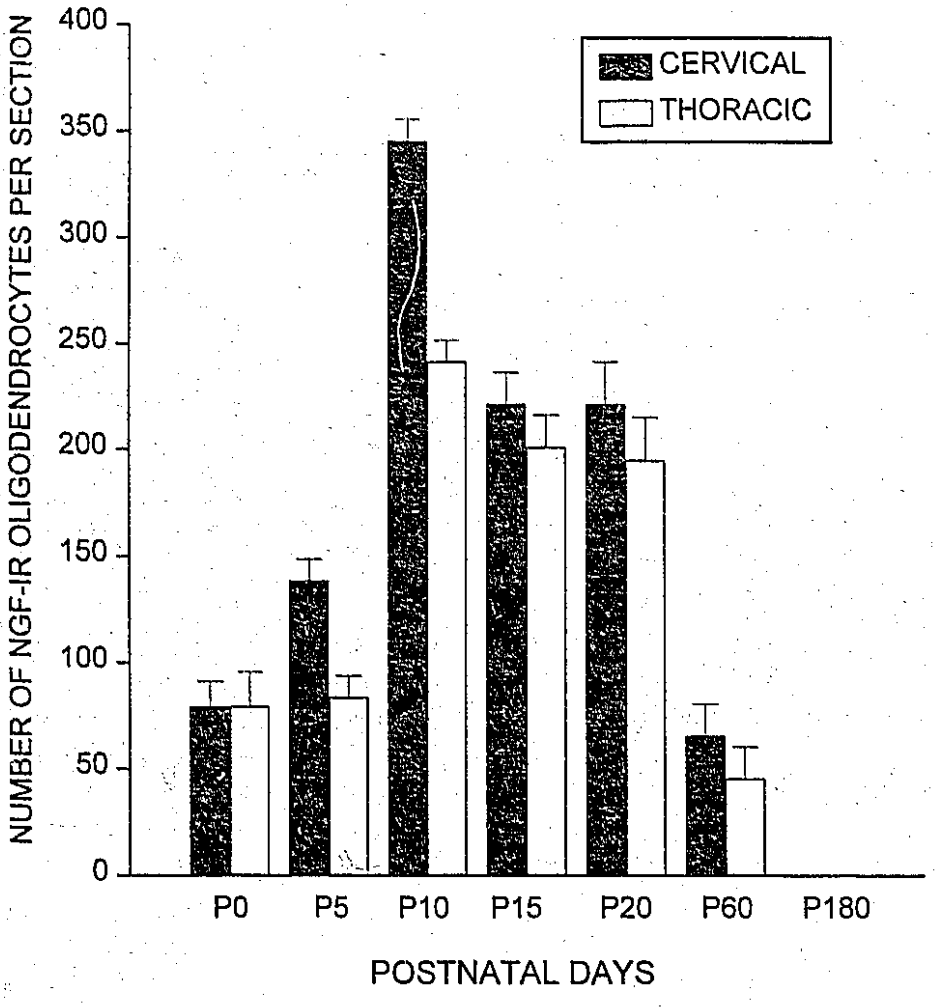
NUMBER OF NGF-IR OLIGODENDROCYTES PER SECTION
400
350
300
250
200
150
100
50
0
CERVICAL
THORACIC
P0
P5
P10
P15
P20
P60
P180
POSTNATAL DAYS

Figure 4. Micrographs at low magnification showing NGF-IR oligodendrocytes and fiber-like structures in several regions of the CNS of 5-day-old transgenic mice. Abundant NGF-IR oligodendrocytes and fibers were observed in the central white matter of the cerebellum (**A**), cerebral cortex (**B**), spinal trigeminal tract (**C**), and brainstem reticular formation (**D** and **E**). No such NGF-IR oligodendrocytes and fibers were found in controls at the same age (not shown). Scale bars =100 μm.

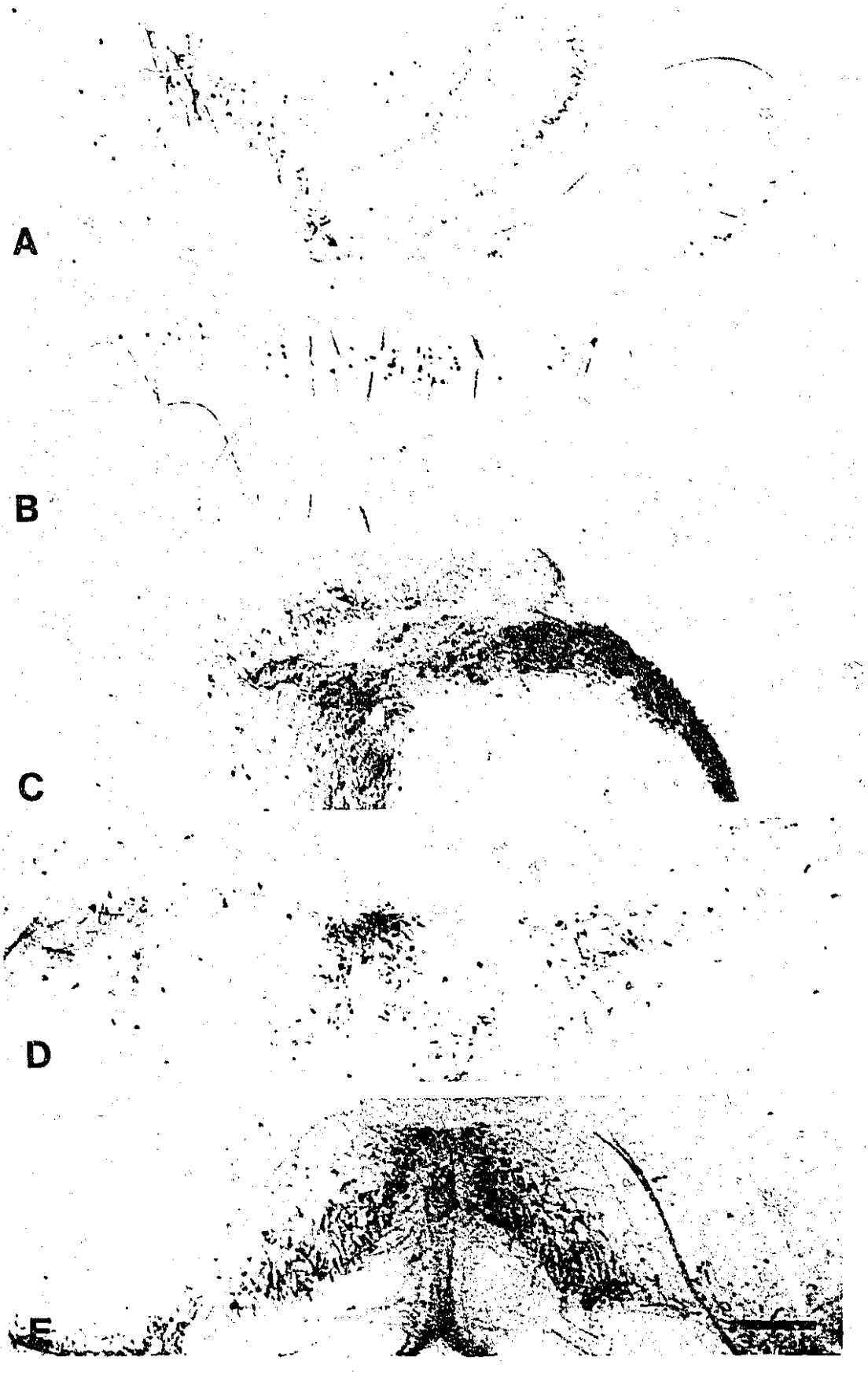
A
B
C
D
E

Figure 5. Micrographs at higher magnification showing NGF-IR oligodendrocytes and fiber-like structures in certain areas of the CNS of 5-day-old transgenic mice. NGF-IR oligodendrocytes were seen in the spinal trigeminal tract (**A**), cerebellum (**B**), reticular formation of medulla oblongata (**C**), and white matter of the cervical spinal cord (**D**, **E** and **F**). Note that some of these NGF-IR fiber-like structures give out branches (arrows in **B**, **D**, **E**, and **F**). NGF-IR oligodendrocytes were distributed in the fiber networks. Note in **E** and **F** that, although some NGF-IR fiber-like structures were detected, no NGF-IR cells were found in the ventral roots (curved arrows). Scale bars =25 μm.

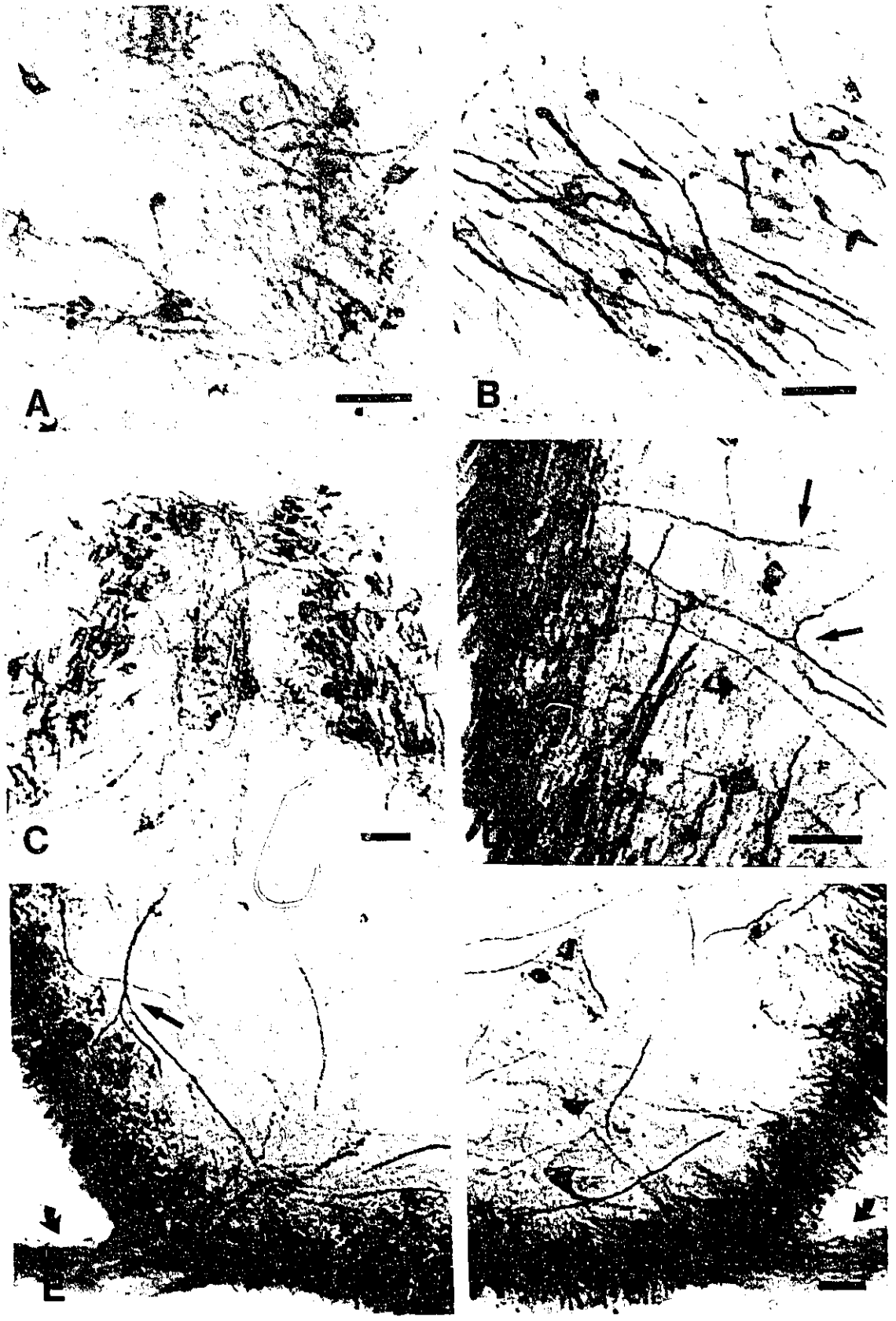
A
B
C

Figure 6. Similarity of morphological appearance at the light microscopy level of NGF-IR fiber-like structures and SP-IR fibers in the cerebellar cortex and spinal cord of 5-day-old transgenic mice. NGF-IR fiber-like structures (**A** and **C**, arrows) appeared similar to SP-IR fibers (**B** and **D**, arrows) in the cerebellar cortex (**A** and **B**) and the spinal cord (**C** and **D**). In the spinal cord, note that both NGF-IR fiber-like structures and SP-IR fibers were observed in the ventral roots (open arrows). Scale bars= 25 μm.

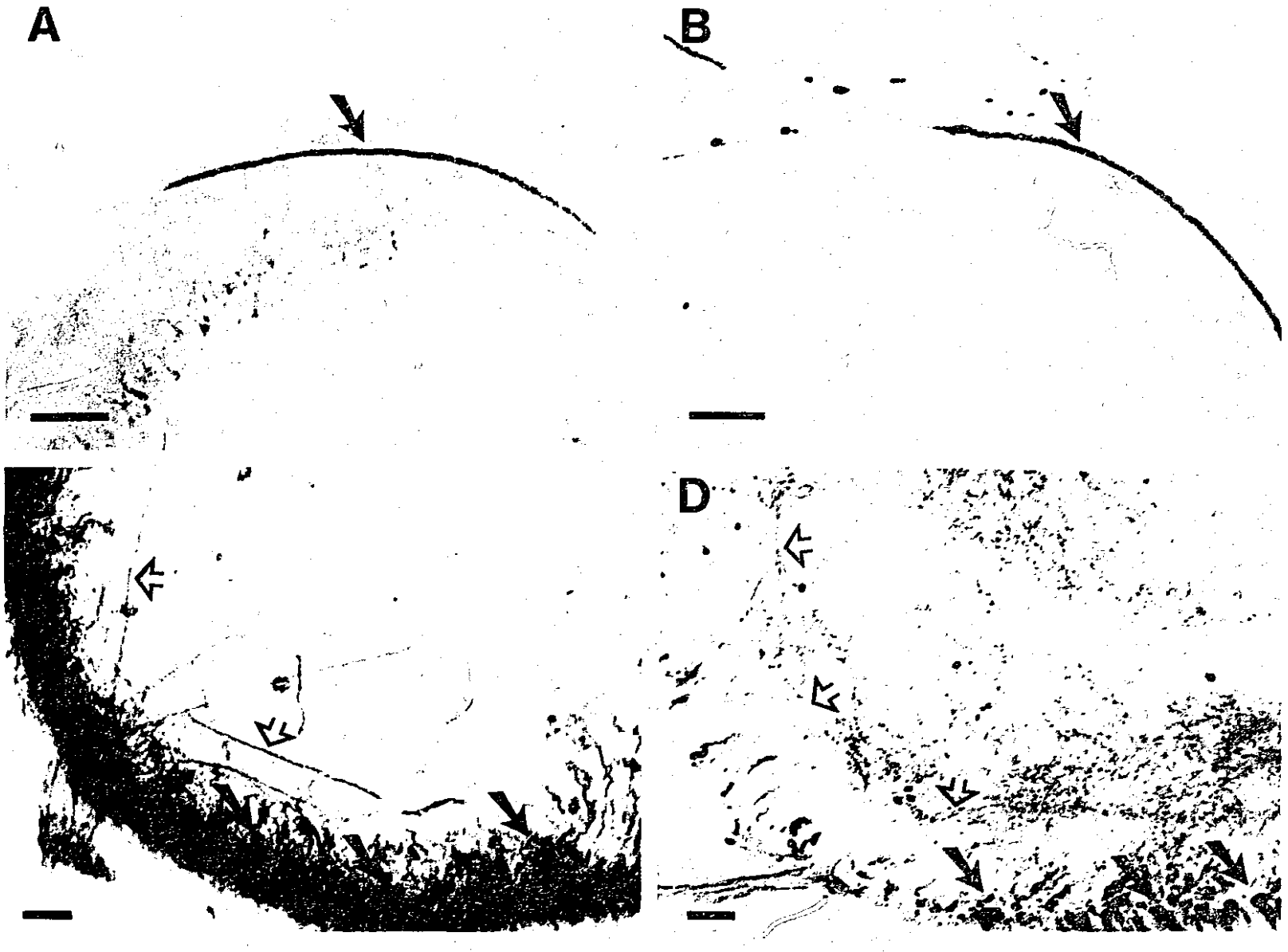
A
B
D

Figure 7. Electron micrographs of a NGF-IR oligodendrocyte in the white matter of the cervical spinal cord of a transgenic mouse at the age of postnatal day 5. **A**, NGF immunoprecipitates were particularly associated with Golgi apparatus (open arrows) and multivesicular bodies (arrows). **B** shows the framed area in **A** at higher magnification. Open arrows indicate NGF-IR in the Golgi apparatus. **C** illustrates DAB reaction product filled multivesicular bodies (arrows) from another NGF-IR oligodendrocyte. Scale bars = 1 μm for A, = 0.5 μm for B and C.

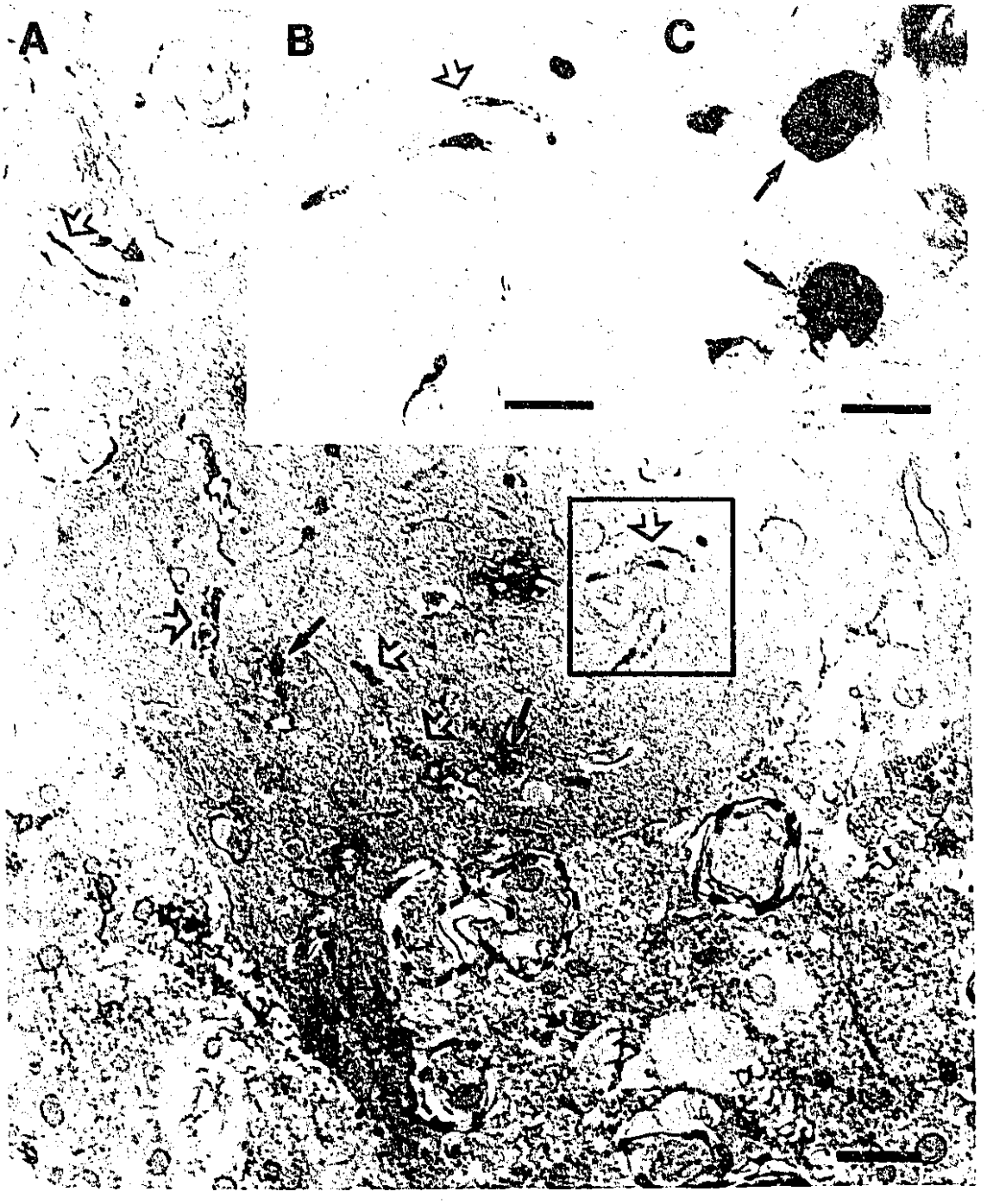
A
B
C

Figure 8. Electron micrographs of NGF immunoreactiviy in the white matter of the cervical spinal cord of a transgenic mouse at the age of postnatal day 5. **A** illustrates the ultrastructural appearance of NGF-IR fiber-like structures seen under light microscopy. Note immunoprecipitates in between and on the membranes of small diameter unmyelinated axon-like structures. Some of these small unmyelinated fibers contain small clear vesicles (arrow). **B** and **C** represent double staining for NGF and SP (**B**) or CGRP (**C**) using a combination of pre-embedding and post-embedding immunocytochemistry as described in Methods. Immunogold particles represent SP or CGRP immunoreactivities. Note that SP (**B**) or CGRP (**C**) immunoreactivities were detected in some of these small diameter fibers which were surrounded by NGF immunoreactivity. Arrows indicate immunogold particles associated with dense core vesicles. Scale bars = 0.5 μm.

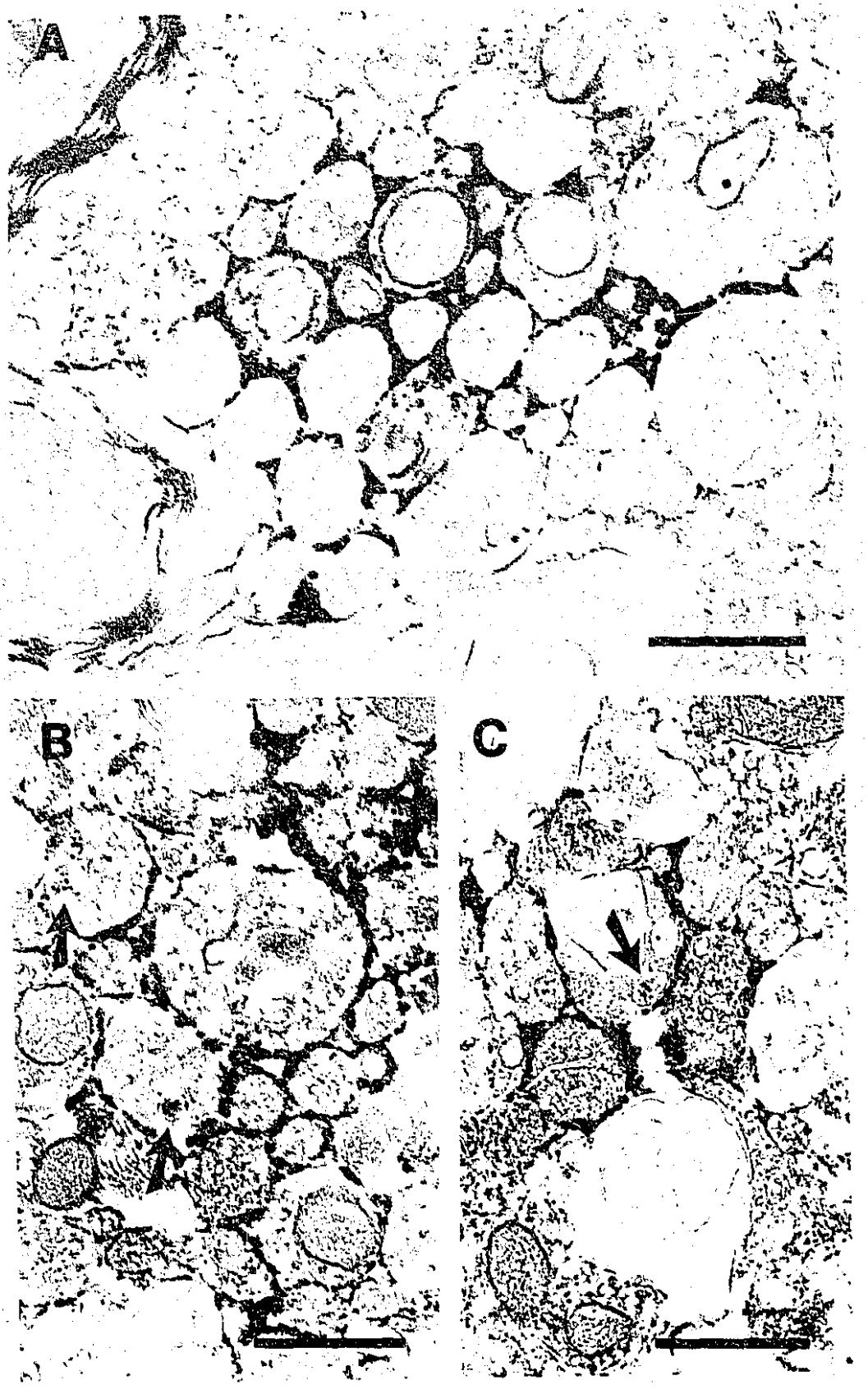
A
B
C

Figure 9. Topographic distribution of ectopic SP-IR fibers in the CNS of 20-day-old transgenic mice. Ectopic SP-IR fibers were observed in the pyramidal tracts, the reticular formation and cochlear nuclei, in the cerebellar cortex and in the central white matter of the cerebellum, and in the white matter of the spinal cord. Ectopic SP-IR fibers were not seen in the forebrain. No ectopic SP-IR fibers were detected in the above regions in control mice. TSV, trigeminal spinal nucleus; RF, reticular formation; P, pyramidal tract.

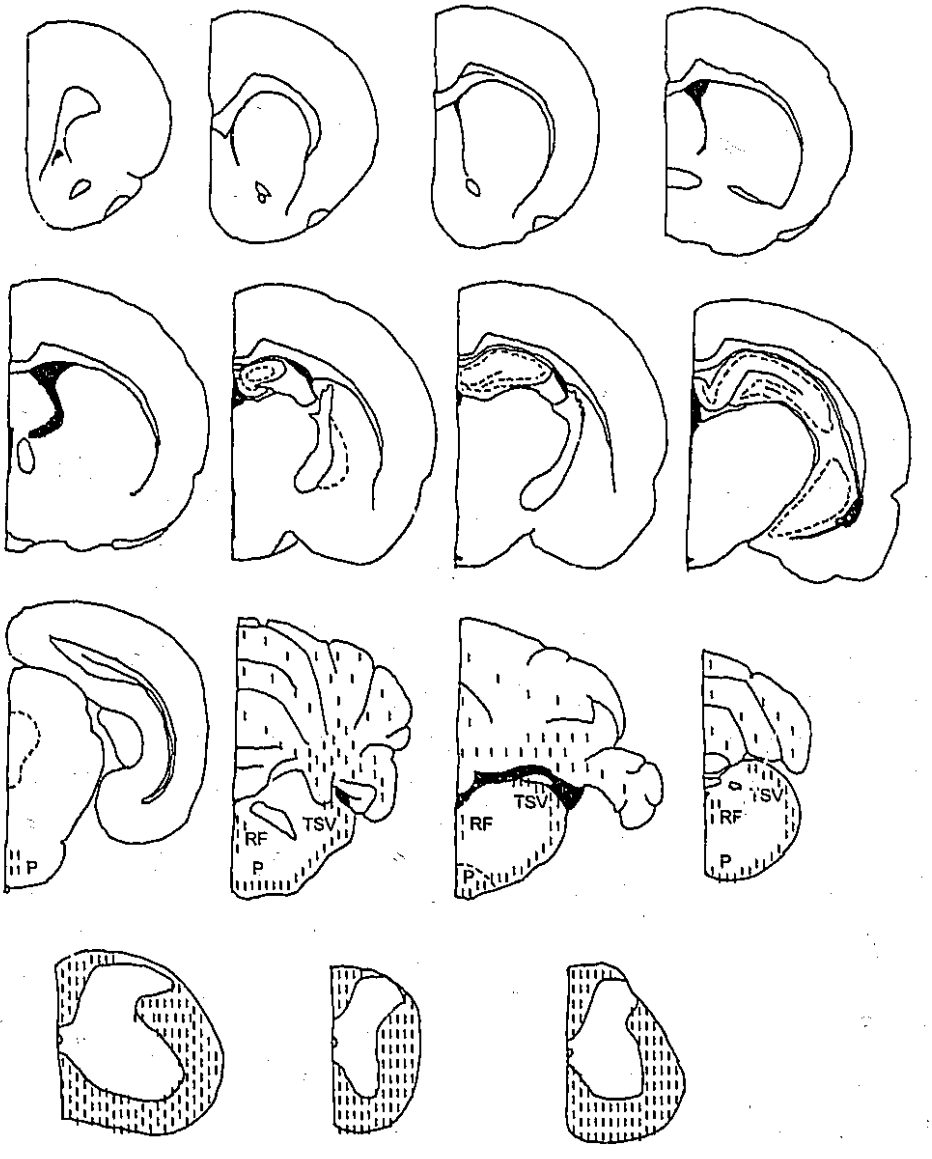
P
RF
TSV
P
RF
TSV
P
RF
TSV
P

Figure 10. Ectopic SP-IR fibers in certain regions of the CNS of 2-month-old transgenic mice. **A** shows ectopic SP-IR fibers in the central white matter of the cerebellum which were arranged at random. Note also the particularly thick fiber bundles in the cerebellar cortex. **B** illustrates the enlargement of the framed area in **A**, note numerous varicosities (arrow) clustered along the fiber bundle. **C** shows transversely oriented ectopic SP-IR fibers in the white matter of the pons; note the branches of the fibers (arrow) crossing the midline. **D** shows ectopic SP-IR fibers in the white matter of the medulla oblongata. Scale bars = 100 μm.

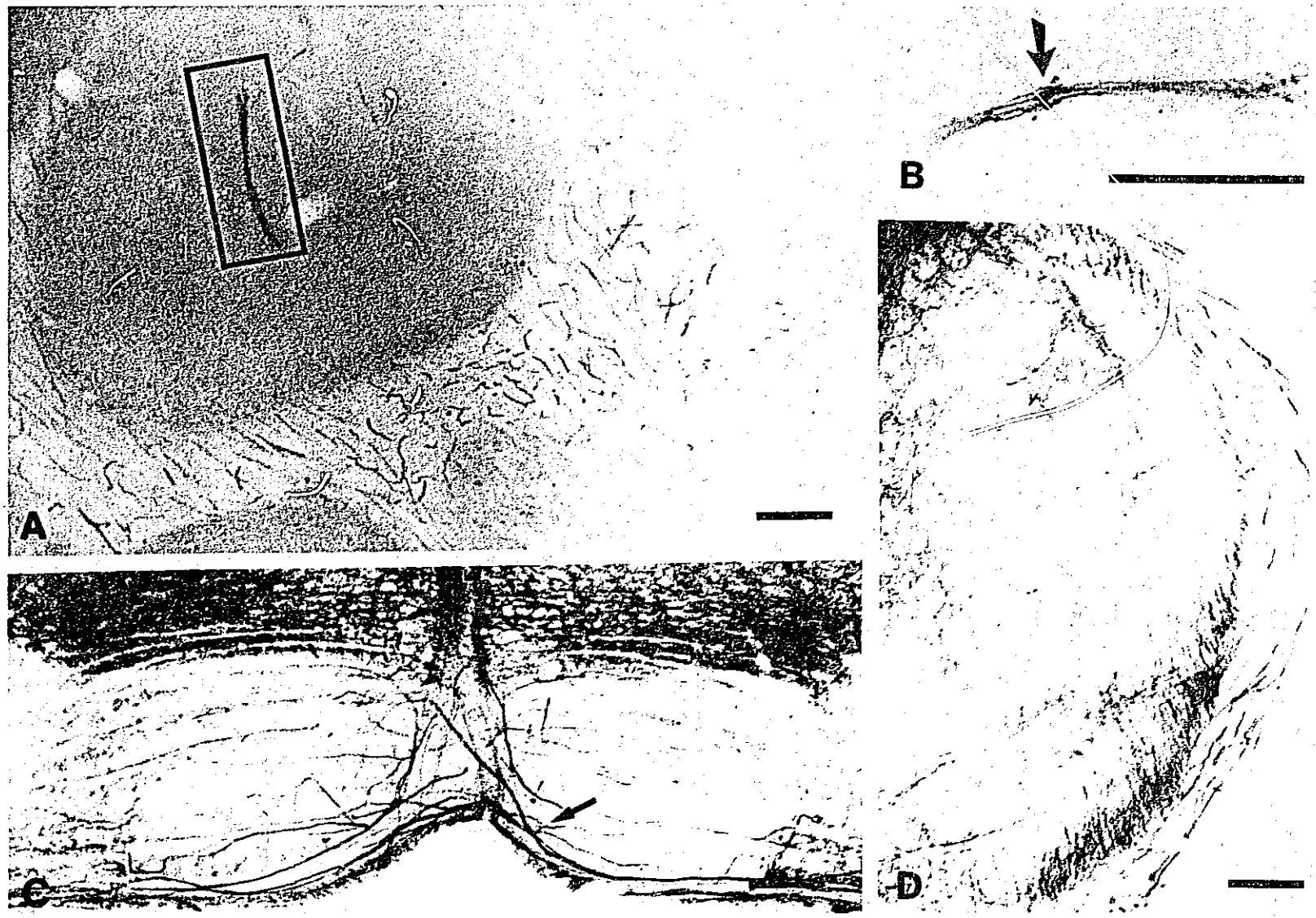
A
B
C
D

Figure 11. Detection of SP-IR fibers in the white matter of the spinal cord of both transgenic mice (**B**, **D** and **F**) and controls (**A**, **B** and **E**) during the early postnatal period. Note abundant SP-IR fine fibers in the spinal cord of newborn transgenic and control mice. The immunostaining was more intense in transgenic specimens (**B**, **D** and **F**) than in controls (**A**, **C** and **E**). SP-IR fibers were present in the white matter of day 0 and day 2 transgenic and control animals. At day 5, SP-IR fibers were almost undetectable in the white matter of the control mouse (**E**), but had increased markedly in number and thickness in the transgenic mouse (**F**). Scale bars = 100 μm.

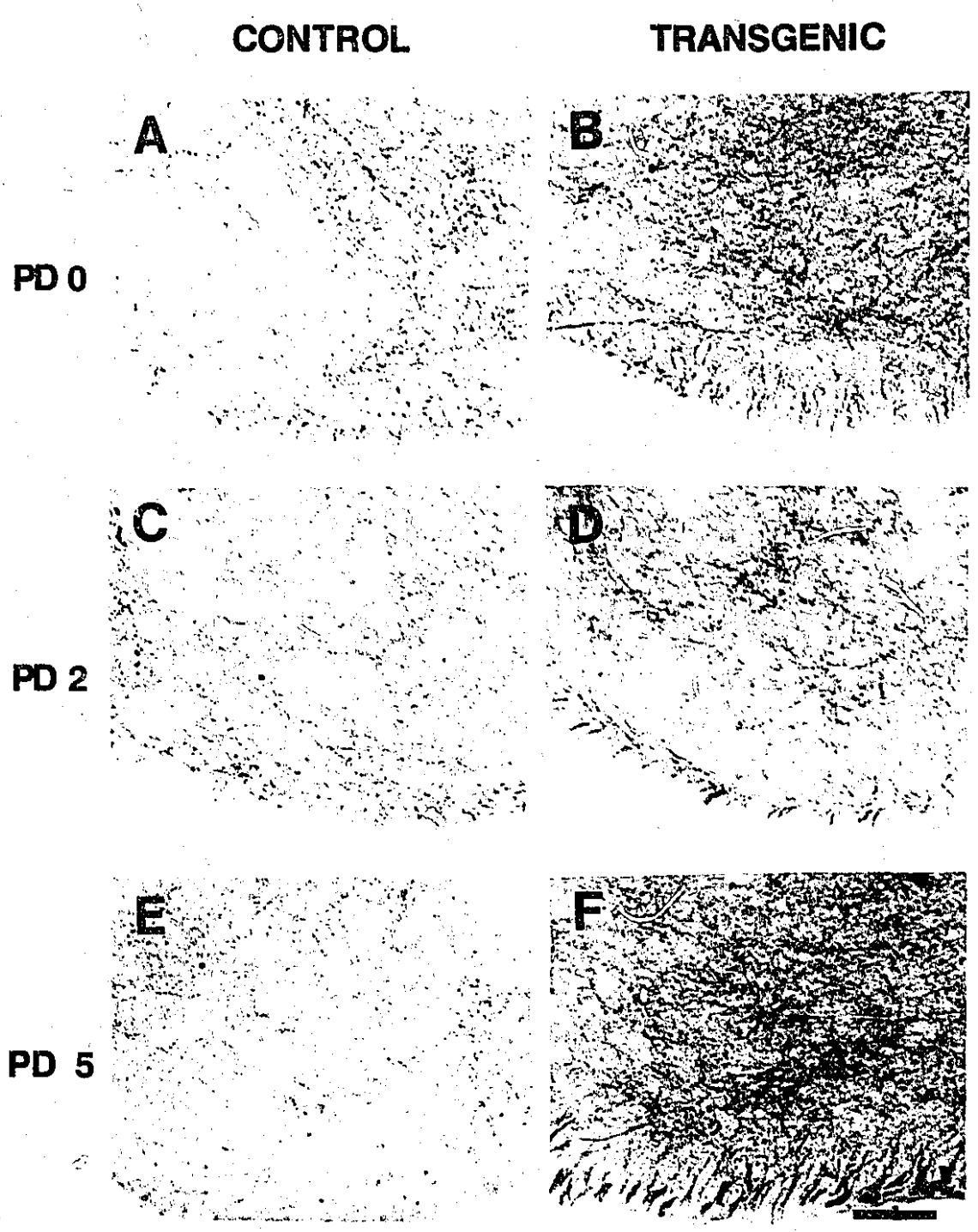
CONTROL
TRANSGENIC
A
B
PD 0
C
D
PD 2
E
F
PD 5

Figure 12. Quantification of ectopic SP-IR fibers in the white matter of the spinal cord of transgenic and control mice in the early postnatal period. The number of intersections of SP-IR fibers with the periphery of the cervical and thoracic spinal cord of transgenic mice at postnatal day 0 and 2 did not differ significantly from controls ($P>0.5$, Student's t-test, mean±SEM, n=5). However, the values in transgenic mice at postnatal day 5 and 10 were significantly higher than in controls (*$P<0.001$, Student's t-test, mean±SEM, n=5).

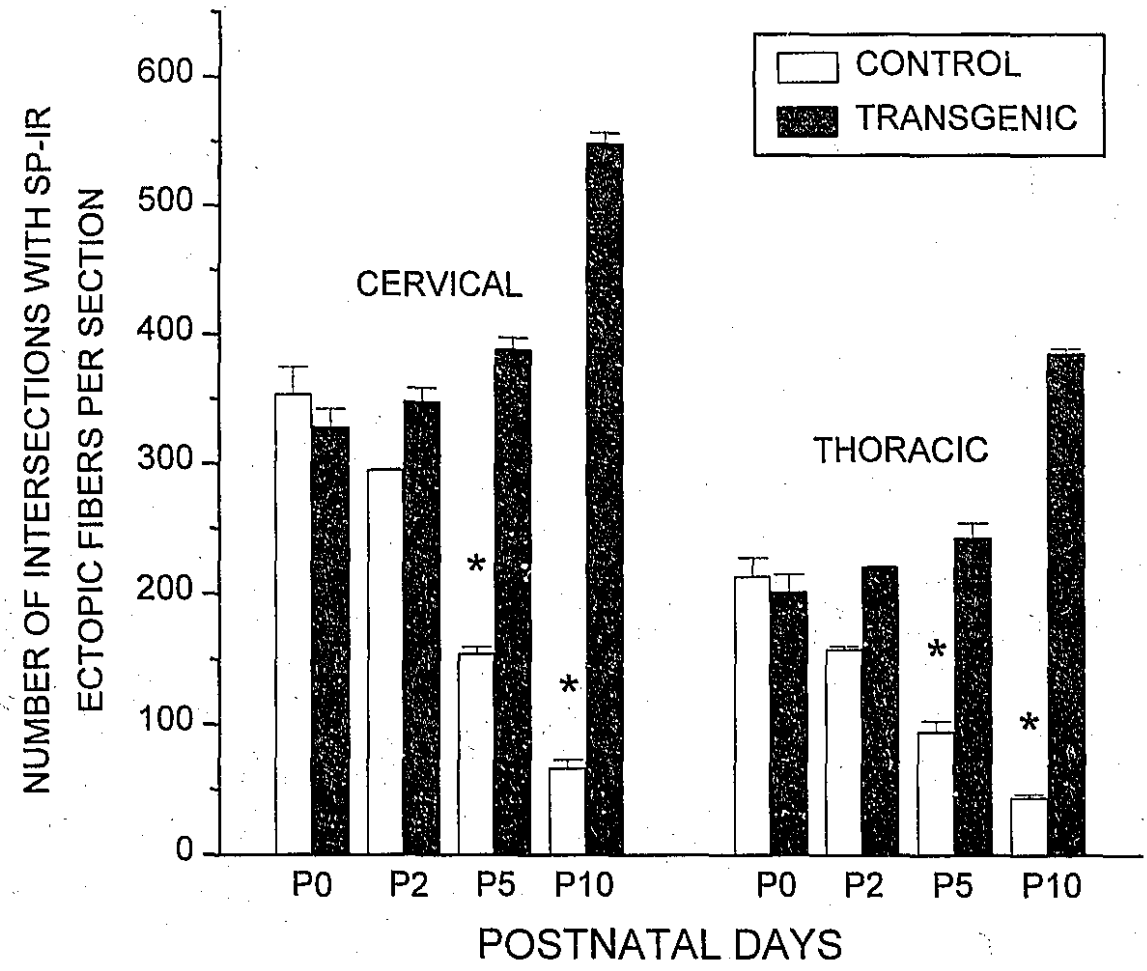
CONTROL
TRANSGENIC
NUMBER OF INTERSECTIONS WITH SP-IR ECTOPIC FIBERS PER SECTION
600
500
400
300
200
100
0
CERVICAL
THORACIC
*
*
*
*
P0
P2
P5
P10
P0
P2
P5
P10
POSTNATAL DAYS

Figure 13. Quantification of ectopic SP-IR fibers in the white matter of the cervical and thoracic spinal cord of transgenic mice at different age groups. The number (mean±SEM, n=5) of intersections of SP-IR fibers with the periphery of the cervical and thoracic spinal cords were counted. These fibers were detected as early as postnatal day 0 and increased gradually in numbers afterwards. The fibers reached the adult level by day 20.

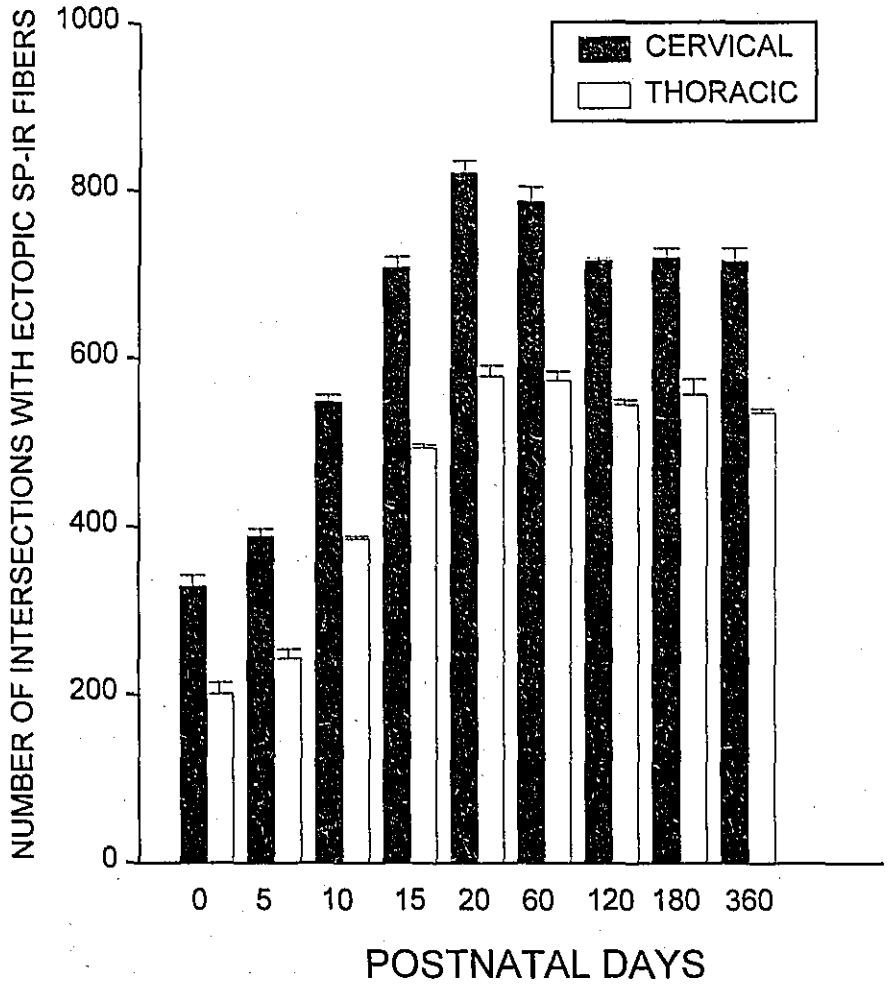
NUMBER OF INTERSECTIONS WITH ECTOPIC SP-IR FIBERS
1000
800
600
400
200
0
CERVICAL
THORACIC
0
5
10
15
20
60
120
180
360
POSTNATAL DAYS

Figure 14. SP-IR cells in the cervical DRG and trigeminal ganglia of 3-month-old transgenic mice (**B** and **D**) and age-matched controls (**A** and **C**), showing the more intense staining of those from transgenic mice over controls. Note the darker staining of small cells in transgenic specimens (arrows in **B** and **D**). Scale bars = 25 μm.

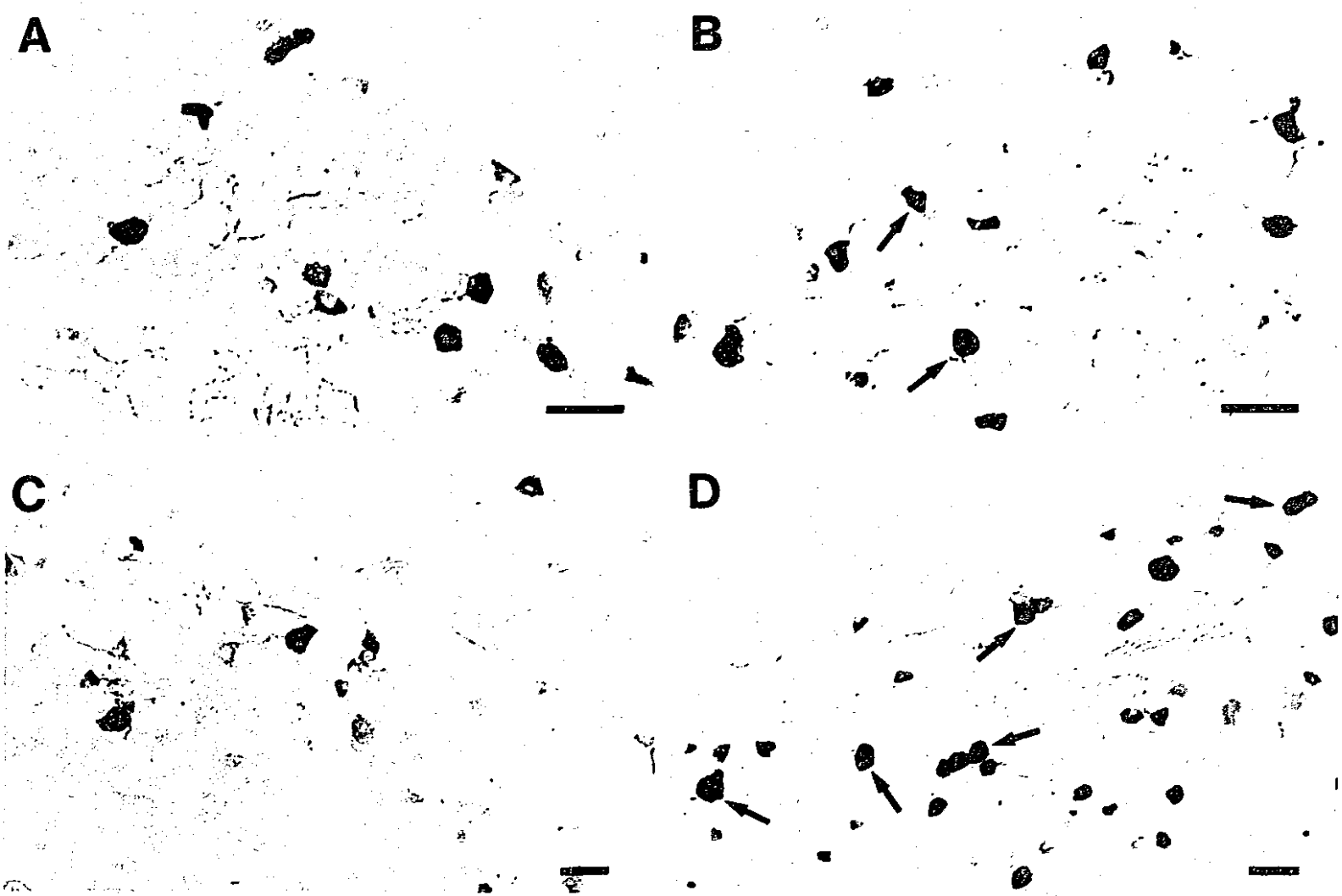
A
B
C
D

Figure 15. Percentages of SP-IR cells in the cervical and lumbar DRG and the trigeminal ganglia of transgenic mice and controls. Values in transgenic mice were significantly higher than in controls. * $P< 0.01$, Student's t-test, mean±SEM, n=4.

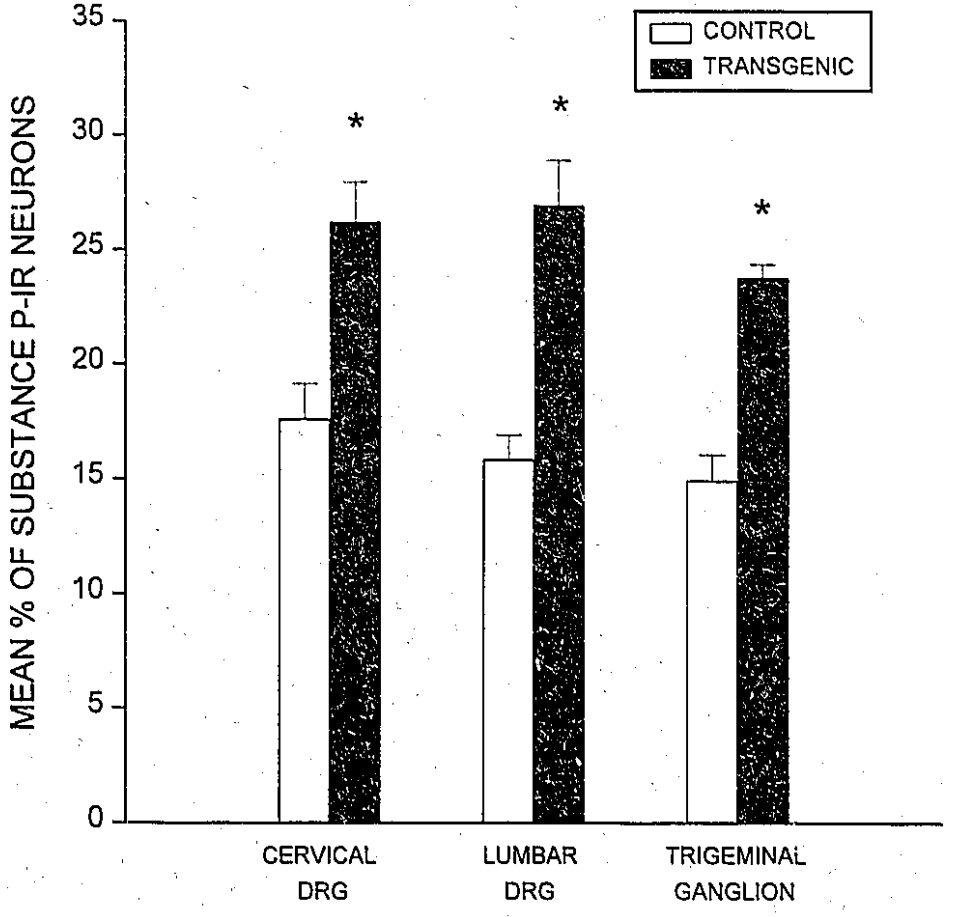
CONTROL
TRANSGENIC
MEAN % OF SUBSTANCE P-IR NEURONS
35
30
25
20
15
10
5
0
*
*
*
CERVICAL DRG
LUMBAR DRG
TRIGEMINAL GANGLION

Figure 16. Size frequency distribution analysis of SP-IR cells in the cervical and lumbar DRG and trigeminal ganglia of transgenic mice and controls. The percentages of SP-IR DRG (**B** and **C**) and trigeminal ganglion cells (**A**) of transgenic mice were not significantly different from those in controls ($P>0.5$, Student's t-test, mean±SEM, n=4). Note that most SP-IR neurons in the primary sensory neurons of both transgenic and control mice are within the range of small size group (mean average soma diameters below 15 μm), with only a small portion of SP-IR neurons belongs to the medium size group (mean average soma diameters between 15 and 25 μm). The size frequency distribution pattern of SP-IR cells in the lumbar DRG (**C**) was similar to that observed in trigeminal ganglia (**A**) in both transgenic and control mice.

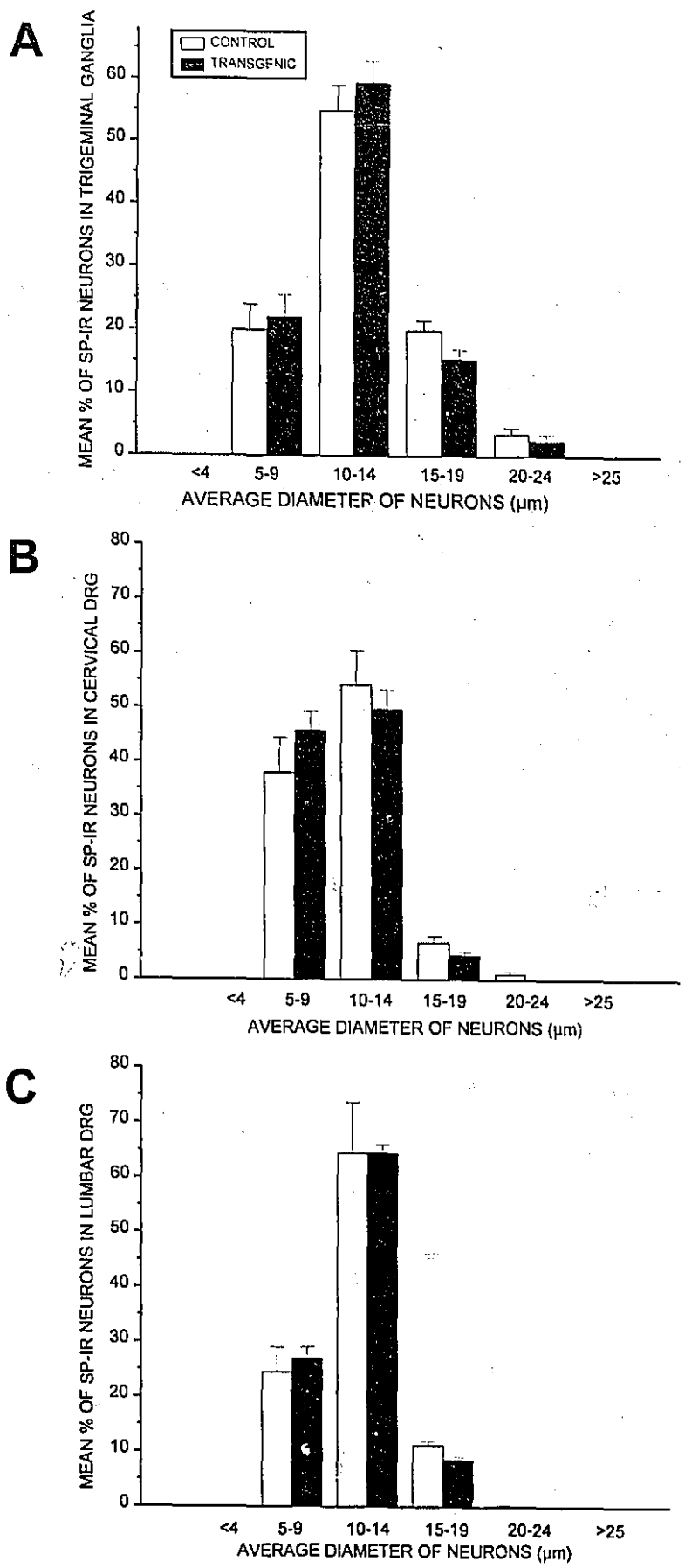
A
CONTROL
TRANSGENIC
MEAN % OF SP-IR NEURONS IN TRIGEMINAL GANGLIA
0
10
20
30
40
50
60
<4
5-9
10-14
15-19
20-24
>25
AVERAGE DIAMETER OF NEURONS (µm)
B
MEAN % OF SP-IR NEURONS IN CERVICAL DRG
0
10
20
30
40
50
60
70
80
<4
5-9
10-14
15-19
20-24
>25
AVERAGE DIAMETER OF NEURONS (µm)
C
MEAN % OF SP-IR NEURONS IN LUMBAR DRG
0
10
20
30
40
50
60
70
80
<4
5-9
10-14
15-19
20-24
>25
AVERAGE DIAMETER OF NEURONS (µm)

Figure 17. Depletion of ectopic SP-IR fibers and SP-IR trigeminal ganglion cells following capsaicin treatment. Ectopic SP-IR fibers in the cerebral cortex (**B**) and the medulla oblongata (**D**) were completely abolished in capsaicin treated 4-month-old transgenic mice. However, these ectopic fibers were still detected in the cerebral cortex (**A**) and medulla oblongata (**C**) of vehicle-treated transgenic mice. Consistently, SP-IR cells in the trigeminal ganglia were considerably reduced in number in a capsaicin-treated 4-month-old transgenic mouse (**F**), compared with a vehicle-treated transgenic mouse (**E**). Scale bars =100 μm.

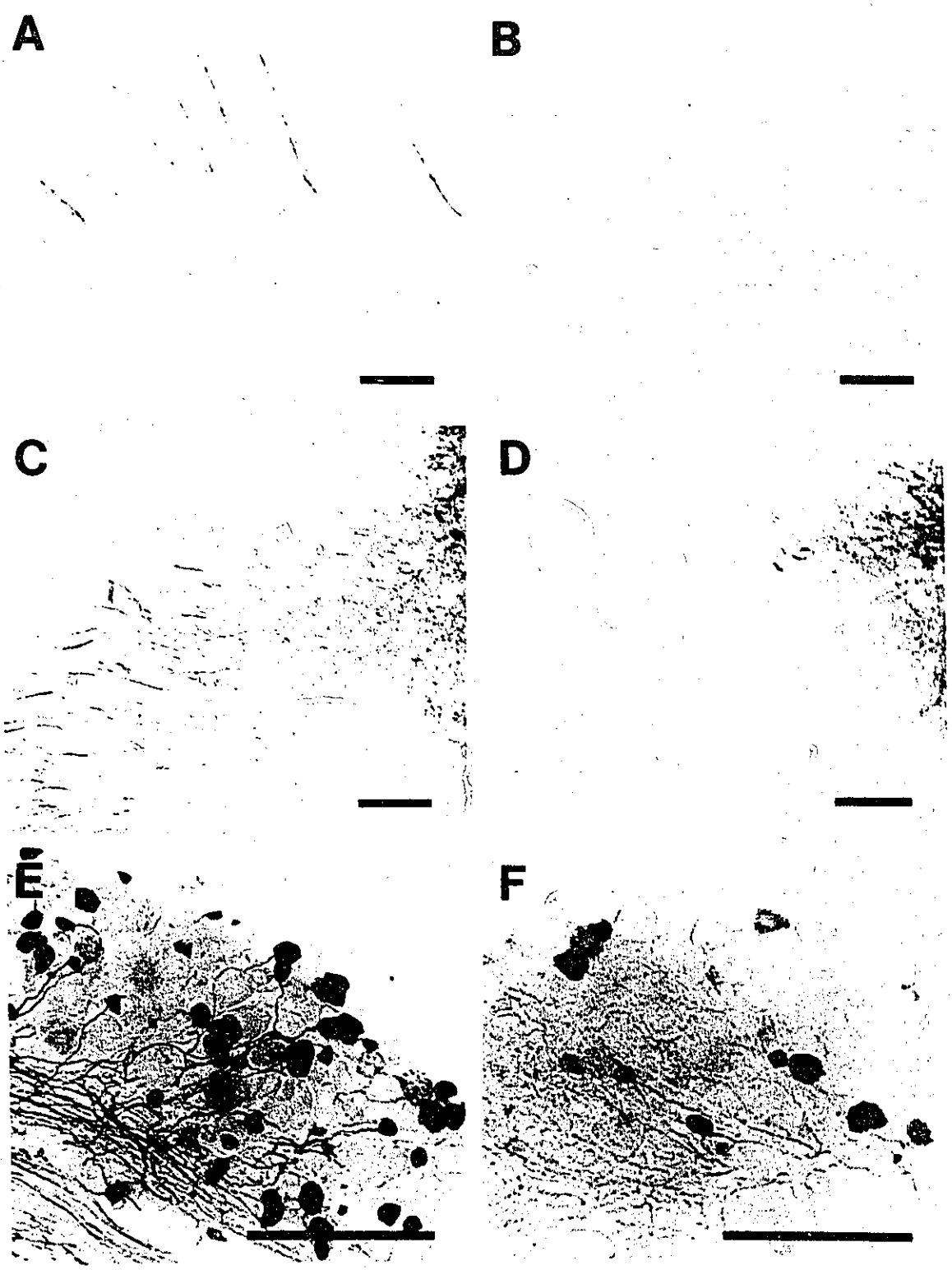
A
B
C
D
E
F

Figure 18. NGF-IR glia-like small cells in the cervical spinal cord and pons of transgenic (**B** and **D**) and control mice (**A** and **C**) at the age of day 5. In **A** and **B** (from the spinal cord), note that these (arrows) possess small cell bodies and a few processes giving rise to multiple thin branches. **C** and **D** show identical NGF-IR cells (arrows) in the pons of transgenic and control mice. In **D**, note that NGF-IR oligodendrocytes (open arrows) in transgenic mice are considerably larger than the small glia-like cells. Scale bar = 25 μm.

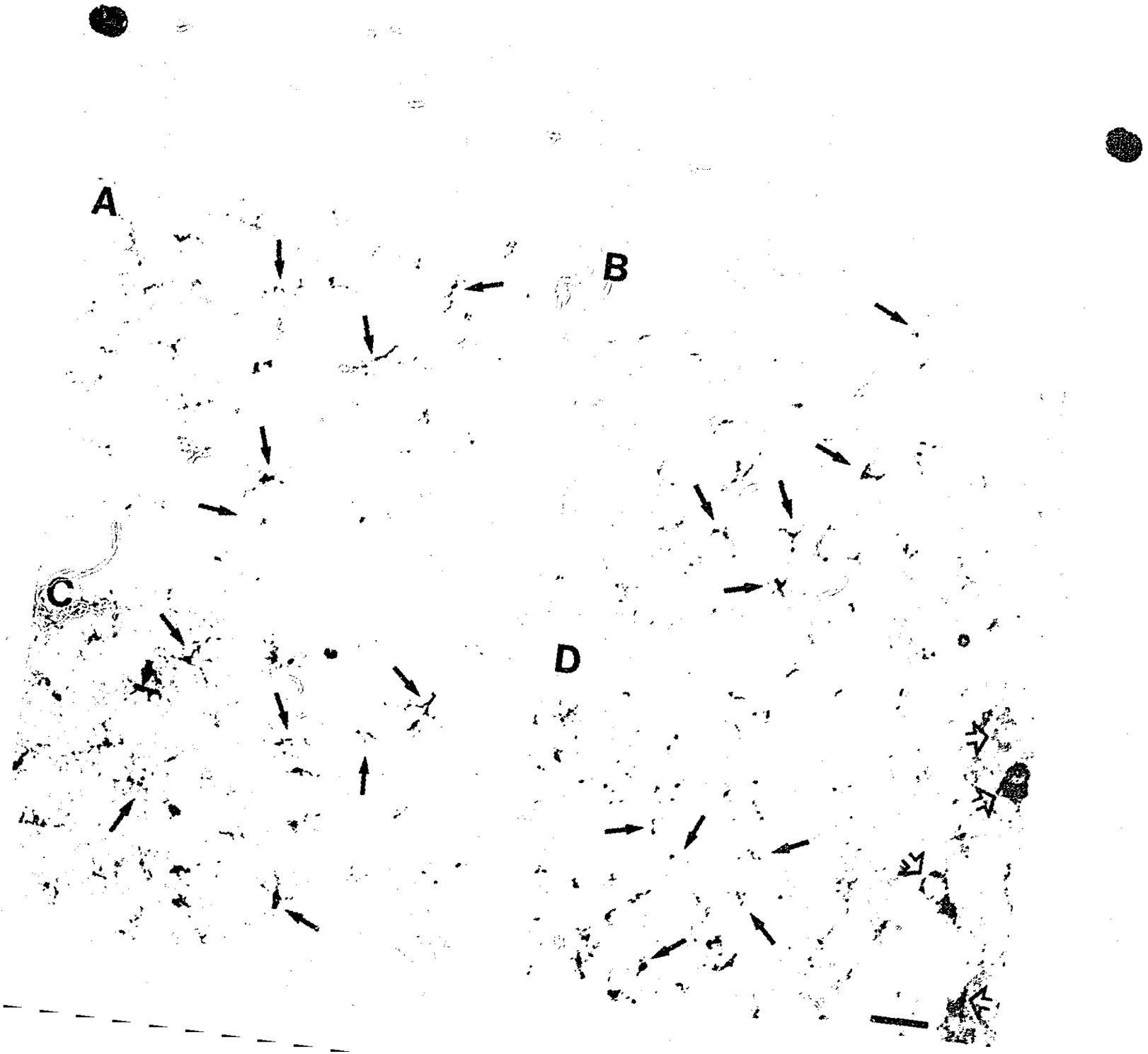
A
B
C
D

Chapter VII

Final discussion

The studies in this thesis dealt with the innervation by SP-IR sensory fibers of CNS target tissues in two experimental models. In the first model, we addressed the issues of how SP-IR axonal terminals are specifically associated with neurons which exhibited a characteristic nociceptive response and how SP-IR axonal terminals interact with CGRP, ENK and GABA in the dorsal horn of the cat spinal cord, under normal physiological conditions. In the second model, we examined the possibility that SP-IR sensory fiber innervation of the central target tissues might be manipulated by the abnormal over-expression of NGF in the CNS of transgenic mice. In this chapter, I will discuss the major findings obtained using the two experimental paradigms and the future studies in which these findings can be integrated. I will also discuss an hypothetic model of the transmission and modulation of nociception in the cat dorsal horn.

I. SP-IR fiber innervation of the dorsal horn of the cat spinal cord

A. *Summary of major findings*

As in a previous study from our laboratory (De Koninck et al., 1992), all nociceptive dorsal horn neurons (nociceptive specific and wide dynamic range) included in this thesis exhibited a characteristic type of nociceptive response, a slow and prolonged depolarization after the end of the noxious stimulation. This nociceptive response was blocked by SP (NK-1) receptor antagonists. Our quantitative data showed that the densities of SP-IR boutons apposed to the cell bodies, proximal dendrites and distal dendrites of nociceptive specific neurons were significantly higher than those of non-nociceptive neurons. The values for the cell body and the proximal dendrite regions

of nociceptive specific neurons were significantly higher than for wide dynamic range neurons, but no significant differences were detected in the distal dendritic region. The values for the proximal and distal dendrite regions of wide dynamic range neurons were significantly higher than those of non-nociceptive neurons, but this was not the case for the cell body region. The percentages of SP-IR boutons apposed to the cell bodies, proximal dendrites and distal dendrites of nociceptive neurons were significantly higher than those of non-nociceptive neurons. Furthermore, the percentages of SP-IR boutons apposed to the three regions of nociceptic specific neurons were significantly higher than those of wide dynamic range neurons. In wide dynamic range neurons, the percentages of SP-IR boutons apposed to the distal dendrites in areas with intense SP immunoreactivity were significantly higher than those located in areas with scarce SP immunoreactivity. In non-nociceptive neurons, the values for the distal dendrites were very low, even in areas of intense SP immunoreactivity. About 30-35% of the SP-IR boutons apposed to nociceptive neurons co-localized CGRP immunoreactivity, indicating that these SP-IR boutons were of primary sensory origin.

Interestingly, all nociceptive specific neurons and most of the wide dynamic range neurons possessed ENK immunoreactivity. However, none of the non-nociceptive neurons were ENK immunoreactive. Axonal boutons co-localizing SP and ENK immunoreactivities (SP+ENK-IR) were apposed to functionally characterized dorsal horn neurons. Quantitatively, the percentages of SP+ENK-IR boutons apposed to the distal dendrites of nociceptive neurons were significantly higher than in non-nociceptive neurons. The percentages of ENK-IR boutons apposed to the cell bodies and the

proximal dendrites of nociceptive neurons were significantly higher than in non-nociceptive neurons; these differences were not detected in the distal dendritic region. Non-nociceptive neurons received a considerable number of ENK-IR only boutons. Both ENK-IR and SP+ENK-IR boutons were never found presynaptic to SP-IR boutons.

For the first time, a co-localization of SP and GABA immunoreactivities in axonal boutons and dendrites in the cat dorsal horn was found. However, this co-localization of SP and GABA was never detected in the rat dorsal horn. SP+GABA-IR boutons were significantly more numerous in lamina I than in other laminae. SP+GABA-IR boutons established synapses with either SP-IR or non-IR dendrites. The synapses thus formed were exclusively symmetric.

B. *A putative model of nociception transmission and modulation by SP, CGRP, ENK and GABA in the dorsal horn of the cat spinal cord*

Based on the findings from previous studies of our group and those included in this thesis, it can be concluded that in the dorsal horn SP fibers innervate specifically neurons which exhibit a characteristic type of nociceptive response. This finding provides direct anatomical and physiological evidence that SP is a neurotransmitter in the first central synapse of pain pathways. Our data enriched current available literature [for review see, (Otsuka and Yoshioka, 1993)].

It has been previously reported that in cat, 80% (Garry et al., 1989) or even 100% (Gibson et al., 1984) of SP-containing DRG cells co-localized CGRP, and also

that many axonal boutons in the dorsal horn co-localized SP and CGRP (Plenderleith et al., 1990; Tuchscherer and Seybold, 1989). Functionally, CGRP potentiated the nociceptive effects elicited by SP in behavioral tests (Wiesenfeld-Hallin et al., 1984; Woolf and Wiesenfeld-Hallin, 1986). Here, we provide the first direct evidence that the axonal boutons co-localizing SP and CGRP are presynaptic to nociceptive dorsal horn neurons. This finding indicates that a considerable number of the SP-IR boutons originate from primary sensory afferents.

Multiple dorsal rhizotomies resulted in a dramatic reduction of opioid receptor binding sites in the superfical layers of the dorsal horn (LaMotte et al., 1976). Also, opoid receptor mRNAs have been detected in DRG neurons using *in situ* hybridization (Maekawa et al., 1994; Minami et al., 1995). These findings indicated that a substantial number of opioid receptors are localized in primary sensory afferents and that opioid peptides may act directly on these afferents. However, ENK-IR boutons were never found to be presynaptic to SP-IR axons (Cuello, 1983; Ribeiro-da-Silva et al., 1991b). Rather, a high number of axodendritic synapses in which the presynaptic axonal terminals were ENK immunoreactive has been detected (Ribeiro-da-Silva et al., 1991b). Therefore, these findings indicate that opioid peptides might inhibit nociception mainly through a postsynaptic mechanism. In this thesis, the finding that nociceptive dorsal horn neurons contained ENK and received synapses from both ENK-IR and SP+ENK-IR boutons lends considerable support to the theory of a postsynaptic mechanism in the enkephalinergic modulation of nociception. Some ENK-IR boutons were detected apposed to non-nociceptive dorsal horn neurons, indicating that ENK might also play

other functional roles besides modulation of nociception.

The detection of a co-localization of SP and GABA immunoreactivities in the axonal boutons in the superficial laminae of the spinal dorsal horn of cat but not rat further contributes to the concept that the modulation in the dorsal horn is extremely complex. In a preliminary study not included in this thesis, we found that some of these boutons co-localizing SP and GABA were apposed to nociceptive neurons, but not to non-nociceptive neurons (Ma et al., 1994). It is interesting to note that both SP+GABA-IR and GABA-IR boutons were never found to be presynaptic to SP-IR boutons. The above findings indicate that, similar to ENK, GABA might modulate SP mediated nociception, mainly through a postsynaptic mechanism.

Based on results obtained using the first experimental paradigm, a hypothetical model is proposed here for the transmission and modulation of nociception in the dorsal horn of the cat spinal cord.

Following the activation of the peripheral nociceptors by noxious stimuli, the noxious information is conveyed by small diameter (Aδ and C) primary sensory fibers to the dorsal horn. This leads to the release of glutamate, SP and CGRP from the central terminals of primary sensory fibers (Battaglia and Rustioni, 1988; De Biasi and Rustioni, 1988; Merighi et al., 1991). The released glutamate excites nociceptive dorsal horn neurons, resulting in an initial fast and brief depolarization (Yoshimura and Jessell, 1989), followed by a second phase of slower responses mediated by the sensory peptides, particularly if the noxious stimulation persists in the peripheral tissue. The component mediated by SP will become prominent in the second phase, represented by

a slow and prolonged depolarization after the end of the noxious stimulus. As wide dynamic range neurons also receive synaptic input from innocuous primary sensory fibers, non-noxious stimulation probably influences the nociceptive transmission of wide dynamic range neurons, as stated by the pain theories of Melzack and Wall (1965) and Cervero and Iggo (1978).

The nociceptive neurons may be divided into several types, of which I will focus on two. The first type comprises cells located mostly in lamina I, which are non-ENK-IR and project their axons to supraspinal structures (mainly to the thalamus) (Ruda, 1986). These cells probably contain excitatory amino acids such as glutamate. The second type of nociceptive neuron is likely the one that we detected more frequently in our studies and represents mostly enkephalinergic cells, either interneurons or, less frequently, projection neurons. Some of the cells of the second type may co-localize ENK and SP. The fact that we detected mostly nociceptive neurons which were enkephalinergic may indicate that the second type of cells is more abundant than the first type, an hypothesis that is in agreement with the fact that, even in lamina I, most of the neurons are interneurons (Light et al., 1979; Cervero et al., 1979).

We can speculate that the ENK contained in the second type of nociceptive neurons is released locally to affect the responsiveness of the nociceptive non-enkephalinergic projection neurons to nociceptive information. However, some of the ENK-IR nociceptive neurons could also be projection neurons (Coffield and Miletic, 1987b; Coffield and Miletic, 1987a), thus exerting their inhibitory effects at higher levels in the pain pathways. But more likely, GABA-IR and ENK-IR interneurons,

through their local axonal terminals, exert a fast and a slow inhibitory effect, respectively, on nociceptive neurons. SP+ENK-IR and SP+GABA-IR interneurons play a role of fine tuning, through the release of SP or, respectively, ENK or GABA, to either enhance or inhibit the transmission of nociception. Finally, as a result of all the above interactions, the transmission and inhibition of nociception will be well balanced to adapt to the interior and exterior environments.

C. *Integration of current results into future studies*

1. Correlation of the intensities of SP elicited nociceptive responses with the amount of SP boutons apposed to nociceptive neurons.

Our data suggest that nociceptive neurons with strong nociceptive responses receive higher numbers of SP-IR boutons than those with moderate nociceptive responses. However, the data is not yet conclusive. Further studies are needed to correlate the intensity of the nociceptive responses of nociceptive specific and wide dynamic range neurons with the number of synapses received from SP-IR boutons apposed to them. If possible, the intensity of peripheral noxious stimuli should be directly correlated with the intensity of the nociceptive responses and the amount of SP-IR boutons apposed to nociceptive neurons. Elucidation of this issue will provide insights into the mechanisms underlying the transmission of nociception mediated by SP in the dorsal horn.

2. Examination of the correlation of NK-1 receptor immunoreactivity with SP

immunoreactivity in relation to functionally characterized dorsal horn neurons.

As mentioned in the general introduction, recent immunocytochemical studies (Bleazard et al., 1994; Liu et al., 1994; Littlewood et al., 1995; Brown et al., 1995) demonstrated that NK-1 receptor immunoreactivity was present in lamina I and in deeper laminae, but was scarce in lamina II. Moreover, using a monoclonal antibody against the NK-1 receptor in a double immunostaining at the EM level, a study showed that SP-IR boutons were seldomly found apposed to NK-1 receptor-IR neurons in the rat dorsal horn (Liu et al., 1994). In our studies, we found that the number of SP-IR boutons received by nociceptive neurons was correlated with the location of the dendritic arborization of the cell. The dendrites of nociceptive neurons which were located in laminae I, II and V, areas rich in SP immunoreactivity (Hökfelt et al., 1975a; Cuello et al., 1978; Ruda et al., 1986), received significantly higher percentages of SP-IR inputs than those located in other laminae. Also, our data favor the idea that SP exerts its effects at synaptic sites. In fact, about one third of all SP-IR boutons exhibited a synapse with the cells, a proportion which was identical to that of non-immunoreactive boutons. Therefore, it is very important to investigate whether the nociceptive neurons which receive higher numbers of SP-IR boutons contain NK-1 receptor immunoreactivity. To overcome the dense DAB reaction product after HRP filling, lucifer yellow will be injected intracellularly (instead of HRP) as described in a recent report (Branchereau et al., 1995). This protocol includes the use of an antibody against lucifer yellow, followed by a secondary antibody labeled with 1 nm gold, and by silver intensification. This protocol will allow us to combine our study with DAB-based

immunocytochemistry for the detection of NK-1 receptor antigenic sites. The two signals should be easy to distinguish, as the silver-gold particles indicate the intracellularly labeled cell, and the DAB precipitates the NK-1 receptor antigenic sites. SP antigenic sites can be detected subsequently using post-embedding immunogold staining.

3. Differentiation of nociceptive neurons with predominant SP-IR primary sensory fiber innervation and those in which SP-IR intrinsic fiber innervation prevails

As mentioned above, CGRP immunoreactivity in the dorsal horn originates exclusively from primary sensory afferents, as shown in studies using dorsal rhizotomies (Traub et al., 1989; Chung et al., 1988) and *in situ* hybridization (Réthelyi et al., 1989). The co-localization of SP and CGRP in axonal boutons in the dorsal horn can be used as a marker for SP-IR boutons of primary sensory origin. In contrast, ENK immunoreactivity in the dorsal horn originates mostly from intrinsic dorsal horn neurons, since thoracic spinal cord transection caused only a negligible reduction of ENK immunoreactivity in the lumbar dorsal horn (Seybold and Elde, 1982). Also, ENK was found to frequently co-localize with SP in the dorsal horn (Senba et al., 1988; Ribeiro-da-Silva et al., 1991b). Therefore, the co-localization of SP and ENK in axonal boutons in the dorsal horn can be used as a maker for SP-IR boutons of intrinsic origin. It will be interesting to determine: 1. whether nociceptive dorsal horn neurons which predominantly receive synapses from SP+CGRP-IR boutons are physiologically different from those which predominantly receive contacts from SP+ENK-IR boutons;

2. whether nociceptive projection neurons receive a predominance of synapses from SP+CGRP-IR boutons or from SP+ENK-IR boutons.

4. Association of axonal boutons co-localizing SP and GABA with nociceptive dorsal horn neurons.

We detected for the first time that SP and GABA are co-localized in axonal boutons in the dosal horn of cat, but not rat, spinal cord. Furthermore, in a preliminary study (Ma et al., 1994) not included in this thesis, axonal boutons co-localizing SP and GABA were found apposed to nociceptive neurons. Therefore, it is important to quantitate the GABA-IR and SP+GABA-IR boutons apposed to the three functional types of dorsal horn neuron. This study will hopefully provide novel information regarding the modulation of nociceptive neurons by a classic neurotransmitter (GABA). ENK was found to co-localize with GABA in some dorsal horn neurons in lamina II and III (Todd et al., 1992). As our studies found that SP co-localized with ENK or GABA in axonal boutons presynaptic to nociceptive neurons, it is possible that SP, ENK and GABA might be co-localized in axonal boutons apposed to nociceptive neurons. The elucidation of this issue will help us to better understand the interactions of excitatory and inhibitory neurotransmitters in the modulation of nociception in the dorsal horn.

II. SP-IR fiber innervation of the white matter of transgenic mice which over-express NGF in myelinating oligodendrocytes

A. *Summary of major findings*

In transgenic mice which bear a chick NGF cDNA driven by a MBP promoter, NGF-IR oligodendrocytes were found in the following regions: at the forebrain level, in the caudate-putamen and corpus callosum; at the brainstem level, in the reticular nuclei of the thalamus, trigeminal spinal tracts, pyramidal tracts, reticular nuclei of brainstem and cochlear nuclei; in the central white matter of the cerebellum and the cerebellar cortex; and in the white matter of the spinal cord. In our time course study, we observed NGF-IR oligodendrocytes as early as postnatal day 0. Then, they increased substantially in number and reached a plateau by day 10. After day 20, these cells decreased gradually in number and completely disappeared by the age of postnatal 2 months. From day 0 to day 5, NGF-IR fiber-like structures were detected in the white matter of the CNS of transgenic mice. Under the electron microscope, these NGF-IR fiber-like structures were characterized as small unmyelinated fibers surrounded by NGF immunoreactivity. Some of these small unmyelinated fibers were characterized as SP-IR or CGRP-IR following double immunostaining. Interestingly, during the early neonatal period, small NGF-IR glia-like cells were observed in the CNS of both transgenic and control mice. These small NGF-IR glia-like cells decreased in number from day 0 to day 10 and were not seen by postnatal day 15.

From day 0 to day 2, SP-IR fibers were detected in the white matter of the pons, medulla oblongata, cerebellum and spinal cord of both transgenic mice and controls. However, SP immunostaining was considerably more intense in transgenic mouse specimens than in controls. These SP-IR fibers decreased dramatically in number in control mice and by day 5 they were not detected. In contrast, SP-IR fibers increased

significantly in transgenic mice from day 0 onwards. By day 5, they became the thick bundles of ectopic fibers in the white matter of transgenic mice. These ectopic SP-IR fiber bundles reached the adult level by day 20, and kept the same level until the age of 12 months (the oldest age examined). At the EM level, these ectopic SP-IR fibers were characterized as bundles of small unmyelinated SP-IR fibers, which displayed boutons with synaptic vesicles. These SP-IR boutons formed synapses with dendrites in the white matter. The SP-IR fibers and boutons co-localized CGRP immunoreactivity. After capsaicin treatment, all the ectopic SP-IR fibers were abolished from the white matter of adult transgenic mice. In adult transgenic mice, the percentages of SP-IR neurons in primary sensory ganglia were significantly higher than in controls. In spite of the increased numbers, the size distribution of SP-IR cells in the dorsal root ganglia of transgenic mice was the same as in controls. In short, most of these SP-IR cells were of small size.

B. *Possible future studies using this transgenic mouse model*

1. Experimental model for pain perception.

As discussed in chapter VI, it is likely that the over-availability of NGF in the white matter of trangenic mice during early the postnatal period induced the normally occurring SP-IR fibers to sprout, thus forming thick ectopic SP-IR fiber bundles in the white matter. The interpretation of these data would be in agreement with the concept established by numerous studies [for review see (Black et al., 1990)], namely that, in addition to fostering connectivity during development, NGF and other neurotrophic

factors are required for the maintenance of pathways and their components during maturity. Primary sensory neurons, in response to NGF over-expression in the white matter of the CNS, were likely induced to synthesize higher amounts of SP and CGRP. The functional consequences from these changes in the transmission and perception of nociception remain to be determined. NGF itself is known to cause hyperalgesia (Lewin et al., 1993), through multiple mechanisms, including mast cell degranulation (Stead et al., 1987), nociceptor stimulation following proteolytic cleavage (Miaskowski et al., 1991), and, possibly, through an effect on the production of peptides in DRG neurons (Wong and Oblinger, 1991; Donnerer et al., 1992; Verge et al., 1995). It will be interesting to find out if these transgenic mice display any hyperalgesia, particularly in the age group from day 0 to 2 months, a period in which NGF-IR oligodendrocytes were detected in the white matter of the CNS. In older transgenic mice, it will be meaningful to determine if there is any alteration in pain perception, since ectopic SP-IR sensory fibers continue to exist independently of NGF over-expression.

2. Experimental models for the *in vivo* study of neurotrophic effects of NGF on basal forebrain cholinergic neurons.

There is overwheming experimental evidence for a neurotrophic role of NGF in adult and aging basal forebrain cholinergic neurons [for reviews, see (Hefti et al., 1989; Hefti et al., 1993)]. Basal forebrain cholinergic neurons react to NGF with an increase in the enzyme responsible for acetylcholine production, choline acetyltransferase (ChAT) (Gnahn et al., 1983; Hefti et al., 1984; Thoenen and Barde, 1980). In our

transgenic mice, numerous NGF-IR oligodendrocytes were observed in the caudate-putamen from postnatal day 10 to 20. These NGF-IR oligodendrocytes in the striatum may be used as natural pumps to administer NGF endogenously. Therefore, it will be interesting to examine ChAT immunostaining of the basal forebrain cholinergic neurons in these transgenic mice, and to determine behaviorally whether these transgenic mice are different from controls in the capability of memorizing and learning, particularly after lesions. This model may present several advantages over the one currently used in the rat which requires the administration of NGF via minipump [for reviews see (Hefti et al., 1989; Hefti et al., 1993; Cuello et al., 1990)]. In fact, the supply of NGF in these transgenic mice is continuous. Indeed, NGF-IR neurons, which were likely cholinergic neurons (Hu et al., 1994), in the septal nuclei and nucleus basalis of day 10 and day 20 transgenic mice were considerably increased in number and size when compared with age-matched controls (Ma et al., unpublished observations).

3. Experimental models for neural regeneration in transected spinal cord

Studies on the regeneration of the lesioned spinal cord are of great clinical importance and have drawn considerable attention in recent years. Neurotrophic factors are thought to be involved in the regeneration and sprouting of pathway tracts in the CNS. However, regeneration of long neural pathways in the CNS is usually very restricted because of the occurrence of myelin-associated inhibitory molecules produced by oligodendrocytes [for reviews see, (Schwab, 1990; Schwab et al., 1993)]. Therefore, results have been very limited to date, as no much regeneration has been achieved. A study (Schnell et al., 1994) has shown that a single injection of NT-3 or NGF induced

the collateral sprouting of the transected corticospinal tract, and that some fibers grew for some distance past the lesion point, representing a true regeneration. To further elucidate this issue, our transgenic mice provide an excellent experimental model, as NGF-IR oligodendrocytes were observed in the white matter of the spinal cord from postnatal day 0 to 2 months and may be used as a natural source of high concentrations of NGF. It is possible that neurotrophins, in concentrations higher than those achieved via injection of exogenous neurotrophic factors, may overcome the inhibitory effects of myelin-associated inhibitors on the regeneration of axons in the CNS. Therefore, it would be interesting to examine whether the corticospinal tracts of transgenic mice sprout and regenerate following spinal cord transection and how significant such sprouting and regeneration may be.

III. General conclusions

The current thesis project studied SP-IR sensory fiber innervation in CNS targets in two experimental models. In the first model, SP-IR boutons innervated nociceptive neurons in significantly higher number than non-nociceptive neurons in the dorsal horn of the cat spinal cord. We also found that a considerable number of such SP-IR boutons were of primary sensory origin as they co-localized CGRP immunoreactivity. In contrast, other SP-IR boutons co-localizing ENK immunoreactivity were very likely from dorsal horn intrinsic neurons. The preferential innervation of nociceptive neurons by SP-IR boutons seemed to be proportional to the specificity and intensity of the nociceptive response, as wide dynamic range neurons with moderate nociceptive

responses were less innervated than both wide dynamic range neurons with strong nociceptive response and nociceptive specific neurons. Boutons co-localizing SP and GABA immunoreactivities were detected in the dorsal horn of cat, but not rat, spinal cord, a finding that indicates species differences in the modulation of nociception. These findings provide anatomical substrates for the transmission and modulation of nociception in the dorsal horn of the cat spinal cord. In the second experimental model, ectopic SP-IR sensory fibers innervated the white matter of the CNS of transgenic mice which over-produced NGF in myelinating oligodendrocytes. These ectopic SP-IR sensory fibers might be involved in nociception, an issue which needs further experiments to elucidate.

LIST OF CONTRIBUTIONS TO ORIGINAL KNOWLEDGE

1. Significantly higher numbers of SP-IR boutons were apposed to nociceptive neurons than to non-nociceptive neurons in the dorsal horn of cat spinal cord. Nociceptive specific neurons received significantly higher numbers of SP-IR boutons than wide dynamic range neurons. In wide dynamic range neurons, the distal dendrites located in areas rich in SP immunoreactivity received significantly higher numbers of appositions from SP-IR boutons than those located in areas with scarce SP immunoreactivity. About 33% of SP-IR boutons apposed to nociceptive neurons co-localized CGRP immunoreactivity.

2. Most nociceptive neurons included in our studies were ENK-IR, and received significantly higher numbers of SP+ENK-IR boutons in the distal dendrites than non-nociceptive neurons. Nociceptive neurons received significantly higher numbers of ENK-IR boutons in the cell bodies and proximal dendrites than non-nociceptive neurons, but this difference was not detected in the distal dendrites.

3. SP and GABA immunoreactivities were co-localized in axonal boutons and dendritic profiles in the superficial laminae, particulary lamina I, of the dorsal horn of cat, but not rat, spinal cord. Such SP+GABA-IR boutons were presynaptic to SP-IR or non-IR dendritic profiles. The synapses thus formed were always symmetric.

4. From postnatal day 0 to 2 months, NGF-IR oligodendrocytes were observed in the white matter of the CNS of transgenic mice which carried a chick NGF cDNA driven by a 1.3 kb MBP promoter. NGF-IR fiber-like structures were detected in the white matter of the CNS of transgenic mice at the ages from postnatal day 0 to day 5. At the EM level, these structures were characterized as small unmyelinated fibers surrounded by NGF immunoreactivity. Some of these unmyelinated fibers contained SP or CGRP immunoreactivities. Small NGF-IR glia-like cells were found in the CNS of both transgenic and control mice from day 0 to day 10.

5. SP-IR fibers were detected in the white matter of the CNS in both transgenic and control mice from postnatal day 0 to day 2. However, these SP-IR fibers disappeared in controls by day 5 and increased in number and thickness in transgenic mice, thus forming ectopic fibers which were present throughout adulthood. At the EM level, these ectopic SP-IR fibers in the white matter were characterized as bundles of small unmyelinated fibers. Some ectopic SP-IR boutons were presynaptic to dendrites. Some SP-IR boutons and axons co-localized CGRP immunoreactivities.

REFRENCE

Adams, J.C. (1981) Heavy metal intensification of DAB-based HRP reaction product. *J. Histochem. Cytochem.* **29**, 775

Akerman, B.S., Rosell, S. and Folkers, K. (1982) Intrathecal (D-Pro^2, D-Trp^{7,9})-SP elicits hypoalgesia and motor blockade in the rat and antagonizes noxious responses induced by substance P. *Acta.Chem.Scand.* **114**, 631-633.

Albers, K.M., Wright, D.E. and Davis, B.M. (1994) Overexpression of nerve growth factor in epidermis of transgenic mice causes hypertrophy of the peripheral nervous system. *J. Neurosci.* **14**, 1422-1432.

Aloe, L., Cozzari, C., Calissano, P. and Levi-Montalcini, R. (1981) Somatic and behavioral postnatal effects of fetal injections of nerve growth factor antibodies in the rat. *Nature,* **291**, 413-415.

Aloe, L., Tuveri, M.A. and Levi-Montalcini, R. (1992) Studies on carrageenan-induced arthritis in adult rats: presence of nerve growth factor and role of sympathetic innervation. *Rheumatol Int,* **12**, 213-216.

Alvarez, F.J., Kavookjian, A.M. and Light, A.R. (1992) Synaptic interactions between GABA-immunoreactive profiles and the terminals of functionally defined myelinated nociceptors in the monkey and cat spinal cord. *J. Neurosci.* **12**, 2901-2917.

Amara, S.G., Arriza, J.L., Leff, S.E., Swanson, L.W., Evans, R.M. and Rosenfeld, M.G. (1985) Expression in brain of a mesenger RNA encoding a novel neuropeptide homologous to calcitonin

gene-related peptide. *Science,* 229, 1094-1097.

Andrews, T.J. and Cowen, T. (1994) In vivo infusion of NGF induces the organotypic regrowth of perivascular nerves following their atrophy in aged rats. *J. Neurosci.* **14 (5)**, 3048-3058.

Barber, R.P., Vaughn, J.E., Saito, K., McLaughlin, B.J. and Roberts, E. (1978) GABAergic terminals are presynaptic to primary afferent terminals in the substantia gelatinosa of the rat spinal cord. *Brain Res.* **141,** 35-55.

Barber, R.P., Vaughn, J.E., Slemmon, J.R., Salvaterra, P.M., Roberts, E. and Leeman, S.E. (1979) The origin, distribution and synaptic relationships of substance P axons in rat spinal cord. *J. Comp. Neurol.* **184,** 331-352.

Barber, R.P., Vaughn, J.E. and Roberts, E. (1982) The cytoarchitecture of GABAergic neurons in rat spinal cord. *Brain Res.* **238,** 305-328.

Basbaum, A.I. (1985) Functional analysis of the cytochemistry of the spinal dorsal horn. In. Fields, H.L., Dubner, R. and Cervero, F. (eds), *Advances in pain research and therapy, vol.9.* Raven Press, New York, pp. 149-175.

Basbaum, A.I., Glazer, E.J. and Oertel, W. (1986) Immunoreactive glutamic acid decarboxylase in the trigeminal nucleus caudalis of the cat: a light- and electron-microscopic analysis. *Somatosens. Res.* **4,** 77-94.

Battaglia, G. and Rustioni, A. (1988) Coexistence of glutamate and substance P in dorsal root ganglion neurons of the rat and monkey. *J. Comp. Neurol.* 277, 302-312.

Beal, J.A., Penny, J.E. and Bicknell, H.R. (1981) Structural diversity of marginal (lamina I) neurons in the adult monkey (Macaca mulatta) lumbosacral spinal cord: a Golgi study. *J. Comp. Neurol.* **202**, 237-254.

Bennett, G.J., Abdelmoumene, M., Hayashi, H. and Dubner, R. (1980) Physiology and morphology of substantia gelatinosa neurons intracellularly stained with horseradish peroxidase. *J. Comp. Neurol.* **194**, 809-827.

Bennett, G.J., Abdelmoumene, M., Hayashi, H., Hoffert, M.J. and Dubner, R. (1981) Spinal cord layer I neurons with axon collaterals that generate local arbors. *Brain Res.* **209**, 421-426.

Bennett, G.J., Ruda, M.A., Gobel, S. and Dubner, R. (1982) Enkephalin immunoreactive stalked cells and lamina IIb islet cells in cat substantia gelatinosa. *Brain Res.* **240**, 162-166.

Bernardi, P.S., Valtschanoff, J.G., Weinberg, R.J., Schmidt, H.H.H.W. and Rustioni, A. (1995) Synaptic interactions between primary afferent terminals and GABA and nitric oxide-synthesizing neurons in superficial laminae of the rat spinal cord. *J. Neurosci.* **15**, 1363-1371.

Bernau, N.A., Dawson, S.D., Kane, L.A. and Pubols, L.M. (1993) Changes in substance P and 5-HT binding in the spinal cord dorsal horn and lamina 10 after dorsolateral funiculus lesions. *Brain Res.* **613**, 106-114.

Black, I.B., DiCicco-Bloom, E. and Dreyfus, C.F. (1990) Nerve growth factor and the issue of mitosis in the nervous system. *Current Topics in Devolopmental Biology*, **24**, 161-192.

Bleazard, L., Hill, R.G. and Morris, R. (1994) The correlation between the distribution of the NK_1

receptor and the actions of tachykinin agonists in the dorsal horn of the rat indicates that substance P does not have a functional role on substantia gelatinosa (lamina II) neurons. *J. Neurosci.* **14**, 7655-7664.

Boehmer, C.G., Norman, J., Catton, M., Fine, L.G. and Mantyh, P.W. (1989) High levels of mRNA coding for substance P, somatostatin and α-tublin are expressed by rat and rabbit dorsal root ganglia neurons. *Peptides*, **10**, 1179-1194.

Branchereau, P., Van Bockstaele, E.J., Chan, J. and Pickel, V.M. (1995) Ultrastructural characterization of neurons recorded intracellularly in vivo and injected with lucifer yellow: Advantages of immunogold-silver vs. immunoperoxidase labeling. *Microsc. Res. Tech.* **30**, 427-436.

Brasch, H. and Zetler, G. (1982) Caerulein and morphine in a model of visceral pain. Effects on the hypotensive response to renal pelvis distension in the rat. *Naunyn Schmiedebergs Arch. Pharmacol.* **319**, 161-167.

Bresnahan, J.C., Ho, R.H. and Beattie, M.S. (1984) A comparison of the ultrastructure of substance P and enkephalin-immunoreactive elements in the nucleus of the dorsal lateral funiculus and laminae I and II of the rat spinal cord. *J. Comp. Neurol.* **229**, 497-511.

Brinster, R.L., Chen, H.Y., Trumbauer, M., Senear, A.W., Warren, R. and Palmiter, R.D. (1981) Somatic expression of herpes thymidine kinase in mice following injection of a fusion gene into eggs. *Cell*, **27**, 223-231.

Brodin, E., Linderoth, B., Gazelius, B. and Ungerstedt, U. (1987) In vivo release of substance P in cat dorsal horn studied with microdialysis. *Neurosci. Lett.* **76**, 357-362.

Brown, A.G., Fyffe, R.E.W., Rose, P.K. and Snow, P.J. (1981) Spinal cord collaterals from axons of type II slowly adapting units in the cat. *J. Physiol.* **316**, 469-480.

Brown, A.G. (1982) The dorsal horn of the spinal cord. *Q. J. Exp. Physiol.* **67**, 193-212.

Brown, J.L., Liu, H., Maggio, J.E., Vigna, S.R., Mantyh, P.W. and Basbaum, A.I. (1995) Morphological characterization of substance P receptor-immunoreactive neurons in the rat spinal cord and trigeminal nucleus caudalis. *J. Comp. Neurol.* **356**, 327-344.

Buck, S.H., Miller, M.S. and Burks, T.F. (1982) Depletion of primary afferent substance P by capsaicin and dihydrocapsaicin without altered thermal sensitivity in rats. *Brain Res.* **233**, 216-220.

Burks, T.F., Buck, S.H. and Miller, M.S. (1985) Mechanisms of depletion of substance P by capsaicin. *Federation Proc.* **44**, 2531-2534.

Campaghoni, A.T. (1988) Molecular biology of myelin proteins from the central nervous system. *J. Neurochem.* **51 (1)**, 1-14.

Campenot, R.B. (1982) Development of sympathetic neurones in compartmentalized cultures. I. Local control of neurite growth by nerve growth factor. *Dev. Biol.* **93**, 1-12.

Carlton, S.M. and Hayes, E.S. (1990) Light microscopic and ultrastructural analysis of GABA-immunoreactive profiles in the monkey spinal cord. *J. Comp. Neurol.* **300**, 162-182.

Carlton, S.M. and Hayes, E.S. (1991) GABAergic vesicle-containing dendrites and spines: A critical element in processing sensory input in the monkey dorsal horn. *Neurosci. Lett.* **121**, 40-42.

Cervero, F., Iggo, A. and Ogawa, H. (1976) Nociceptor-driven dorsal horn neurones in the lumbar spinal cord of the cat. *Pain*, **2**, 5-24.

Cervero, F., Iggo, A. and Molony, V. (1979) Ascending projections of nociceptor-driven lamina I neurones in the cat. *Exp. Brain Res.* **35**, 135-149.

Cervero, F. and Iggo, A. (1978) Reciprocal sensory interaction in the spinal cord. *J. Physiol. (Lond.)*, **284**, 84P-85P.

Cervero, F. and Iggo, A. (1980) The substantia gelatinosa of the spinal cord. A critical review. *Brain*, **103**, 717-772.

Chan-Palay, V. and Palay, S.L. (1977) Ultrastructural identification of substance P cells and their processes in rat sensory ganglia and their terminals in the spinal cord by immunocytochemistry. *Proc. Natl. Acad. Sci. USA*, **74**, 4050-4054.

Chang, M.M., Leeman, S.E. and Niall, H.D. (1971) Amino-acid sequence of substance P. *Nature New Biol.* **232**, 86-87.

Chirgwin, J.M., Przybyla, A.E., MacDonald, R.J. and Ruller, W.J. (1977) Isolation of biologically active ribonucleic acid form sources enriched in ribonuclease. *Biochemistry*, **18**, 5294-5299.

Chung, K., Lee, W.T. and Carlton, S.M. (1988) The effects of dorsal rhizotomy and spinal cord isolation on calcitonin gene-related peptide-labeled terminals in the rat lumbar dorsal horn. *Neurosci. Lett.* **90**, 27-32.

Coffield, J.A. and Miletic, V. (1987a) Enkephalinergic trigeminal and spinal neurons projecting to the rat thalamus. *Soc. Neurosci. Abstr.* **13**, 522

Coffield, J.A. and Miletic, V. (1987b) Immunoreactive enkephalin is contained within some trigeminal and spinal neurons projecting to the rat medial thalamus. *Brain Res.* **425**, 380-383.

Coimbra, A., Ribeiro-da-Silva, A. and Pignatelli, D. (1984) Effects of dorsal rhizotomy on the several types of primary afferent terminals in laminae I-III of the rat spinal cord. An electron microscope study. *Anat. Embryol. (Berl.)*, **170**, 279-287.

Cridland, R.A. and Henry, J.L. (1988a) Facilitation of the tail-flick reflex by noxious cutaneous stimulation in the rat: antagonism by a substance P analogue. *Brain Res.* **462**, 15-21.

Cridland, R.A. and Henry, J.L. (1988b) Intrathecal administration of substance P in the rat: spinal transection or morphine blocks the behavioural responses but not the facilitation of the tail-flick reflex. *Neurosci. Lett.* **84**, 203-208.

Cridland, R.A. and Henry, J.L. (1988c) Effects of intrathecal administration of neuropeptides on a spinal nociceptive reflex in the rat: VIP, galanin, CGRP, TRH, somatostatin and angiotensin II. *Neuropeptides*, **11**, 23-32.

Crowley, C., Spencer, S.D., Nishimura, M.C., Chen, K.S., Pitts-Meek, S., Armanini, M.P., Ling, L.H., McMahon, S.B., Shelton, D.L., Levinson, A.D. and Phillips, H.S. (1994) Mice lacking nerve growth factor display perinatal loss of sensory and sympathetic neurons yet develop basal forebrain cholinergic neurons. *Cell*, **76**, 1001-1011.

Cuello, A.C., Emson, P., Del Fiacco, M., Gale, J., Iversen, L.L., Jessell, T.M., Kanazawa, I., Paxinos, G. and Quik, M. (1977a) Distribution and release of substance P in the central nervous system. In Hughes, J. (ed), *Centrally acting peptides.* Univ. Park Press, Baltimore, pp. 135-155.

Cuello, A.C., Jessell, T.M., Kanazawa, I. and Iversen, L.L. (1977b) Substance P: localization in synaptic vesicles in rat central nervous system. *J. Neurochem.* **29,** 747-751.

Cuello, A.C., Del Fiacco, M. and Paxinos, G. (1978) The central and peripheral ends of the substance P-containing sensory neurones in the rat trigeminal system. *Brain Res.* **152,** 499-509.

Cuello, A.C., Galfre, G. and Milstein, C. (1979) Detection of substance P in the central nervous system by a monoclonal antibody. *Proc. Natl. Acad. Sci. USA,* **76,** 3532-3536.

Cuello, A.C., Gamse, R., Holzer, P. and Lembeck, F. (1981) Substance P immunoreactive neurons following neonatal administration of capsaicin. *Naunyn-Schmiedeberg's Arch. Pharmacol.* **315,** 185-194.

Cuello, A.C. (1983) Central distribution of opioid peptides. *Br. Med. Bull.* **39,** 11-16.

Cuello, A.C. (1987) Peptides as neuromodulators in primary sensory neurons. *Neuropharmacology,* **26,** 971-979.

Cuello, A.C., Garofalo, L., Maysinger, D., Pioro, E.P. and Ribeiro-da-Silva, A. (1990) Injury and repair of central cholinergic neurons. *Prog. Brain Res.* **84,** 301-311.

Cuello, A.C., Ribeiro-da-Silva, A., Ma, W., De Koninck, Y. and Henry, J.L. (1993) Organization of

substance P primary sensory neurons: ultrastructural and physiological correlates. *Regul. Pept.* **46**, 155-164.

Cuello, A.C. and Côté, A. (1993) Preparation and application of conventional and non-conventional monoclonal antibodies. In Cuello, A.C. (ed), *Immunohistochemistry II*. John Wiley & Sons, Chichester, pp. 107-145.

Cuello, A.C. and Kanazawa, I. (1978) The distribution of substance P immunoreactive fibers in the rat central nervous system. *J. Comp. Neurol.* **178**, 129-156.

Dam, T.-V., Martinelli, B. and Quirion, R. (1990) Autoradiographic distribution of brain neurokinin-1/substance P receptors using a highly selective ligand [^{3}H]-[Sar9,met(O_2)11]-substance P. *Brain Res.* **531**, 333-337.

Davis, B.M., Lewin, G.R., Mendell, L.M., Jones, M.E. and Albers, K.M. (1993) Altered expression of nerve growth factor in the skin of transgenic mice leads to changes in response to mechanical stimuli. *Neuroscience,* **56**, 789-792.

De Biasi, S. and Rustioni, A. (1988) Glutamate and substance P coexist in primary afferent terminals in the superficial laminae of spinal cord. *Proc. Natl. Acad. Sci. USA,* **85**, 7820-7824.

De Koninck, Y., Ribeiro-da-Silva, A., Henry, J.L. and Cuello, A.C. (1992) Spinal neurons exhibiting a specific nociceptive response receive abundant substance P-containing synaptic contacts. *Proc. Natl. Acad. Sci. USA,* **89**, 5073-5077.

De Koninck, Y., Ribeiro-da-Silva, A., Henry, J.L. and Cuello, A.C. (1993) Ultrastructural

immunocytochemistry combined with intracellular marking of physiologically identified neurons *in vivo*. In Cuello, A.C. (ed), *Immunohistochemistry II*. John Wiley & Sons , Chichester, pp. 369-393.

De Koninck, Y. and Henry, J.L. (1991) Substance P-mediated slow excitatory postsynaptic potential elicited in dorsal horn neurons *in vivo* by noxious stimulation. *Proc. Natl. Acad. Sci. USA*, **88**, 11344-11348.

De Koninck, Y. and Henry, J.L. (1992) Peripheral vibration causes an adenosine-mediated postsynaptic inhibitory potential in dorsal horn neurons of the cat spinal cord. *Neuroscience*, **50**, 435-443.

Del Fiacco, M. and Cuello, A.C. (1980) Substance P-and enkephalin-containing neurones in the rat trigeminal system. *Neuroscience*, **5**, 803-815.

Diamond, J., Holmes, M. and Coughlin, M. (1992) Endogenous NGF and nerve impulses regulate the collateral sprouting of sensory axons in the skin of the adult rat. *J. Neurosci.* **12**, 1454-1466.

Dickenson, A.H., Sullivan, A., Feeney, C., Fournie-Zaluski, M.C. and Roques, B.P. (1986) Evidence that endogenous enkephalins produce delta-opiate receptor mediated neuronal inhibitions in rat dorsal horn. *Neurosci. Lett.* **72**, 179-182.

DiFiglia, M., Aronin, N. and Leeman, S.E. (1982) Light microscopic and ultrastructural localization of immunoreactive substance P in the dorsal horn of the monkey spinal cord. *Neuroscience*, **7**, 1127-1139.

Ding, Y.-Q., Takada, M., Shigemoto, R. and Mizuno, N. (1995) Spinoparabrachial tract neurons

showing substance P receptor-like immunoreactivity in the lumbar spinal cord of the rat. *Brain Res.* **674**, 336-340.

Donnerer, J., Schuligoi, R. and Stein, C. (1992) Increased content and transport of substance P and calcitonin gene-related peptide in sensory nerves innervating inflamed tissue: Evidence for a regulatory function of nerve growth factor *in vivo*. *Neuroscience*, **49**, 693-698.

Dray, A. (1992) Neuropharmacological mechanisms of capsaicin and related substances. *Biochem. Pharmacol.* **44**, 611-615.

Duggan, A.W., Hall, J.G. and Headley, P.M. (1976) Morphine, enkephalin and the substantia gelatinosa. *Nature*, **264**, 456-458.

Duggan, A.W., Hall, J.G. and Headley, P.M. (1977) Enkephalin and dorsal horn neurones of the cat: effects on responses to noxious and innocuous skin stimuli. *British Journal of Pharmacology*, **61**, 399-408.

Duggan, A.W., Johnson, S.M. and Morton, C.R. (1981) Differing distributions of receptors for morphine and Met5-enkephalinamide in the dorsal horn of the cat. *Brain Res.* **229**, 379-387.

Duggan, A.W., Morton, C.R., Zhao, Z.Q. and Hendry, I.A. (1987) Noxious heating of the skin releases immunoreactive substance P in the substantia gelatinosa of the cat: a study with antibody microprobes. *Brain Res.* **403**, 345-349.

Duggan, A.W., Hendry, I.A., Morton, C.R., Hutchison, W.D. and Zhao, Z.Q. (1988) Cutaneous stimuli releasing immunoreactive substance P in the dorsal horn of the cat. *Brain Res.* **451**, 261-273.

Duncan, D. and Morales, R. (1978) Relative numbers of several types of synaptic connections in the substantia gelatinosa of the cat spinal cord. *J. Comp. Neurol.* **182,** 601-610.

Ebendal, T. (1992) Function and evolution in the NGF family and its receptors. *J. Neurosci. Res.* **32,** 461-470.

Enfiejian, H.J., Chiaia, N.L., Macdonald, G.J. and Rhoades, R.W. (1989) Neonatal transection alters the percentage of substance-P-positive trigeminal ganglion cells that contribute axons to the regenerate infraorbital nerve. *Somatosens. Mot. Res.* **6,** 537-552.

Fields, H.L., Emson, P.C., Leigh, B.K., Gilbert, R.F. and Iversen, L.L. (1980) Multiple opiate receptor sites on primary afferent fibres. *Nature,* **284,** 351-353.

Finn, P.J., Ferguson, I.A., Wilson, P.A., Vahaviolos, J. and Rush, R.A. (1987) Immunohistochemical evidence for the distribution of nerve growth factor in the embryonic mouse. *J. Neurocytol.* **16,** 639-647.

Fitzgerald, M. (1983) Capsaicin and sensory neurons- a review. *Pain,* **15,** 109-130.

Fitzgerald, M., Wall, P.D., Goedert, M. and Emson, P.C. (1985) Nerve growth factor counteracts the neurophysiological and neurochemical effects of chronic sciatic nerve section. *Brain Res.* **332,** 131-141.

Foran, D.R. and Peterson, A.C. (1992) Myelin acquisition in the central nervous system of the mouse revealed by an MBP-lacZ transgene. *J. Neurosci.* **12,** 4890-4897.

Gamse, R., Molnar, A. and Lembeck, F. (1979) Substance P release from spinal cord slices by capsaicin. *Life Sci.* **25**, 629-636.

Garofalo, L., Ribeiro-da-Silva, A. and Cuello, A.C. (1992) Nerve growth factor-induced synaptogenesis and hypertrophy of cortical cholinergic terminals. *Proc. Natl. Acad. Sci. USA*, **89**, 2639-2643.

Garry, M.G., Miller, K.E. and Seybold, V.S. (1989) Lumbar dorsal root ganglia of the cat: a quantitative study of peptide immunoreactivity and cell size. *J. Comp. Neurol.* **284**, 36-47.

Gibbins, I.L., Furness, J.B., Costa, M., MacIntyre, I., Hillyard, C.J. and Girgis, S. (1985) Co-localization of calcitonin gene-related peptide-like immunoreactivity with substance P in cutaneous, vascular and visceral sensory neurons of guinea-pigs. *Neurosci. Lett.* **57**, 125-130.

Gibson, S.J., Polak, J.M., Bloom, S.R., Sabate, I.M., Mulderry, P.M., Ghatei, M.A., McGregor, G.P., Morrison, J.F., Kelly, J.S., Evans, R.M. and Rosenfeld, M.G. (1984) Calcitonin gene-related peptide immunoreactivity in the spinal cord of man and of eight other species. *J. Neurosci.* **4**, 3101-3111.

Gilbert, R.F., Emson, P.C., Hunt, S.P., Bennett, G.W., Marsden, C.A., Sandberg, B.E., Steinbusch, H.W. and Verhofstad, A.A. (1982) The effects of monoamine neurotoxins on peptides in the rat spinal cord. *Neuroscience*, **7**, 69-87.

Glazer, E.J. and Basbaum, A.I. (1983) Opioid neurons and pain modulation: an ultrastructural analysis of enkephalin in cat superficial dorsal horn. *Neuroscience*, **10**, 357-376.

Gnahn, H., Hefti, F., Heumann, R., Schwab, M.E. and Thoenen, H. (1983) NGF-mediated increase of

choline acetyltransferase (ChAT) in the neonatal rat forebrain: Evidence for a physiological role of NGF in the brain? *Dev. Brain Res.* **9**, 45-52.

Gobel, S. (1975) Golgi studies of the substantia gelatinosa neurons in the spinal trigeminal nucleus. *J. Comp. Neurol.* **162**, 397-416.

Gobel, S. (1978a) Golgi studies of the neurons in layer I of the dorsal horn of the medulla (trigeminal nucleus caudalis). *J. Comp. Neurol.* **180375**, 375-393.

Gobel, S. (1978b) Golgi studies of the neurons in layer II of the dorsal horn of the medulla (trigeminal nucleus caudalis). *J. Comp. Neurol.* **180**, 395-414.

Gorin, P.D. and Johnson, E.M. (1979) Experimental autoimmune model of nerve growth factor deprivation: effects of developing peripheral sympathetic and sensory neurons. *Proc. Natl. Acad. Sci. USA*, **76**, 5382-5386.

Gorin, P.D. and Johnson, E.M.J. (1980) Effects of long term nerve growth factor deprivation on the nervous system of rat: an experimental autoimmune approach. *Brain Res.* **198**, 27-42.

Gouardères, C., Jhamandas, K., Cridland, R., Cros, J., Quirion, R. and Zajac, J.M. (1993) Opioid and substance P receptor adaptations in the rat spinal cord following sub-chronic intrathecal treatment with morphine and naloxone. *Neuroscience*, **54**, 799-807.

Goujet-Zalc, C., Babinet, C., Monge, M., Timsit, S., Cabon, F., Gansmüller, M., Miura, M., Sanchez, M., Pournin, S., Mikoshiba, K. and Zalc, B. (1993) The proximal region of the MBP gene promoter is sufficient to induce oligodendroglial-specific expression in transgenic mice. *Eur. J. Neurosci.* **5**,

624-632.

Gow, A., Friedrich, V.L., Jr and Lazzarini, R.A. (1992) Myelin basic protein gene contains separate enhancers for oligodendrocyte and Schwann cell expression. *J. Cell Biol.* **119**, 605-616.

Gray, E.G. (1969) Electron microscopy of excitatory and inhibitory synapses: a brief review. *Prog. Brain Res.* **31**, 141-155.

Gulbenkian, S., Merighi, A., Wharton, J., Varndell, I.M. and Polak, J.M. (1986) Ultrastructural evidence for the coexistence of calcitonin gene-related peptide and substance P in secretory vesicles of peripheral nerves in the guinea-pig. *J. Neurocytol.* **15**, 535-542.

Gundersen, R.W. and Barrett, J.N. (1979) Neuronal chemotaxis: chick dorsal root axons turn toward high concentrations of nerve growth factor. *Science*, **206**, 1079-1081.

Hayes, A.G., Skingle, M. and Tyers, M.B. (1981) Effects of single doses of capsaicin on nociceptive thresholds in the rodent. *Neuropharmacology*, **20**, 505-511.

Hefti, F., Dravid, A. and Hartikka, J. (1984) Chronic intraventricular injections of nerve growth factor elevate hippocampal choline acetyltransferase activity in adult rats with partial septo-hippocampal lesions. *Brain Res.* **293**, 305-311.

Hefti, F., Hartikka, J. and Knusel, B. (1989) Function of neurotrophic factors in the adult and aging brain and their possible use in the treatment of neurodegenerative diseases. *Neurobiol. Aging*, **10**, 515-533.

Hefti, F., Knusel, B. and Lapchak, P.A. (1993) Protective effects of NGF and BDNF on basal forebrain cholinergic neurons in adult rats with partial fimbrial transections. *Prog. Brain Res.* **98**, 257-263.

Helke, C.J., Dimicco, J.A., Jacobowitz, D.M. and Kopin, I.J. (1981) Effect of capsaicin administration to neonatal rats on the substance P content of discrete CNS regions. *Brain Res.* **222**, 428-431.

Henderson, T.A., Johnson, E.M.J., Osborne, P.A. and Jacquin, M.F. (1994) Fetal NGF augmentation preserves excess trigeminal ganglion cells and interrupts Whisker-related pattern formation. *J. Neurosci.* **14**, 3389-3403.

Henry, J.L. (1976) Effects of substance P on functionally identified units in cat spinal cord. *Brain Res.* **114**, 439-452.

Henry, J.L. (1982) Relation of substance P to pain transmission: neurophysiological evidence. *Substance P in the Nervous System (Ciba Foundation Symposium No. 91).* Pitman, London, pp. 206-224.

Henry, J.L. (1994) Roles of substance P in spinal nociceptive pathways. In. Hökfelt, T., Schaible, H.-J. and Schmidt, R.F. (eds), *Neuropeptides, Nociception and Pain.* Chapman & Hall, Weinheim, pp. 209-220.

Holzer, P., Jurna, I., Gamse, R. and Lembeck, F. (1979) Nociceptive threshold after neonatal capsaicin treatment. *Eur. J. Pharmacol.* **58**, 511-514.

Holzer, P. (1988) Local effector functions of capsaicin-sensitive sensory nerve endings: involvement of tachykinins, calcitonin gene-related peptide and other neuropeptides. *Neuroscience*, **24**, 739-768.

Holzer, P. (1991) Casaicin as a tool for studying sensory neuron functions. In. Costa, M. and et al. (eds), *Sensory nerves and neuropeptides in gastroenterology*. Plenum Press, New York, pp. 3-16.

Hoyle, G.W., Mercer, E.H., Palmiter, R.D. and Brinster, R.L. (1993) Expression of NGF in sympathetic neurons leads to excessive axon outgrowth from ganglia but decreased terminal innervation within tissues. *Neuron*, **10**, 1019-1034.

Hökfelt, T., Kellerth, J.O., Nilsson, G. and Pernow, B. (1975a) Substance P: localization in the central nervous system and in some primary sensory neurons. *Science*, **190**, 889-890.

Hökfelt, T., Kellerth, J.O., Nilsson, G. and Pernow, B. (1975b) Experimental immunohistochemical studies on the localization and distribution of substance P in cat primary sensory neurones. *Brain Res.* **100**, 235-252.

Hökfelt, T., Elde, R., Johansson, O., Luft, R., Nilsson, G. and Arimura, A. (1976) Immunohistochemical evidence for separate populations of somatostatin-containing and substance P-containing primary afferent neurons in the rat. *Neuroscience*, **1**, 131-136.

Hökfelt, T., Ljungdahl, A., Terenius, L., Elde, R. and Nilsson, G. (1977) Immunohistochemical analysis of peptide pathways possibly related to pain and analgesia: enkephalin and substance P. *Proc. Natl. Acad. Sci. USA*, **74**, 3081-3085.

Hökfelt, T., Ljungdahl, A., Steinbusch, H.W., Verhofstad, A.N., Nilsson, G., Brodin, E., Pernow, B.

and Goldstein, M. (1978) Immunohistochemical evidence of substance P-like immunoreactivity in some 5-hydroxytryptamine-containing neurons in the rat central nervous system. *Neuroscience,* **3,** 517-538.

Hökfelt, T., Arvidsson, U., Ceccatelli, S., Cortés, R., Cullheim, S., Dagerlind, Å., Johnson, H., Orazzo, C., Piehl, F., Pieribone, V., Schalling, M., Terenius, L., Ulfhake, B., Verge, V.M., Villar, M., Wiesenfeld-Hallin, Z., Xù, X.-J. and Xu, Z. (1992) Calcitonin gene-related peptide in the brain, spinal cord, and some peripheral systems. *Ann. NY Acad. Sci.* **657,** 119-134.

Hökfelt, T., Zhang, X. and Wiesenfeld-Hallin, Z. (1994) Messenger plasticity in primary sensory neurons following axotomy and its functional implications. *Trends Neurosci.* **17,** 22-30.

Hu, L., Ribeiro-da-Silva, A., Garofalo, L. and Cuello, A.C. (1994) Subcellular localization of NGF immunoreactivity in basal forebrain cholinergic neurons. An ultrastructural double-labelling study in the rat. *Soc. Neurosci. Abstr.* **20,** 1305

Hulsebosch, C.E., Perez-Polo, J.R. and Coggeshall, R.E. (1987) In vivo anti-NGF induces sprouting of sensory axons in dorsal roots. *J. Comp. Neurol.* **259,** 445-451.

Hunt, S.P., Kelly, J.S. and Emson, P.C. (1980) The electron microscopic localization of methionine-enkephalin within the superficial layers (I and II) of the spinal cord. *Neuroscience,* **5,** 1871-1890.

Hunt, S.P., Kelly, J.S., Emson, P.C., Kimmel, J.R., Miller, R.J. and Wu, J.-Y. (1981) An immunohistochemical study of neuronal populations containing neuropeptides or gamma-aminobutyrate within the superficial layers of the rat dorsal horn. *Neuroscience,* **6,**

1883-1898.

Hylden, J.L.K. and Wilcox, G.L. (1981) Intrathecal substance P elicits a caudally-directed biting and scratching behavior in mice. *Brain Res.* **217**, 212-215.

Iadarola, M.J., Tang, J., Costa, E. and Yang, H.Y. (1986) Analgesic activity and release of [MET5] enkephalin-Arg6-Gly7-Leu8 from rat spinal cord in vivo. *Eur. J. Pharmacol.* **121**, 39-48.

Inaishi, Y., Kashihara, Y., Sakaguchi, M., Nawa, H. and Kuno, M. (1992) Cooperative regulation of calcitonin gene-related peptide levels in rat sensory neurons via their central and peripheral processes. *J. Neurosci.* **12**, 518-524.

Isaacson, L.G., Saffran, B.N. and Crutcher, K.A. (1992) Nerve growth factor-induced sprouting of mature, uninjured sympathetic axons. *J. Comp. Neurol.* **326**, 327-336.

Iversen, L.L. (1986) Chemical signalling in the nervous system. *Prog. Brain Res.* **68**, 15-21.

Jancsó, G., Király, E. and Jancsó-Gabor, (1977) Pharmacologically induced selective degeneration of chemosensitive primary sensory neurones. *Nature,* **270**, 741-743.

Jancsó, G., Hökfelt, T., Lundberg, J.M., Király, E., Halasz, N., Nilsson, G., Terenius, L., Rehfeld, J., Steinbusch, H., Verhofstand, A., Elde, R., Said, S. and Brown, M. (1981) Immunohistochemical studies on the effect of capsaicin on spina and medullary peptide and monoamine neurons using antisera to substance P, gastrin/CCK, somatostatin, VIP, enkephalin, neurtensin and 5-hydroxytryptamine. *J. Neurocytol.* **10**, 963-980.

Jancsó, G., Király, E., Joo, F., Such, G. and Nagy, A. (1985) Selective degeneration by capsaicin of a subpopulation of primary sensory neurons in the adult rat. *Neurosci. Lett.* **59**, 209-214.

Janig, W. and Morrison, J.F.B. (1986) Functional properties of spinal visceral afferents supplying abdominal and pelvic organs, with special emphasis on visceral nociception. *Prog. Brain Res.* **67**, 87-114.

Jeftinija, S. (1988) Enkephalins modulate excitatory synaptic transmission in the superficial dorsal horn by acting at mu-opioid receptor sites. *Brain Res.* **460**, 260-268.

Jessell, T., Tsunoo, A., Kanazawa, I. and Otsuka, M. (1979) Substance P: depletion in the dorsal horn of rat spinal cord after section of the peripheral processes of primary sensory neurons. *Brain Res.* **168**, 247-259.

Jessell, T.M., Iversen, L.L. and Cuello, A.C. (1978) Capsaicin-induced depletion of substance P from primary sensory neurones. *Brain Res.* **152**, 183-188.

Jessell, T.M., Yoshioka, K. and Jahr, C.E. (1986) Amino acid receptor-mediated transmission at primary afferent synapses in rat spinal cord. *J. Exp. Biol.* **124**, 239-258.

Jessell, T.M. and Iversen, L.L. (1977) Opiate analgesics inhibit substance P release from rat trigeminal nucleus. *Nature*, **268**, 549-551.

Johnson, E.M., Jr., Rich, K.M. and Yip, H.K. (1986) The role of NGF in sensory neurons *in vivo*. *Trends Neurosci.* **9**, 33-36.

Ju, G., Hökfelt, T., Brodin, E., Fahrenkrug, J., Fischer, J.A., Frey, P., Elde, R.P. and Brown, J.C. (1987) Primary sensory neurons of the rat showing calcitonin gene-related peptide immunoreactivity and their relation to substance P-, somatostatin-, galanin-, vasoactive intestinal polypeptide- and cholecystokinin-immunoreactive ganglion cells. *Cell Tissue Res.* **247,** 417-431.

Kachidian, P., Poulat, P., Marlier, L. and Privat, A. (1991) Immunohistochemical evidence for the coexistence of substance P, thyrotropin-releasing hormone, GABA, methionin-enkephalin, and leucin-enkephalin in the serotonergic neurons of the caudal raphe nuclei: A dual labeling in the rat. *J. Neurosci. Res.* **30,** 521-530.

Kangrga, I., Larew, J.S. and Randic, M. (1990) The effects of substance P and calcitonin gene-related peptide on the efflux of endogenous glutamate and aspartate from the rat spinal dorsal horn in vitro. *Neurosci. Lett.* **108,** 155-160.

Kangrga, I. and Randic, M. (1990) Tachykinins and calcitonin gene-related peptide enhance release of endogenous glutamate and aspartate from the rat spinal dorsal horn slice. *J. Neurosci.* **10,** 2026-2038.

Kawamura, M., Kuraishi, Y., Minami, M. and Satoh, M. (1989) Antinociceptive effect of intrathecally administered antiserum against calcitonin gene-related peptide on thermal and mechanical noxious stimuli in experimental hyperalgesic rats. *Brain Res.* **497,** 199-203.

Kaway, Y., Takami, K., Shiosaka, S., Emson, P.C., Hillyard, C.J., Girgis, S., MacIntyre, I. and Tohyama, M. (1985) Topographic localization of calcitonin gene-related peptide in the rat brain: an immunohistochemical analysis. *Neuroscience,* **15,** 747-763.

Kenigsberg, R.L., Semenenko, F.M. and Cuello, A.C. (1990) Development of a bi-specific monoclonal antibody for simultaneous detection of rabbit IgG and horseradish peroxidase: use as a general reagent in immunocytochemistry and enzyme-linked immunosorbent assay. *J. Histochem. Cytochem.* **38,** 191-198.

Kenins, P. (1982) Responses of single nerve fibres to capsaicin applied to the skin. *Neurosci. Lett.* **29,** 83-88.

Kessler, J.A. and Black, I.B. (1980) Nerve growth factor stimulates the development of substance P in sensory ganglia. *Proc. Natl. Acad. Sci. USA,* **77,** 649-652.

Kopriwa, B.M. (1973) A reliable standardized method for ultrastructural electron microscopic radioautography. *Histochemistry,* **37,** 1-17.

Kopriwa, B.M. (1975) A comparison of various procedures for fine grain development in electron microscopic radioautography. *Histochemistry,* **44,** 201-224.

Kosaka, K., Hama, K., Nagatsu, I., Wu, J.-Y. and Kosaka, T. (1988) Possible coexistence of amino acid (gamma-aminobutyric acid), amine (dopamine) and peptide (substance P): neurons containing immunoreactivities for glutamic acid decarbooxylase, trrosine hydroxylase and substance P in the hamster main olfactory bulb. *Exp. Brain Res.* **71,** 633-642.

Kosaka, T., Nagatsu, I., Wu, J.-Y. and Hama, K. (1986) Use of high concentrations of glutaraldehyde for immunocytochemistry of transmitter-synthesizing enzymes in the central nervous system. *Neuroscience,* **18,** 975-990.

Kream, R.M., Kato, T., Shimonaka, H., Marchand, J.E. and Wurm, W.H. (1993) Substance P markedly potentiates the antinociceptive effects of morphine sulfate administered at the spinal level. *Proc. Natl. Acad. Sci. USA*, **90**, 3564-3568.

Kuchel, G.A., Hellendall, R. and Blum, M. (1992) Transynaptic regulation of low-affinity p75 nerve growth factor receptor mRNA precedes and accompanies lesion-induced collateral neuronal sprouting. *Exp. Neurol.* **118**, 73-84.

LaMotte, C.C., Pert, C.B. and Snyder, S.H. (1976) Opiate receptor binding in primate spinal cord: distribution and changes after dorsal root section. *Brain Res.* **112**, 407-412.

Le Greves, P., Nyberg, F., Terenius, L. and Hökfelt, T. (1985) Calcitonin gene-related peptide is a potent inhibitor of substance P degradation. *Eur. J. Pharmacol.* **115**, 309-311.

Le Greves, P., Nyberg, F., Hökfelt, T. and Terenius, L. (1989) Calcitonin gene-related peptide is metabolized by an endopeptidase hydrolyzing substance P. *Regul. Pept.* **25**, 277-286.

LeBars, D., Menetrey, D. and Besson, J.M. (1976) Effects of morphine upon the lamina V type cells activities in the dorsal horn of the decerebrate cat. *Brain Res.* **113**, 293-310.

Lee, Y., Kaway, Y., Shiosaka, S., Takami, K., Kiyama, H., Hillyard, C.J., Girgis, S., MacIntyre, I., Emson, P.C. and Tohyama, M. (1985a) Coexistence of calcitonin gene-related peptide and substance P-like peptide in single cells of the trigeminal ganglion of the rat: immunohistochemical analysis. *Brain Res.* **330**, 194-196.

Lee, Y., Takami, K., Kaway, Y., Girgis, S., Hillyard, C.J., MacIntyre, I., Emson, P.C. and Tohyama,

M. (1985b) Distribution of calcitonin gene-related peptide in the rat peripheral nervous sytem with reference to its coexistence with substance P. *Neuroscience,* **15,** 1227-1237.

Lemay, G., Waksman, G., Roques, B.P., Crine, P. and Boileau, G. (1989) Fusion of a cleavable signal peptide to the ectodomain of neutral endopeptidase (EC 3.4.24.11) results in the secretion of an active enzyme in COS-1 cells. *J. Biol. Chem.* **264,** 15620-15623.

Levi-Montalcini, R. and Angeletti, P.U. (1968) Nerve growth factor. *Physiol. Rev.* **48,** 534-569.

Lewin, G.R., Lisney, S.J.W. and Mendell, L.M. (1992a) Neonatal anti-NGF treatment reduces the Aσ- and C-fibre evoked vasodilator responses in rat skin: Evidence that nociceptor afferents mediate antidromic vasodilation. *Eur. J. Neurosci.* **4,** 1213-1218.

Lewin, G.R., Ritter, A.M. and Mendell, L.M. (1992b) On the role of nerve growth factor in the development of myelinated nociceptors. *J. Neurosci.* **12,** 1896-1905.

Lewin, G.R., Ritter, A.M. and Mendell, L.M. (1993) Nerve growth factor-induced hyperalgesia in the neonatal and adult rat. *J. Neurosci.* **13,** 2136-2148.

Lewin, G.R. and Mendell, L.M. (1992) NGF induced heat and mechanical hyperalgesia in adult rats. *Soc. Neurosci. Abstr.* **18,** 130

Lewin, G.R. and Mendell, L.M. (1993) Nerve growth factor and nociception. *Trends Neurosci.* **16,** 353-359.

Lewin, G.R. and Mendell, L.M. (1994) Regulation of cutaneous C-fiber heat nociceptors by nerve

growth factor in the developing rat. *J. Neurophysiol.* **71**, 941-949.

Light, A.R., Trevino, D.L. and Perl, E.R. (1979) Morphological features of functionally defined neurons in the marginal zone and substantia gelatinosa of the spinal dorsal horn. *J. Comp. Neurol.* **186**, 151-172.

Light, A.R. (1992) Organization of the spinal cord. In Light, A.R. (ed), *The initial processing of pain and its descending control: spinal and trigeminal systems. Pain and Headache series, vol. 12 (Series editor: P.L. Gildenberg).* Karger, Basel, pp. 75-86.

Light, A.R. and Perl, E.R. (1979a) Spinal termination of functionally identified primary afferent neurons with slowly conducting myelinated fibers. *J. Comp. Neurol.* **186**, 133-150.

Light, A.R. and Perl, E.R. (1979b) Reexamination of the dorsal root projection to the spinal dorsal horn including observations on the differential termination of coarse and thin fibers. *J. Comp. Neurol.* **186**, 117-132.

Lima, D., Mendes-Ribeiro, J.A. and Coimbra, A. (1991) The spino-latero-reticular system of the rat: Projections from the superficial dorsal horn and structural characterization of marginal neurons involved. *Neuroscience*, **45**, 137-152.

Lima, D., Avelino, A. and Coimbra, A. (1993) Morphological characterization of marginal (lamina I) neurons immunoreactive for substance P, enkephalin, dynorphin and gamma-aminobutyric acid in the rat spinal cord. *J. Chem. Neuroanat.* **6**, 43-52.

Lima, D. and Coimbra, A. (1986) A Golgi study of the neuronal population of the marginal zone

(lamina I) of the rat spinal cord. *J. Comp. Neurol.* **244**, 53-71.

Lima, D. and Coimbra, A. (1988) The spinothalamic system of the rat: structural types of retrogradely labelled neurons in the marginal zone (lamina I). *Neuroscience*, **27**, 215-230.

Lima, D. and Coimbra, A. (1989) Morphological types of spinomesencephalic neurons in the marginal zone (lamina I) of the rat spinal cord, as shown after retrograde labelling with cholera toxin subunit B. *J. Comp. Neurol.* **279**, 327-339.

Lima, D. and Coimbra, A. (1990) Structural types of marginal (lamina I) neurons projecting to the dorsal reticular nucleus of the medulla oblongata. *Neuroscience*, **34**, 591-606.

Lindsay, R.M., Lockett, C., Sternberg, J. and Winter, J. (1989) Neuropeptide expression in cultures of adult sensory neurons: modulation of substance P and calcitonin gene-related peptide by nerve growth factor. *Neuroscience*, **33**, 53-65.

Lindsay, R.M. and Harmar, A.J... (1989) Nerve growth factor regulates expression of neuropeptide genes in adult sensory neurons. *Nature*, **337**, 362-364.

Littlewood, N.K., Todd, A.J., Spike, R.C., Watt, C. and Shehab, S.A.S. (1995) The types of neuron in spinal dorsal horn which possess neurokinin-1 receptors. *Neuroscience*, **66**, 597-608.

Liu, H., Brown, J.L., Jasmin, L., Maggio, J.E., Vigna, S.R., Mantyh, P.W. and Basbaum, A.I. (1994) Synaptic relationship between substance P and the substance P receptor: Light and electron microscopic characterization of the mismatch between neuropeptides and their receptors. *Proc. Natl. Acad. Sci. USA*, **91**, 1009-1013.

Ljungdahl, A., Hökfelt, T. and Nilsson, G. (1978) Distribution of substance P-like immunoreactivity in the central nervous system of the rat - I. Cell bodies and nerve terminals. *Neuroscience*, **3**, 861-943.

Lu, B., Yokoyama, M., Dreyfus, C.F. and Black, I.B. (1991) NGF gene expression in actively growing brain glia. *J. Neurosci.* **11**, 318-326.

Ma, W., Ribeiro-da-Silva, A., Radhakrishnan, V., De Koninck, Y., Henry, J.L. and Cuello, A.C. (1994) Co-localization of substance P- and GABA-immunoreactivities in axonal varicosities presynaptic to functionally identified spinal dorsal horn neurons of the cat. *Soc. Neurosci. Abstr.* **20**, 554

Ma, W., Ribeiro-da-Silva, A., De Koninck, Y., Radhakrishnan, V., Henry, J.L. and Cuello, A.C. (1995a) Quantitative analysis of substance P immunoreactive boutons on physiologically characterized dorsal horn neurons in the cat lumbar spinal cord. *J. Comp. Neurol.* **Submitted,**

Ma, W., Ribeiro-da-Silva, A., Noel, G., Julien, J.-P. and Cuello, A.C. (1995b) Ectopic substance P and calcitonin gene-related peptide immunoreactive fibers in the spinal cord of transgenic mice over-expressing nerve growth factor. *Eur. J. Neurosci.* (in press)

Maekawa, K., Minami, M., Yabuuchi, K., Toya, T., Katao, Y., Hosoi, Y., Onogi, T. and Satoh, M. (1994) In situ hybridization study of μ- and kappa-opioid receptor mRNAs in the rat spinal cord and dorsal root ganglia. *Neurosci. Lett.* **168**, 97-100.

Magoul, R., Onteniente, B., Geffard, M. and Calas, A. (1987) Anatomic l distribution and ultrastructural organization of the GABAergic system in the rat spinal cord. An immunocytochemical

study using monoclonal antibodies. *Neuroscience,* **20,** 1001-1009.

Mantyh, P.W., Gates, T., Mantyh, C.R. and Maggio, J.E. (1989) Autoradiographic localization and characterization of tachykinin receptor binding sites in the rat brain and peripheral tissues. *J. Neurosci.* **9,** 258-279.

Maxwell, D.J., Fyffe, R.E.W. and Réthelyi, M. (1983) Morphological properties of physiologically caracterized lamina III neurones in the cat spinal cord. *Neuroscience,* **10,** 1-22.

Maxwell, D.J., Christie, W.M., Short, A.D. and Brown, A.G. (1990) Direct observations of synapses between GABA-immunoreactive boutons and muscle afferent terminals in lamina VI of the cat's spinal cord. *Brain Res.* **530,** 215-222.

Maxwell, D.J. and Noble, R. (1987) Relationship between hair-follicle afferent terminations and glutamic acid decarboxylase-containing boutons in cat's spinal cord. *Brain Res.* **408,** 308-312.

Maxwell, D.J. and Réthelyi, M. (1987) Ultrastructure and synaptic connections of cutaneous afferent fibres in the spinal cord. *Trends Neurosci.* **10,** 117-123.

McCarthy, P.W. and Lawson, S.N. (1989) Cell type and conduction velocity of rat primary sensory neurons with substance P-like immunoreactivity. *Neuroscience,* **28,** 745-753.

McCarthy, P.W. and Lawson, S.N. (1990) Cell type and conduction velocity of rat primary sensory neurons with calcitonin gene-related peptide-like immunoreactivity. *Neuroscience,* **34,** 623-632.

Melzack, R. and Wall, P.D. (1965) Pain mechanisms: a new theory. *Science,* **150,** 971-979.

Menétrey, D. and Basbaum, A.I. (1987) The distribution of substance P-, enkephalin- and dynorphin-immunoreactive neurons in the medulla of the rat and their contribution to bulbospinal pathways. *Neuroscience,* **23,** 173-187.

Merighi, A., Polak, J.M., Gibson, S.J., Gulbenkian, S., Valentino, K.L. and Peirone, S.M. (1988) Ultrastructural studies on calcitonin gene-related peptide-, tachykinins- and somatostatin-immunoreactive neurones in rat dorsal root ganglia: Evidence for the colocalization of different peptides in single secretory granules. *Cell Tissue Res.* **254,** 101-109.

Merighi, A., Polak, J.M., Fumagalli, G. and Theodosis, D.T. (1989) Ultrastructural localization of neuropeptides and GABA in rat dorsal horn: a comparison of different immunogold labeling techniques. *J. Histochem. Cytochem.* **37,** 529-540.

Merighi, A., Polak, J.M. and Theodosis, D.T. (1991) Ultrastructural visualization of glutamate and aspartate immunoreactivities in the rat dorsal horn, with special reference to the co-localization of glutamate, substance P and calcitonin-gene related peptide. *Neuroscience,* **40,** 67-80.

Miaskowski, C., Taiwo, Y.O. and Levine, J.D. (1991) Contribution of supraspinal μ- and δ-opioid receptors to antinociception in the rat. *Eur. J. Pharmacol.* **205,** 247-252.

Miletic, V. and Tan, H. (1988) Iontophoretic application of calcitonin gene-related peptide produces a slow and prolonged excitation of neurons in the cat lumbar dorsal horn. *Brain Res.* **446,** 169-172.

Miller, K.E. and Seybold, V.S. (1987) Comparison of met-enkephalin-, dynorphin A-, and neurotensin immunoreactive neurons in the cat and rat spinal cords: I. Lumbar cord. *J. Comp. Neurol.* **255,** 293-304.

Miller, K.E. and Seybold, V.S. (1989) Comparison of met-enkephalin, dynorphin A, and neurotensin immunoreactive neurons in the cat and rat spinal cords: II. Segmental differences in the marginal zone. *J. Comp. Neurol.* **279**, 619-628.

Millhorn, D.E., Hökfelt, T., Seroogy, K., Oertel, W., Verhofstad, A.A.J. and Wu, J.Y. (1987) Immunohistochemical evidence for colocalization of gamma-aminobutyric acid and serotonin in neurons of the ventral medulla oblongata projecting to the spinal cord. *Brain Res.* **410**, 179-185.

Minami, M., Maekawa, K., Yabuuchi, K. and Satoh, M. (1995) Double in situ hybridization study on coexistence of μ-, δ- and kappa-opioid receptor mRNAs with preprotachykinin A mRNA in the rat dorsal root ganglia. *Mol. Brain Res.* **30**, 203-210.

Miskimins, R., Knapp, L., Dewey, M.J. and Zhang, X. (1992) Cell and tissue-specific expression of a heterologous gene under control of the myelin basic protein gene promoter in transgenic mice. *Dev. Brain Res.* **65**, 217-221.

Molander, C., Xu, Q. and Grant, G. (1984) The cytoarchitectonic organization of the spinal cord in the rat. I. The lower thoracic and lumbosacral cord. *J. Comp. Neurol.* **230**, 133-141.

Morton, C.R., Hutchison, W.D. and Lacey, G. (1992) Baclofen and the release of neuropeptides in the cat spinal cord. *Eur. J. Neurosci.* **4**, 243-250.

Morton, C.R. and Hutchison, W.D. (1989) Release of sensory neuropeptides in the spinal cord: studies with calcitonin gene-related peptide and galanin. *Neuroscience,* **31**, 807-815.

Murase, K., Nedeljkov, V. and Randic, M. (1982) The actions of neuropeptides on dorsal horn

neurons in the rat spinal cord slice preparation: an intracellular study. *Brain Res.* **234**, 170-176.

Murray, M. and Goldberger, M.E. (1986) Replacement of synaptic terminals in lamina II and Clarke's nucleus after unilateral lumbosacral dorsal rhizotomy in adult cats. *J. Neurosci.* **6**, 3205-3217.

Nagy, J.I., Vincent, S.R., Staines, W.A., Fibiger, H.C., Reisine, T.D. and Yamamura, H.I. (1980) Neurotoxic action of capsaicin on spinal substance P neurons. *Brain Res.* **186**, 435-444.

Nagy, J.I., Hunt, S.P., Iversen, L.L. and Emson, P.C. (1981) Biochemical and anatomical observations on the degeneration of peptide-containing primary afferent neurons after neonatal capsaicin. *Neuroscience*, **6**, 1923-1934.

Nagy, J.I., Iversen, L.L., Goedert, M., Chapman, D. and Hunt, S.P. (1983) Dose-dependent effects of capsaicin on primary sensory neurons in the neonatal rat. *J. Neurosci.* **3**, 399-406.

Nagy, J.I. and Van der Kooy, D. (1983) Effects of neonatal capsaicin treatment on nociceptive thresholds in the rat. *J. Neurosci.* **3**, 1145-1150.

Nakaya, Y., Kaneko, T., Shigemoto, R., Nakanishi, S. and Mizuno, N. (1994) Immunohistochemical localization of substance P receptor in the central nervous system of the adult rat. *J. Comp. Neurol.* **347**, 249-274.

Nance, P.W., Sawynok, J. and Nance, D.M. (1987) Modality specific analgesia produced by intrathecal anti-substance P antibody. In. Henry, J.L., Couture, R., Cuello, A.C., Pelletier, G., Quirion, R. and Regoli, D. (eds), *Substance P and Neurokinins.* Springer-Verlag, New York, pp. 282-284.

Naranjo, J.R., Arnedo, A., De Felipe, M.C. and Del Rio, J. (1986) Antinociceptive and Met-enkephalin releaseing effects of tachykinins and substance P fragments. *Peptides*, **7**, 419-423.

Nawa, H., Hirose, T., Takashima, H., Inayama, S. and Nakanishi, S. (1983) Nucleotide sequences of cloned cDNAs for two types of bovine brain substance P precursor. *Nature*, **306**, 32-36.

Oku, R., Satoh, M., Fujii, N., Otaka, A., Yajima, H. and Takagi, H. (1987) Calcitonin gene-related peptide promotes mechanical nociception by potentiating release of substance P from the spinal dorsal horn in rats. *Brain Res.* **403**, 350-354.

Oku, R., Nanayama, T. and Satoh, M. (1988) Calcitonin gene-related peptide modulates calcium mobilization in synaptosomes of rat spinal dorsal horn. *Brain Res.* **475**, 356-360.

Otsuka, M. and Konishi, S. (1976) Release of substance P-like immunoreactivity from isolated spinal cord of newborn rat. *Nature*, **264**, 83-84.

Otsuka, M. and Yanagisawa, M. (1987) Does substance P act as a pain transmitter? *Trends Pharmacol. Sci.* **8**, 506-510.

Otsuka, M. and Yanagisawa, M. (1990) Pain and neurotransmitters. *Cell. Mol. Neurobiol.* **10**, 293-302.

Otsuka, M. and Yoshioka, K. (1993) Neurotransmitter functions of mammalian tachykinins. *Physiol. Rev.* **73**, 229-308.

Otten, U., Goedert, M., Mayer, N. and Lembeck, F. (1980) Requirement of nerve growth factor for

development of substance P-containing sensory neurones. *Nature*, **287**, 158-159.

Otten, U. and Lorez, H.P. (1983) Nerve growth factor increases substance P, cholecystokinin and vasoactive intestinal polypeptide immunoreactivities in primary sensory neurons of newborn rats. *Neurosci. Lett.* **34**, 153-158.

Otto, D., Unsicker, K. and Grothe, C. (1987) Pharmacological effects of nerve growth factor and fibroblast growth factor applied to the transected sciatic nerve on neuron death in adult rat dorsal root ganglia. *Neurosci. Lett.* **836**, 156-160.

Pearson, J., Brandeis, L. and Cuello, A.C. (1982) Depletion of axons containing substance P in the substantia gelatinosa of patients with diminuished pain sensitivity. *Nature*, **275**, 61-63.

Pickel, V.M., Reis, D.J. and Leeman, S.E. (1977) Ultrastructural localization of substance P in neurons of rat spinal cord. *Brain Res.* **122**, 534-540.

Pickel, V.M., Sumal, K.K. and Miller, R.J. (1982) Early prenatal development of substance P and enkephalin-containing neurons in the rat. *J. Comp. Neurol.* **210**, 411-422.

Piercey, M.F., Dobry, P.J.K., Schroeder, L.A. and Einspahr, F.J. (1981) Behavioral evidence that substance P may be a spinal cord sensory neurotransmitter. *Brain Res.* **210**, 407-412.

Pignatelli, D., Ribeiro-da-Silva, A. and Coimbra, A. (1989) Postnatal maturation of primary afferent terminations in the substantia gelatinosa of the rat spinal cord. An electron microscopic study. *Brain Res.* **491**, 33-44.

Plenderleith, M.B., Haller, C.J. and Snow, P.J. (1990) Peptide coexistence in axon terminals within the superficial dorsal horn of the rat spinal cord. *Synapse,* **6,** 344-350.

Pourcho, R.G. and Goebel, D.J. (1988) Colocalization of substance P and gamma-aminobutyric acid in amacrine cells of the cat retina. *Brain Res.* **447,** 164-168.

Powell, J.J. and Todd, A.J. (1992) Light and electron microscope study of GABA-immunoreactive neurones in lamina III of rat spinal cord. *J. Comp. Neurol.* **315,** 125-136.

Price, D.D., Hayashi, H., Dubner, R. and Ruda, M.A. (1979) Functional relationships between neurons of marginal and substantia gelatinosa layers of primate spinal cord. *J. Neurophysiol.* **42,** 1590-1608.

Priestley, J.V., Bramwell, S., Butcher, L.L. and Cuello, A.C. (1982a) Effect of capsaicin on neuropeptides in areas of termination of primary sensory neurones. *Neurochem. Int.* **4,** 57-65.

Priestley, J.V., Somogyi, P. and Cuello, A.C. (1982b) Immunocytochemical localization of substance P in the spinal trigeminal nucleus of the rat: a light and electron microscopic study. *J. Comp. Neurol.* **211,** 31-49.

Purves, D., Snider, W.D. and Voyvodic, J.T. (1988) Trophic regulation of nerve cell morphology and innervation in the autonomic nervous system. *Nature,* **336,** 123-128.

Quirion, R., Shults, C.W., Moody, T.W., Pert, C.B., Chase, T.N. and O'Donohue, T.L. (1983) Autoradiographic distribution of substance P receptors in rat central nervous system. *Nature,* **303,** 714-716.

Radhakrishnan, V., Ma, W., Ribeiro-da-Silva, A., De Koninck, Y., Cuello, A.C. and Henry, J.L. (1993) Correlation of quantitated substance P-immunoreactive synapses and NK-1 receptor mediated nociceptive responses in lumbar spinal neurones in the cat. *Soc. Neurosci. Abstr.* **19**, 108

Radhakrishnan, V. and Henry, J.L. (1991) Novel substance P antagonist, CP-96,345, blocks responses of cat spinal dorsal horn neurons to noxious cutaneous stimulation and to substance P. *Neurosci. Lett.* **132**, 39-43.

Radhakrishnan, V. and Henry, J.L. (1995) Antagonism of nociceptive responses of cat spinal dorsal horn neurons *in vivo* by the NK-1 receptor antagonists CP-96,345 and CP-99,994, but not by CP-96,344. *Neuroscience,* **64**, 943-958.

Ramón y Cajal, S. (1909) Histologie du Système Nerveux de l'Homme et des Vertébrés. Vol. 1. Translated by L. Azoulay. A.Maloine, Paris,

Randic, M., Hecimovic, H. and Ryu, P.D. (1990) Substance P modulates glutamate-induced currents in acutely isolated rat spinal dorsal horn neurones. *Neurosci. Lett.* **117**, 74-80.

Randic, M. and Miletic, V. (1977) Effect of substance P in cat dorsal horn neurones activated by noxious stimuli. *Brain Res.* **128**, 164-169.

Randic, M. and Miletic, V. (1978) Depressant actions of methionine-enkephalin and somatostatin in cat dorsal horn neurones activated by noxious stimuli. *Brain Res.* **152**, 196-202.

Readhead, C., Popko, B., Takahashi, N., Shine, H.D., Saavedra, R.A., Sidman, R.L. and Hood, L. (1987) Expression of a myelin basic protein gene in transgenic shiverer mice: correction of the

dysmyelinating phenotype. *Cell,* **48,** 703-712.

Regoli, D., Drapeau, G., Dion, S. and Couture, R. (1988) New selective agonists for neurokinin receptors: pharmacological tools for receptor characterization. *Trends Pharmacol. Sci.* **9,** 290-295.

Rexed, B. (1952) The cytoarchitectonic organization of the spinal cord in the cat. *J. Comp. Neurol.* **96,** 415-495.

Rexed, B. (1954) A cytoarchitectonic atlas of the spinal crd in the cat. *J. Comp. Neurol.* **100,** 297-397.

Réthelyi, M., Metz, C.B. and Lund, P.K. (1989) Distribution of neurons expressing calcitonin gene-related peptide mRNA in the brain stem, spinal cord and dorsal root ganglia of rat and guinea-pig. *Neuroscience,* **29,** 225-239.

Ribeiro-da-Silva, A., Tagari, P. and Cuello, A.C. (1989) Morphological characterization of substance P-like immunoreactive glomeruli in the superficial dorsal horn of the rat spinal cord and trigeminal subnucleus caudalis: a quantitative study. *J. Comp. Neurol.* **281,** 497-415.

Ribeiro-da-Silva, A., De Koninck, Y., Henry, J.L. and Cuello, A.C. (1991a) Co-localization of substance P and enkephalin immunoreactivities in synaptic boutons apposed onto physiologically identified dorsal horn neurones: an ultrastructural multiple-labelling study. *Soc. Neurosci. Abstr.* **17,** 1007

Ribeiro-da-Silva, A., Pioro, E.P. and Cuello, A.C. (1991b) Substance P- and enkephalin-like immunoreactivities are colocalized in certain neurons of the substantia gelatinosa of the rat spinal

cord. An ultrastructural double-labeling study. *J. Neurosci.* **11**, 1068-1080.

Ribeiro-da-Silva, A., De Koninck, Y., Cuello, A.C. and Henry, J.L. (1992) Enkephalin-immunoreactive nociceptive neurons in the cat spinal cord. *NeuroReport*, **3**, 25-28.

Ribeiro-da-Silva, A., Priestley, J.V. and Cuello, A.C. (1993) Pre-embedding ultrastructural immunocytochemistry. In Cuello, A.C. (ed), *Immunohistochemistry II*. John Wiley & Sons, Chichester, pp. 181-227.

Ribeiro-da-Silva, A. (1995) Substantia Gelatinosa of spinal cord. In Paxinos, G. (ed), *The Rat Nervous System*. 2nd. Academic Press, Sydney, pp. 47-59.

Ribeiro-da-Silva, A. and Coimbra, A. (1980) Neuronal uptake of ^{3}H-GABA and ^{3}H-glycine in laminae I-III substantia gelatinosa Rolandi) of the rat spinal cord. An autoradiographic study. *Brain Res.* **188**, 449-464.

Ribeiro-da-Silva, A. and Coimbra, A. (1982) Two types of synaptic glomeruli and their distribution in laminae I-III of the rat spinal cord. *J. Comp. Neurol.* **209**, 176-186.

Ribeiro-da-Silva, A. and Coimbra, A. (1984) Capsaicin causes selective damage to type I synaptic glomeruli in rat substantia gelatinosa. *Brain Res.* **290**, 380-383.

Rich, K.M., Luszczinski, J.R., Osborne, P.A. and Johnson, E.M., Jr. (1987) Nerve growth factor protects adult sensory neurons from cell death and atrophy caused by nerve injury. *J. Neurocytol.* **16**, 261-268.

Richardson, P.M., Verge Issa, V.M.K. and Riopelle, R.J. (1986) Distribution of neuronal receptors for nerve growth factor in the rat. *J. Neurosci.* **6**, 2312-2321.

Richardson, P.M. and Riopelle, R.J. (1983) Uptake of nerve growth factor along peripheral and spinal axons of primary sensory neurons. *J. Neurosci.* **4**, 1683-1689.

Rosenfeld, M.G., Mermod, J.J., Amara, S.G., Swanson, L.W., Sawchenko, P.E., Rivier, J., Vale, W.W. and Evans, R.H. (1983) Production of novel neuropeptide encoded by the calcitonin gene via tissue specific RNA processing. *Nature*, **304**, 129-135.

Ruda, M.A. (1982) Opiates and pain pathways: demonstration of enkephalin synapses on dorsal horn projection neurons. *Science*, **215**, 1523-1525.

Ruda, M.A., Coffield, J. and Dubner, R. (1984) Demonstration of postsynaptic opioid modulation of thalamic projection neurons by the combined techniques of retrograde horseradish peroxidase and enkephalin immunocytochemistry. *J. Neurosci.* **4**, 2117-2132.

Ruda, M.A. (1986) The pattern and place of nociceptive modulation in the dorsal horn. A discussion of the anatomically characterized neural circuitry of enkephalin, serotonin, and substance P. In Yaksh, T.L. (ed), *Spinal afferent processing.* Plenum Press, New York, pp. 141-164.

Ruda, M.A., Bennett, G.J. and Dubner, R. (1986) Neurochemistry and neural circuitry in the dorsal horn. *Prog. Brain Res.* **66**, 219-268.

Ruit, K.G., Osborne, P.A., Schmidt, R.E., Johnson, E.M., Jr. and Snider, W.D. (1990) Nerve growth factor regulates sympathetic ganglion cell morphology and survival in the adult mouse. *J. Neurosci.*

10, 2412-2419.

Ryu, P.D., Gerber, G., Murase, K. and Randic, M. (1988) Actions of calcitonin gene-related peptide on rat spinal dorsal horn neurons. *Brain Res.* **441**, 357-361.

Sakuma, M., Yoshioka, K., Suzuki, H., Yanagisawa, M., Onishi, Y., Kobayashi, N. and Otsuka, M. (1991) Substance P-evoked release of GABA from isolated spinal cord of the newborn rat. *Neuroscience*, **45**, 323-330.

Sambrook, J., Fritsch, E.F. and Maniatis, T. (1989) Molecular Cloning: a Laboratory Manual. Cold Spring Harbor, New York,

Scadding, J.W. (1980) The permanent anatomical effects of neonatal capsaicin in somatosensory nerves. *J. Anat.* **131**, 471-482.

Scheibel, M.E. and Scheibel, A.B. (1968) Terminal axonal patterns in the cat spinal cord. II. The dorsal horn. *Brain Res.* **9**, 32-58.

Scheibel, M.E. and Scheibel, A.B. (1969) Terminal patterns in cat spinal cord. III. Primary afferent collaterals. *Brain Res.* **13**, 417-443.

Schnell, L., Schneider, R., Kolbeck, R., Barde, Y.-A. and Schwab, M.E. (1994) Neurotrophin-3 enhances sprouting of corticospinal tract during development and after adult spinal cord lesion. *Nature*, **367**, 170-173.

Schnell, L. and Schwab, M.E. (1990) Axonal regeneration in the rat spinal cord produced by an

antibody raised against myelin-associated neurite growth inhibitors. *Nature*, **343**, 269-272.

Schwab, M.E. (1990) Myelin-associated inhibitors of neurite growth and regneration in the CNS. *Trends Neurosci.* **13(11)**, 452-456.

Schwab, M.E., Kapfhammer, J.P. and Bandtlow, C.E. (1993) Inhibitors of neurite growth. *Annu. Rev. Neurosci.* **16**, 565-595.

Schwartz, J.P., Pearson, J. and Johnson, E.M. (1982) Effect of exposure to anti-NGF on sensory neurons of adult rats and guinea-pigs. *Brain Res.* **244**, 378-381.

Senba, E., Yanaihara, C., Yanaihara, N. and Tohyama, M. (1988) Co-localization of substance P and Met-enkephalin-Arg^6-Gly^7-Leu^8 in the intraspinal neurons of the rat, with special reference to the neurons in the substantia gelatinosa. *Brain Res.* **453**, 110-116.

Seybold, V.S. and Elde, R.P. (1982) Neurotensin immunoreactivity in the superficial laminae of the dorsal horn of the rat: I. Light microscopic studies of cell bodies and proximal dendrites. *J. Comp. Neurol.* **205**, 89-100.

Sholl, D.A. (1953) Dendritic organization in the neurons of the visual and motor cortices of the cat. *J. Anat.* **87**, 387-406.

Skilling, S.R., Smullin, D.H. and Larson, A.A. (1990) Differential effects of C- and N-terminal substance P metabolites on the release of amino acid neurotransmitters from the spinal cord: potential role in nociception. *J. Neurosci.* **10**, 1309-1318.

Skofitsch, G. and Jacobowitz, D.M. (1985) Calcitonin gene-related peptide: detailed immunohistochemical distribution in the central nervous system. *Peptides*, **6**, 721-745.

Smeyne, R.J., Klein, R., Schnapp, A., Long, L.K., Bryant, S., Lewin, A., Lira, S.A. and Barbacid, M. (1994) Severe sensory and sympathetic neuropathies in mice carrying a disrupted Trk/NGF receptor gene. *Nature*, **368**, 246-249.

Smullin, D.H., Skilling, S.R. and Larson, A.A. (1990) Interactions between substance P, calcitonin gene-related peptide, taurine and excitatory amino acids in the spinal cord. *Pain*, **42**, 93-101.

Stead, R.H., Tomioka, M., Quinonez, G., Simon, G.T., Felten, S.Y. and Bienenstock, J. (1987) Intestinal mucosal mast cells in normal and nematode-infected rat intestines are in intimate contact with peptidergic nerves. *Proc. Natl. Acad. Sci. USA*, **84**, 2975-2979.

Stewart, J.M., Getto, C.J., Neldner, K., Reeve, E.B., Krivoy, W.A. and Zimmermann, E. (1976) Substance P and analgesia. *Nature*, **262**, 784-785.

Stöckel, K., Schwab, M.E. and Thoenen, H. (1975) Specificity of retrograde transport of nerve growth factor (NGF) in sensory neurons: a biochemical and morphological study. *Brain Res.* **89**, 1-14.

Sugiura, Y., Lee, C.L. and Perl, E.R. (1986) Central projections of identified, unmyelinated (C) afferent fibers innervating mammalian skin. *Science*, **234**, 358-361.

Suresh, M.R., Cuello, A.C. and Milstein, C. (1986) Advantages of bispecific hybridomas in one-step immunocytochemistry and immunoassays. *Proc. Natl. Acad. Sci. USA*, **83**, 7989-7993.

Szolcsanyi, J. (1977) A pharmacological approach to elucidation of the role of different nerve fibres and receptor endings in mediation of pain. *J. Physiol. ,Paris,* **73,** 251-259.

Tang, J., Chou, J., Yang, H.Y. and Costa, E. (1983) Substance P stimulates the release of Met5-enkephalin-Arg6-Phe7 and Met5-enkephalin from rat spinal cord. *Neuropharmacology,* **22,** 1147-1150.

Tashiro, T., Takahashi, O., Satoda, T., Matsushima, R. and Mizuno, N. (1987) Immunohistochemical demonstration of coexistence of enkephalin-and substance P-like immunoreactivities in axonal components in the lumbar segments of cat spinal cord. *Brain Res.* **424,** 391-395.

Theriault, E., Otsuka, M. and Jessell, T. (1979) Capsaicin-evoked release of substance P from primary sensory neurons. *Brain Res.* **170,** 209-213.

Thoenen, H., Bandtlow, C. and Heumann, R. (1987) The physiological function of nerve growth factor in the central nervous system: Comparison with the periphery. *Rev. Physiol. Biochem. Pharmacol.* **109,** 145-178.

Thoenen, H. and Barde, Y.-A. (1980) Physiology of nerve growth factor. *Physiol. Rev.* **60,** 1284-1335.

Todd, A.J., Spike, R.C., Russell, G. and Johnston, H.M. (1992) Immunohistochemical evidence that Met-enkephalin and GABA coexist in some neurones in rat dorsal horn. *Brain Res.* **584,** 149-156.

Todd, A.J. and Lochhead, V. (1990) GABA-like immunoreactivity in type I glomeruli of rat substantia gelatinosa. *Brain Res.* **514,** 171-174.

Todd, A.J. and McKenzie, J. (1989) GABA-immunoreactive neurons in the dorsal horn of the rat spinal cord. *Neuroscience*, **31**, 799-806.

Todd, A.J. and Sullivan, A.C. (1990) Light microscope study of the coexistence of GABA-like and glycine-like immunoreactivities in the spinal cord of the rat. *J. Comp. Neurol.* **296**, 496-505.

Traub, R.J., Solodkin, A. and Ruda, M.A. (1989) Calcitonin gene-related peptide immunoreactivity in the cat lumbosacral spinal cord and the effects of multiple dorsal rhizotomies. *J. Comp. Neurol.* **287**, 225-237.

Traub, R.J., Allen, B., Humphrey, E. and Ruda, M.A. (1990) Analysis of calcitonin gene-related peptide-like immunoreactivity in the cat dorsal spinal cord and dorsal root ganglia provide evidence for a multisegmental projection of nociceptive C-fiber primary afferents. *J. Comp. Neurol.* **302**, 562-574.

Tuchscherer, M.M. and Seybold, V.S. (1985) Immunohistochemical studies of substance P, cholecystokinin-octapeptide and somatostatin in dorsal root ganglia of the rat. *Neuroscience*, **14**, 593-605.

Tuchscherer, M.M. and Seybold, V.S. (1989) A quantitative study of the coexistence of peptides in varicosities within the superficial laminae of the dorsal horn of the rat spinal cord. *J. Neurosci.* **9**, 195-205.

Tuszynski, M.H., Peterson, D.A., Ray, J., Baird, A., Nakahara, Y. and Gage, F.H. (1994) Fibroblasts genetically modified to produce nerve growth factor induce robust neuritic ingrowth after grafting to the spinal cord. *Exp. Neurol.* **126**, 1-14.

Uchizono, K. (1965) Characteristics of excitatory and inhibitory synapses in the central nervous system of the cat. *Nature,* **207,** 642-643.

Urban, L. and Randic, M. (1984) Slow excitatory transmission in rat dorsal horn: possible mediation by peptides. *Brain Res.* **290,** 336-341.

Valtschanoff, J.G., Phend, K.D., Bernardi, P.S., Weinberg, R.J. and Rustioni, A. (1994) Amino acid immunocytochemistry of primary afferent terminals in the rat dorsal horn. *J. Comp. Neurol.* **346,** 237-252.

Van der Zee, C.E.E.M., Fawcett, J. and Diamond, J. (1992) Antibody to NGF inhibits collateral sprouting of septohippocampal fibers following entorhinal cortex lesion in adult rats. *J. Comp. Neurol.* **326,** 91-100.

Vedder, H., Affolter, H.-U. and Otten, U. (1993) Nerve growth factor (NGF) regulates tachykinin gene expression and biosynthesis in rat sensory neurons during early postnatal development. *Neuropeptides,* **24,** 351-357.

Verge, V.M.K., Richardson, P.M., Benoit, R. and Riopelle, R.J. (1989a) Histochemical characterization of sensory neurons with high-affinity receptors for nerve growth factor. *J. Neurocytol.* **18,** 583-591.

Verge, V.M.K., Riopelle, R.J. and Richardson, P.M. (1989b) Nerve growth factor receptors on normal and injured sensory neurons. *J. Neurosci.* **9,** 914-922.

Verge, V.M.K., Merlio, J.-P., Grondin, J., Ernfors, P., Persson, H., Riopelle, R.J., Hökfelt, T. and

Richardson, P.M. (1992) Colocalization of NGF binding sites, trk mRNA, and low-affinity NGF receptor mRNA in primary sensory neurons: Responses to injury and infusion of NGF. *J. Neurosci.* **12**, 4011-4022.

Verge, V.M.K., Richardson, P.M., Wiesenfeld-Hallin, Z. and Hökfelt, T. (1995) Differential influence of nerve growth factor on neuropeptide expression *in vivo*: A novel role in peptide suppression in adult sensory neurons. *J. Neurosci.* **15**, 2081-2096.

Vigna, S.R., Bowden, J.J., McDonald, D.M., Fisher, J., Okamoto, A., McVey, D.C.P., DG and Bunnett, N.W. (1994) Characterization of antibodies to the rat substance P (NK-1) receptor and to a chimeric substance P receptor expressed in mammalian cells. *J. Neurosci.* **14**, 834-845.

Von Euler, U.S. and Gaddum, J.H. (1931) An unidentified depressor substance in certain tissue extracts. *J. Physiol. (Lond.)*, **72**, 74-86.

Weskamp, G. and Otten, U. (1987) An enzyme-linked immunoassay for nerve growth factor (NGF): a tool for studying regulatory mechanisms involved in NGF production in brain and peripheral tissues. *J. Neurochem.* **48**, 1779-1786.

Wiesenfeld-Hallin, Z., Hökfelt, T., Lundberg, J.M., Forssmann, W.G., Reinecke, M., Tschopp, F.A. and Fischer, J.A. (1984) Immunoreactive calcitonin gene-related peptide and substance P coexist in sensory neurons to the spinal cord and interact in spinal behavioral responses of the rat. *Neurosci. Lett.* **52**, 199-204.

Wiesenfeld-Hallin, Z. (1986a) Substance P and somatostatin modulate spinal cord excitability via physiologically different sensory pathways. *Brain Res.* **372**, 172-175.

Wiesenfeld-Hallin, Z. (1986b) Somatostatin and calcitonin gene-related peptide synergistically modulate spinal sensory and reflex mechanisms in the rat: behavioral and electrophysiological studies. *Neurosci. Lett.* **67,** 319-323.

Willis, W.D., Westlund, K.N. and Carlton, S.M. (1995) Pain. In Paxinos, G. (ed), *The Rat Nervous System.* 2nd. Academic Press, Sydney, pp. 725-750.

Willis, W.D. and Coggeshall, R.E. (1991) Sensory mechanisms of the spinal cord. Plenum Press, New York,

Wong, J. and Oblinger, M.M. (1991) NGF rescues substance P expression but not neurofilament or tubulin gene expression in axotomized sensory neurons. *J. Neurosci.* **11,** 543-552.

Woolf, C. and Wiesenfeld-Hallin, Z. (1986) Substance P and calcitonin gene-related peptide synergistically modulate the gain of the nociceptive flexor withdrawal reflex in the rat. *Neurosci. Lett.* **66,** 226-230.

Woolf, C.J. and Fitzgerald, M. (1983) The properties of neurones recorded in the superficial dorsal horn of the rat spinal cord. *J. Comp. Neurol.* **221,** 313-328.

Yaksh, T.L., Jessell, T.M., Gamse, R., Mudge, A.W. and Leeman, S.E. (1980) Intrathecal morphine inhibits substance P release from mammalian spinal cord. *Nature,* **286,** 155-156.

Yashpal, K., Dam, T.-V. and Quirion, R. (1990) Quantitative autoradiographic distribution of multiple neurokinin binding sites in rat spinal cord. *Brain Res.* **506,** 259-266.

Yashpal, K. and Henry, J.L. (1983) Endorphins mediate overshoot of substance P-induced facilitation of a spinal nociceptive reflex. *Can. J. Physiol. Pharmacol.* **61**, 303-307.

Yashpal, K. and Henry, J.L. (1984) Substance P analogue blocks SP-induced facilitation of a spinal nociceptive reflex. *Brain Res. Bull* **13**, 597-600.

Yip, H.K., Rich, K.M., Lampe, P.A. and Johnson, E.M., Jr. (1984) The effects of nerve growth factor and its antiserum on the postnatal development and survival after injury of sensory neurons in the rat dorsal root ganglia. *J. Neurosci.* **4**, 2986-2992.

Yoshimura, M. and Jessell, T.M. (1989) Primary afferent evoked synaptic responses and slow potential generation in rat substantia gelatinosa neurons in vitro. *J. Neurophysiol.* **62**, 96-108.

Zhang, L., Schmidt, R.E., Yan, Q. and Snider, W.D. (1994) NGF and NT-3 have differing effects on the growth of dorsal root axons in developing mammalian spinal cord. *J. Neurosci.* **14**, 5187-5201.

Zieglgansberger, W. and Bayerl, H. (1976) The mechanism of inhibition of neuronal activity by opiates in the spinal cord of cat. *Brain Res.* **115**, 111-128.

AUTHORIZATION OF REPRINTS

ELSEVIER SCIENCE B.V.

Amsterdam Publishing Division

Sara Burgerhartstraat 25
1055 KV Amsterdam
The Netherlands

P.O. Box 521
1000 AM Amsterdam
The Netherlands

Tel (+31) 20 5862 833
Fax (+31) 20 5862 722

Mc Gill University
Pharmacology and Therapeutics
3655 Drummond Street
Room 1325
Montreal, Quebec
Canada H33 1Y6
Attn. Weiya Ma

Direct Line: (020) 5862 833

Amsterdam, 11 August 1995

Dear Sir/Madam,

We herewith grant you and The National Library of Canada permission to reproduce the material as mentioned in the enclosed copy of your letter in your thesis/dissertation, provided that:

- full acknowledgement is given to the original source of the publication
- your work is not distributed commercially

Should your thesis be published commercially, please reapply for permission.

Yours sincerely,
ELSEVIER SCIENCE B.V.
Amsterdam Publishing Division

Linda Versteeg
Rights & Permissions

Imprints:
Elsevier
Pergamon
North-Holland
Excerpta Medica

Bankers: Hollandsche Bank-Unie